Tyre - Road Noise, Surface Characteristics and Material Properties

Mingliang LI

Tyre - Road Noise, Surface Characteristics and Material Properties

Proefschrift

ter verkrijging van de graad van doctor
aan de Technische Universiteit Delft,
op gezag van de Rector Magnificus prof. ir. K.C.A.M. Luyben,
voorzitter van het College voor Promoties,
in het openbaar te verdedigen
op dinsdag 17 september 2013 om 10:00 uur

door

Mingliang LI

Master of Science in Municipal Engineering,
Dalian University of Technology, China
geboren te Fuxin, Liaoning Province, China

Dit proefschrift is goedgekeurd door de promotor:
Prof. dr. ir. A.A.A. Molenaar

Copromotor:
Ir. M.F.C. van de Ven

Samenstelling promotiecommissie:

Rector Magnificus,	voorzitter
Prof. dr. ir. A.A.A. Molenaar,	Technische Universiteit Delft, promotor
Ir. M.F.C. van de Ven,	Technische Universiteit Delft, copromotor
Prof. H. Ceylan, MSc, PhD	Iowa State University, USA
Prof. dr. ir. A. de Boer,	Universiteit Twente
Prof. dr. A. Scarpas	Technische Universiteit Delft
Dr. ir. R. Hofman,	Rijkswaterstaat
Ir. G. Gaarkeuken,	DIBEC Materiaalkunde
Prof. dr. ir. S.M.J.G. Erkens,	Technische Universiteit Delft, reservelid

ISBN 978-94-6186-206-8

Key Words: Tyre - Road Noise; Thin Layer Surfacing; Surface Texture; Sound Absorption; Mechanical Impedance; Modeling

Printing: Wohrman Print Service, Zutphen (the Netherlands)

To my parents

Acknowledgements

After a long journey, someone needs to be recalled and something to be remembered. This is a right moment to preserve all the memories and to say "thank you" to all those who accompanied me in the last five years. We walked, we met, and we made the history.

My PhD work was sponsored by China Scholarship Council (CSC) and Delft University of Technology (TU Delft). It was also partly sponsored by VAN KEULEN advies. The research was carried out in the Section of Road and Railway Engineering in the Faculty of Civil Engineering and Geosciences in TU Delft. The support from all these institutes is greatly acknowledged.

Deepest gratitude to my promotor, Prof. André Molenaar. He provided the chance which brought me from DUT (Dalian University of Technology) to TUD to start my search for the PhD. He not only gave me the guidance and conduct throughout my research, but I also profited greatly from his life philosophy, work behavior and wisdom of being a boss. He is a very important supervisor in my life. At the same time, I am grateful to my copromotor Associate Prof. Martin van de Ven, who is a very nice man and always helped me when I asked for help. His professional knowledge and experience in road engineering helped me to accomplish this research and to solve problems in many practical cases. Discussions with him were valuable and rewarding experiences.

Sincere thanks go to my daily supervisor Dr. Wim van Keulen, owner of VAN KEULEN advies. He is the one who lead me into the world of "noise", which was totally strange for me five years ago. Thanks for the remarkable ideas and suggestions on my research work, the opportunities to join practical tests carried out in the field and the lab, supporting me in attending international conferences and introducing me to experts in this field.

My sincere appreciation also goes to Prof. Halil Ceylan from Iowa State University. It was really a busy but fruitful time for me when he was at TU Delft as a visiting scholar. I am grateful for his guidance on data analysis and the frequent discussions which happened nearly every day. The whole research speeded up with this American rhythm.

Special thanks for people and institutes that provided contributions and assistance to my research work. The thesis could not have been completed without their involvement and support. My gratitude goes to Bert Gaarkeuken and Ballast Nedam b.v. for producing and providing the slab samples which are the most important materials used in the research. Peter The, from DVS, with whom I cooperated so many times. I thank him for his help for the measurements on the Kloosterzande trial sections and for taking me to lots of practical projects. Thanks are also for Dr. Rob Hofman and Andre Kleis from DVS for providing

measurement data from Dutch highways which facilitated my modeling work. I appreciate the help from Fred van Dishoeck and Hogeschool Windesheim for lending the device to test flow resistance and measuring the sound absorption with their impedance tube. I also would like to thank my friend Mingzhong Zhang from the Microlab in TU Delft, who put effort in the analysis of CT scanning results. Appreciations also go to my master supervisor Prof. Yang Zhong from DUT, and my former boss Dr. Wing-Gun Wong from Hong Kong Road Research Laboratory. Thanks for the kind care and encouragement.

I am grateful to all my colleagues in the group of Road and Railway Engineering who worked and are still working with me. Many thanks for Associate Prof. Lambert Houben, Prof. Tom Scarpas, Prof. Sandra Erkens, Prof. Rolf Dollevoet, Associate Prof. Zili Li, Ad Pronk, Dr. Rien Huurman and Dr. Xueyan Liu for the support and encouragement in my research work. Appreciations to Jacqueline, Sonja and Abdol, for the careful arrangements and help in daily affairs. Great thanks to Jan, Marco, Jan-Willem, Dirk and Wim Verwaal for the technical support to my laboratory work. My officemates, Milliyon, Yue and Pungky, I had so much wonderful time when sitting in the same office with them. My thanks to all the PhD students who worked together with me during all these years, Liantong, Gang, Jian, Dongxing, Alem, Xin, Oscar, Marija, Ning, Diederik, Sadegh, Mohamad, Jingang, Maider, Nico, Dongya, Yuan, Mauricio, Shaoguang, Xiangyun, Pengpeng, Chang, Lizuo, Haoyu and all the new PhD students in Railway Engineering. I am lucky for being a member of such a big family. Kai Chang, the master student, thanks for the asphalt mixture stiffness tests in a hot summer. Of course, how can I forget the lovely Italian guys and girls who have visited here? Claudio, Luca, Chiara, Serena, Stefania, Lorenzo and Elisa, Grazie! in bocca al lupo!

Thanks to all my friends, who were around me, thanks for all the beautiful and fantastic time we have spent together: Xu and Xuhong, Xun and Xuefei, Lin Liu and Huisu Chen, Zhan Zhang, Chen Zhou, Hua Zhong, Yutian Yao, Junchao Shi, Wenchao and Sizhu, Lu Wang, Tao Qian, Jiao Yuan, Tingting Jiang, Yaya, Xiaoshi, Harmony my sister and Xin Wang etc. Thanks everyone! You make me happy, you make me strong, and you make me what I am today.

Many thanks for the understanding and support of all my relatives and friends in China and other countries.

Last but not least, thanks to my parents, for their continuous support and endless love.

Mingliang Li 李明亮

August 2013, Delft

Summary

Noise levels due to road traffic have reached intolerable high levels in and around many urban areas all around the world. Because of health reasons and reasons of well- being these noise levels have to be reduced. The noise produced from the interaction between the rolling tyre and road surface is one of the most important contributions in the overall traffic noise. Therefore solutions for noise level reduction have to be found in that interface. A noise reducing pavement is considered as an effective way to reduce the tyre - road noise from the source where it generates. Towards further understanding and improvement of the noise reduction ability of pavements, research was carried out in this PhD thesis to determine the relationship between the road material properties, surface characteristics and the noise levels, and to develop models which can be used for guiding the design of noise reducing pavements.

As one of existing road surfaces, the thin layer surfacing eliminates the tyre - road noise by combining a small surface texture and a high porosity. In recent years, it became popular for using it on urban and provincial road sections in the Netherlands and some other European countries. Replacing porous asphalt with thin layer surfacings on highways is also considered an option in the Netherlands. As there are limited investigations on the relation between tyre - road noise and the influencing parameters for this type of surface, the research in this thesis focuses on thin layer surfacings.

The study starts with a review of existing researches on tyre - road noise. It provides basic knowledge about tyre - road noise and the influencing parameters related to the road surface. The related measurement methods and models developed were summarized. Comments were made on these existing studies and the shortcomings were pointed out. A research plan was then proposed based on the comments of the current researches and aiming for improving the existing knowledge of tyre - road noise on thin layer surfacings.

Measurements were carried out for investigating the influence of mixture compositions on surface characteristics. Both laboratory and in-situ measurements were involved. In the laboratory tests, thin layer surfacing samples with different mixture compositions were designed and produced; core samples were also used which were drilled from trial road sections in the Netherlands. The surface characteristics studied included: surface texture, sound absorption, mechanical impedance and stiffness.

Methods for testing the surface characteristics and mixture compositions were discussed. Experimental work was also undertaken for developing new methods in testing the surface characteristics. A contribution of this thesis to tyre - road noise related measurement is the application of a new type of technology for

measuring the sound absorption of a road surface. It is based on testing the sound pressure and sound particle velocity close to the sample surface. According to the analysis of the test results, this measurement method proved to provide reliable results of sound absorption for road surface samples. Furthermore, suggestions were given for the application of the method in road engineering measurements.

Surface characteristics and mixture compositions of thin layer surfacings were then measured. The influence of the material properties on surface characteristics, including texture, sound absorption, mechanical impedance and stiffness, were observed based by comparing test results obtained on materials with different mixture compositions. Moreover, in the study, the degree of connectivity of air voids in the road surface sample was determined. A relationship between the mechanical impedance and stiffness of road surface material was also developed. Comments were given for noise reduction by taking into account the mechanical impedance of road surfaces.

The investigation of the effect of surface characteristics on tyre - road noise was performed by means of statistical analyses. Data used in the analysis were from thin layer surfacing sections in the Netherlands. The two important surface characteristics, surface texture and sound absorption were taken in to account. Correlation analysis and linear regression analysis were adopted for observing the relationship between the surface characteristics and noise levels. The individual effect of a certain surface characteristic can be reflected by the regression equations. Furthermore, the influence of driving speed of the vehicle, the tyre types and small changes of surface characteristics were also discussed.

In the end, a model which predicts the tyre - road noise levels for thin layer surfacings was developed. The model was built by means of regression analysis by using the data from the laboratory measurements and an existing database. With the model, noise levels can be predicted using a small number of input parameters of material properties or surface characteristics. The model was validated by using data from in service thin layer road surfaces. The model can be used for predicting noise levels and helps to improve the design of noise reducing surfaces.

Samenvatting

Geluidniveaus veroorzaakt door wegverkeer hebben onaanvaardbare hoogtes bereikt in en rond veel stedelijke gebieden over de hele wereld. Omwille van gezondheids- en welzijnsredenen moeten deze geluidniveaus worden gereduceerd. Het geluid veroorzaakt door de interactie tussen band en wegdek is een van de belangrijkste bijdragen aan verkeerslawaai en boven een snelheid van ca 50 km/h zelfs de dominante bijdrage. Daarom moeten oplossingen voor beperking van het geluid door de interactie tussen band en wegdek worden gezocht. Geluidsreducerende verhardingen worden beschouwd als een effectieve manier om het lawaai veroorzaakt door de band - weg interactie bij de bron te reduceren. Voor het verbeteren van het geluidsreducerend vermogen van verhardingen, is het belangrijk om de relatie tussen materiaaleigenschappen van de deklagen, oppervlaktekenmerken en het geluidsniveau te bepalen en modellen te ontwikkelen die als standaard kunnen worden gebruikt voor het ontwerp van geluidsreducerende wegdekken.

Als een van de bestaande wegdekken, reduceert de dunne deklaag het geluid ten gevolge van de band - weg interactie door een combinatie van een geringe oppervlaktextuur en een relatief hoge porositeit. De laatste 10 jaren is het gebruik van deze dunne deklagen op stedelijke en provinciale wegvakken sterk toegenomen. Het vervangen van ZOAB door dit soort dunne deklagen wordt ook als optie overwogen in Nederland. Omdat er nog slechts beperkt onderzoek is gedaan naar de relatie tussen het geluid veroorzaakt door de band - weg interactie en de eigenschappen van dit type deklaag, richt het onderzoek in dit proefschrift zich op deze dunne deklagen.

Begonnen is met een overzicht van onderzoek dat reeds verricht is naar de geluidproductie ten gevolge van band - wegdek interactie. Dit deel geeft basiskennis over geluid veroorzaakt door de band - wegdek interactie en de wegdek parameters die van invloed zijn op dit geluid. De bijbehorende meetmethoden en ontwikkelde modellen zijn samengevat. Deze bestaande studies zijn becommentarieerd en enkele tekortkomingen zijn geduid. Op basis hiervan is een onderzoeksplan geformuleerd dat als doel heeft de bestaande kennis over het geluid veroorzaakt door de band - wegdek interactie op dunne deklagen te vergroten.

Metingen zijn uitgevoerd voor het onderzoeken van de invloed van de samenstelling van het mengsel op de oppervlak-eigenschappen. Zowel laboratorium als veldmetingen zijn verricht. In de laboratorium experimenten, zijn dunne deklaag monsters met verschillende mengselsamenstellingen ontworpen en geproduceerd; kernen die werden geboord uitproefvakken van Rijkswaterstaat in Kloosterzande in Nederland zijn ook gebruikt. De bestudeerde

deklaag-eigenschappen zijn: oppervlaktextuur, geluidsabsorptie, mechanische impedantie en stijfheid.

Meetmethoden voor het bepalen van de oppervlakeigenschappen en de mengselsamenstellingen worden besproken. Experimenteel werk is uitgevoerd voor het ontwikkelen van nieuwe methoden voor het bepalen van de oppervlakeigenschappen. Een relatief nieuwe techniek voor het meten van de geluidsabsorptie van een wegdek is hierbij gebruikt. Deze methode is gebaseerd op het meten van de geluidsdruk en de snelheid van het geluid dichtbij het monsteroppervlak. Uit een analyse van de testresultaten bleek dat deze meetmethode betrouwbare resultaten oplevert m.b.t. geluidsabsorptie van wegdekken en wegdekmonsters. Op basis van de analyse is ookaangegeven hoe de methode kan worden toegepast voor metingen in de wegenbouw.

Metingen aan de oppervlakeigenschappen en mengselsamenstellingen van dunne deklagen zijn vervolgens verricht. De invloed van de materiaaleigenschappen op oppervlakkenmerken, zoals textuur, geluidsabsorptie en mechanische impedantie , is vervolgens bepaald door de testresultaten van materialen met verschillende mengselsamenstellingen met elkaar te vergelijken. Thevens is in het onderzoek de mate van connectiviteit van holle ruimten in de wegdekmonsters bepaald, omdat dit een belangrijke parameter is voor het verklaren van de resultaten. Ook is een relatie tussen de mechanische impedantie en de stijfheid van een wegdekmateriaal ontwikkeld. Aangetoond wordt dat mechanische impedantie alleen een rol gaat spelen als de stijfheid van de deklaag (zeer) gering is.

Het onderzoek naar het effect van oppervlakte-eigenschappen op het geluid veroorzaakt door de band - weg interactie is uitgevoerd met behulp van statistische analyses. Gegevens afkomstig uit metingen aan dunne deklagen toegepast op een aantal wegen in Nederland zijn gebruikt bij de analyse. Correlatieanalyse en lineaire regressieanalyse zijn gebruikt voor het bepalen van de relatie tussen de oppervlakeigenschappen en de geluidsniveaus. Het individuele effect van een bepaalde oppervlakeigenschap is met regressievergelijkingen beschreven. Ook de invloed van de rijsnelheid van het voertuig, de bandtypes en kleine veranderingen van oppervlakkenmerken is geanalyseerd.

Tot slot is een model ontwikkeld dat de geluidsniveaus veroorzaakt door de band - wegdek interactie op dunne deklagen voorspelt. Het model is opgebouwd door middel van regressieanalyse uitgevoerd op gegevens verkregen uit laboratoriummetingen en die welke beschikbaar waren in een bestaande database. Met het model kunnen geluidsniveaus worden voorspeld met behulp van een klein aantal parameters die betrekking hebben op materiaaleigenschappen en oppervlakeigenschappen. Het model is gevalideerd met gegevens van momenteel gebruikte dunne deklagen. Het model kan worden gebruikt voor het voorspellen van geluidsniveaus en als ontwerp hulpbij het verbeteren van geluidreducerende oppervlakken.

List of Symbols

a	constant [-]
a_c	acceleration [m/s^2]
a_T	shifting factor [-]
b	constant [-]
AL_i	sound absorption coefficient at frequency f_i [-]
BC	binder content [%]
B_j'	standardized partial regression coefficient of the standardized principal component regression [-]
c_0	speed of sound in atmosphere [m/s]
c_{ij}	eigenvector corresponding to the jth principal component and the ith explanatory variable [-]
CA	coarse aggregate content [%]
C_{ij}	correlation coefficient [-]
$Croad$	correction of noise prediction due to the road surface influence [dB]
d	diameter [m]
d_s	maximum size of the aggregate [m]
D_{Ag}	density of the coarse aggregate [kg/m^3]
D_s	density of the specimen [kg/m^3]
h	thickness [m]
h_s	distance from the source of sound to the sample [m]
h_p	distance from the probe to the sample [m]
f	frequency [Hz]
$f_{\alpha,max}$	frequency corresponding to the maximum sound absorption coefficient [Hz]
f_{red}	the loading frequency where the master curve to be read [Hz]
f_{sh}	the frequency shift factor [Hz]
f_u	upper frequency of impedance tube measurement [Hz]
F	force [N]
FA	fine aggregate content [%];
k	wavenumber [m^{-1}]
K_g	bulk modulus [Pa]
K_t	roughness caused stiffness variation [-]
l	length [m]
l_s	number of selected latent vectors in regression with partial least square method [-]
$L_{A,eq}$	equivalent sound level [dB(A)]
$L_{A,max}$	the maximum sound pressure level [dB(A)]
L_i	sound pressure level at frequency band f_i [dB]
L_p	logarithmic sound pressure level (SPL) [dB]
L_Z	decibel expression of mechanical impedance [dB, Ref=1 Ns/m]
M_{max}	maximum resilient modulus of mixture [MPa]
M_{min}	minimum resilient modulus of mixture [MPa]
M_{mix}	resilient modulus of mixture [MPa]

MI'	a new indicator of mechanical impedance proposed in this research [dB, Ref=1 Ns/m]
M_R	resilient modulus [Pa]
MS	maximum aggregate size [mm]
n	number of observations of explanatory variable in linear regression [-]
n'	grain shape factor [-]
N_{pr}	Prandtl number [-]
p	number of explanatory variables in linear regression [-]
p_0	ambient atmospheric pressure [kPa]
p'	selected number of principal component [-]
P	the linear sound pressure [Pa]
P_{ref}	an internationally standardized reference sound pressure of [Pa]
P_{Ag}	content of coarse aggregate by mass [%]
PC	principal component [-]
P_M	content of coarse mortar by mass [%]
Q	sound strength from the source [m^3/s]
R	air flow resistance [Pa·s/m]
R_p	plane-wave reflection coefficient [-]
R_s	air flow resistivity [Pa·s/m^2]
R^2	coefficient of determination [-]
s_{norm}	standard stiffness value for a slick tyre [Pa]
s_1	the stiffness of tyre tread [Pa]
s_2	the stiffness of road surface [Pa]
S	cross-sectional area [m^2]
SEL	sound exposure level [dB]
$Sig.$	statistical significance [-]
t	time [s]
T	temperature [ºC]
TA	age of the surface in years [year]
TL_i	texture level at wavelengths λ_i [dB, Ref=10^{-6}m]
$TL_i^{(e)}$	enveloped texture level at wavelengths λ_i [dB, Ref=10^{-6}m]
T_R	reference temperature [ºC]
U	the velocity of sound particle [m/s]
v	the complex velocity vector [m/s]
v_i	velocity of vibration of the road surface [m/s]
V	speed of the vehicle [km/h]
V_{ref}	reference speed of the vehicle [km/h]
V_{Ag}	volume fraction of coarse aggregate [%]
V_M	volume fraction of mortar [%]
X	explanatory variables in linear regression [-]
$\boldsymbol{X}$	matrix of explanatory variables in linear regression [-]
y	response variables in linear regression [-]
$\boldsymbol{y}$	vector of response variables in linear regression [-]
$Y_{model,i}$	predicted value from the model [-]
$Y_{obs,i}$	observed values from measurement [-]

Z	mechanical impedance [N·s/m^3]
Z_c	specific acoustical impedance [N·s/m^3]
Z_{ff}	acoustical impedance for the free field [N·s/m^3]
$Z_{measure}$	acoustical impedance measured close to the sample surface [N·s/m^3]
Z_n	acoustical impedance [N·s/m^3]
Z_{ref}	reference mechanical impedance [Ns/m]
α	sound absorption coefficient [-]
α_{max}	maximum sound absorption coefficient [-]
$\alpha_{t,i}$	root mean square value of the vertical displacement of the surface profile [m]
$\alpha_{t,ref}$	reference value of the vertical displacement of the surface profile [m]
β	regression coefficient [-]
γ	shape parameter [-]
Δ	difference value [-]
Δd	total recoverable horizontal deformation of core sample in the indirect tension test [mm]
$\Delta \upsilon_i$	change of a certain surface characteristic [-]
ε	regression error [-]
η	shape parameter [-]
λ	wavelength [mm]
λ_{max}	the maximum wavelength can be reached in testing the texture level with laser profilometer [mm]
ν	Poisson's ratio [-]
ρ_0	the density of air [kg/m^3]
ρ_g	dynamic density [kg/m^3]
σ	standard deviation [-]
φ	angel [º]
Ω	air void content by volume [%]
ω	angular frequency [rad/s]

List of Abbreviations

AGEL	Age-reduced Level
ANOVA	One way analysis of variance
AOT	Acoustic Optimization Tool
AR	Auto-Regressive (filter)
CB	Coast-By method
COP	Conformity of Production
CPB	The Controlled Pass-By method
CPX	The Close-Proximity method
$CRNL_C$	Combined Road Noise Level for cars
CT	Computerized Tomography
DAC	Dense Asphalt Concrete
DIS	Draft International Standard
DVS	Centre for Transport and Navigation in the Netherlands
ENR_α	Expected pass-by Noise level Reduction from sound absorption
ERNL	Estimated Road Noise Level
ESM	Extended Surface Method
ETD	Estimated Texture Depth
EU	European Union
FFT	Fast Fourier Transform
HU	Hounsfield Units
HyRoNE	Hybrid Rolling Noise Estimation model
INRETS	National institute for transport and safety research of France
IPG	the Dutch Noise Innovation Programme
ISO	International Organization for Standardization
ITT	Indirect Tension Test
LVDT	Linear Variable Differential Transformers
MIRIAD	Mobile Inspection of Road surfaces: In-situ Absorption Determination
MLSSA	Maximum-Length-Sequence System Analyzer
MPD	Mean Profile Depth
MSE	Mean Squared Error
NIPALS	Non-linear Iterative Partial Least Squares
PAC	Porous Asphalt Concrete
PC	Principal Component
PCR	Principal Component Regression
PERS	Poro-Elastic Road Surfaces
PIN	Probability of *F*-value due to which the variable is selected in the regression equation
PLS	Partial Least Squares
POUT	Probability of *F*-value due to which the variable is removed from the regression equation
P-U	Sound Pressure and Particle Velocity
PWRI	Japanese Public Works Research Institute

RMS	Root Mean Square value
RMSE	Root Mean Square Error
RODAS	ROad Design Acoustic Simulation
SILVIA	Sustainable road surfaces for traffic noise control
SIMPLS	SIMple Partial Least Squares regression
SMA	Stone Mastic Asphalt
SPB	Statistical Pass-By method
SPERoN	Statistical Physical Explanation of Rolling Noise
SPL	Sound Pressure Level
TCB	Trailer Coast-By method
TLPA	Two-Layer Porous Asphalt
TNO	Netherlands Organisation for Applied Scientific Research
TRIAS	Tyre Road Interaction Acoustic Simulation model
TRL	Transport Research Laboratory of UK
TYDAS	TYre Design Acoustic Simulation
UTM	Universal Testing Machine
VIF	Variance inflation factor
WHO	World Health Organization
WLF	Williams – Landel – Ferry model

Table of Contents

CHAPTER 1 INTRODUCTION

1.1 Background

Noise is defined as sound that is undesired or unwanted by the recipient. Road traffic is a predominant source of noise in modern societies. In European Union countries, it is estimated that around 50% of the population is regularly exposed to over 55 dB of road traffic noise, a level potentially dangerous to health [1]. In cities of developing countries, the noise pollution caused by traffic on the densely travelled roads is more severe and the equivalent sound pressure levels for 24 hours can reach 75-80 dB [2].

The World Health Organization (WHO) pointed out that environmental noise, including traffic noise, has direct as well as cumulative adverse effects on the health and/or well-being of exposed people on the following aspects [1, 2]:

- annoyance;
- sleep disturbance;
- interference with communication and intellectual performance;
- cardiovascular disease;
- adverse effects on mental health.

In addition, noise also affects socio-cultural, aesthetic and economic aspects. Traffic noise therefore causes increasing complaints from large groups of people who are affected. Significant progress has been made in Europe since 1970 in terms of measurement and evaluation of traffic noise as well as legislation.

Road traffic noise is generated from three major sources: propulsion (power train) noise, aerodynamic noise and tyre - road interaction noise. Previous studies showed that noise generated from the interaction between tyre and road surface is the dominant source at speeds above 30 to 50 km/h [3]. Reduction of the noise level produced at the tyre - pavement surface interface is thus considered as an effective way to eliminate the overall traffic noise. The term tyre - road noise implies the noise generated from the interaction between a rolling tyre and the road surface [4]. Tyre - road surface noise and especially the effects of the condition of the pavement surface on noise is the topic of this thesis.

1.2 Existing Studies

1.2.1 Influencing parameters

Tyre - road noise can be studied from either the tyre or road surface point of view. In this thesis, the research mainly focuses on road surface properties. It is known that the generation of tyre - road noise is an extremely complicated process which is related to various mechanisms and influencing parameters. Much work has been undertaken to understand the generation of tyre - road noise and related influencing parameters [5, 6]. Figure 1-1 gives an overview of these parameters and their relationships with noise. It can be seen that the road surface characteristics, vehicle properties and environmental factors act cooperatively on the tyre - road noise production through different mechanisms. The three main surface characteristics, namely the texture, sound absorption and mechanical impedance, are determined by basic material properties, such as, stone gradation, binder content and air voids, etc. The existing research and developments are mainly on topics like measurement methods, noise reducing pavements and prediction models. Measurement methods, noise reducing surfaces and models are introduced in brief in the sub-sections here-after. Details can be found in the literature review given in Chapter 2.

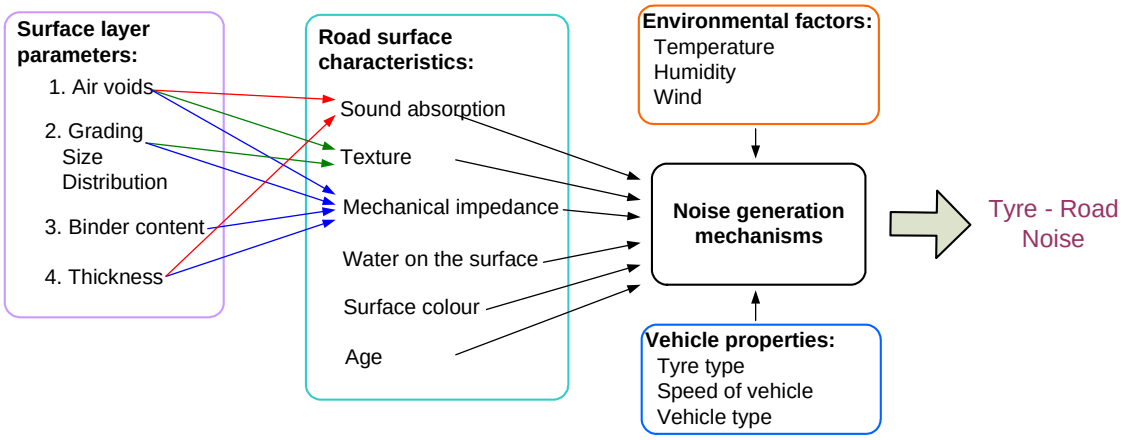

Figure 1-1 Major influencing factors on tyre - road noise

1.2.2 Measurement methods

In studying tyre - road noise, generally noise measurements and measurements of the relevant surface characteristics are included. Noise measurements can be performed at near field positions as well as far field positions. The close proximity (CPX) test is a typical method for measuring the near field noise. The measurements are carried out with microphones which are placed close to the test tyres on a special testing vehicle. The method can be seen as a procedure specifically designed to detect the influence of the road surface characteristics on noise generation. The Statistical Pass-By method (SPB), Coast-By method (CB) and Controlled Pass-By method (CPB) are all used for testing noise at the far field. In general, the noise is measured by microphones standing on the road side, and noise generated at and propagating over the road surface can be detected.

The three important surface characteristics to be measured for studying tyre - road noise are: surface texture, sound absorption and mechanical impedance. Standard methods have been developed for testing the road surface texture. According to ISO 13473, the texture of a road surface is generally measured by scanning the road surface with a laser sensor. In terms of sound absorption, measurements can be performed in situ with the Extended Surface Method (ESM) or in the laboratory with the impedance tube. However, the sound absorption at high frequencies cannot be measured with the impedance tube as it is limited by the diameter of the tube. With regards mechanical impedance, there is no standard method for measuring this property. Measurements based on the impedance hammer were referred to in some studies and an impedance shaker was developed by the company M+P in the Netherlands.

1.2.3 Noise reducing surfaces

Development and application of noise reducing pavements can be regarded as the most direct way to attenuate the tyre - road noise from the source. It is a cost-effective measure when compare to other technologies available to road authorities to reduce traffic noise [7, 8]. Currently, the most effective and commonly used low noise road surfaces in Europe are porous asphalt and thin layer surfaces [9].

Porous asphalt is a wearing course with high air voids content (usually > 20%) [10]. Sound energy at the source as well as in the path of propagation can be partly absorbed due to the porosity. One of the problems for using porous asphalt is the clogging of the pores in time by dirt and dust, which results in a decrease of the acoustical performance during the service life [11]. In order to counter the clogging effect, two-layer porous asphalt (TLPA) was developed. The TLPA consists of a bottom layer of porous asphalt with a coarse grading (typically 0/14, 0/16, 11/16) and a thin top layer of fine graded aggregate (typically 4/8, but sometimes 2/4 or 2/6). The initial noise reduction is excellent: 4-6 dB (A) for passenger cars at 50 km/h. It is one of the quietest road surfaces which are actually in use [12].

Thin layer noise reducing surfacings are commonly used in the Netherlands and some other European countries at present. This type of surfacing generally has a typical thickness of 25 mm. The tyre - road noise is mainly reduced by two properties:
1) Small maximum size aggregates are used to increase the smoothness of the road surface and to reduce the noise generated by tyre vibration.
2) The open surface structure absorbs sound waves like it does with porous asphalt [6].

Thin noise reducing surfacings are commonly used on provincial and urban roads. It is also used as the top layer of TLPA.

So-called third generation silent pavements such as Poro-Elastic Road Surfaces (PERS) [13] and Roll Pave [14] are also under investigation. These surfaces provide both a very fine texture and high air voids for noise reduction. The rubber is used for decreasing the mechanical impedance of the surface, which is also considered as a way to reduce the vibration generated noise. However, the durability and the mechanical properties of this type of surface still need to be improved.

1.2.4 Tyre - road noise prediction models

There is an increasing need for prediction models which provide information about noise generation before the road is constructed. Such models play an important role in predicting tyre - road noise, optimizing the pavement design and improving the materials and building technology [15].

Tyre - road noise models can be classified into three categories: statistical models, physical models and hybrid models. The statistical models usually characterize the relationship between noise level and the influencing parameters by regression equations. For example, the models developed respectively by Sandberg and Klein evaluate the tyre - road noise level from the surface texture levels and sound absorption coefficient of porous asphalt [5, 16]. Physical models focus on specific noise production mechanisms. In current studies, the vibration mechanism is widely simulated by mechanical models or finite element models (FEM). A great deal of work has been done and is still going on at Chalmers University for developing such a physical model [17]. The hybrid models combine both the statistical and physical elements in the framework. The structure is complicated but it gives an overall simulation on the emission and propagation of tyre - road noise. Two typical examples of hybrid models are the so-called Acoustic Optimization Tool (AOT) [18] and the Tyre Road Interaction Acoustic Simulation (TRIAS) model [19].

The road parameters in existing models are normally derived parameters such as a texture spectrum but they are not linked directly to the construction materials [20]. For road engineers, a model linking the noise level to the composition of the road surface mixture is essential for being able to design and constructing noise reducing surfacings. Such models would allow to determine the changes in noise caused by the variation of the material properties. In this way, the model helps to guide and optimize the design of road surfaces. In addition, the physical and hybrid models generally require a large number of input variables. Furthermore, some models are very much based on theory which implies that simplification of reality had to be made. This makes these models less practical for reflecting the generated noise. It is necessary to develop a model which has a simple structure and needs a small number of inputs, but makes accurate predictions.

1.3 Research Objectives and Methods

1.3.1 Research objectives

In this thesis, the research especially focuses on thin layer surfacing. From current studies, it is known that thin layer surfacings are designed to reduce the tyre - road noise by both texture and sound absorption. This type of surface got very popular in the last decades in the Netherlands, and the potential replacement of porous asphalt with thin layer surfacings on Dutch highways has already been proposed [14]. Porous asphalt has already been systematically studied and different models (statistical or physical models) have been developed for evaluating the noise generation of this type of surface. In contrast, for thin surfacings, there is still a lack of information on the relation between tyre - road noise and surface properties. As the mixture composition and surface layer characteristics are different from those of dense and porous layers, the acoustical performance of a thin surfacing is also different. Special investigations and improvements of the existing models are helpful for a better understanding of the properties of thin layer surfacings in reducing tyre - road noise and for improving the acoustical design.

The main objectives of this thesis are:

- Develop and improve laboratory measurement methods of surface characteristics which are related to tyre - road noise.
- Investigate the influence of material properties on the surface characteristics which are related to tyre - road noise of thin layer surfacings.
- Investigate the influence of surface characteristics on tyre - road noise for thin layer surfacings.
- Develop a practical model which is suitable for predicting the tyre - road noise of thin layer surfacings and which can be applied for road engineers.

The three surface characteristics which are mainly studied in this thesis are:

- Surface texture;
- Sound absorption;
- Mechanical impedance and stiffness.

1.3.2 Research methods

The research can be divided into three parts being: 1) laboratory measurement; 2) statistical analysis; 3) model development.

1) Laboratory measurement

Laboratory measurements are performed to determine the material properties and surface characteristics. Thin layer surfacing samples produced in the lab and

extracted from the road sections are included in the test program. Features to be measured include the mixture composition, surface texture, sound absorption, mechanical impedance and stiffness. Besides the standard methods for testing the surface texture and the stiffness, CT scanning is employed to determine the mixture composition of the samples. Measurements of sound absorption by using the surface impedance technology are performed. The mechanical impedance is measured by an impedance hammer device. These are all new methods for testing the noise related parameters of a road surface.

The influence of the material properties on the surface characteristics is determined using measurement results on mixture composition, texture and absorption. Besides, a statistical relationship between the mechanical impedance and stiffness is also developed. This information on noise elimination by means of mechanical impedance is important for road engineers involved in mixture design.

2) Statistical analysis

Statistical analyses are performed for investigating the influence of surface characteristics on tyre - road noise. In the study, data are obtained from a database which contains the measurement results from trial sections in Kloosterzande in the Netherlands. As general observations on these test results have been given in a previous study [21], this thesis will concentrate on exploring the influence of specific indicators of surface characteristics on tyre - road noise. It can be seen as refined or complementary work to the former research. In this thesis, the correlations between surface characteristics and tyre - road noise are evaluated. Linear regression equations relating noise levels with texture and sound absorption are developed. Principal component regression (PCR) and partial least square regression (PLS) are used to eliminate the multicollinearity between surface characteristic parameters. Influence of texture with different wavelengths and sound absorption at various frequencies on noise levels can be investigated specifically from the linear relationships. The influence of driving speed and truck tyres are also analyzed by means of regression analysis.

3) Model development

Model development can also be considered as a statistical analysis. However, in this part, the study aims for building a tool which is applicable for noise prediction in the road design stage. This requires that material properties, such as gradation etc, are used as inputs for the model. A small number of input variables is also preferred. The models are developed by means of regression analyses with data from both the laboratory measurements and the field database. Final selection of the model is based on the prediction power of the model and by validation using data from practical road surfaces.

1.4 Outline

The thesis consists of 8 chapters in total. The outline of the thesis is illustrated in Figure 1-2. The chapters are organized as follows:

Chapter 1 serves as a general introduction. The background, important topics in the field of tyre - road noise study, the objectives and the outline of the PhD research are presented.

Chapter 2 gives a detailed overview on the existing studies on tyre - road noise. Basic knowledge of tyre - road noise, road surface characteristics and other properties is provided.

Chapter 3 proposes the research plan of the PhD study. Comments are firstly given on the existing studies from the literature review. A research plan is then presented which shows the organization of the whole research work in this thesis.

Chapter 4 shows the materials and test methods used in the measurements. Properties to be measured include mixture compositions, surface texture, sound absorption, mechanical impedance and stiffness of the thin layer surfacing samples. In this chapter, a new method of testing sound absorption of asphalt samples by means of surface impedance devices is also investigated and developed.

Chapter 5 investigates the influence of mixture compositions on the surface characteristics for thin layer surfacings based on measurement results. The test results are shown, and comparisons are made between surfaces with different material properties. Regression analyses are used to relate the texture and maximum absorption with different material properties. An acoustical model is used to simulate the sound absorption of thin layer surfacings. A relationship between mechanical impedance and stiffness is developed.

Chapter 6 studies the influence of the surface characteristics on tyre - road noise by means of statistical analyses using data collected from the trial sections. The combined effect of the surface texture and sound absorption on noise levels are investigated by using principal component regression (PCR) and partial least square regression (PLS). The influence of driving speed and truck tyre are also discussed.

Chapter 7 describes the development of a statistical model which is specially used for predicting tyre - road noise level of thin layer surfacings. Different regression methods, model type and input combinations are taken into account. The selection of the model is based on the fit with the measured data used in developing the model and is based on validation of the model with measurement data from in service road sections. Two models are finally proposed which evaluate the tyre - road noise level from the surface characteristics and from

material properties respectively. Only a small number of input variables are required for using these models.

Chapter 8 presents the conclusions from the thesis and gives recommendations for future work.

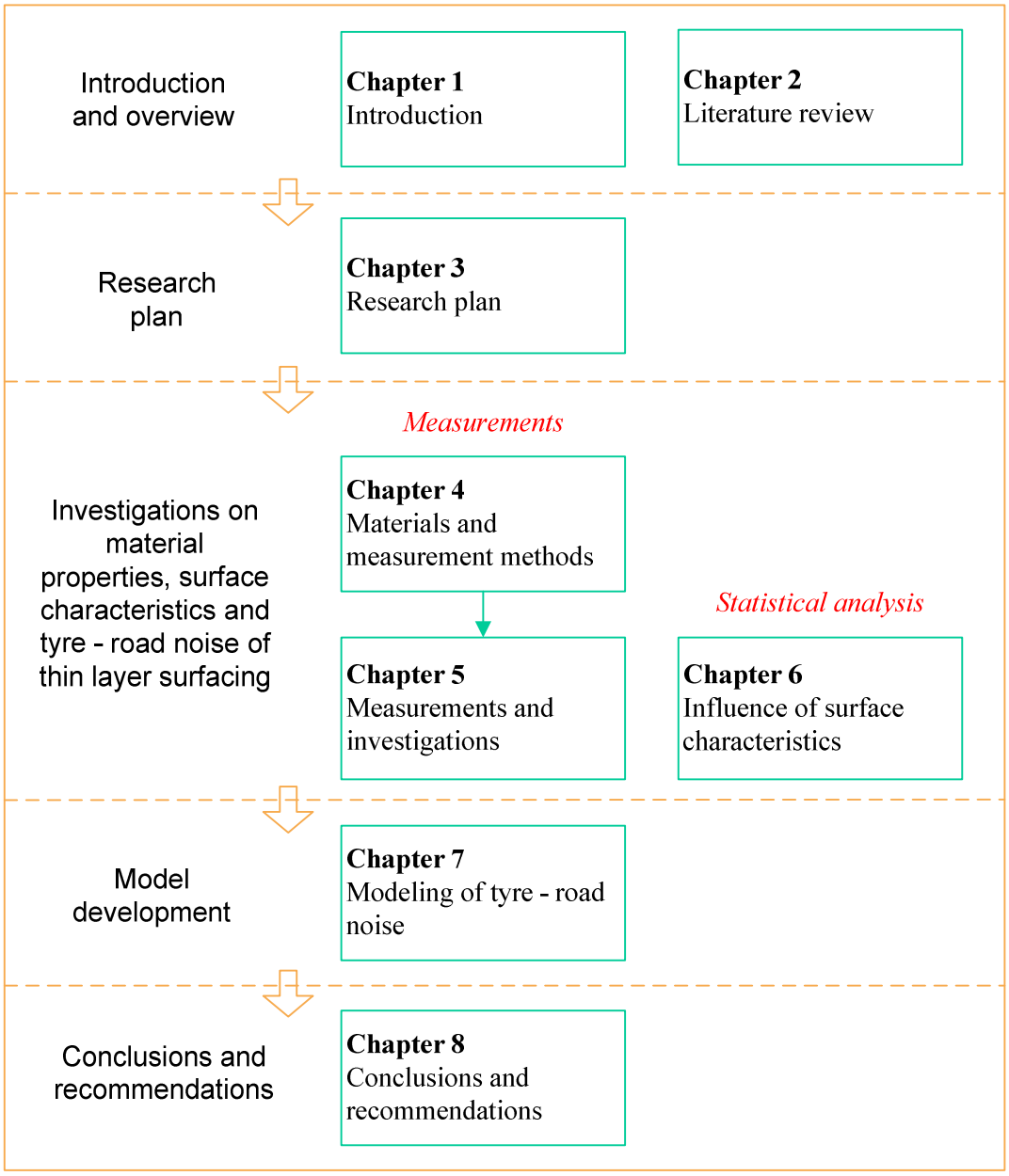

Figure 1-2 Outline of the thesis

References

1. World Health Organization, *Burden of disease from environmental noise - Quantification of healthy life years lost in Europe*. 2011, World Health Organization: Copenhagen, Denmark.
2. Berglund, B., Lindvall, T., and Schwela, D.H., *Guidelines for Community Noise*. 1999, World Health Organization: Geneva.
3. Sandberg, U. *Tyre/road Noise-Myths and Realities*. in *Proceedings 2001 International Congress and Exhibition on Noise Control Engineering*. 2001. The Hague, The Netherlands.
4. Donavan, P.R., *Handbook of Noise and Vibration Control*. 2007: Malcolm Crocker, John Wiley and Sons.
5. Sandberg, U. and Ejsmont, J., *Tyre/Road Noise Reference Book*. 2002, Kisa, Sweden: Informex.
6. van Keulen, W. and Duškov, M., *Inventory study of basic knowledge on tyre/road noise,* in *IPG Report DWW-2005-022,*. 2005: Delft, the Netherlands.
7. den Boer, L.C. and Schroten, A., *Traffic noise reduction in Europe - Health effects, social costs and technical and policy options to reduce road and rail traffic noise*, in *CE Delft*. 2007.
8. Bendtsen, H., Kragh, J., and Nielsen, E., *Use of noise reducing pavements. - European experience*. 2008, Danish Road Institute: Copenhagen, Denmark.
9. Nilsson, R., Nordlander, J., and Silwa, N., *Design guidelines for durable, noise-reducing pavements*, in *SILVIA Project Report SILVIA-SKANSKA-018-01-WP4-231105*. 2005.
10. COWI, *Noise classification of road pavements :Task 1: Technical background information*. 2006, European Commission - DG Environment: Brussels, Belgium.
11. Tan, S.A., Fwa, T.F., and Guwe, Y.K., *Laboratory Measurements and analysis of clogging mechanism of porous asphalt mixes.* Journal of testing and evaluation, 2000. **28**(3): p. 207-216.
12. Abbott, P.G., Morgan, P.A., and McKell, B., *A Review of Current Research on Road Surface Noise Reduction Techniques*, in *Transport Research Laboratory report for the Rural and Environment Research Analysis Directorate of the Scottish Government*. 2010.
13. Sandberg, U., Goubert, L., Biligiri, K.P., and Kalman, B., *State-of-the-art regarding poroelastic road surfaces*, in *Deliverable D8.1*. 2010.
14. Morgan, P.A., *IPG Research Report - Innovative mitigation measures for road traffic noise*, in *Report DVS-2008-018*. 2008, Road and Hydraulic Engineering Division of Rijkswaterstaat: Delft, the Netherlands.
15. Beckenbauer, T. and Kropp, W. *A hybrid model for analysis and design of low noise road surfaces*. in *EuroNoise 2006 conference*. 2006. Tampere, Finland.

16. Klein, P. and Hamet, J.F., *Tyre/road noise prediction with the HyRoNE model*, in *Proceedings of INTER-NOISE conference*. 2007: Istanbul, Turkey.
17. Larsson, K., Barrelet, S., and Kropp, W., *The modelling of the dynamic behaviour of tyre tread blocks.* Applied Acoustics, 2002. **63**(6): p. 659-677.
18. Kuijpers, A.H.W.M., Peeters, H.M., Kropp, W., and Beckenbauer, T., *Acoustic optimization tool, RE4 - Modelling refinements in the SPERoN framework*, in *M+P Report DWW.06.04.7*. 2007: Vught, the Netherlands.
19. Gerretsen, E. and Mulder, E.H., *TRIAS: a comprehensive tyre-road noise model and its validation*, in *TNO-report, HAG-RPT-000121a* 2001.
20. Peeters, B. and Blokland, G.J.v., *The noise emission model for European road traffic*, in *IMAGINE project no. 503549*. 2007.
21. van Blokland, G.J., Reinink, H.F., and Kropp, W., *Acoustic optimization tool. RE3: Measurement data Kloosterzande test track*, in *M+P Report DWW.06.04.8*. 2007, M+P Raadgevende Ingenieurs bv: Vught, the Netherlands.

CHAPTER 2 LITERATURE REVIEW

2.1 Introduction

The generation of tyre - road noise is an extremely complicated process which is related to various mechanisms and influencing parameters. Much work has been undertaken to understand the tyre - road noise generation and relevant influencing parameters [1, 2]. In this thesis, the relationships between mixture composition, road surface characteristics and tyre - road noise are to be investigated. It is essential to gather information for each aspect related to tyre - road noise before starting the work. This literature study focuses on reviewing the characteristics of tyre - road noise and each influencing parameter. Basic knowledge on tyre - road noise, road surface characteristics and other properties is provided, which is useful for investigation and developing models, a topic that will be discussed in the chapters here-after.

Section 2.2 is an introduction on the basics of noise. The generation mechanisms, measurement methods, noise reducing pavements and modeling work of tyre - road noise are all discussed. Section 2.3 presents those properties of road surface related factors which are related to tyre - road noise. The influence of surface texture, sound absorption and the mechanical impedance of the road surface on tyre - road noise as well as, measurement methods and prediction models from previous research are discussed. Section 2.4 provides a general review of other factors, including the age of surface, temperature and vehicle speed. In Section 2.5, a summary from the literature is given.

2.2 Basic Knowledge of Tyre - Road Noise

2.2.1 Measuring methods of sound and noise

Noise is defined as sound that is undesired or unwanted by the recipient. Identical with characterizing the sound wave, the quantity that is employed to describe the “strength” of noise is the sound pressure. Sound pressure (or acoustic pressure) is the local pressure deviation from the ambient (average, or equilibrium) atmospheric pressure caused by a sound wave. It is expressed in the SI unit pascal - Pa. The working range of human ear is from 20×10^{-6} Pa to 20 Pa. In order to compress this wide range in linear scale, a logarithmic scale, called Sound Pressure Level (SPL), is introduced. SPL or sound level L_p is a logarithm

of the effective sound pressure relative to a reference value and the unit is decibel (dB).

$$L_p = 10 \cdot \lg(P / P_{ref})^2 \quad (2\text{-}1)$$

with
L_p – logarithmic sound pressure level (SPL), dB;
P – the linear sound pressure, Pa;
P_{ref} – an internationally standardized reference sound pressure of 20 $\times 10^{-6}$ Pa [1].

The formula used to combine multiple sources of sound is:

$$L_{p,t} = 10 \cdot \lg(\sum 10^{\frac{L_{p,i}}{10}}) \quad (2\text{-}2)$$

where
Lp,t – the total sound pressure level, dB;
$L_{p,i}$ – the sound pressure level of the number i individual source, dB.

Sound pressure levels in practice cover the range from 0 (the threshold of hearing) to 120 dB (the threshold of pain). As human hearing is not equally sensitive to sound of all frequencies, when imitating human ear's response to sound, an analogue or digital filter is required before the signals are measured and presented. The filter which performs the best in approximating the human perception of sounds is the so-called "A" filter. The unit dB (A) is used when referring to the sound levels that are A-weighted.

The most commonly used noise measure in Europe for assessing the noise impact from road traffic is the equivalent sound level $L_{A,\,eq}$, which is the steady sound level over a certain span of time. The equivalent level for a continuous sound is defined as follows:

$$L_{A,eq} = 10 \cdot \log\left[\frac{1}{t_2 - t_1}\int_{t_1}^{t_2}\frac{P^2(t)}{P_{ref}^2}\cdot dt\right] \quad (2\text{-}3)$$

where
t_1 – the start time of the integration;
t_2 – the stop time of the integration;
$P(t)$ – the sound pressure.

Another common and traditional measure for individual vehicle or tyre - road noise is the maximum sound pressure level $L_{A,\,max}$, the highest sound pressure level recorded during a vehicle pass-by. The maximum level is often reached at a point in time which quite closely corresponds to the moment when the vehicle is at its closest position to the microphone.

2.2.2 Tyre - road noise generation mechanisms

The generation mechanisms for tyre - road noise have been investigated since the 1970s. Several physical processes are related to tyre - road noise generation and they are categorized into different groups by various researchers [1, 3, 4]. A classification into three-groups is used in this study:

1) Vibrational mechanisms (structure-borne): impacts resulting from the contact between the tyre tread and road surface are leading to radial (also known as impact mechanism) and tangential vibrations (adhesion mechanism);
2) Aerodynamical mechanism (air-borne): processes that are related to the movement of air between, and within, the tyre tread and road surface patterns;
3) Amplification/reduction mechanisms: acoustical impedance related properties of the surface that influence the noise in transmission paths.

Specific items that belong to each mechanism group are shown in Table 2-1. A general summary from the table is that the mechanisms related to vibration mostly occur below 1000 Hz, while the aerodynamical mechanisms are mostly effective above 1000 Hz.

Table 2-1 Tyre - road noise generation mechanisms ([1], with small modification)

Classification			Effective frequency	Definition
Vibrational mechanism	Impact mechanism	Tread impact	300-1500 Hz	impact of tyre tread blocks or other pattern elements on road surfaces, leading to vibrations in the tyre
		Texture impact	800-1250 Hz	impact of road surface texture on the tyre tread, causing vibrations in the tyre
		Running deflection		deflection around tyre circumference when rotating, producing tyre vibrations
	Adhesion mechanism	Stick/slip		tread element movement relative to the road surface, tangential tyre vibrations is caused by frictional forces
		Stick/snap	above 1000-2000 Hz	breaking of adhesive bonds between rubber and road, causing either tangential or radial vibrations
Aerodynamical mechanism	Air turbulence		300 Hz	turbulence around tyre due to the tyre displacing air when rolling on the road and air dragged around by the spinning tyre/rim
	Air pumping		>1000 Hz	air displaced into/out of cavities in or between tyre tread and road surface, without necessarily being in resonance
	Pipe resonances		900-2000 Hz	air displacement in grooves (pipes) in the tyre tread pattern amplified by resonances
	Helmholtz resonance		1000-2500 Hz	air displacement into/out of connected air cavities in the tyre tread pattern and the road surface amplified by resonances
Amplification/reduction mechanisms	The horn effect			tyre leading and trailing edges and the road surface form a structure similar to an exponential horn which amplify the sound
	The acoustical impedance effect			connecting voids in porous surfaces absorb sound near the noise generation source and on the propagation path
	Tyre resonance	Belt resonances	600-1300 Hz	mechanical resonances in the belt
		Torus cavity resonance	230-280 Hz	resonance in the air column of the tyre

2.2.3 Measurement of tyre - road noise

Standardized measurement methods and equipments have been developed for testing the level of noise emission. With these methods, the noise generated from the interaction between the tyre and road surface can either be collected on far field positions, like the road side, or positions close to the source of the noise. Several methods used for measuring the tyre - road noise on road surfaces are presented in this sub-section.

2.2.3.1 Statistical Pass-By method (SPB)

The Statistical Pass-By method involves measuring the noise levels generated by different categories of vehicles (cars, dual-axle heavy vehicles, multi-axle heavy vehicles, etc.) under constant or nearly constant speed conditions. The measurement is performed by using a road side microphone together with simultaneous recordings of vehicle speed and type. Afterwards, noise levels for certain types of vehicle running at certain speeds are achieved from regression analysis with the collected data. According to the International Standardization Organization (ISO) 11819-1 [5], the microphone is placed at 7.5 m from the center of the driving lane. The standard microphone height is 1.2 m. As this height is very sensitive to environmental conditions and unwanted propagation effects, a higher position is preferred by some parties. In the Dutch standard, the microphone height is set at 5.0 m. In the Harmonoise project, a height of 3.5 m was selected [2]. A schematic diagram of the SPB measurement in accordance with the Dutch standard and a picture of the field test set-up are shown in Figure 2-1.

In the measurement process, the A-weighted sound pressure level and the vehicle speed are recorded at each vehicle pass-by. With valid measurements on at least 100 cars and 80 heavy vehicles, a linear regression relationship of the noise level versus the logarithm of speed is calculated for each vehicle category. Based on this relation, the average maximum A-weighted sound pressure level is determined at the reference speed.

The SPB measurement provides a good assessment of the actual traffic noise emission and the influence of the road surface for different vehicle types. It has gained acceptance from professionals all over the world and is widely applied. However, the time consuming measurement procedure and the strict requirements of the test conditions are considered as drawbacks of this method.

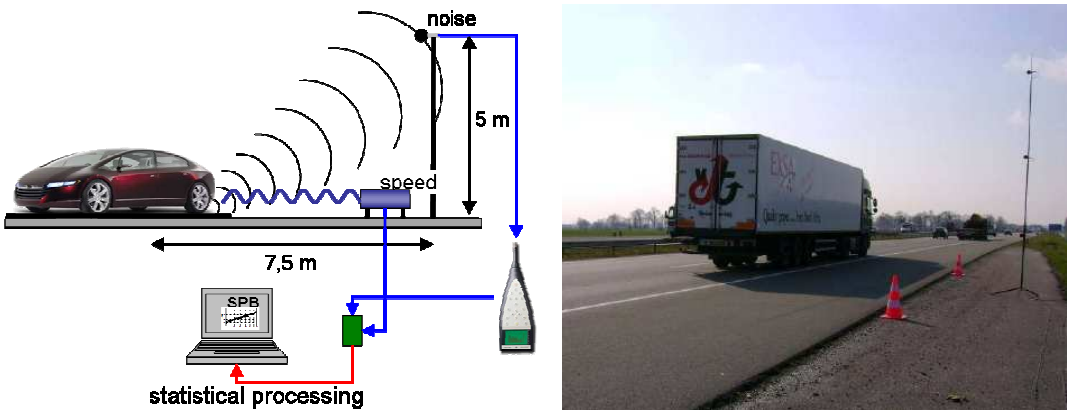

Figure 2-1 Schematic diagram of SPB method and measurement on a Dutch highway

2.2.3.2 The Close-Proximity method (CPX)

The Close Proximity (CPX) method as described in ISO 11819-2 [6] is developed to assess the sound pressure level close to the tyre - road interface. Some pictures of the test are given in Figure 2-2. In the method, rolling noise emitted by two or four standard tyres over a specified distance, together with the vehicle speed are recorded. The data are collected by two microphones located close to the tyres. Positions of the front and rear mandatory microphones are illustrated in Figure 2-2(b). In the specification, four types of standard tyres are involved for the measurement, i.e. Avon ZV1 185/65R15, Avon Enviro CR322 185/65R15, Avon Turbogrip CR65 185/65R15 and Dunlop AP Arctic 185R14, which are simply marked as tyre A, B, C and D respectively. The image of the four standard tyres is illustrated in Figure 2-2 (d). The average noise level determined from tyres A, B, and C has been found to be representative for the interaction of road surface and car tyres, and the results of tyre D, a coarser tread pattern, was observed to correlate well with the surface effect of truck tyres [7].

The test tyres can either be mounted on a trailer, which is towed over the test surface, or can be incorporated in a specially designed vehicle. The test trailer developed by M+P in the Netherlands is shown in Figure 2-2 (c). The measured noise levels are averaged over short distances (20 m segments) and over both the microphones. The rolling noise level at a certain reference speed is the output of CPX test.

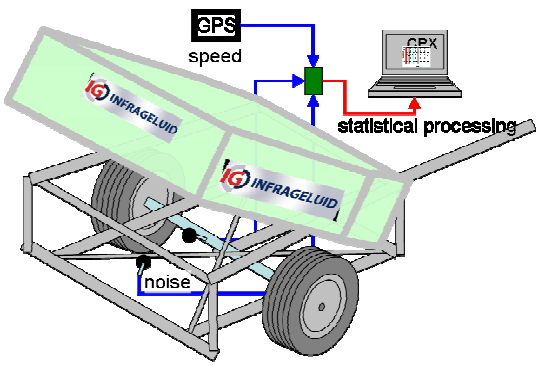

(a) Schematic diagram

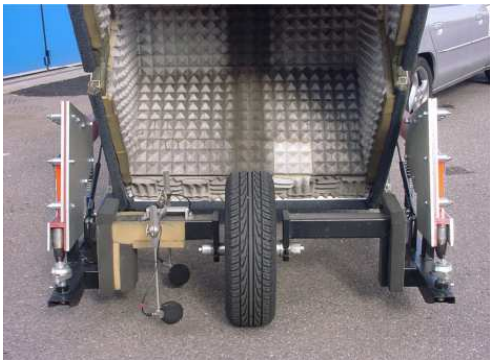

(b) Standard microphone position

(c) Test trailer

(d) Standard tyre types

Figure 2-2 CPX measurement

For better studying the sound power at different positions around the tyre, more microphones are also used. In developing the Acoustic Optimization Tool (AOT) model, 11 microphones were mounted around one test tyre in the CPX measurements performed on the trial sections [8]. The microphones were placed in the horizontal plane of the normal CPX test, and two of them were set at the standard CPX inner positions. Passenger car and truck tyres were both investigated. Photographs of the microphone positions for both the car and truck tyre measurements are given in Figure 2-3. The final noise level is calculated from the integration of noise levels tested with different microphones over a spherical segment [9].

(a) Passenger car tyre

(b) Truck tyre

Figure 2-3 Positions for 11 microphones in CPX measurement by M+P [8]

2.2.3.3 Coast-By method (CB)

The Coast-By (CB) method is standardized in the ISO standard 13325 [10] and is related to the SPB measurement. According to the Coast-By method, four identical test tyres are mounted on the test vehicle. The engine is switched off and the transmission is disengaged before the vehicle drives into the measuring area. During the measurement, the vehicle is only moved by inertia force. In this case, it is assumed that only the tyre - road noise is generated. The noise is measured by two road-side microphones at 7.5 m distance from the central line of the track and at 1.2 m above the road surface.

The maximum sound pressure level in each pass of the test vehicle and the vehicle speed *V* are recorded. The subsequent statistical analysis is the same as that used for the SPB test results. By this type of measurement, the sound level is obtained as generated for a certain combinations of tyre type and road surface.

2.2.3.4 The Controlled Pass-By method (CPB)

The same setups as in SPB are used in the Controlled Pass-By (CPB) method. For the CPB test, a limited number of vehicles are selected and driven at a constant speed passing by the measurement spot. In the national French standard NSF 31-119-2 [11], two standard cars and four standard tyre sets are specified to be used. In the Netherlands, the CPB measurements are performed with 15 or more vehicles which are chosen form a randomly selected population. The European Union (EU) is currently developing standards for the method.

The CPB method takes less time compared with the SPB measurement but does not account for the potential deviations in selecting the vehicle and tyre types. Moreover, traffic closure might be required in order to eliminate the interference of sound from other vehicles when testing on a road with heavy traffic.

From the results of the pass-by measurements, a regression analysis is performed to obtain a linear relationship between $L_{A,max}$ or sound exposure level (SEL) and the logarithm of *V*. This yields the sound level as function of the vehicle speed for each combination of tyre and road surface.

2.2.3.5 The Trailer Coast-By method (TCB)

The Trailer Coast-By (TCB) method is regarded as a combination of CPB and CPX methods and specified in ISO/DIS 13325 [10], Annex B. A trailer on which two tyres are mounted is towed by a low-noise vehicle along the track. For each pass-by, the $L_{A,max}$, the time history of the overall A-weighted *SPL* is measured. Since the time history of the passing tow vehicle is recorded, it is necessary to separate the peak values from the vehicle and the trailer. A long length of the tow bar connecting the vehicle and the trailer is also preferred for minimizing this problem; this tow bar needs to be at least 5 m. The analysis procedure is identical to that of the SPB method. It should be noted that only the sound coming from the tyre - road interaction is recorded in the TCB method.

2.2.3.6 Relationship between different measurement results

From the introduction above, one can conclude that the CPX is a typical method for measuring the near field noise in the tyre - road contact path, and that SPB, CB and CPB methods are generally applied for examining the noise level at the road sides. The CB method can be used for measuring the noise purely from tyre - road interaction, while SPB and CPB methods provide a representative noise level gained from statistics by concerning a number of vehicles. In practice, the CPX, CB and TCB can be used in the cases focusing on tyre - road noise. The SPB and CPB methods give general description on how much noise can be expected by the receiver at the road side.

In existing studies, relationships between far and near field noise levels were also set up by some researchers. In the Silvia (Sustainable road surfaces for traffic noise control) project, relationships between SPB (or CPB) and CPX results are established by linear regression based on multiple surface types and databases [12]. A fairly accurate CPX-SPB (/CPB) relation is observed when data from the same dataset is used. However, the CPX-SPB model is not reproducible between different datasets. Therefore, no generalized equation could be developed to describe this relationship.

In the study carried out by M+P, relationships based on comparison of the SPB and CPX results obtained with various microphone positions for combinations of different surface and tyre types were obtained. Figure 2-4 gives an example of the SPB-CPX relation at speed 80 and 110 km/h. The linear relationship was determined corresponding to specific type of tyre, but the regression coefficients also varied between different combinations of surface and tyre [13].

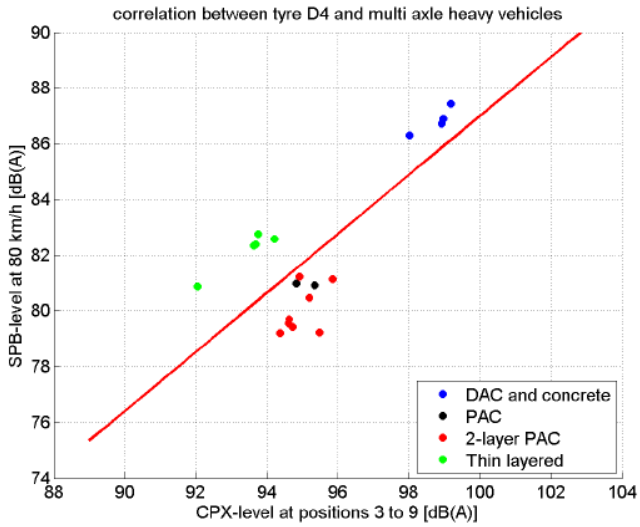

Figure 2-4 SPB-CPX relation between the results for passenger cars (DAC: dense asphalt concrete; PAC: porous asphalt concrete) [13]

2.2.4 Noise reducing surfaces

Noise generated from interaction between tyre and road surface is one of the most significant contributions to traffic noise. Reduction of the noise level from this interface is thus urgently required for abating the harmful influence of traffic noise. Development and application of low noise pavements can be regarded as the most direct way to attenuate the tyre - road noise from the source and it is also the most cost-effective when considering other technologies which are available to road authorities. Low-noise pavements are a cost-effective option to reduce traffic noise. It has been revealed that a low noise asphalt pavement can reduce investments in noise abatement measures by up to 80% compared to noise barriers [15]. Because of this, noise reducing pavements are intensively studied and built all over the world [16].

Up till now, scenarios for developing a low noise road surface have mainly been based on the following experimental findings [17]:

1) surface textures with a wavelength greater than 10 mm tend to increase noise excited by the tyre vibration;
2) surface textures with a wavelength less than 10 mm tend to reduce noise from air pumping;
3) porosity of the pavement helps to reduce aerodynamic effects on noise;
4) a stiffer surface generates a higher noise level than a softer one;
5) a negative texture is much more favorable for noise reduction than positive texture.

Currently, the most effective and commonly used low noise road surfaces are porous asphalt and thin layer surfacings. The third generation silent pavements such as Poro-Elastic Road Surfaces (PERS) and Poll Pave are also under investigation. However, it should be noted that noise is only one of several characteristics of a road surface which are determining the choice of the pavement layers. The overall performance of a road surface also depends on other parameters such as safety, fuel economy and overall cost-life benefits. Considerations of skid resistance, rolling resistance and durability are often more important than noise and will in most cases limit the choice to one or a few categories of road surfacings within which acoustical optimization is possible.

2.2.4.1 Porous asphalt

Porous asphalt is defined as a wearing course with a high stone content (typically 81-85%), the typical grading of which is 0/11, 0/16 or 0/20 with a gap at 2/7, and a high air voids content (usually > 20%). The layer thickness is typically 40-50 mm [18].

In Europe, porous asphalt was developed by the Transport Research Laboratory (TRL) in the UK in the late 1950s for use on airport runways; trials were made on public roads in the 1960s. It has been used on highways since the beginning of the 1980s in a number of countries, such as France, Belgium, Italy and the Netherlands. In the Netherlands, it was regulated as the standard road surface for highways since the end of the 1980s. At present, nearly 90% of the Dutch primary road network has this type of surface layer.

Porous asphalt is generally gap-graded, consisting mainly of coarse aggregates and a small proportion of sand and filler, which are held together by a bituminous binder (in other countries, polymer modified binder is used). This results in a permeable skeleton with a large volume of open and inter-connected voids (20-28% at the time of laying). Sound absorption is thus provided by porous asphalt which is believed to be one of the important characteristics related to noise reduction. Tyre - road noise produced at the source as well as propagating noise can be partly absorbed. Furthermore, the horn effect and the air pumping noise are both virtually eliminated. According to the experience from the Netherlands, the resulting noise reduction at high speeds compared to the reference surfacing

of DAB 0/16 is around 4 dB(A) [2]. In addition, as a result of the high porosity and the good stone quality (micro-texture), porous asphalt provides a good skid resistance and reduces significantly splash and spray in wet conditions.

However, there are problems with the durability of porous surfaces due to the open mix design and rapid aging of the binder. The loss of aggregate from the road surface, called raveling, is the dominating defect influencing service life and the average service life of the slow lane is not more than 11 years, resulting in high maintenance cost. Another problem is clogging of the pores due to dirt and dust, which is the primary cause for a decrease of the acoustical performance of the porous surface in time [19]. The clogging can be investigated by CT-scanning of samples drilled from the road surface or by monitoring the decrease in permeability of cores taken from the field [20]. From an assessment on highways A28 and A17 in the Netherlands, it was found that clogging is more pronounced at the older road surfaces and concentrated between the wheel paths and in the emergency lane. Although the passing of vehicle tyres generates a certain degree of self-cleaning in the wheel tracks of high speed roads, this type of surface requires periodical special cleaning techniques [21]. In most cases, the road surfaces are cleaned by spraying water on the surface and then using vacuum-cleaning. In the procedure, water is pressed into the voids with a pressure of about 60 to 80 bar by means of a spray bar with static or rotating valves. At a short distance behind the spray bar, the water is sucked out from the porous surface by using a vacuum cleaner. Observations show that absorption can be two times more effective for cleaned porous asphalt compared to a clogged surface [22].

2.2.4.2 Two-layer porous asphalt

In order to counter the clogging effect in urban areas, the concept of two-layer porous asphalt (TLPA) was developed. This type of surface is an improvement of the single-layer porous asphalt. The first TLPA trial was made in France and it is well developed in the Netherlands. The first sections with this material have been built in the Netherlands in the beginning of 1990s by the company Hijmans. From then on, about 40 sections were constructed on local and secondary roads. Since mid-1990s, about 20 main trial sections were built on the Dutch highways and in several other European countries. More than 90 sections have also been paved in Japan so far [23].

The TLPA is made up of a bottom layer of porous asphalt with a coarse grading (typically 0/14, 0/16, 11/16) and a thin top layer of fine graded aggregate (typically 4/8, but sometimes 2/4 or 2/6). The typical thickness of the bottom layer is 4 to 5 cm for the bottom layer, and the top layer is 2 to 3 cm for top layer. A schematic figure of single- and two-layer porous asphalt is shown in Figure 2-5. The fine graded upper layer of double layer porous asphalt is claimed to work as a filter for the coarse dirt, while the fine dirt moves downwards and thus prevents/minimises clogging of the layer underneath. A relatively small macro-texture is achieved by using small sized chips in the top layer, which helps to

reduce the noise generation due to the vibration mechanism. The thick bottom layer has a high void content, which works well for absorbing sound waves [24, 25].

Initially, the acoustical performance is excellent: a noise reduction of 4-6 dB (A) for passenger cars at 50 km/h has been observed, and double layer porous asphalt is among the quietest types of road surfacing which are in use.

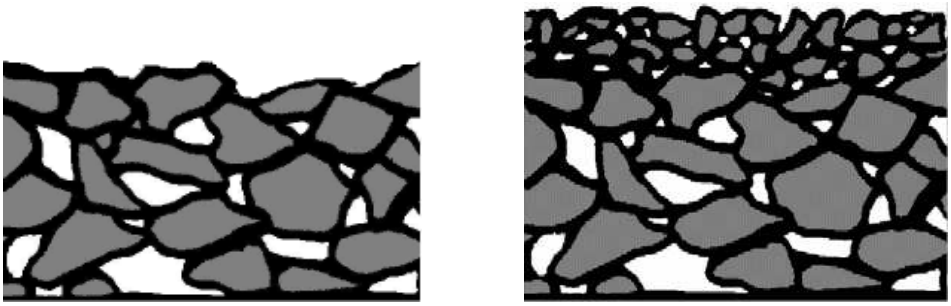

(a) Single layer (b) Double layer

Figure 2-5 The stone skeleton of single and double layer porous asphalt

However, there are also drawbacks of applying two-layer porous asphalt. It is more sensitive to raveling compared with conventional pavements, and thus the technical lifetime is relatively short as with single layer porous asphalt. And, unfortunately, the voids of the surface also tend to be clogged, which results in the deterioration of acoustical properties and hence a shorter functional lifetime.

2.2.4.3 Thin layer surfacing

Thin layers are commonly used as a silent surface in the Netherlands and quite some other European countries at present. It is a single top layer with a thickness varying between 20 and 40 mm, with 25 mm is considered as a typical thickness. Thin layers were introduced and came into wide application as wearing courses in the beginning of the 1990's in France and some other European countries. Around 2000, the noise reduction property of the surface was noticed. The tyre - road noise is mainly reduced by two features:

1) small maximum size aggregates are used in order to increase the smoothness of the road surface and reduce the noise generated by tyre vibration;
2) an open surface structure is created by relatively high air voids content aiming for absorbing sound waves.

In order to fulfill these requirements, the thin layers were optimised by using small maximum aggregates sizes (6-8 mm), and an open and smooth surface is created. In Japan, a thin layer with 5 mm maximum aggregate size was produced and utilized. In the test sections of Kloosterzande in the Netherland, a 4 mm maximum aggregate size layer was also paved and investigated. According to different levels of air voids, thin layer surfacing are classified into 4 groups [26, 27]:

1) dense layers (air voids <9%);
2) semi-dense (air voids 9%-14%);
3) semi-open (air voids 14%-19%);
4) open layers (air voids >19%), they are also known as porous thin layers.

Most of the thin layer surfacings are gap-graded and rely on interaction of the stone fraction for stability and a relatively high content of bituminous mortar in the voids for durability. It is claimed that this mixture type combines both the acoustical performance of porous asphalt and the durability of normal SMA. The fine surface texture of thin layer surfacings helps to prevent the tyre tread vibration, while the air voids absorb sound waves. In this way, the tyre - road noise is considered to be reduced. It should also be noted that there is a large risk of raveling/stripping with semi-open or open types of thin layer surfacings.

According to French studies, the noise reduction of thin layers is between 0 and 3 dB (A) with respect to their reference surface dense asphalt concrete [28]. Another investigation was made in France on a thin layer surfacing (stone size 0/6 mm, air voids content 20 to 25%) during a period eight years. It was found that the SPB level was 1 dB lower than for a dense surface in the first year. But then it reached and exceeded the noise level from the dense surface after one year [29]. The Dutch Noise Innovation Program (IPG) reports a reduction of 4 up to 7 dB (A) for porous thin layers and 3 up to 5 dB (A) for the semi-dense type mixtures in comparison with the reference surface DAC 0/16 [26]. They are also considered in the frame of the IPG as a valuable alternative (reasonable costs for construction and maintenance, same durability as TLPA and quite good acoustical properties) for two-layer porous asphalt, the quietest road surface so far. In the IPG program, thin layer surfacings for medium speed roads are studied. Results obtained from more than 100 sections of the Dutch secondary road network are analyzed. For light vehicles driving at 80 km/h, the average initial noise reduction for both the semi-dense type and porous type thin layer surfacing turned out to be 5.1 dB (A), which is much more than the 2.6 dB (A) reduction from single PAC. In the Danish study of thin quiet SMA surfacings in urban areas, noise reductions achieved from different mixtures are from 1 dB to 4.3 dB. The most significant noise reduction is obtained by adding 10% of oversized (8 mm) aggregate in the size of 8mm into SMA with a maximum grain size of 6 mm. In this way the openness of the surface structure increases.

Due to the limited layer thickness, clogging does not play a significant role because of the self-cleaning effect of traffic for this type of surface. Similar to SMA, the surface texture becomes larger with trafficking as fine aggregates surrounding the coarse ones are gradually swept away by the rolling vehicle tyres. Like porous asphalt, the thin layer surfacings are not laid in roundabouts. The durability is about 6 to 8 years depending on the porosity and the noise reduction compares to or exceeds that of PAC.

2.2.4.4 Third generation low-noise road surfaces

(1) PERS

Since 1993, the Japanese Public Works Research Institute (PWRI) has been developing a new type of low-noise pavement named "Porous Elastic Road Surface" (PERS). It has a porous structure composed of granular rubber made from recycled tyres as aggregate and poly-urethane (PUR) resin as binder. The porosity of this type of surface is approximately 40 percent (generally at least 20% by volume). The thickness is 3 to 4 cm. The PERS can either be produced on site or prefabricated as carpet, and it is to be glued with epoxy resin onto the underlying sub layer [30-32]. Figure 2-6 shows an illustration of this type of surface.

PERS generally shows high noise reductions, typically 10 up to 12 dB (A). However, problems arise in terms of insufficient binding to the hard asphalt sub layer, damage by snow ploughs and low skid resistance [33].

The PERS was also tested in the IPG program. The material used was designed by Japanese and supplied as prefabricated panels (1m x 1m and 30 mm thick). Three test sections with different mixture compositions were laid. The initial noise reduction from these surfaces was 6.9 dB(A) relative to DAC 0/16 for passenger cars at a speed of 100 km/h. Temperature is affecting the stiffness of the panel and the width of individual joints between the panels, as a 2 dB(A) difference was found between the measurements in spring and autumn in 2007 [8].

Figure 2-6 PERS and its application [34]

(2) Roll Pave

Roll Pave is a rollable porous surface that was invented and developed by the company Dura Vermeer-Intron in the Netherlands. The layer is made by mixing

polyurethane resin, rubber and quartz. The air voids content is around 30%. It is prefabricated in the factory and the slab has a length of 50-60 m with a width of 3.5 m. The thickness is 30 mm. For transportation, each pave is rolled onto a drum which is transported to the site. During construction, the rubber surface is unrolled. A special type of glue is sprayed between the Roll Pave and the underlying asphalt layer surface. Then a roller is used to flatten the mat and glue the Roll Pave glued on the underlying surface. Figure 2-7 shows the transportation and paving of this surface a test trial at a parking site alongside the A50 in the Netherlands.

The expected noise reduction of the surface is 8 dB(A). On the basis of the measured initial noise reduction from the test section on the A50, the noise reduction at 100 km/h for light vehicles was extrapolated from the data and found to be 6 dB(A) relative to a DAC16 reference surface. The durability and the mechanical properties of this type of surface still need to be investigated and improved [34].

Figure 2-7 Transportation and laying of the Roll Pave

2.2.5 Modeling of tyre - road noise

Developing a quiet road surface turns out to be an effective way for decreasing the noise at the source. Therefore noise reducing surfaces, such as porous surfaces, gap graded thin overlays, and rubber modified asphalt, receive much interest and are commonly built all over the world. As a result, there is an increasing demand for an optimization criterion for balancing durability and noise reduction. Tyre - road noise models, part of the typical traffic noise prediction models, provide information of noise generation before the road is constructed. They play an important role in quantifying the tyre - road noise, optimizing the pavement design and improving the materials and building technology. Figure 2-8 shows the function of a tyre - road noise model in surface layer design optimization and construction technique improvement [35].

Tyre - road noise models are classified into three categories: statistical models, physical models and hybrid models. Statistical models generally characterize the relationship between noise level and the influencing parameters by means of regression equations. Physical models concentrate on specific noise production

mechanisms. Hybrid models combine both the statistical and physical elements in the framework. The structure is complicated but it gives an overall simulation of the emission and propagation of tyre - road noise.

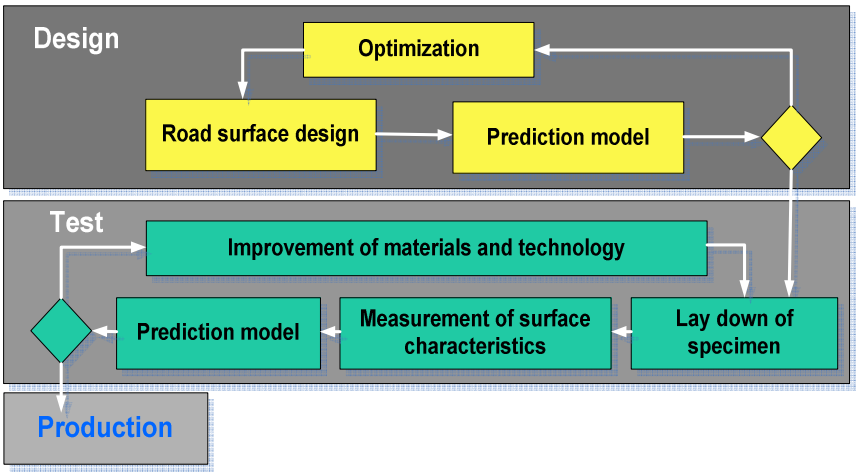

Figure 2-8 Prediction model function in road surface design and test [35]

2.2.5.1 Statistical model

Sandberg and Descornet were the first to relate surface texture to noise emission using regression techniques. The model was suggested for investigating the influence of road surfaces on average noise emission levels and is written as follow [1]:

$$CRNL_C = 0.5L_{80} - 0.25L_5 - a(2-T) - b\ln(\Omega h) + 67 \quad (2\text{-}4)$$

where

$CRNL_C$– combined pass by road noise level for cars, dB;

L_{80} – texture level in the octave band with center at 80 mm texture wavelength, dB, in relation to the ref. level of 10^{-6} m;

L_5 – as above, but for a wavelength of 5 mm;

T – age of the surface in years;

a – constant, which is 0.8 for 0<T<2, 0 for T≥2, and 0 for all surfaces with MPD >1.0 mm;

Ω – air void content, % by volume;

h – thickness of layer, mm;

b – constant, which is 0 for $\Omega h \leq 4.5$, 4.7 for $4.5 < \Omega h < 20$ and 7 for $\Omega h \geq 20$.

The noise prediction model developed by Klein and Hamet gives a relationship between road texture properties and noise levels, and an excess attenuation was introduced to take the acoustic absorption into account [36]. The specific expression of the model is shown in Section 2.3.1.4.

The statistical regression method was also employed in developing the interaction model in the hybrid model AOT [9]. This statistical part links the predicted force which applied on the road by the tyre with the predicted sound

pressure level. The assumption is that the overall tyre - road noise is the linear superposition of different sound sources. The contribution of each individual source to the total sound power can be described as:

$$P_{total}^2 = P_{vibration}^2 + P_{airflow}^2 + P_{cavity}^2 \quad (2\text{-}5)$$

where $P_{vibration}$, $P_{airflow}$ and P_{cavity} are respectively the sound power from tyre vibration, from airflow related mechanisms and from the radiation from interior resonances of the cavity between tyre structure and rim cavity. These three items can all be determined by means of regression models. The explanatory variables used in the regression include: the pre-calculated contact forces from a physical model, the air flow resistance, the tyre width, tread stiffness and driving speed of the vehicle.

2.2.5.2 Physical model

Physical models simulate the mechanical processes in tyre road interaction and sound radiation. In the mid-1980s, the tyre - road noise modeling focused on tyre vibration was started by Kropp [4]. The model simulates a smooth tyre rolling over a rough surface with constant speed. It is composed of three modules, namely a tyre model, a contact model and a radiation model. The model was refined and further developed by Prof. Kropp and Chalmers University. The latest work takes into account the adhesion mechanisms, stick-slip mechanisms and aero-acoustic mechanisms (e.g. Helmholtz resonance) etc.

In the Chalmers model, the structure-borne sound behaviour of a tyre is described by a double-layered isotropic plate, as shown in Figure 2-9. Two elastic layers with different thicknesses and material properties are coupled together. The bottom layer models the stiff belt, while the top layer stands for the soft rubber surface. An elastic bedding which supports the layers in all three directions simulates the effect of air pressure inside the tyre and the sidewalls stiffness. Deformation at any discrete point in the solid can be achieved by solving the general field equations. A 12 × 12 global matrix containing expressions of displacements and stresses is assembled to describe the layer coupling [37].

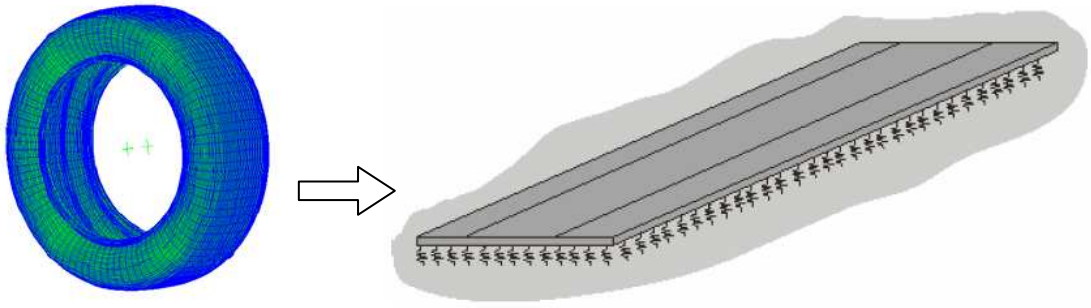

Figure 2-9 Simplified plate model for the unfolded tyre [37]

D.J. O'Boy and A.P. Dowling developed a method to predict the noise produced by a patterned tyre rolling on a rough road surface by using a tyre belt model

composed of multiple viscoelastic layers [38, 39]. The response of a cylinder with infinite length of the belt material is deduced. Then the boundary conditions were specified and this equivalent bending plate could be used to represent the belt in a finite width tyre model to predict the sound as the tyre rolls on a rough road. The viscoelastic cylindrical model used in the work is illustrated in Figure 2-10.

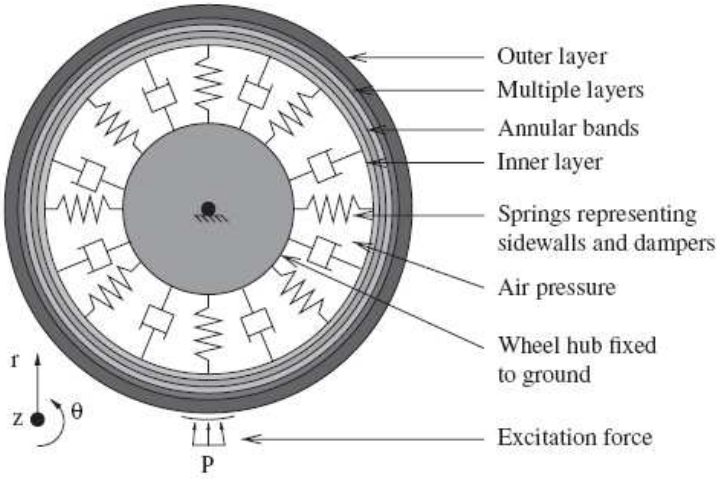

Figure 2-10 The multi-layer viscoelastic cylindrical model of the tyre belt [38]

For the physical models, the tyre properties are generally indispensable for learning the sound emission from the tyre - road contact. Representative parameters are required for simulating the dynamic behaviour of tyres in global models, such as the orthotropic plate model, circular ring model, etc. These tyre related parameters include:

1) the mass per unit area of the tyre structure;
2) bedding stiffness, in radial, circumferential and lateral direction;
3) tension, which depends on the inflation pressure in the tyre;
4) as to the curvature of the tyre, the influence is omitted by existing models though it leads to deviation in the low frequency range (i.e. below 400 Hz). For the higher frequency range (above 400 Hz), the influence is not important.

2.2.5.3 Hybrid model

(1) SPERoN and AOT

SPERoN is an acronym for Statistical Physical Explanation of Rolling Noise. It is a hybrid tyre - road interaction model for predicting rolling noise. The first version was developed by M+P and Müller-BBM which aimed to describe the noise induced by the road texture [40]. The Acoustic Optimization Tool (AOT) is a comprehensive model developed from the SPERoN model v2.0 framework. In the latest version, extensions were made on the following aspects:

- inclusion of tangential forces and adhesion effects;
- prediction of near-field and far-field noise level at different receiver heights, i.e. 1.2 m, 3 m and 5m;
- truck tyre consideration;
- mechanical impedance of poro-elastic surfaces.

The framework of the SPERoN model is shown in Figure 2-11. It consists of one physical sub-model, namely the contact model and two statistical models, i.e. the tyre - road interaction model and the sound propagation model. The contact model is a physical simulation of contact between the rolling tyre and the pavement. The interacting force in the contact surface can be derived from this part. The interaction model provides insight into the contributions of different mechanisms on the tyre - road noise emission. In the current version of AOT, mechanisms considered are vibration, air pumping and tyre cavity. The propagation model is used for describing the transfer of the sound from the source to the receiver positions near the tyre and in far field.

When running AOT simulations, the surface texture, acoustical impedance and flow resistance are required as inputs. The mechanical impedance is an optional input.

The output of the model is the prediction of total noise level and the noise level spectra for the following receiver positions:

$L_{A,eq}$ levels at the CPX inner positions, as an average over the front and rear microphones;
$L_{A,max}$ levels at the SPB positions at 7.5 m from the road lane center, at three heights: 1.2 m, 3.0 m and 5.0 m.

Besides, the contribution of various noise generation mechanisms, including vibration, airflow and cavity noise can also be displayed in the form of the noise spectra and the global noise level.

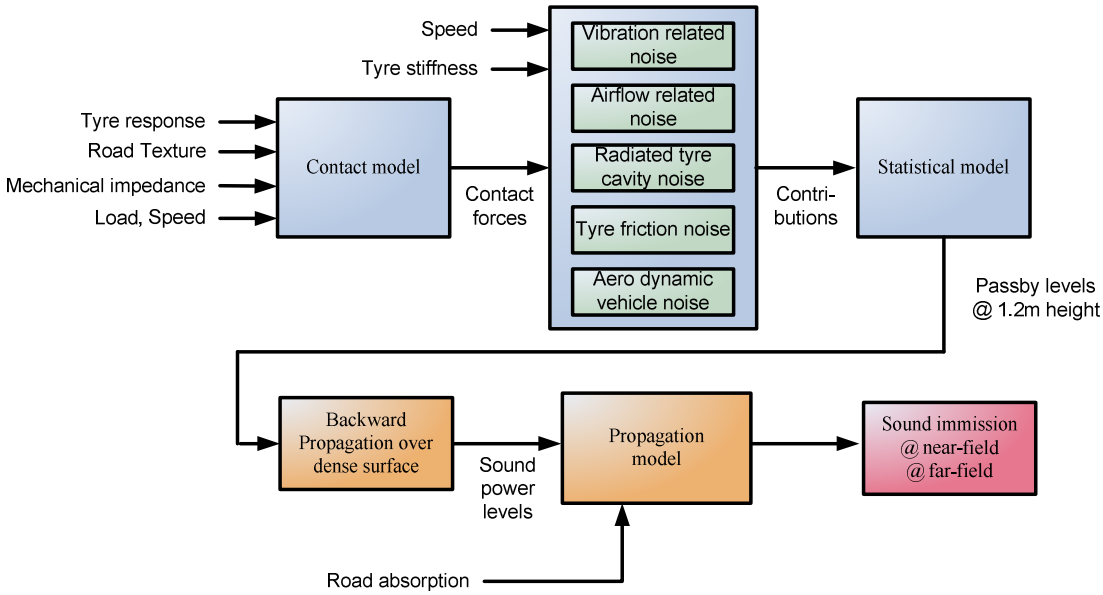

Figure 2-11 Schematic overview of the SPERoN framework [9]

The AOT is considered one of the best commercially available software packages for predicting tyre - road noise, as the commonly used surface types are all

included in the model and influences of different surface parameters are combined. However, the mixture compositions of the road surface are not used as input variables of the model. Predictions need to be made by giving the measured surface characteristics, such as surface profile, sound absorption. This limits the application of the model for guiding the road surface mixture design.

(2) TRIAS

The TRIAS model (Tyre Road Interaction Acoustic Simulation) is a comprehensive mathematical simulation model developed by TNO in the Netherlands. The model attempts to simulate the excitation and radiation of tyre - road noise based on all relevant aspects from tyre and road properties [41].

A schematic overview of the TRIAS model is given in Figure 2-12. In this model, the central component is the interaction rolling model which calculates the tyre vibration caused by road roughness. Both the road surface characteristics and the tyre parameters are needed as input. When no measurement result is available, the input properties of the road can be deduced from road construction parameters by a sub-model, namely, ROad Design Acoustic Simulation (RODAS). On the other hand, the TYre Design Acoustic Simulation (TYDAS) is used for generating the tyre properties from basic data on materials and construction of the tyre. The framework is comprised of the following modules:

- Interaction rolling model: this calculates the displacement caused by the vibration of the tyre which is excited by the road roughness in the contact area.

- Air pumping model: this determines the noise radiation caused by changes in the volume of the air in the grooves of tyre tread and porous spaces of the road surface.

- Vibration model: this model is used for calculating the sound radiation due to tyre vibrations.

- Source transmission model: this model consists of semi-empirical transfer functions for horn effect, directivity and road reflection.

- The situation transmission model: this takes into account effects on the sound levels at the receiver due to absorption or reflection of the roadside material, the vehicle configuration and the observer location.

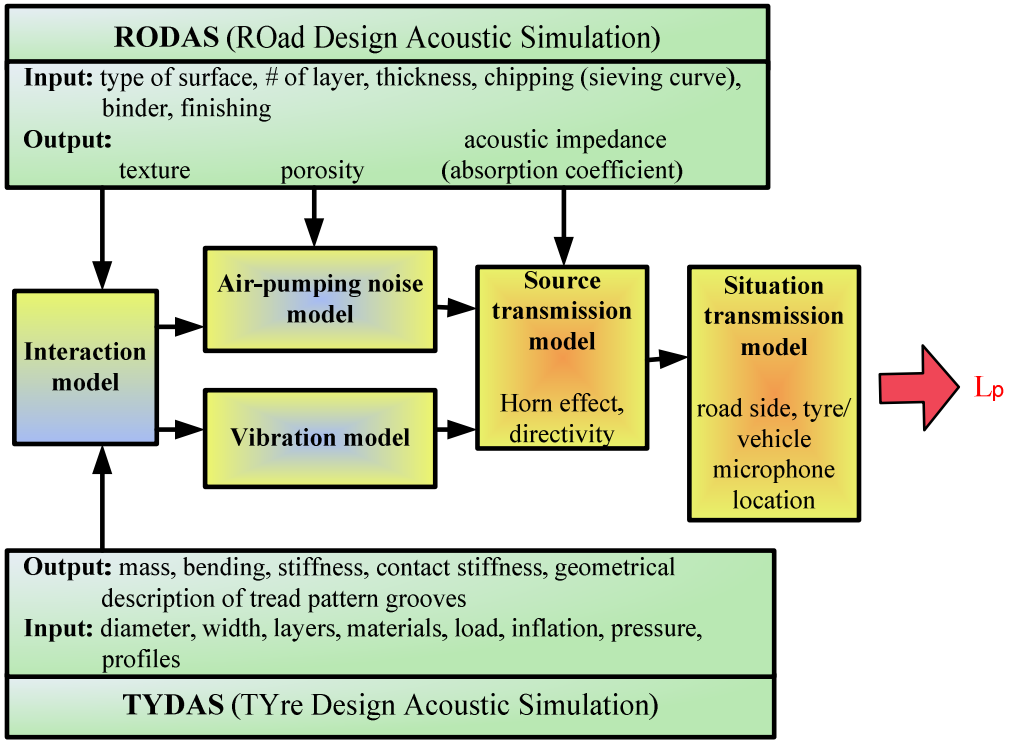

Figure 2-12 Schematic overview of the TRIAS model

2.3 Road Surface Characteristics

2.3.1 Surface texture

2.3.1.1 Introduction

Pavement texture is defined as the deviation of a pavement surface from a planar surface. Based on the wavelength of the irregularities, the road surface texture can be divided into three ranges [42]:
1) < 0.5 mm micro-texture;
2) 0.5-50 mm macro-texture;
3) 50-500 mm mega-texture.

Road surface characteristics in wavelength between 0.5 m-50 m are referred to as unevenness.

The micro-texture is generally produced by the sharpness and harshness of the individual chippings or other particles. It is important for safety but does not play a significant role in tyre - road noise generation. According to a report by the ISO, the macro- and megatexture have a substantial effect on the noise production. As the influences of these two ranges of texture are interrelated, the two characteristics together are called “texture” in the following chapters.

Research by Sandberg and Descornet has shown that increasing texture amplitudes at wavelengths in the range of 0.5 to 10 mm reduces noise generation particularly at high frequencies above 1 kHz [43]. This high frequency range

response is attributed to the air-pumping or air-resonant mechanism, which is associated with the small asperities in the surface. On the contrary, increasing the texture at wavelengths between 10 and 500 mm was observed to cause the noise level to increase at frequencies below 1 kHz. The mechanism is believed to be the impact of road chippings on the tyre tread or the impact of the tyre tread elements on road surface. The frequency where the correlation changes of sign (from positive to negative, and vise versa) is called the crossover frequency and appears to be around 1000 Hz for passenger car tyres and 500 Hz for truck tyres. Moreover, the relation between texture and noise level found in the low and high frequency ranges, respectively, are not associated with each other.

2.3.1.2 Measurement of surface texture

For characterization of the road surface texture, the Mean Profile Depth (MPD), the Estimated Texture Depth (ETD) and the effective root mean square value (RMS) are commonly employed. Determination of these parameters from the measured texture profile is shown in Figure 2-13.

In addition, a texture profile spectrum in third-octave bands is also useful to characterize the surface texture. This spectrum shows the texture profile level (in dB relative to a reference amplitude) along the spatial frequency. In accordance with ISO/DIS 13473-2 [44], the texture profile level is expressed by:

$$TL_i = 20 \cdot \lg(a_i / a_{ref}) \tag{2-6}$$

where:

TL_i – texture profile level (dB ref. 10^{-6} m),
a_i – root mean square value (m),
a_{ref} – reference root mean square value ($a_{ref}=10^{-6}=1\mu m$),
i – subscript indicating a value obtained with a certain filter.

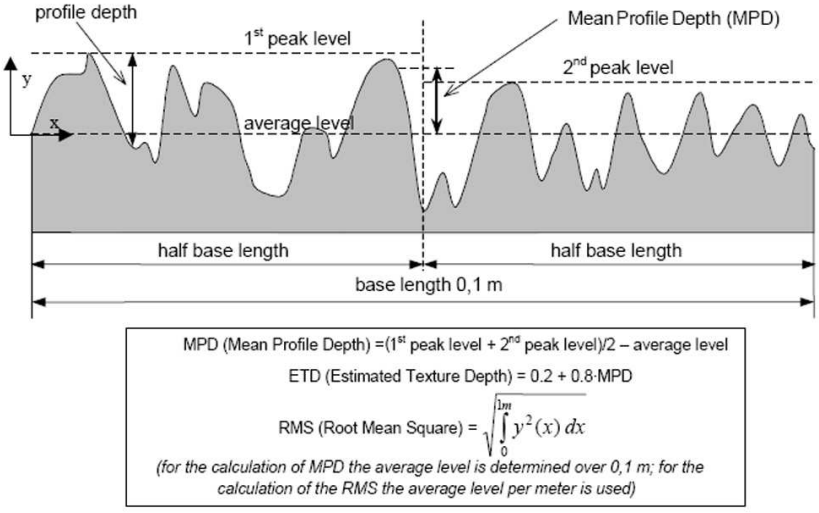

Figure 2-13 Illustration of the terms measuring the surface texture

The classification of texture levels based on the wavelength is shown in Figure 2-14 [44]. The influences of texture levels with different wavelengths are also given in the figure. In the ISO standard, the octave bands with the center wavelengths of 4 and 63 mm are chosen as the representative adjacent third octave band center wavelengths. Thus texture levels at octave band 4 mm and 63 mm are considered to be predictors of tyre - road characteristics in the high (1000 Hz and above) and low (below 1000 Hz) frequency range respectively.

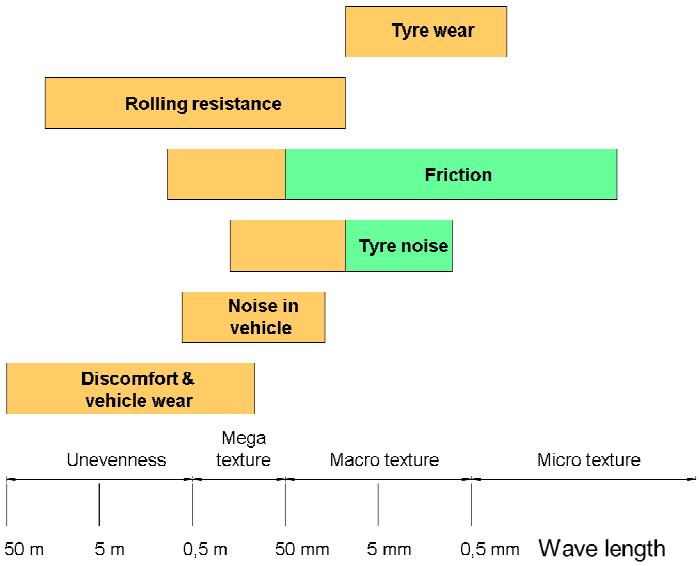

Figure 2-14 Ranges in terms of texture wavelength and the influences of texture and unevenness

The ways in which the textures are formed can differ in vertical direction though the values could be identical on a texture spectrum basis. Therefore, two other concepts are introduced to describe the difference: positive texture, which is formed by particles or ridges protruding above the plane of the surface, and negative texture, which is composed of voids below the plane of the road surface. A positive texture is generally provided by various types of surface dressings or special surfaces such as hot rolled asphalt, while a negative texture is often found in porous asphalt and thin surface materials. The positive texture is considered more aggressive to excite the vibration in the rolling tyre and makes the surface noisier than the negative one.

2.3.1.3 Texture simulation

The texture of the surface is determined by various factors such as aggregate size, gradation, grain shape, binder content, porosity, compaction method, etc. However, in the literature, no evidence or methods have been found to estimate the texture profile considering all these parameters. It seems only be possible to estimate texture from these factors.

Texture simulation as developed in the TRIAS model is one of the attempts to realize this [45]. In this model, the aggregate size is assumed to follow a log-normal distribution. The granular form (top half of a grain) can be described by a

half-sinus, a rectangle or a triangle, and the height of the texture varies randomly up to the value of the maximum grain size. The peaks of the granules are positioned randomly with respect to the horizontal surface up to a certain maximum altitude. The gaps between the stones are decided by the density of the mixture and the porosity. For DAC and SMA, the gaps are filled up to a fixed distance from the highest peaks. For porous asphalt, the gaps caused by the porosity are randomly deepened to the maximum aggregate size. This simulation progress is involved in the sub-model RODAS of TRIAS. The texture profile and the spectrum can thus be deduced from the given mixture properties.

In another research program of TNO in the Netherlands, the road surface texture was simulated using a 2-D (3-D in a later version) model [46, 47]. In the model, the road surface texture is described as a 2-D auto-regressive (AR) filtered white noise sequence. It is a completely mathematical simulation of the texture, and it is not related to the mixture compositions of the surface layer. This artificial surface has similar properties as a real road surface.

2.3.1.4 Modeling the influence of texture

(1) Envelopment of the texture

As mentioned in section 4.3.1.2, there are two texture forms, the positive and the negative texture, corresponding to the ridges and valleys in the measured profile respectively. Surfaces with an identical texture spectrum could result in different tyre - road noise levels due to different effect of the ridges and the valleys. In a porous layer where negative texture is dominant, it is believed that the depth of the valley has no influence on the tyre vibration when it is beyond a certain critical value. Predictions which are solely based on raw texture levels thus provide wrong results on these surfaces.

One feasible way to solve this problem is to envelope the road profile before calculating the spectrum. Von Meier et al. proposed an empirical procedure which is based on the mathematical limitation of the second-order derivative of the discrete texture sample [48]. A physical simulation was developed by Clapp to evaluate the distance of the elastic medium (tyre tread) penetrated by the rigid road profile [49]. The algorithm is executed by iterative balancing the road surface reaction force and the tyre inflation pressure.

The texture envelopment method, as a choice for optimizing the tyre - road noise simulation, has already been employed in several models, such as former versions of SPERoN [40], the INRETS (National institute for transport and safety research of France) model [50] and HyRoNE model. Figure 2-15 shows the enveloped profiles for three types of road surfaces achieved by the INRETS model. According to their study, the envelopment procedure substantially improves the texture and noise correlations as compared to the measured texture in the low and medium frequency range [51]. As an application in HyRoNE model, the enveloped texture is taken into account in the frequency range below 1250 Hz, where the vibration mechanism is considered dominant.

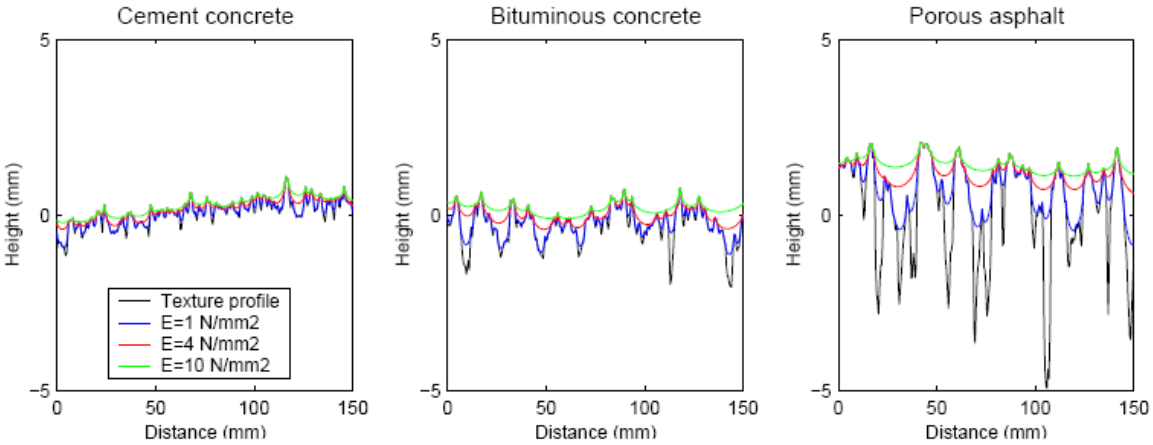

Figure 2-15 Enveloped profiles for three road pavements and different Young's modulus of the rubber body [50]

(2) Statistical model

The representative texture parameters, such as MPD and texture spectrum level are sometimes directly used as predictors in a statistical model. These simple structure models based on several representative parameters are also highly preferred by engineers.

1) Descornet and Sandberg suggested that the road noise level can be described reasonably by a linear combination of the texture levels with two representative wavelengths. The expression is as follows [1]:

$$ERNL = a \cdot TL_{80} - b \cdot TL_5 + c \quad [dB(A)] \tag{2-7}$$

where:

$ERNL$ – estimated Road Noise Level, dB;

TL_{80} – texture level in the octave band with centre at 80 mm texture wavelength, in relation to the ref. level of 10^{-6} m rms;

TL_5 – as above, but for a wavelength of 5 mm;

The constants used were: a=0.50; b=0.25; c=60 and are based on measurement results.

The model is an empirical one and has no relation with the physical properties of the tyre involved. The main purpose of the formula is to display the influence of the road surface texture and not to give typical noise emission levels.

2) HyRoNE

The Hybrid Rolling Noise Estimation (HyRoNE) model aims at predicting the pass-by noise level from the surface texture and the acoustical characteristics of the impervious or porous road surface [36]. It estimates the 1/3 octave noise levels L_i at frequencies f_i from raw or enveloped texture levels TL_i and $TL_i^{(e)}$ at wavelengths λ_i. The calculation scheme is shown in Figure 2-16. The enveloped texture levels are used in the low and medium frequency range, while raw texture levels are adopted in the high frequency range, where the noise is mainly caused by the aerodynamical mechanisms. The enveloped texture profile is obtained by

using the INRETS envelopment procedure. Pass-by noise levels without absorption are generated by linear statistical formulas.

The effective frequency range of HyRoNE is from 100 Hz to 5000 Hz. L_i is given by the following linear expressions:

$$L_i = a_i + b_i TL_i^{(e)} + \Delta L_i^{(p)} \qquad \text{for} \quad f_i \le 1250 \text{ Hz} \tag{2-8a}$$

$$L_i = a_i + b_i TL_i + \Delta L_i^{(p)} \qquad \text{for} \quad f_i > 1250 \text{ Hz} \tag{2-8b}$$

where a_i and b_i are the coefficients of the linear regression, $\Delta L_i^{(p)}$ is the excess attenuation caused by the sound absorption of the road surface.

The global level $L^{(T)}$ simulated by the HyRoNE model is written as

$$L^{(T)} = 10 \log \sum_i 10^{L_i/10} \tag{2-9}$$

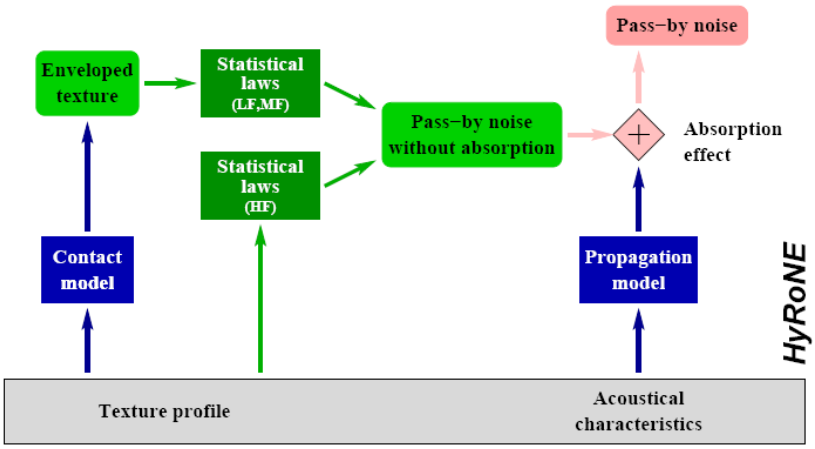

Figure 2-16 Framework of HyRoNE Model (LF: low frequency; MF: medium frequency; HF: high frequency)

3) Model in the Silvia project

In the Silvia project, a study was carried out to relate the pass-by noise level with the surface texture level. The correlation coefficients between the texture level and noise level were evaluated. The highest correlations were found between texture levels and noise levels at the same frequency band f_i [51]. Thus the regressions were performed only between the texture levels and noise levels at the same frequency band f_i.

The Expected pass-by Noise level Difference (END_T) is provided by the relationship:

$$\text{For a porous surface, } END_T = 10 \log \frac{\sum_i 10^{(L_i + b_i \cdot L_i^{(eT)})/10}}{\sum_i 10^{L_i/10}} \tag{2-10a}$$

For a dense surface, $END_T = 10\log\frac{\sum_i 10^{(L_i + b_i \cdot \Delta L_i^{(eT)})/10}}{\sum_i 10^{L_i/10}} - 0.25\Delta L_{5mm}^{(T)}$ (2-10b)

where

L_i – 1/3rd octave noise level measured at the frequency band f_i, dB;

$\Delta L_i^{(eT)}$ – the 1/3rd octave enveloped texture level difference between the enveloped texture measured in practice and the enveloped texture measured at the conformity of production (COP), dB

b_i – coefficient calculated for each 1/3rd band below 1 kHz; it equals 0 above 1kHz.

The coefficient b_i is found to be highly dependent on the rolling speed. For the dense surface where air pumping occurs, the texture level difference in the 5 mm wavelength octave band is added (see also Eq.(2-7)) [52].

4) Japan

Fujikawa from the Japan Automobile Research Institute, has studied the modeling tyre - road noise reduction related to road surface parameters since 2004 [53]. In his model, the noise level in each octave band is approximated by the tyre vibration noise and the air pumping noise, and is described as a function of surface unevenness and *MPD* [54]:

$$\left(\frac{P^2}{P_0^2}\right)_{500} = 53300000 h_d N^* + 168200000$$

$$\left(\frac{P^2}{P_0^2}\right)_{1k} = 23300000 h_d N^* + 145800000$$

$$\left(\frac{P^2}{P_0^2}\right)_{2k} = 238000000 h_d N^* - 4090000000 MPD + 2878000000 \quad (2\text{-}11)$$

where $P^2/P_0^2 = 10^{Lp/10}$, P is the sound pressure, P_0 is 2×10^5 Pa and L_p is the measured sound pressure level. $h_d N^*$ represents the total asperity height unevenness in the frequency range from 355 Hz to 1.41 kHz, where

$$h_d N^* = h_{d500} N_{500} + h_{d1k} N_{1k} \quad (2\text{-}12)$$

where h_{d500} and h_{d1k} are the average height unevenness in the frequency bands of 500 Hz and 1 kHz, respectively. N_{500} and N_{1k} are the numbers of asperities in the frequency bands of 500 Hz and 1 kHz, respectively.

(3) Physical model

In a physical model, the road surface profile is generally included in the contact model which aims to calculate the contact force between the tyre and road surface. As the physical models reflect the actual state of the tyre - road contact,

the surface profile parameters required are not the derived ones, such as MPD or texture levels, but the real surface roughness of the road.

According to the physical model built up by Kropp, as shown in Figure 2-9, the force at any point in the contact surface is determined by the stiffness of the bedding and its compression. The compression of the spring $\Delta y(\varphi, t)$, at the angle φ is a function of the centre of the rim $y_0(t)$, the curvature $k_2(\varphi)$ of the tyre, the vibration $\xi(\varphi, t)$ of the tyre belt and the roughness $k_1(\varphi, t)$ of the road [9].

$$\Delta y(\varphi,t) = y_0(t) + k_1(\varphi,t) + \xi(\varphi,t) - k_2(\varphi) \tag{2-13}$$

The contact force is then:

$$F(\varphi,t) = s_1 \Delta y(\varphi,t) H[-\Delta y(\varphi,t)] \tag{2-14}$$

with s_1 the stiffness of tyre tread, $H[x]$ is the Heaviside step function.

2.3.1.5 Measurement

The volumetric patch method and the profilometer method are generally used with regard to road surface measurements.

The volumetric patch method, commonly called the sand patch method, is a manual way to determine the Mean Texture Depth (MTD). A given volume of the sand is spread out on the road surface and the MTD is calculated from the measured radius of the sand area. The method is standardized in ISO 10844 [55] and ASTM E965 [56].

In the profilometer measurement, the texture profile as function of the position is recorded by scanning the road surface with a certain type of sensor. The measured texture profiles can then be transferred into a spectrum by means of a Fast Fourier Transformation (FFT), and the indexes MPD, ETD and RMS can also be generated to quantify the road surface. Profilometers are considered to be of two types depending on whether the sensor contacts the surface or not. Due to the type of the sensor, 4 principles of operation are listed in the ISO standard, namely the laser, light sectioning, stylus and the ultrasonic profilometer. The device can either be mounted on a vehicle or be used in stationary setups such as a beam [44, 57-59].

2.3.2 Sound absorption

On porous roads, sound energy can be absorbed by the road surface due to its porosity. Sound waves enter the upper layer of the road surface and are partly reflected and partly absorbed. Absorbed means that sound energy is transformed into another kind of energy. In road surfaces, this is mainly due to two effects: 1) by viscous losses, as the pressure wave pumps air in and out of the cavities in the road; 2) by thermal elastic damping. The absorption efficiency of a material varies with frequency and with the angle at which the sound wave impinges upon the material.

2.3.2.1 Evaluation of sound absorption

The absorption coefficient α is a commonly used parameter showing of the efficiency of a surface or material in absorbing sound. It is a frequency dependent parameter and basically defines the ratio of the energy lost in the reflection process to the energy incident on the surface. If 55 percent of the incident sound energy is absorbed, the absorption coefficient is said to be 0.55. A typical absorption coefficient curve is described by two parameters: (1) α_{max}, which is the value of the first maximum on the measured absorption curve; (2) $f_{\alpha,max}$, the frequency at which the first maximum absorption coefficient occurs.

Another measure that describes the reflection and absorption of the sound field impinging on the surface is the acoustical impedance (Z_n). Mathematically, it is the ratio of sound pressure P to the sound particle velocity U at the reference plane. This term is related to (but not equal to) the acoustic absorption of the road surface.

$$Z_n = P / U \tag{2-15}$$

2.3.2.2 Parameters influencing absorption

The following parameters are influencing the sound absorption of a road surface [1]:

1) the porosity (residual air void content) Ω: the percentage of connected air cavities;
2) the air flow resistivity (airflow resistance per unit length) R_s:

It is a measure of how easily air can enter a porous layer and the resistance that air flow encounters through a structure. Flow resistivity relates to the inverse of permeability, high flow resistivity implies low permeability. Considering a steady flow of air passing through a porous layer, the flow resistivity is defined as the ratio of static pressure drop ΔP to a volume flow U over a small sample length h:

$$R_s = \frac{\Delta P}{Uh} \ [\mathrm{Ns/m^4}] \tag{2-16}$$

For most granular or fibrous sound absorbing materials, it is difficult to predict the flow resistivity analytically; it has to be measured. For a few idealized absorbing materials, such as stack of identical spheres, it is possible to make a prediction. In terms of a road surface, the air flow resistivity is considered to be dependent on the porosity and the aggregate grading by the relation $R_s = a/(\Omega^n d_s^2)$, with a is a constant, Ω air voids content and d_s maximum size of the aggregate.

If the material is considered as homogeneous, with cross-sectional area S and thickness h, the flow resistivity is [60]:

$$R_s = RS / h \tag{2-17}$$

where R is the airflow resistance, which can be measured directly following the method described in ISO 9053 .

3) thickness of the layer;

4) tortuosity q^2 (or "shape factor" as it is sometimes called):

It is a measure of the shape of the air void passages. This is a somewhat artificial parameter describing the influence of the internal structure of the material on the acoustic behaviour. The more complex the path, the more time a wave is in contact with the pore structure. The parameter can be estimated from the porosity Ω of the sample with the following equation [61]:

$$q^2 = 1 - a(1 - 1/\Omega), \quad 0 < a < 1 \tag{2-18}$$

where a is a coefficient.

It is interpreted as the inverse of the formation factor used in studying of gas diffusion in porous materials [62], given by:

$$q^2 = \Omega^{-n'} \tag{2-19}$$

where n' is the grain shape factor.

This parameter is in some cases, i.e. in phenomenological models, also expressed by a structure factor [63].

In general, the air void content affects the value and frequency spectral bandwidth of the absorption coefficient, the air flow resistance influences the peak value, and the absorption peak frequency is determined by the layer thickness and the tortuosity.

2.3.2.3 Acoustic models

Since mid-1980, considerable work has been carried out for modeling the acoustical properties of porous surfacings. Two basic approaches developed by European researchers are the phenomenological approach and the microstructural approach. In the model, pores are assumed to be present in a rigid body. In both models, the sound absorption coefficient can be derived from the specific impedance Z_c and the complex wavenumber k.

For a surface with thickness h and a dense bottom layer, the surface impedance Z_n is given by [64, 65]:

$$Z_n = Z_c \coth(-ikh) \tag{2-20}$$

The plane-wave reflection coefficient R_p for porous asphalt can be expressed as:

$$R_p = (Z_n \sin\varphi - \chi)/(Z_n \sin\varphi + \chi) \tag{2-21}$$

with

$$\chi = \left[1 - (k_0/k)^2 \cos^2\varphi\right]^{1/2} \tag{2-22}$$

where

φ – grazing angle of the sound wave, it is considered to be 90º in this study;

k_0 $-2\pi f/c_0$, with f the frequency and c_0 the sound speed in the air, which equals to 343.2 m/s.

The absorption coefficient can be derived from the reflection coefficient by:

$$\alpha = 1 - \left| R_p \right|^2 \tag{2-23}$$

It can be seen that the Z_c and k need to be calculated for modeling the sound absorption of the porous material. The two modeling methods, namely phenomenological and the microstructural approach, can be treated as two different ways to determine Z_c and k.

(1) The phenomenological model

The phenomenological approach considers the porous medium as a globally compressive fluid where dissipations occur. In the model developed by Hamet and Bérengier [63], both the viscous dissipation which is due to velocity gradient and the thermal dissipation caused by thermal gradients in the medium are introduced. This has particular implications for materials with a very low flow resistance, like porous surfaces. Three parameters of the porous structure, including content of air-filled connected pores, tortuosity and flow resistivity need to be provided for presenting the specific impedance Z_c and the complex wave number k [60, 66].

(2) The microstructural model

Microstructural models have been set up by different researchers for describing the propagation of acoustic waves through porous materials. In the model of Champoux and Stinson [65], and two shape factors are introduced separately to describe the viscous and thermal effects in addition to the porosity, tortuosity and flow resistivity. There are different expressions of the model for describing pores with various shapes, such as slit-like pores, cylindrical pores, etc. As the acoustical properties of pavements are relatively insensitive to these two shape factors, they are not taken into account in most applications modeling the road surface. In a previous study, the microstructural model was introduced for modeling the sound propagation through two layer porous asphalt [67]. This method is also used in this thesis for modeling the sound absorption of thin layer surfacings. Specific expressions of the microstructural model can also be seen in Section 5.4.3.

(3) RODAS

In the RODAS module of the hybrid model TRIAS, the acoustical impedance is also determined from basic theory of sound absorption [68]. Taking the surface of the absorbing layer as a rigid frame, the impedance for sound incidence angle φ_o to normal on the surface $Z'(\varphi_o)$ can be calculated when the practical porosity,

flow resistance and the structure factor are known. Correspondingly, the absorption coefficient at the angle φ_o, $\alpha(\varphi_o)$, is derived from:

$$\alpha(\varphi_o) = 1 - \left| \frac{Z'(\varphi_o)\cos\varphi_o - 1}{Z'(\varphi_o)\cos\varphi_o + 1} \right|^2 \quad (2\text{-}24)$$

(4) Multi-layered perforated panel model

The multi-layered perforated panel model is normally used for modeling the sound absorption of an absorbing layer built from components with a regular shape. However, when the medium is simplified into a stack of sphere aggregates, this method could be applicable for materials with irregular shaped pores, such as porous concrete. Kim and Lee did research on predicting the sound absorption of porous concrete based on the multi-layered perforated panel model [69]. The scheme of stacked sphere aggregates and the transferred multi-layered model are shown in Figure 2-17. Theories mentioned here are from the publications of Lu [70] and Maa [71]. The acoustic impedance of the system is mainly determined by the size of the aperture in the panel, which is related to the gradation and shape of the aggregates, thickness of the layer and the target air voids content. In the current studies, the approach is still not yet used in simulating the acoustic properties of porous asphalt.

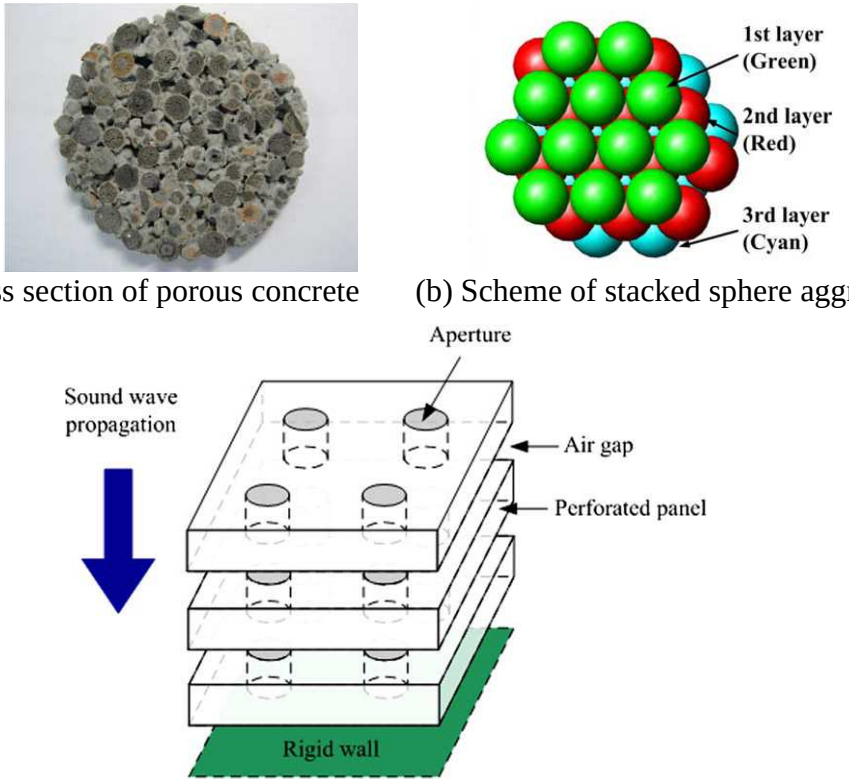

(a) Cross section of porous concrete (b) Scheme of stacked sphere aggregates

(c) Multi-layered perforated panel model

Figure 2-17 Multi-layered perforated panel model of porous concrete [69]

It should be noticed that all these acoustic models mentioned above are built based on a simplified structure of the porous asphalt layer. The structure contains

well connected pores. However, this is only the case when the surface is newly paved. After being used for a certain period of time, the air voids tend to be clogged, and correspondingly there are changes in porosity, flow resistivity, tortuosity and the resulting sound absorption. Therefore, a time related compensation should be considered for the continuous prediction during service life of the sound absorption by these acoustic models. Moreover, the commonly used semi-dense thin layer surfacing, with air voids content around 12% and less connected pores compared to porous asphalt, cannot be regarded as an absolute porous structure. Correction is also needed when using these acoustic models for simulating the sound absorption property of such thin layer surfacings.

2.3.2.4 Effect of sound absorption on noise reduction

Another effect of sound absorption on noise attenuation is the reduction of horn amplification in the space between the curved tyre tread and the road surface. It also works effectively to eliminate of sound waves reflected from the road surface.

In a recent study, the relationship between the sound absorption performance of porous asphalt and the noise reduction was investigated by M+P [9]. Several conclusions were drawn from the experimental observations: the maximum noise reduction due to road surface absorption occurs at frequencies around the maximum absorption coefficient. However, frequency shifts are observed between the absorption and noise reduction curves. Generally, the sound absorption under normal incidence at a certain frequency (e.g. $f_{\alpha,max}$ = 800 Hz) is found at a higher frequency (around 900 to 1000 Hz) in the attenuation curve of the propagation measurements. Sound absorption is more effective in the frequency range between 800 and 1600 Hz, where the horn effect is significant.

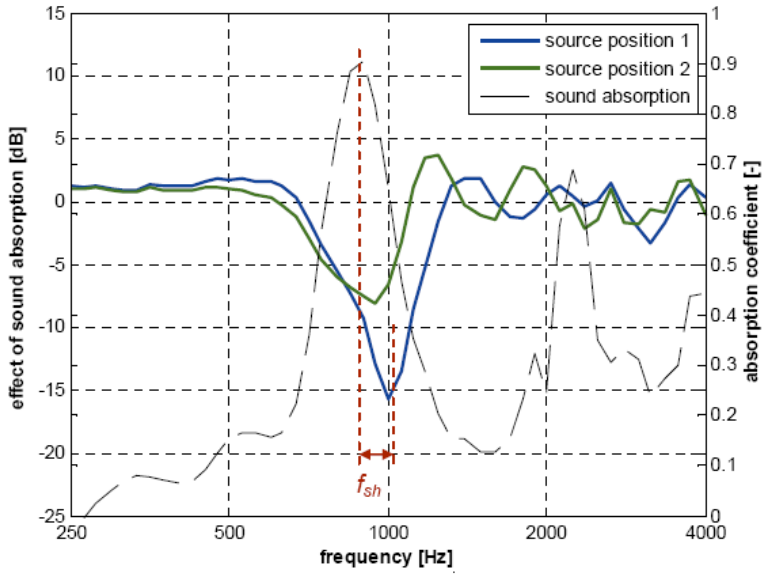

Figure 2-18 Sound absorption effect on noise reduction; the noise measurements were taken on a 50 mm thickness two-layer porous asphalt and at two source positions on the tyre [9]

2.3.2.5 Modeling the absorption effect on tyre - road noise

As the sound absorption of road surface acts on both the noise radiation and propagation, absorption models take into account these two aspects. Considering the peak shift in the frequency spectrum between the absorption and the noise reduction curve, a model was proposed by Hamet in the Silvia project [72], which relates the reduction of propagating noise to the absorption coefficient α:

$$\Delta L_p(f) = A \cdot \alpha\left(\frac{f}{f_{sh}}\right) \tag{2-25}$$

where f_{sh} is the frequency shift factor, and A denotes the amplification factor. Both factors can be determined from the measurement results obtained from far field tests. If the microphone is located at 5 m height for pass-by measurements, no frequency shifting is necessary, i.e. f_{sh} =1.

A single number, called the Expected pass-by Noise level Reduction from sound absorption of the road surface (ENR_α), was proposed in the Silvia project. It is calculated as follow [73]:

$$END_\alpha = 10\log\frac{\sum_i 10^{(L_i-\Delta L_i)/10}}{\sum_i 10^{L_i/10}} \tag{2-26}$$

with L_i is the reference noise level at frequency band f_i.

In AOT a modified version of Hamet's model is used to take into account the horn effect [9]:

$$\Delta L_{i,j}(f) = A_{i,j} \cdot H_{horn,i}(f) \cdot \alpha\left(\left(\frac{f}{f_{sh,i}}\right)\right) \tag{2-27}$$

where $H_{horn,i}$ describes the influence of the horn effect at frequency band f_i.
In the hybrid model HyRoNE, Klein and Hamet introduced an excess attenuation caused by acoustic absorption to correct the pass-by noise prediction [36]. It only addresses the absorption influence in noise propagation, but does not consider the horn effect.

2.3.2.6 Measurement

Absorption coefficients of the road surface can be measured either in-situ or on cores in the laboratory. The result of the measurement is the sound absorption as a function of the frequency.

(1) Measurement on cores

The measurement is performed according to ISO 10534-1 [74], by using the standing wave impedance tube and the two microphone impedance tube. The rationale is shown in Figure 2-19. In a measurement, the core sample is mounted at one end of a straight, rigid, smooth impedance tube. The incident plane sound wave is generated by the loudspeaker at the other end of the tube. At each

frequency, the minimum and maximum pressure of the sound pressure amplitudes are recorded, and then they are used for calculating the sound absorption coefficient at this frequency.

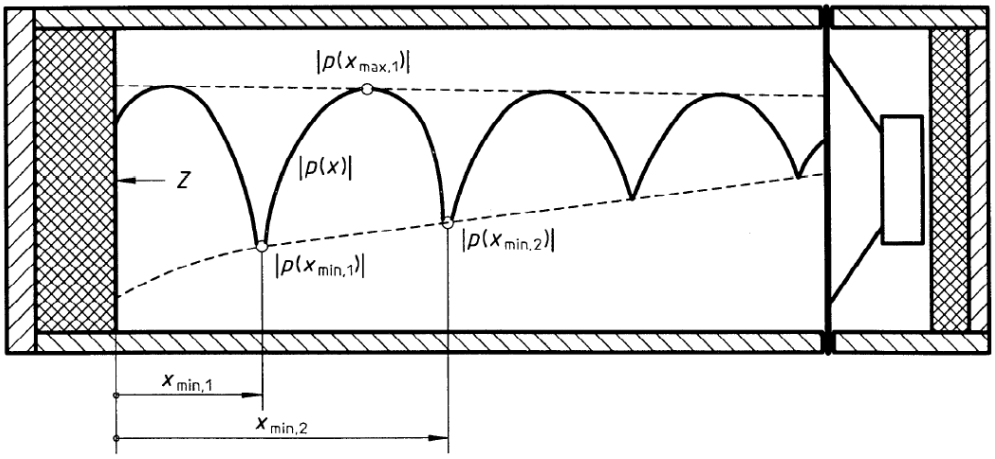

Figure 2-19 Sound absorption measurement in an impedance tube

For both methods described in the standards, the upper frequency f_u is limited to frequencies where only plane waves can propagate in the impedance tube. This frequency f_u is proportional to the inverse of the tube diameter: $f_u<0.586c_0/d$, where c_0 is the speed of sound (m/s), d is the diameter (m). Upper frequency limits are in the order of 4 kHz (with a 5cm diameter tube).

(2) In-situ measurement

In-situ measurements are preferred since no core has to be taken from the road surface. A commonly used approach is the Extended Surface Method (ESM) specified in ISO 13472-1 [74].

The schematic of the ESM measurement system is shown in Figure 2-20. The microphone which is located between the sound source and the test surface measures the sound signal from the source. The signal contains both the direct and reflected sound. With suitable time domain processing (e.g. signal subtraction techniques), these signals can be separated and transferred into the frequency domain by Fourier transformation. The frequency dependent absorption coefficient is then achieved from the transfer functions.

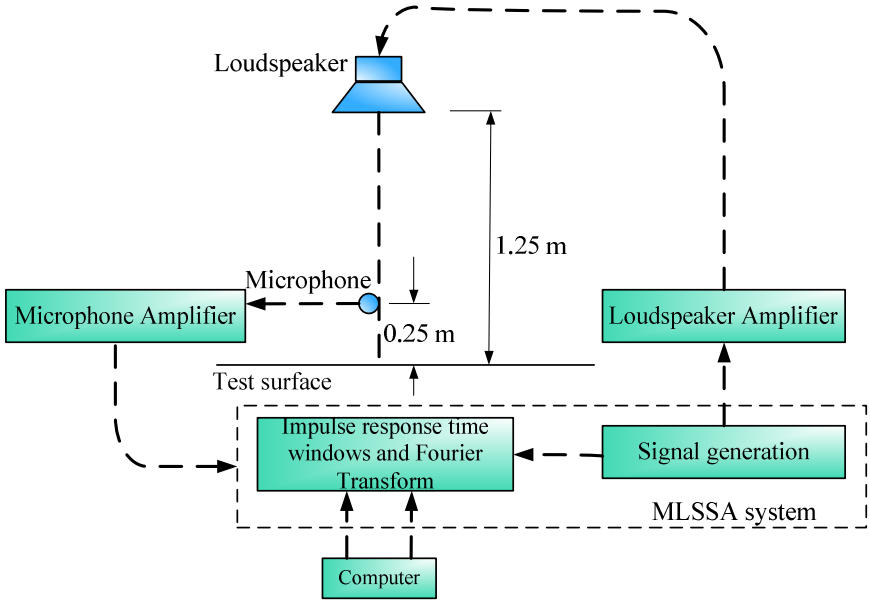

Figure 2-20 Extended surface measurement system (MLSSA= Maximum-Length-Sequence System Analyzer)

The EMS is widely examined and applied for in-situ porous surface absorption measurements, and the results show a good repeatability, reproducibility [75], and are in agreement with predictions by physical models.

A mobile system, known as MIRIAD (Mobile Inspection of Road surfaces: In-situ Absorption Determination), was developed by TRL to enable tests to be done under traffic [76]. The system comprises an experimental mobile measurement rig and a towing vehicle, as shown in Figure 2-21. Studies have shown that a reliable test can be performed at a speed up to 30 km/h.

The sealed tube method is also used for absorption measurements in the field. The equipment and procedure are similar to the impedance tube measurement stated in ISO 10534-1. The only difference is that one end of the tube is open and sealed onto the surface to be tested.

Figure 2-21 Mobile MIRIAD system, developed by TRL [76]

(3) Measurement by P-U technology

A new type of sound absorption (or surface impedance) measurement is based on measuring the sound pressure (P) and particle velocity (U) at the surface [77]. A device based on this P-U technology is developed by the company Microflown Technologies in the Netherlands. Free field measurement can be performed. The main advantages compared to other methods, is that it is not required to core a sample and it shows a low susceptibility to background noise. In some of the previous studies, the surface impedance method was applied to test the road surface impedance in a laboratory as well as outdoors on practical road surfaces. In the in-situ measurement on porous asphalt, high sound absorption coefficients were measured around 1 kHz, which also confirms the noise reduction effect of this type of surface [78].

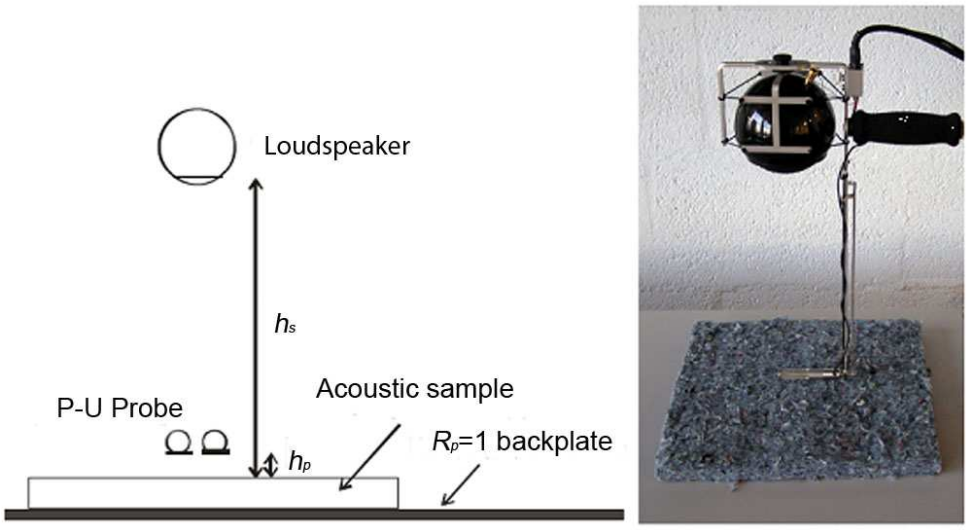

Figure 2-22 Microflown impedance setup and the schema

For field measurements, the setup was mounted behind a driving car and it was possible to measure the surface acoustic impedance in the 300 Hz-10 kHz bandwidth, at a speed up to 40 km/h. However, at a speed of 80 km/h the sensor signal is affected by wind and the vibration caused by the road surface [79]. As it is a newly developed technology, there is no standard for using the setup on a road surface. In this research, this device is extensively used. The achievements from the research will be important for standardizing and applying the P-U technology for measuring on road surface in the field and on samples in the lab.

2.3.3 Mechanical impedance

2.3.3.1 Introduction

The mechanical impedance is a measure of the ability of a structure to resist motion when subjected to a given force [80]. It is defined as the ratio of the driving force acting on the system to the resulting displacement velocity of the system:

$$Z = \frac{F}{v} \tag{2-28}$$

where F is the complex force vector and v the complex velocity vector. The reciprocal of the mechanical impedance, which is defined as point mobility, is also a physical property related to the elasticity of a road surface.

For decades it was assumed that the impedance has no influence on tyre - road noise production since the impedance of the conventional road surface is much higher than that of the tyre rubber. However, an increasing number of researchers believe that mechanical impedance could explain the difference between asphalt and concrete roads with comparable texture.

In an earlier experiment undertaken by M+P, coast-by noise measurements were taken on a concrete surface and on an elastic layer glued on the same type of concrete surface. The similar texture was achieved by gluing the same sanding paper on both the surfaces. A substantial noise reduction was found in the 800 to 1600 Hz frequency range by adding the elastic layer. The test result is shown in Figure 2-23.

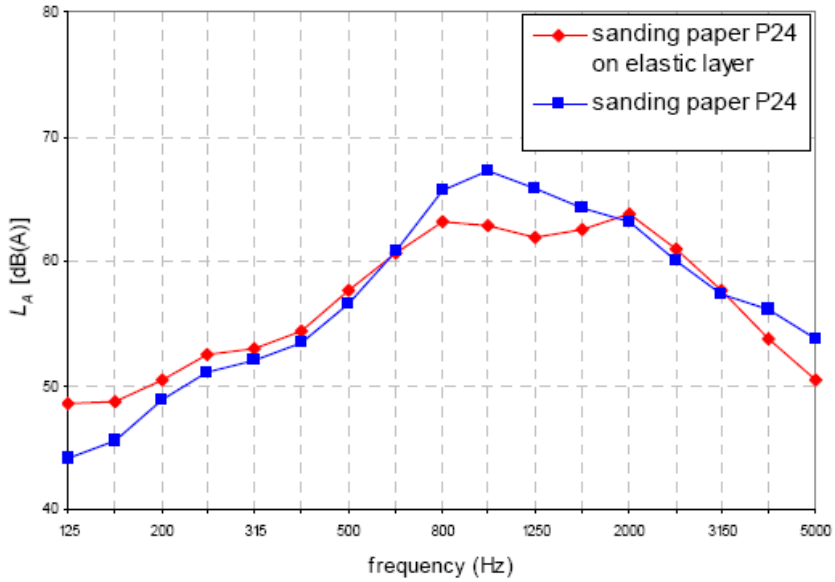

Figure 2-23 Maximum coast-by noise level at 80 km/h for elastic and rigid surface

Meanwhile, Japanese experiments showed that the differences in stiffness of various rubber-based surfaces did not influence noise emission as much as it was expected and the softest surface was not even the most silent surface. However, it is still expected that soft surfaces may perform better against clogging [2]. Hence, the mechanical impedance is proposed to be an important design parameter for new experimental road surfaces.

2.3.3.2 Modeling the effect of the mechanical impedance of the road surface

In most existing tyre - road noise models, the dynamic properties (e.g. mechanical impedance, dynamic stiffness) of the road surface are not taken into

account. It was introduced in AOT as an input parameter when considering poroelastic surfaces [9]. In the contact sub-model of AOT, the force in each position *m* on the tyre tread is given by:

$$F_m = s_{nom} \psi p_m K_t(\Delta\xi) \tag{2-29}$$

where s_{norm} is a standard stiffness value for a slick tyre (reference value), ψ a correction factor for the hardness of the tyre, p_m a function taking into account the stiffness variation of the tread due to the pattern and K_t the roughness caused stiffness variation (i.e. different area in contact as function of the road roughness indenting the tyre). When the road stiffness is similar or even smaller than the tread stiffness, both the tread and the road surface contribute to the total stiffness, which thus can be considered as a system of two springs in series.

$$s_{nom} = \frac{s_1 s_2}{s_1 + s_2} \tag{2-30}$$

with s_1 the stiffness of tread and s_2 the stiffness of the road.

2.3.3.3 Measurement methods

Because the mechanical impedance is a newly considered influential parameter on tyre - road noise, there is no existing standard method to determine this parameter. Generally speaking, it can be measured by applying an impact to the road surface and recording the response of the material in terms of its vibration. Several researchers have made efforts for developing a measurement method.

1) Laboratoire Central des Ponts et Chaussées (LCPC) developed a trailer prototype, called COLIBRI, to measure the mechanical impedance of road surfaces. It consists of a trailer, a measurement beam supporting three accelerometers and a hammer for producing the impact; the device is shown in Figure 2-24. The distances between the hammer and the accelerometers are 10, 35 and 95 cm respectively. Instead of the impedance at the driving point, the transfer impedance is measured by this prototype.

Figure 2-24 COLIBRI in action during the Silvia Round Robin test of 2003 [81].

2) A device developed by Nilsson and Sylwan [81] is based upon a classic impedance hammer, which is called the "matched impedance head". In the setup, the force and acceleration transducer are mounted in-line.

Figure 2-25 Impedance head developed by Nilsson and Sylwan [81]

3) An in situ method was explored by M+P based on the work of Nilsson et al. The device consists of an aluminum ground plate with a diameter of 40 mm and a height of 10 mm. A force sensor is mounted on the top of this ground plate. The housing for the accelerometer on its turn is attached to the force sensor. When the system is impacted by the hammer striking on the housing, the force and acceleration are measured. The resonance frequency of the whole system is above 2500 Hz, which is beyond the range that noise reduction due to mechanical impedance is observed, i.e. 630 to 1600 Hz.

Figure 2-26 Measurement device for mechanical impedance [81]

4) In the development of the SPERoN model a device to measure the driving point mechanical impedance on road samples in the laboratory is designed by M+P [82]. Figure 2-27 gives an overview of the measurement setup. A shaker is used to impact the road surface sample and a so-called impedance head measures the input force and driving point vibration simultaneously. The shaker is placed upside down in springs, so as to avoid unwanted vibrations of the measured surface. The impedance head is connected rigidly to the shaker and excited with a sinusoidal force using a frequency sweep. Since both the input (force) and the output (acceleration) are measured with the impedance head, the results are

independent of the exact force amplitude and of the configurations of the system above the impedance head.

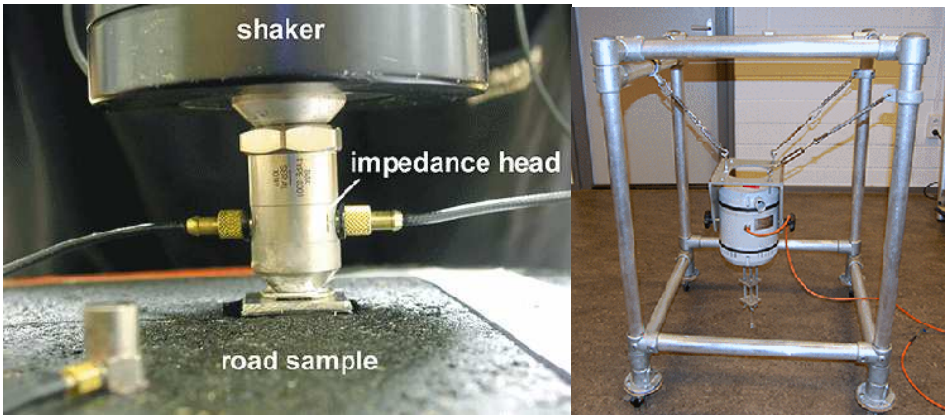

Figure 2-27 Measurement setup for mechanical impedance measurements [82]

2.4 Other Influencing Parameters

2.4.1 Age

Characteristics of road surface changes with the time of service, and this leads to changes of the noise level from the tyre and road interaction. Ageing influences the following phenomena:

The mega- and macro-texture change as particles and other material are worn away. The mega- and macro-texture, as well as stiffness, are changing due to the pavement deterioration and post compaction caused by traffic. The micro-texture is also changing due to the polishing effect of numerous tyres passing over the surface (studs on tyres may counteract this effect, however).

The chemical effects from the weather, accelerated by road salt, create a weathering and crumbling of the surface (loss of fine material), and both micro-texture and macro-texture could be affected.

Normally, surfaces like DAC and SMA exhibit an increased noise level with time for their first 1-2 years in service. For porous surfaces, air voids become clogged with accumulated dirt and raveling occurs which is creating a rougher texture, and the initially smooth-rolled top part of the pavement will deteriorate. This is an ongoing process, and sometimes noise reduction properties are lost very rapidly.

Models related to influence of on age on noise reduction:

Sanberg suggested an age influencing parameter which can be used for estimating the overall tyre - road noise generation [1]:

$$AGEL = -a(2 - TA) \tag{2-31}$$

where:
TA – age of the surface in years;
AGEL – age-reduced level, dB(A);
a – constant.

2.4.2 Temperature

It was realized in the 1980's that the temperature effect is substantial for exterior tyre - road noise emission. The influence of temperature is important for the measurements. For good repeatability and reproducibility, it requires either measurement in a rather narrow temperature interval or some type of temperature correction needs to be applied.

With more refined prediction methods for road traffic noise now being developed, the increased demand for accuracy means that the temperature influence can no longer be ignored, particularly when establishing the basic emission levels and when conducting validation studies.

It has already been recognized that a temperature increase results in a decrease of the tyre – road noise levels. In most studies, the relationship between sound level and temperature are assumed as:

$$L_p = -bT + a \tag{2-32}$$

where:
T – temperature, °C;
a, *b* – constants.

The slope *b* is called the temperature coefficient. A negative sign means decreasing noise with increasing temperature [1].

In the EU Directive on tyre noise (2001/43/EC), a road temperature correction for passenger car tyres is shown in Figure 2-28. The coefficients achieved are -0.06 dB(A)/°C and -0.03 dB(A)/°C when the road surface temperature is below and above 20 °C respectively.

A problem for investigating the influence of the temperature on noise emission is that the standard deviation of the measurement is probably close to the temperature effect. It means that the temperature effect could be difficult to distinguish from the normal random variations. Therefore, a semi-generic procedure is suggested to be employed to reduce the tyre - road noise deviation by categorizing the tyre - road combinations into different groups and assigning separate temperature coefficient for each group [83].

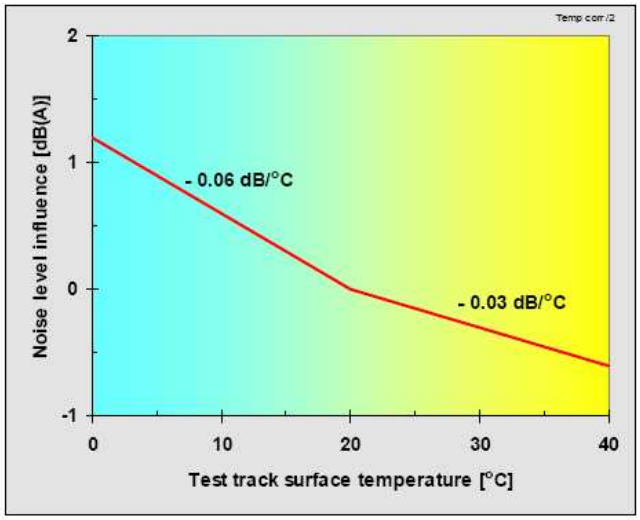

Figure 2-28 The noise-temperature relationship used for car tyres in the EU tyre noise directive 2001/43/EC [83]

A study in the Netherlands took into account a large set of tyre and road combinations, including truck tyres [84]. Both the air temperature and the road surface temperature are included in the regression model together with the speed of the car. The reference temperature is 20°C:

$$\begin{aligned} L_{A,\max} &= a_{air}(T_{air}-20)+b10\log(V/V_{ref})+c, \\ L_{A,\max} &= a_{road}(T_{road}-20)+b10\log(V/V_{ref})+c, \\ L_{A,\max} &= 0.5a_{air\&road}[(T_{air}-20)+0.7(T_{road}-20)]+b10\log(V/V_{ref})+c. \end{aligned} \quad (2\text{-}33)$$

Air temperature coefficient values a_{air} between -0.04 and -0.13 dB/ °C were obtained on two dense asphalt road surfaces. Lower values were obtained for a porous asphalt surface (between -0.02 and -0.07 dB/ °C). The coefficient of determination R^2 for the regression showed that there was no statistical improvement by using T_{road}, or a combination of T_{road} and T_{air} in comparison with using T_{air} only.

On the noise spectrum, the influence of temperature was mainly found at high frequencies. The relation between tyre stiffness and temperature was also studied. Nearly all tyres display the same trend: when the temperature increases, the tyre tread stiffness decreases.

In the study of Anfosso-Lédée, the tyre temperature is also introduced in the model [85]. The statistical relationship between the noise and temperature is given as follows:

$$\begin{aligned} L_{A90}(T) &= a(T_{air}-20)+L_{A90}(20) \\ L_{A90}(T) &= a(T_{road}-20)+L_{A90}(20) \\ L_{A90}(T) &= a(T_{tyre}-20)+L_{A90}(20) \end{aligned} \quad (2\text{-}34)$$

The $L_{A90}(20)$ is the noise level of the road surface at the reference speed 90 km/h, and at the reference air temperature 20°C. According to the measurement results, the air temperature coefficients *a* are close to -0.10 dB(A)/°C and -0.06 dB(A)/°C for dense and porous asphalt respectively. It is also found that the correlation between the pass-by noise level and the road or tyre temperature is not stronger than with air temperature. This indicates that the air temperature can be used as a representative parameter in the temperature correction procedures. In the spectral analysis, linear relationships between the noise and temperature variation are observed in the low frequency range from 125 to 400 Hz and high frequency range from 1.6 kHz to 5 kHz. For medium frequencies (500 Hz to 1.25 kHz), the correlation is low.

2.4.3 Vehicle speed

For vehicle speed, a linear relationship between the sound pressure levels of tyre - road noise and the logarithm of the speed has been identified and coefficients are derived by different researchers. The relationship can be written as follows:

$$L_{A,eq} = a + b \cdot \log(V) \tag{2-35}$$

In the Dutch specifications, a correction term for the road surface influence called C_{road} is provided for noise calculations. It is given as [18]:

$$\text{Simplified procedure: } C_{road,m} = \Delta L_m + b_m \cdot \log(\frac{V_m}{V_{ref}}) \tag{2-36}$$

$$\text{Full procedure: } C_{road,m,i} = \Delta L_{m,i} + b_m \cdot \log(\frac{V_m}{V_{ref}}) \tag{2-37}$$

where *m* and *i* are the subscripts for vehicle category and frequency band respectively, V_{ref} the reference speed of 70 km/h, and ΔL the noise level difference with respect to the observed surface and the reference dense asphalt concrete surface.

2.5 Summary

This chapter have summarized existing researches on tyre - road noise. The literature review shows, it is known that reducing the noise level from the interaction between the rolling tyre and road surface involves many factors. It includes learning the noise generation mechanism, noise level measurement, investigation of influencing parameters, noise reducing pavement design and production and development of models for predicting the tyre - road noise. Comments on these existing studies will be given in the next chapter. Research work as carried out in this PhD thesis is also to be presented in Chapter 3.

References

1. Sandberg, U. and Ejsmont, J., *Tyre/Road Noise Reference Book*. 2002, Kisa, Sweden: Informex.
2. van Keulen, W. and Duškov, M., *Inventory study of basic knowledge on tyre/road noise*, in *IPG Report DWW-2005-022,*. 2005: Delft, the Netherlands.
3. Rasmussen, R.O., Bernhard, R.J., Sandberg, U., and Miller, N.P., *The little book of quieter pavements*, in *FHWA-IF-08-004* 2007.
4. Blom, R., *Report on tyre/road noise. Generation mechanisms, influence of tyre parameters and experiment on belt resonances*, in *DCT. 2004.20. Traineeship report*. 2004: Eindhoven, The Netherlands.
5. ISO11819-1, *Acoustics - Measurement of the influence of road surfaces on traffic noise -- Part 1: Statistical Pass-By method*. 1997, International Organisation for Standardization (ISO): Geneva, Switzerland.
6. ISO11819-2, *Acoustics - Method for measuring the influence of road surfaces on traffic noise -- Part 2: Close-proximity method*. 2000, International Organisation for Standardization (ISO): Geneva, Switzerland.
7. Steven, H., Küppers, D., van Blokland, G.J., van Houten, M.H., and van Loon, R., *International Validation Test for the 'Close Proximity Method' (CPX)*, in *CDROM from M+P Raadgevende ingenieurs bv*. 2000: CDROM from M+P Raadgevende ingenieurs bv.
8. van Blokland, G.J., Reinink, H.F., and Kropp, W., *Acoustic optimization tool. RE3: Measurement data Kloosterzande test track*, in *M+P Report DWW.06.04.8*. 2007, M+P Raadgevende Ingenieurs bv: Vught, the Netherlands.
9. Kuijpers, A.H.W.M., Peeters, H.M., Kropp, W., and Beckenbauer, T., *Acoustic optimization tool, RE4 - Modelling refinements in the SPERoN framework*, in *M+P Report DWW.06.04.7*. 2007: Vught, the Netherlands.
10. ISO13325, *Tyres -- Coast-by methods for measurement of tyre-to-road sound emission*. 2003: International Organisation for Standardization (ISO).
11. Norme, *NFS 31 119-2 Acoustique : Caractérisation in situ des qualités acoustiques des revêtements de chausses - Mesurages acoustiques au passage* 2000, Procédure Véhicules Maîtrisés
12. Roovers, M.S. and Peeters, H.M., *CPX-SPB/CPB Relation*, in *SILVIA Project Report SILVIA-M+P-008-00-WP2-080904*. 2004.
13. Schwanen, W., van Blokland, G.J., and van Leeuwen, H.M., *IPG 1.4 Robust CPX - Comparison of potential CPX tyres -Comparison of CPX- and SPB-measurements (M+P.DWW.07.04.1, Revision 3)*, in *M+P Report*. 2008, M+P Raadgevende Ingenieurs bv: Vught, the Netherlands.
14. Anfosso-LédéE, F. *Modeling the Local Propagation Effects of Tire-Load Noise : Propagation Filter between CPX and CPB Measurements*. in *Proceedings of Inter-Noise 2004*. 2004. Prague, Czech Republic.

15. den Boer, L.C. and Schroten, A., *Traffic noise reduction in Europe - Health effects, social costs and technical and policy options to reduce road and rail traffic noise*, in *CE Delft*. 2007.
16. Nilsson, R., Nordlander, J., and Silwa, N., *Design guidelines for durable, noise-reducing pavements*, in *SILVIA Project Report SILVIA-SKANSKA-018-01-WP4-231105*. 2005.
17. Sandberg, U., *Design and maintenance of low noise road surfacing*, in *Proceedings of the 3rd international symposium on surface characteristics*. 1996: Christchurch, New Zealand. p. 2-4.
18. COWI, *Noise classification of road pavements :Task 1: Technical background information*. 2006, European Commission - DG Environment: Brussels, Belgium.
19. Danish Road Institute, R.D., *Clogging of porous pavements - International experiences*, in *DRI, technical note 55*. 2007.
20. Tan, S.A., Fwa, T.F., and Guwe, Y.K., *Laboratory Measurements and analysis of clogging mechanism of porous asphalt mixes.* Journal of testing and evaluation, 2000. **28**(3): p. 207-216.
21. Danish Road Institute, *Clogging of porous pavements - The cleaning experiment*, in *DRI, technical note 60*. 2007.
22. Kropp, W., Kihlman, T., Forssén, J., and Ivarsson, L., *Reduction potential of road traffic noise*. 2007, Royal Swedish Academy of Engineering Sciences.
23. Abbott, P.G., Morgan, P.A., and McKell, B., *A Review of Current Research on Road Surface Noise Reduction Techniques*, in *Transport Research Laboratory report for the Rural and Environment Research Analysis Directorate of the Scottish Government*. 2010.
24. Morgan, P.A., Nelson, P.M., and Steven, H., *Integrated assessment of noise reduction measures in the road transport sector*, in *TRL Project Rep. No. PR SE/652/03*. 2003: Crowthorne, U.K.
25. Goubert, L., Hooghwerff, J., and Hofman, R., *Twolayer porous asphalt: an international survey in the frame of the Noise Innovation Programme (IPG)*, in *Inter-Noise 2005*. 2005: Brazil.
26. Morgan, P.A., *Scientific Strategy Document, End report*, in *DVS-2008-016*. 2008.
27. Bendtsen, H., Raaberg, J., and Thomsen, S.N., *International experiences with thin layer pavements*. 2005, The Danish Road Directorate Hedehusene, Denmark.
28. Brosseaud, Y., Abadie, R., and Legonin, R., *Wearing very thin and ultra-thin hot bituminous materials (in French: Couches de roulement très minces et ultra-minces en matériaux bitumineux à chaud).* 1997, LCPC: France. p. 55-71.
29. Brosseaud, Y. and Anfosso-LédéE, F., *Review of existing low-noise pavement solutions in France*, in *SILVIA Project Report SILVIA-LCPC-011-01-WP4-310505*. 2005.

30. Sandberg, U., Kalman, B., and Nilsson, R., *Design guidelines for construction and maintenance of poroelastic road surfaces*, in *SILVIA Project Report SILVIA-VTI-005-02-WP4-141005*. 2005.
31. Meiarashi, S. *Porous Elastic Road Surface as an Ultimate Highway Noise Measure*. in *the 22nd World Road Congress*. 2003. Durban, South Africa.
32. Sandberg, U., Goubert, L., Biligiri, K.P., and Kalman, B., *State-of-the-art regarding poroelastic road surfaces*, in *Deliverable D8.1*. 2010.
33. Sandberg, U. and Kalman, B., *The Poroelastic Road Surface - Results of an Experiment in Stockholm*, in *SILVIA Project Report SILVIA-VTI-006-00-WP4-030605*. 2005.
34. Morgan, P.A., *IPG Research Report - Innovative mitigation measures for road traffic noise*, in *Report DVS-2008-018*. 2008, Road and Hydraulic Engineering Division of Rijkswaterstaat: Delft, the Netherlands.
35. Beckenbauer, T. and Kropp, W. *A hybrid model for analysis and design of low noise road surfaces*. in *EuroNoise 2006 conference*. 2006. Tampere, Finland.
36. Klein, P. and Hamet, J.F., *Tyre/road noise prediction with the HyRoNE model*, in *Proceedings of INTER-NOISE conference*. 2007: Istanbul, Turkey.
37. Larsson, K., Barrelet, S., and Kropp, W., *The modelling of the dynamic behaviour of tyre tread blocks.* Applied Acoustics, 2002. **63**(6): p. 659-677.
38. O'Boy, D.J. and Dowling, A.P., *Tyre/road interaction noise—Numerical noise prediction of a patterned tyre on a rough road surface.* Journal of Sound and Vibration, 2009. **323**(1–2): p. 270-291.
39. O'Boy, D.J. and Dowling, A.P., *Tyre/road interaction noise—A 3D viscoelastic multilayer model of a tyre belt.* Journal of Sound and Vibration, 2009. **322**(4–5): p. 829-850.
40. Kuijpers, A.H.W.M., *Tyre/road noise modelling, the road from a tyre' s point of view*, in *M+P report MVW 01.8.1* 2001.
41. Gerretsen, E. and Mulder, E.H., *TRIAS: a comprehensive tyre-road noise model and its validation*, in *TNO-report, HAG-RPT-000121a* 2001.
42. Wayson, R.L., *NCHRP Synthesis 268 - Relationship between pavement surface texture and highway traffic noise*, in *Transportation Research Board, National Academy Press*. 1998: Washington D.C.
43. Sandberg, U., *Road traffic noise—The influence of the road surface and its characterization.* Applied Acoustics, 1987. **21**(2): p. 97-118.
44. ISO13473-2, *Characterization of pavement texture by use of surface profiles -- Part 2: Terminology and basic requirements related to pavement texture profile analysis*. 2002, International Organisation for Standardization (ISO): Geneva, Switzerland.
45. Gerretsen, E., *Tyre-road noise model, part B, fase 2: validation of road model RODAS (Model Geluidemissie band-wegdek, Deel B, fase 2: validatie wegdekmodel RODAS)*, in *TNO report HAG-RPT-990086*. 1999.
46. Doelman, N.J., *Characterisation of road surface textures*, in *TNO-report, HAG-RPT-990151a*. 2001: The Hague, The Netherlands.

47. Doelman, N.J., Mulder, E.H., M. van der Eerden, F.J., and de Roo, F. *3-D characterisation of road surface textures in TRIAS*. in *Proc. Inter-noise 2004*. 2004. Proc. Internoise 2004.
48. von Meier, A., van Blokland, G.J., and Descornet, G., *The influence of texture and sound absorption on the noise of porous road surfaces*, in *PIARC 2nd International Symposium on Road Surface Characteristics*. 1992: Berlin, Germany. p. 7 - 19.
49. Clapp, T.G., Eberhardt, A.C., and Kelley, C.T., *Development and Validation of a Method for Approximating Road Surface Texture‐Induced Contact Pressure in Tire‐Pavement Interaction.* Tire Science and Technology, 1988. **16**(1): p. 2-17.
50. Klein, P. and Hamet, J.F., *An envelopment procedure for tyre/road contact*, in *Technical Report SILVIA-INRETS-009-WP2, INRETS*. 2003.
51. Klein, P. and Hamet, J.F., *Texture and noise correlations using a dynamic rolling model*, in *SILVIA-INRETS-020-WP2, INRETS*. 2005.
52. Klein, P. and Hamet, J.F., *END_T, Expected pass-by noise level difference from texture level variation of the road surface*, in *SILVIA Report SILVIA-INRETS-021-01-WP2-070705*. 2005.
53. Fujikawa, T., Oshino, Y., Mikami, T., and Tachibana, H. *Examination on effects of road roughness parameters for abating tire/road noise*. in *Proceedings of Inter-Noise 2004*. 2004. Prague, Czech Republic.
54. Fujikawa, T., Oshino, Y., Mikami, T., and Tachibana, H. *Prediction of tire/road noise reduction by road-surface improvements*. in *Proceedings of Inter-Noise 2009*. 2009. Ottawa, Canada.
55. ISO10844, *Acoustics -- Specification of test tracks for measuring noise emitted by road vehicles and their tyres*. 2011.
56. ASTM, *E965 - 96 Standard Test Method for Measuring Pavement Macrotexture Depth Using a Volumetric Technique*. 2006.
57. ISO13473-1, *Characterization of pavement texture by use of surface profiles -- Part 1: Determination of Mean Profile Depth*. 1997, International Organisation for Standardization (ISO): Geneva, Switzerland.
58. ISO13473-3, *Characterization of pavement texture by use of surface profiles -- Part 3: Specification and classification of profilometers*. 2002, International Organisation for Standardization (ISO): Geneva, Switzerland.
59. ISO/TS13473-4, *Characterization of pavement texture by use of surface profiles -- Part 4: Spectral analysis of surface profiles*. 2008, International Organisation for Standardization (ISO): Geneva, Switzerland.
60. Berengier, M.C., Stinson, M.R., Daigle, G.A., and Hamet, J.F., *Porous road pavements: Acoustical characterization and propagation effects.* The Journal of the Acoustical Society of America, 1997. **101**(1): p. 155-162.
61. Ogushwitz, P.R., *Applicability of the Biot theory. I. Low-porosity materials.* The Journal of the Acoustical Society of America, 1985. **77**(8): p. 429-440.

62. Berryman, J.G., *Long-wavelength propagation in composite elastic media II. Ellipsoidal inclusions.* Journal of the Acoustical Society of America, 1980. **68**(6): p. 1820-1831.
63. Hamet, J.F. and Be´rengier, M., *Acoustical characteristics of porous pavements: A new phenomenological model*, in *Internoise 93*. 1993: Leuven, Belgium. p. 641–646
64. Berengier, M.C., Stinson, M.R., Daigle, G.A., and Hamet, J.F., *Porous road pavements: Acoustical characterization and propagation effects.* Journal of the Acoustical Society of America, 1997. **101**(1): p. 155–162.
65. Champoux, Y. and Stinson, M.R., *On acoustical models for sound propagation in rigid frame porous materials and the influence of shape factors.* The Journal of the Acoustical Society of America, 1992. **92**(2): p. 1120-1131.
66. Attenborough, K., Bashir, I., and Taherzadeh, S., *Outdoor ground impedance models.* The Journal of the Acoustical Society of America, 2011. **129**(5): p. 2806-2819.
67. Kuijpers, A.H.W.M. and Blokland, G.v. *Modelling and optimization of two-layer porous asphalt roads*. in *Proceeding of Inter-noise 2000*. 2002. Nice, France.
68. Gerretsen, E., *Model for tyre-road sound emission Part B, phase 1: relation between road properties and material data (in Dutch: Model geluidemissie band-wegdek Deel B, fase 1: relaties wegdekeigenschappen met materiaalgegevens)*, in *TPD-HAG-RPT-970118 for CROW*. 1997.
69. Kim, H.K. and Lee, H.K., *Acoustic absorption modeling of porous concrete considering the gradation and shape of aggregates and void ratio.* Journal of Sound and Vibration, 2010. **329**(7): p. 866-879.
70. Lu, T.J., Chen, F., and He, D., *Sound absorption of cellular metals with semiopen cells.* The Journal of the Acoustical Society of America, 2000. **108**(4): p. 1697-1709.
71. Maa, D.Y., *Micro perforated-panel wide band absorbers.* Noise Control Engineering Journal, 1987. **29**: p. 77-84.
72. Hamet, J.F., *Estimation of the attenuation of rolling noise by acoustic absorption*, in *SILVIA report SILVIA-INRETS-013-00-WP2-09/06/2004*. 2004: Bron Cedex, France.
73. Hamet, J.F. and Klein, P., *ENRa, Expected pass-by noise level reduction from acoustic absorption of the road surface*, in *SILVIA Project Report SILVIA-INRETS-018-02-WP2-040505*. 2005.
74. ISO13472-1, *Measurement of sound absorption properties of road surfacings in situ - Part 1: Extended surface method*. 2002.
75. van Blokland, G. and Roovers, M.S., *SILVIA Deliverable D14: Measurement methods*, in *SILVIA Project Report SILVIA-M+P-015-02-WP2-140705*. 2005.
76. Morgan, P.A. and Watts, G.R., *A novel approach to the acoustic characterisation of porous road surfaces.* Applied Acoustics, 2003. **64**(12): p. 1171-1186.

77. de Bree, H.-E., Nosko, M., and Tijs, E. *A handheld device to measure the acoustic absorption in situ*. in *NVH GRAZ*. 2008.
78. Tijs, E. and de Bree, H.E. *An in situ method to measurement the acoustic absorption of roads whilst driving*. in *NAG/DAGA 2009, International Conference on Acoustics*. 2009. Rotterdam, The Netherlands.
79. Iwase, T. and Yoshihisa, K. *Measuring Method of Sound Reflection and Absorption Characteristics Based on the Particle Velocity and its Applications to Measurements on Such as Drainage Pavement of Road Surface*. in *Proc. Internoise 2003*. 2003. Seogwipo, Korea.
80. Harris, C.M. and Piersol, A.G., *Harris' shock and vibration handbook*. 2002, New York: McGraw-Hill.
81. Schwanen, W. and Kuijpers, A.H.W.M., *Development of a measurement system for mechanical impedance*, in *SILVIA Project Report SILVIA-M+P-013-01-WP2-230605*. 2005.
82. Kuijpers, A.H.W.M., Peeters, B., Beckenbauer, T., and Kropp, W. *Acoustic optimization tool user manual for version 3.1*. http://www.speron.net/html/userguide.html.
83. Sandberg, U. *Semi-generic temperature corrections for tyre/road noise*. in *Proceedings of Internoise 2004*. 2004. Prague, Czech Republic.
84. Kuijpers, A.H.W.M., *Memo on temperature effects on tyre/road noise and on tyre stiffness*, in *M + P.WG27/2002/2/ak report*. 2002.
85. Anfosso-LédéE, F. and Pichaud, Y., *Temperature effect on tyre–road noise.* Applied Acoustics, 2007. **68**(1): p. 1-16.

CHAPTER 3 RESEARCH PLAN

3.1 Introduction

Most of the existing researches related to tyre - road noise is presented in the literature review in Chapter 2. From that, we learned what research has been done on different aspects of tyre - road noise and the measures for reducing noise levels. As a follow up of the literature review, this chapter gives comments on the existing tyre - road noise studies and points out research which should be carried out in this PhD research. A research plan is then proposed. It provides the whole research program of the thesis and shows the scheme of work that will be carried out in the various chapters following this chapter.

In this chapter, comments on the existing studies of tyre - road noise are given in section 3.2. The research plan for this PhD thesis is presented in section 3.3.

3.2 Comments on Existing Studies

In this section, comments are given on the existing work which was presented in the literature review in Chapter 2. The discussion focuses on three aspects: influencing parameters and investigation methods; measurement methods; tyre - road noise model development.

3.2.1 Influencing parameters and investigation methods

The air voids content of asphalt wearing courses is one of the most important parameters influencing the surface characteristics, including surface texture and sound absorption, and consequently affecting the tyre - road noise levels. In nearly all the investigations on the noise reducing effect of porous asphalt concrete, the influence of the air voids content was considered. However, it should be noted that not all the air voids are effective for sound absorption. Only those connected to the exposed pores at the surface are effective in absorbing sound waves [1]. Knowledge on the content of the connected air voids and the influence of the connected air voids is essential to understand the acoustical properties of the road surface. In addition, the maximum aggregate size, stone grading and binder content are also considered to be important factors that affect those road surface characteristics which are related to tyre - road noise.

Surface texture can be characterised by an individual index, such as MPD, ETD and RMS, or by texture levels on the spectral band of wavelength. The sound absorption can be expressed simply by the maximum absorption coefficient and the corresponding frequency or by the absorption coefficients on the spectral band of frequency. In existing studies, some of the expressions for texture and sound absorption are used to develop relationships for tyre - road noise. However, the combined effect of texture and sound absorption were not demonstrated, especially the combination of texture levels and sound absorption coefficients on the spectral bands. Combinations of the surface characteristics expressed by different indices should be taken into account for analysing the influence of surface characteristics on tyre - road noise.

In previous research, the influence of the mechanical impedance on tyre – road noise has been investigated. In pavement engineering and asphalt mixture design, the mechanical impedance is never used to characterize mixtures but mixture stiffness is a commonly used parameter for denoting the mechanical properties. It is of interest to relate the mechanical impedance with the stiffness. In this way, the mechanical impedance can possibly be related to stiffness tests which are regularly done in mixture design and evaluation. Such a relationship would be very useful and helpful for pavement engineers.

3.2.2 Measurement methods

The CB (or SPB) and CPX methods are typical measurements for testing the far and near field noise level from the tyre - road interaction respectively. They are commonly used for collecting noise data and for developing prediction models. Noise level data to be used in this study were from the Kloosterzande test sections which were specially built under contract with the Dutch Ministry of Transport for tyre – road noise studies. As the data in the database were collected by the CPX and CB methods, only those data were taken into account in this thesis

For road surface texture, profilometer measurements have the advantages of high accuracy and enlarged measuring range. Texture expressions, such as MPD, ETD and texture level spectrum can be easily gained from the results. A device which is feasible to be applied both for in-situ measurement and laboratory measurement makes sense for this study and future work. Therefore such a device was developed for this study.

With regards sound absorption, the laboratory test with the impedance tube confines the frequency range of the resulting absorption curve. By means of ESM tests, sound absorption is measured on a much wider frequency range, but a much larger surface, such as a real road surface, is required. The P-U based surface impedance setup is a portable device, and can be used in the laboratory as well as in the field. However, the effect of using the device on testing road surface samples in the lab needs to be investigated. This was done as part of this study.

The mechanical impedance is a newly considered parameter, and there is also no standardized method for the measurement. Measurements using an improved version of the impedance hammer device are considered since this technology can be used in both the laboratory and field trails. In addition, it is also thought that the mechanical impedance can be related to the stiffness of the material and can be deduced from the stiffness measurement results. Therefore this interrelationship was also investigated in this study.

3.2.3 Modeling of tyre - road noise

Physical models simulate the noise production based on noise generation mechanisms and simplified mechanical models of tyre and road surface. They describe part of the noise generation process, and cannot work independently for predicting the noise level. The physical models are generally used as sub-models in hybrid models, such as AOT and Trias. In most of the physical models, only the tyre vibration is taken into account. Other mechanisms are not involved due to the complexity or lack of related knowledge. The physical models used for simulating the tyre - road interaction are theoretical, and simplify the real state of the road surface. Moreover, a large amount of data, such as original surface profile, needs to be collected to run the contact model. For certain models, the tyre indexes should also be known, and this makes no sense to road engineers. Therefore, it can be concluded that the physical model is essential for describing the tyre - road noise generation in a theoretical way, but long term efforts still need to be made in order to make them applicable for practice. Physical models are not employed in this research.

In statistical models, the noise level is predicted using relationships that relate the noise level to certain parameters of the surface layer, such as surface texture, porosity, etc. These relationships are always derived from a correlation analysis or curve fitting, without clear rationale-based support. They can make good predictions for pavements with properties similar as those used for developing the regression equation, but it is difficult to provide a general rule for all types of surfaces. Therefore statistical models should better be developed for a single type of road surface rather than for all surface types.

Mixture properties and road surface characteristics are directly related to each other. Furthermore mixture properties are of interest to pavement engineers because they affect durability and strength of the layer. However, the road parameters in most of the existing noise predicting models are surface layer parameters, such as a texture spectrum, surface profile, absorption coefficient, and not directly mixture parameters. Furthermore, some parameters can only be obtained by means of special measurements which are uncommon in road engineering, e.g. flow resistance and tortuosity. Thus it is quite important to develop models linking the noise level to the material properties of the road surface layer. The input variables are preferred to be those indices which are typical for road engineers and which can be easily measured. In addition, road

surface characteristics are changing with service time, and an age based correction is important for long term evaluation of the tyre - road noise.

Most of the current modeling focuses on dense and porous asphalt road surfaces. However, much less attention is paid to thin layer surfacings, which are also a commonly used quiet pavement in the Netherlands and some other European countries. This type of surface combines both the advantages of SMA and porous asphalt. The mixture composition and surface layer characteristics are different from those of the dense and porous layers. As a result, the acoustical performance is also different. Special investigation, modeling and improvement of the existing acoustic models are necessary for an accurate prediction of tyre - road noise from thin layer surfaces. Therefore this was taken as one of the topics for this PhD research

3.3 Research Plan for the Thesis

Section 3.2 showed what need to be done in terms of measurements and noise prediction models. Research will therefore be carried out by considering those comments and to solve problems found in existing studies. The research of this PhD thesis focuses on thin layer surfacings.
The main objectives of the study are:
1) finding the relationships between the material properties, surface characteristics and tyre - road noise of thin layer surfacings;
2) developing models for predicting tyre - road noise from material properties.

The scheme of the whole study is shown in Figure 3-1. According to the organization of the chapters, the research can be divided into four main parts:

- development and discussion of laboratory measurement methods (Chapter 4);
- investigation into the influence of mixture composition on surface characteristics (Chapter 5);
- investigation into the influence of surface characteristics on tyre - road noise (Chapter 6);
- tyre - road noise modeling (Chapter 7).

Two types of methods are used in the research:

- measurements (including laboratory measurements and in-situ measurements);
- data analysis.

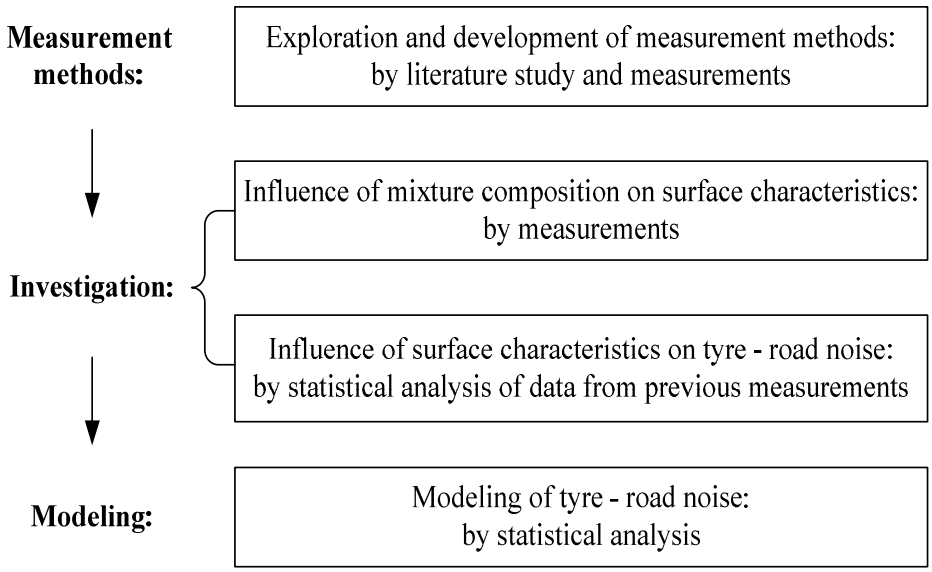

Figure 3-1 Scheme of the research plan of the thesis

Measurements, including laboratory measurements and in-situ measurements, are organized for developing test methods (in Chapter 4) and investigating the influence of mixture composition on surface characteristics (in Chapter 5). Table 3-1 gives a summary of all the measurements to be carried out in the research. Details about the tested materials, samples and the measurement methods will be provided in Chapter 4.

Table 3-1 Summary of measurements in the research

Investigation	Testing property	Laboratory measurement		Field measurement	
		Test method	Sample type	Test method	Test sections
Using P-U technology in laboratory measurement of sound absorption (in Chapter 4)	Sound absorption	P-U surface impedance setup	slab, core samples, and PERS slab	P-U surface impedance setup	Kloosterzande trial sections
		Impedance tube	core		
Investigation on the influence of mixture compositions on surface characteristics (in Chapter 5)	Mixture composition	CT Scanning	core	-	-
	Surface Texture	Laser profilometer	slab and core	-	-
	Sound absorption	P-U surface impedance setup	slab and core	-	-
	Mechanical impedance	Impedance hammer	slab	Impedance hammer	Kloosterzande trial sections
	Resilient modulus	Cyclic indirect tension testes (ITT)	core	-	-

Data analysis is employed for observing the influence of surface characteristics on tyre - road noise (in Chapter 6) and tyre - road noise modeling (in Chapter 7). A database which contains measurement results from Kloosterzande sections obtained in a previous project is used in the investigation of the influence of

surface characteristics on tyre - road noise. With regards the modeling of tyre - road noise, both the database and the laboratory measurements results are involved.

In this thesis, research will be carried out according to the four aspects as shown in Figure 3-1. The research plans for each part are described in the sub-sections hereafter.

3.3.1 Measurement methods

Objective:
The study in this part is to introduce and develop test methods to be used in the laboratory.

Research methods:
Measurements and literature review.

Description:
The measurements to be carried out are shown in Figure 3-2. As shown in the figure, surface characteristics to be measured in this research include: surface texture, sound absorption, mechanical impedance and stiffness. The material properties, including coarse aggregate and binder content, are also to be measured. The relevant measurement methods used are the following:

1) Surface texture

A laser profilometer device is developed for testing the surface texture in this PhD study. The device is applicable on both the laboratory samples and the road surface.

2) Sound absorption

The P-U technology is used for testing the sound absorption of asphalt mixture samples. The device works well on large surfaces, such as in situ road surfaces. The applicability of the device for testing on lab (made) samples is to be investigated in this research. The influences of the distance between the probe and the sample surface, dimension and height of the sample, and the testing positions on slab samples is investigated. Suggestions will be given for using the setup in the laboratory tests.

3) Mechanical impedance

A test method using the impedance hammer is developed. The method can be used on slab samples in the lab or directly on the road surface.

4) Stiffness

Mixture stiffness is measured by the standard indirect tensile test (ITT) method. The resilient modulus is used to describe the stiffness of the samples.

5) Mixture composition

The mixture composition is to be investigated by means of CT scanning. The test methods will be introduced in the study.

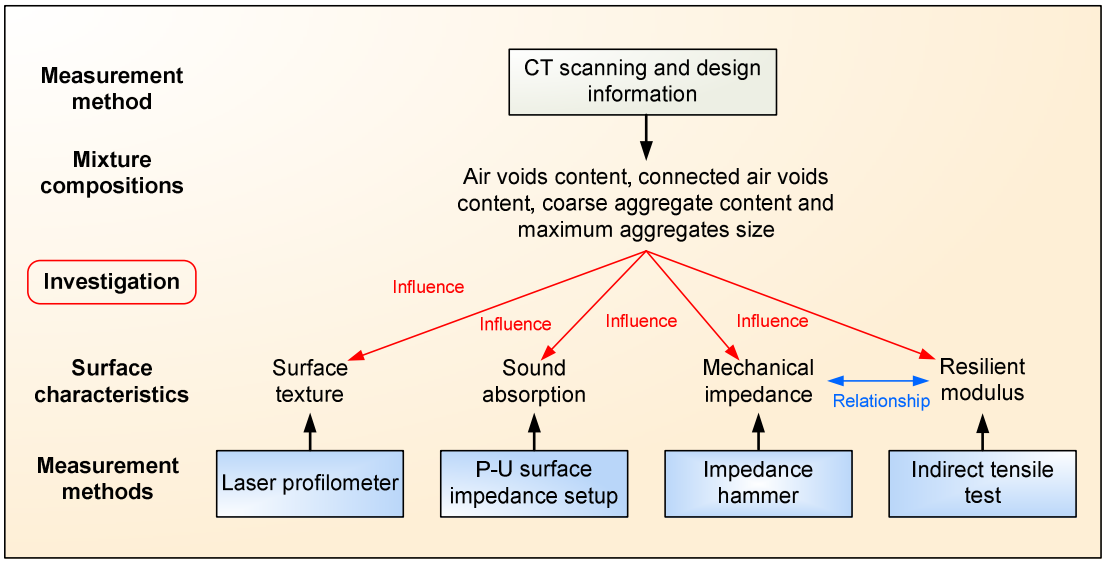

Figure 3-2 Investigation on the influence of mixture composition on surface characteristics by measurements

3.3.2 Influence of mixture composition on surface characteristics

Objective:

Investigate the influence of the mixture composition on the surface characteristics which are related to tyre - road noise of thin layer surfacings.

Research methods:

Measurements.

Description:

The surface characteristics and mixture compositions are measured by the methods mentioned in Section 3.3.1. The influences of mixture compositions on the surface characteristics is investigated based on the measurement results. The scheme of the research is shown in Figure 3-2. More detail descriptions of the study are as follows.

1) Mixture composition

The contents of air voids, coarse aggregate and mortar are obtained from CT scanning images. The content of connected air voids is calculated by using a cluster-labeling algorithm. A relationship between the overall air voids content and the connected air voids content will be presented.

2) Surface texture

Laboratory measurement results of surface texture performed on slab and core samples will be shown. The influences of mixture composition on texture levels and MPD will be discussed.

3) Sound absorption

Sound absorption curves from the laboratory measurements will be shown and comparisons between different surfaces will be made. The influences of mixture composition will be investigated. Physical models will be developed for evaluating the sound absorption of thin layer surfacings.

4) Mechanical impedance and stiffness

The influences of the material properties on the measured mechanical impedance and stiffness will be discussed. A relationship between the mechanical impedance and stiffness as developed by means of regression analysis will be presented.

3.3.3 Influence of surface characteristics on tyre - road noise

Objective:

Investigate the combined influence of different surface characteristics on tyre - road noise of thin layer surfacings.

Research methods:

Data analysis.

Description:

Analyses are to be made by using data from the Kloosterzande trial sections database. The surface characteristics taken into account are surface texture and sound absorption. The combined effect of texture and sound absorption on tyre - road noise is investigated by means of regression analyses. The scheme of the study is given in Figure 3-3.

1) Regression analysis

A relationship between surface characteristics and the tyre - road noise will be developed by means of linear regression. Combinations of the surface texture and sound absorption coefficients will be used as explanatory variables; tyre - road noise is the response variable.

Principal component regression (PCR) and partial least square (PLS) methods will be used to reduce the multicollinearity between the explanatory variables. The influence of surface characteristics will be determined from the regression results. A pre-treatment of the data will be accomplished before the regression analysis.

2) Influence of vehicle speed

The influence of the driving speed of the car will be studied by using speed as an explanatory variable in the regression analysis.

3) Influence of truck tyres

Data from passenger tyres are going to be used in most of the analyses in this research. However, the influence of the truck tyre will also be discussed by using data obtained with truck tyres.

4) Investigation on change of surface characteristics

Investigations are going to be made on the changes of tyre - road noise caused by the small changes in the road surface characteristics. In the regression only the difference value of the surface characteristics and noise levels will be taken into account. This makes that changes in noise levels from variations of the surface characteristics can directly be determined.

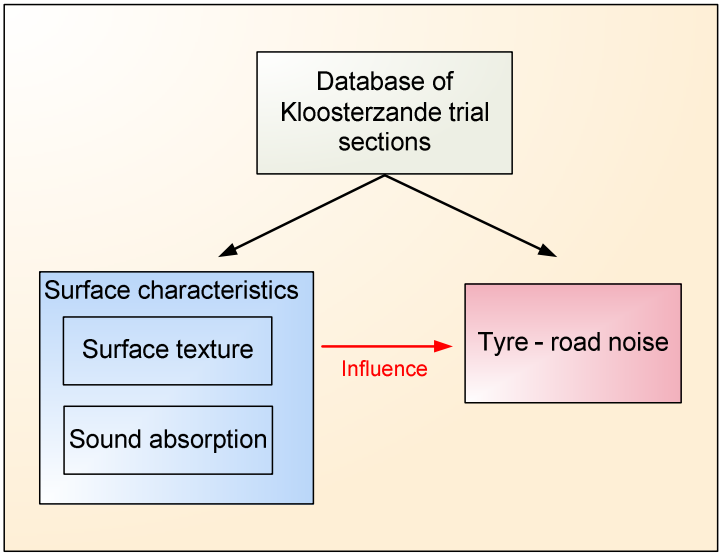

Figure 3-3 Investigation on the combined influence of surface characteristics on tyre - road noise by data analysis

3.3.4 Tyre - road noise modeling

Objective:

Develop a model which can predict the tyre - road noise from basic material properties of the road surface. The model should be attractive for pavement engineers allowing them to predict noise levels when designing mixtures, and helping them to optimize the design of noise reducing pavements.

Research method:

Data analysis.

Description:

Models are going to be developed for predicting tyre - road noise levels. The target model is illustrated in Figure 3-4. The modeling will be based on regression analyses with data from the laboratory measurements and the Kloosterzande database. The development of the model will be done according to the following steps:

1) Initial modeling

Linear regression models are going to be developed by linking tyre - road noise levels to surface characteristics as well as the mixture compositions. A number of candidate models will firstly be developed by using different combinations of input variables and different regression methods.

2) Model selection

Models which show a good prediction capacity are going to be selected from the available candidates.

3) Validation and final selection

Validation of the selected models will be performed. Data used for the validation will come from in situ road surfaces in the Netherlands. Models which present a good fit with the validation data and which require a small number of input variables will be selected as the final models.

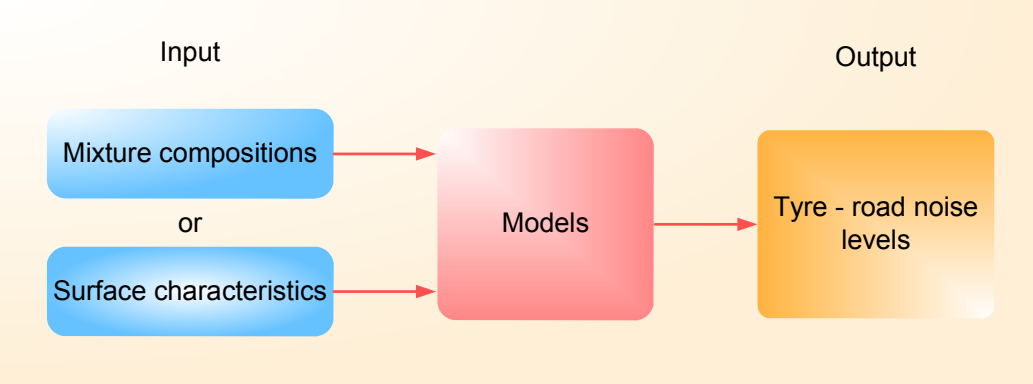

Figure 3-4 Target model for predicting tyre - road noise

3.4 Summary

Comments are given on existing studies of tyre - road noise. Shortcomings of and improvements required for these existing researches are addressed. The research plans for this PhD thesis are proposed and cover four main components being: development and discussion of laboratory measurement methods; investigation of the influence of mixture composition on surface characteristics; investigation of the combined influence of surface characteristics on tyre - road noise; and tyre - road noise modeling. These four components will be discussed in detail in the chapters to follow.

References

1. Sandberg, U. and Ejsmont, J., *Tyre/Road Noise Reference Book*. 2002, Kisa, Sweden: Informex.

CHAPTER 4

MATERIALS AND MEASUREMENT METHODS

4.1 Introduction

Laboratory measurements are carried out to investigate the relationship between the material properties and the surface characteristics of thin layer surfacings. The measurement data are also to be used in the development of the prediction model described in Chapter 7. Two groups of measurements can be distinguished: measurement on the mixture composition and measurement on the surface characteristics. Tests on the mixture composition include: measurement of the air voids content, coarse aggregate content and mortar content. This was partly conducted by means of CT-scanning.

From the literature review, it is known that the three important road surface characteristics related to tyre - road noise are surface texture, sound absorption and mechanical impedance. Therefore, these three surface characteristics are measured and investigated as well. Different types of samples are required according to the various measurement methods. An overview of the measured properties, corresponding test methods and sample type are listed in Table 4-1. Details about the materials, samples and the test methods are given in this chapter.

Table 4-1 Measurements and methods

Testing property	Laboratory measurement		Field measurement	
	Test method	Sample type	Test method	Test sections
Mixture composition	CT Scanning	core	-	-
Surface Texture	Laser profilometer	slab and core	-	-
Sound absorption	P-U surface impedance setup	slab and core	-	-
Mechanical impedance	Impedance hammer	slab	Impedance hammer	Kloosterzande trial sections
Resilient modulus	Cyclic indirect tension test (ITT)	core	-	-

4.2 Material Information

4.2.1 Slab samples of thin layer surfacing

The thin layer surfacing is the main object of the study. Different thin layer surface mixtures were designed based on adjustments from the reference surface Micro-Top, which is a noise reducing thin layer surface developed by Ballast Nedam contracting company in The Netherlands. Table 4-2 gives the design parameters for each type of mixture. Cells with a yellow background indicate the properties which are changed. Different mixtures were made to investigate the influence of mixture composition on different acoustical and mechanical properties:

Mixture 1 and 2: influence of variation of the air voids content;
Mixture 3 and 4: influence of aggregate gradation and lower air void content;
Mixture 5: influence of using a larger size coarse aggregate;
Mixture 6 and 7: influence of different types of coarse aggregate;
Mixture 8: influence of the binder content.

Three aggregate sources were applied in the study. Bestone is employed in most of the mixtures and considered as a reference type of aggregate. It is a type of sandstone mined from a quarry in Norway. The other two types of stone are Tillred and Irish Greywacke, used in mixture P06 and P07 respectively. Tillred is a red coloured chipping from the UK, and Irish Greywacke is a sandstone obtained from Ireland.

The binder used in all mixtures except P06 is Cariphalte DA. P06 is made with colorless bitumen Sealoflex Color with addition of Bayferrox synthetic iron oxide pigments. The result of this is that the colour of P06 is red. Properties of the two types of bitumen, Cariphalte DA and Sealoflex Color are given in Table 4-3.

Table 4-2 Designs of the investigated thin layer surfacings

	Coarse aggregate content, % by mass	Max. Aggregate size, mm	Air voids content, % by volume	Binder content, % by mass of mxiture	Aggregate type
Ref.	78	2/6	12	6.1	Bestone
P01	78	2/6	8	6.1	Bestone
P02	78	2/6	18	6.1	Bestone
P03	72	2/6	8	6.1	Bestone
P04	68	2/6	8	6.1	Bestone
P05	78	4/8	12	6.1	Bestone
P06	78	2/6	12	6.1	Tillred
P07	78	2/6	12	6.1	Irish Greywacke
P08	78	2/6	12	7	Bestone

For testing the surface characteristics, samples with a large surface area are preferred. Large samples facilitate the measurement procedure and provide more

accurate results. Use of small samples, such as drilled cores has its limitations because of all kinds of undesired side effects. The Influence of the dimension of the sample is discussed specifically in the following sections for the different test methods.

Table 4-3 Binder properties of the investigated thin layer surfacings

Items	Cariphalte DA	Sealoflex Color
Penetration, at 25 °C, unit: 0.1 mm	85-130	70-100
Ring and ball softening point, unit: °C	≥ 80	50-56

Because of the above mentioned considerations, slab samples are produced for the thin layer surfacing materials. A typical example of the produced slabs is shown in Figure 4-1. The length and width of the slabs are 700 mm and 500 mm respectively. This size ensures that the surface area is large enough for any tests on the surface characteristics, including surface texture, sound absorption and mechanical impedance. The overall thickness of the slab is 70 mm, with a 30 mm thin top layer and a 40 mm dense asphalt concrete bottom layer. The combination of the two layers is shown in Figure 4-1 (b). The setting can be considered as a simulation of a practical road surface structure.

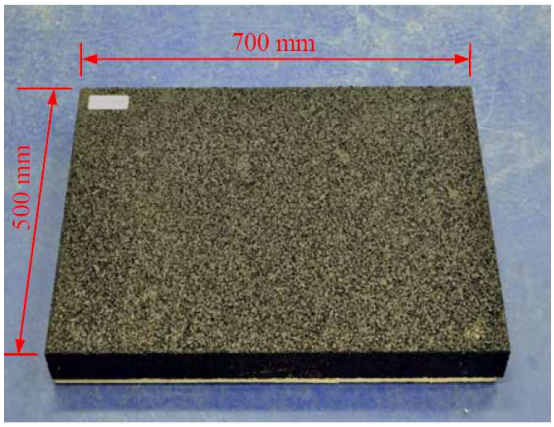

(a) Top view of the slab

(b) Side view of the slab

(c) Label on the sample

(d) Top surface of the sample

(e) Top view of the slab P06

Figure 4-1 Slab sample of thin layer surfacing

The mixtures and the samples were produced with the mixing and compaction unit available in the lab of Ballast Nedam. One slab was made based on each of the mixture design in Table 4-2. The 40 mm bottom layer was first laid and compacted. The thin surfacing was then compacted on top of the bottom layer. In the production, P01 and P02 had the same mixture composition as Ref, but they were made with different compaction energy. Ref. had 100% level of compaction. For P01 and P02, the levels of compaction were 93% and 105% respectively. In this way, different air voids contents shown in Table 4-2 were achieved.

4.2.2 Core samples from Kloosterzande trial sections

The Kloosterzande trial sections are located in the most northern part of the N60 road in the Netherlands. The sections were built with the purpose of developing a prediction tool for tyre - road noise, called Acoustic Optimization Tool (AOT). 40 sections with different surface types were laid in the year 2005 and 2007 respectively [1]. Surface characteristics and the tyre - road noise were measured on the sections. A database was built containing the measurement results and the prediction software AOT was developed. The sections were constructed specifically for experiments and were not opened to traffic. A number of the sections were removed after the project was finished. The sections can be seen as a comprehensive collection of noise reducing surfaces used in The Netherland, and it is an important data source for related to tyre - road noise. For this research, cores were taken from the Kloosterzande surfaces and used in the laboratory measurements as a supplement to the slab samples. In this research, certain in-situ measurements (sound absorption and mechanical impedance measurements) in this research were also performed on the Kloosterzande sections.

Cores were drilled on 17 trial sections in Kloosterzande on May 3rd, 2010. Two cores were drilled from each side of a section and 34 were obtained in total. The positions where the cores were taken are shown in Figure 4-2. All samples had a diameter of 150 mm. Each drilled core consisted of the surface and the bottom layers. Only in the case of the cores from section No. 12 the Rollpave section, the surface layers were separated from the bottom ones. The cores have different

ages as sections numbered 1-15 were built in 2005, while the No. 24 and No. 31 sections were paved in 2007. As mentioned before, none of the sections were ever trafficked. The trial section, coring process and example of the extracted cores are shown in Figure 4-3.

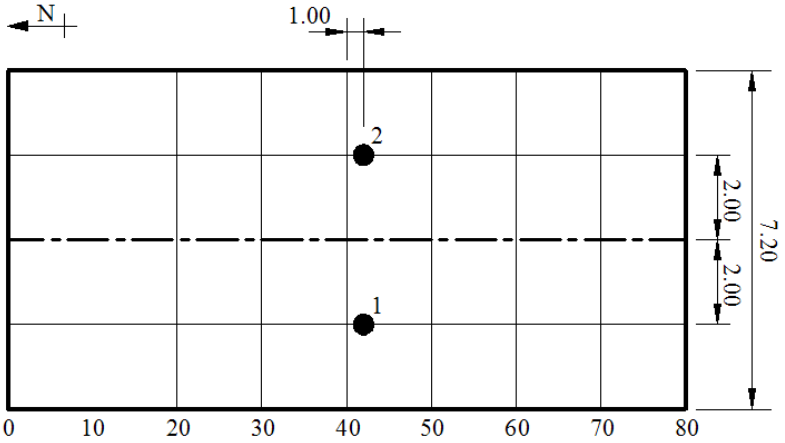

Figure 4-2 Coring positions on each section, Unit: m

Details of the mixture design of each surface layer for each section are summarized in Table 4-4. The 17 trial sections consisted of four thin layer surfacings (Sections No.2 to 5), seven porous asphalt surfaces (Sections No.6-9, 15, 24 and 31), four two-layer porous asphalt (Sections No.10, 11, 13 and 14), one dense surface (Section No.1) and one poroelastic surface (Section No 12). Sections No.9, 15 and 24 are built with a 25 mm thick surface, and can also be treated as porous type thin layer surfacings. Although samples of a wide variety of surface layers are available, this research focuses on thin layer surfacings with a thickness of approximately 25 mm.

(a) The trial section

(b) Mark of drilling position

(c) Drilling the core (d) One of the extracted cores

Figure 4-3 Coring on Kloosterzande sections

In addition to testing on the cores, sound absorption tests and the mechanical impedance measurements by means of a hammer device were also performed on the original sections. This is done, because a large area of a surface is required in these two methods, so field testing is the most appropriate way of carrying out these measurements. The results obtained on the field sections will be compared with those obtained from laboratory tests.

Table 4-4 Basic information about the mixtures used in the Kloosterzande test sections

Trial section No.	Top layer type	Thickness (mm)	Air voids content (%)	Bottom layer type	Thickness (mm)	Air voids content (%)
1	ISO surface, dense	30	4			
2	thin layer surfacing 2/4	25	12			
3	thin layer surfacing 2/6	25	8			
4	thin layer surfacing 2/6	25	12			
5	thin layer surfacing 4/8	25	12			
6	porous 0/11	50	>20			
7	porous 0/16	50	>20			
8	porous 4/8	50	>20			
9	porous 4/8	25	>20			
10	porous 4/8	25	>20	porous 11/16	65	>20
11	porous 4/8	25	>20	porous 11/16	45	>20
12	Rollpave	30	≈30	porous 8/11+11/16	25+45	>20
13	porous 2/4	25	>20	porous 8/11	25	>20
14	porous 2/6	25	>20	porous 8/11	25	>20
15	porous 2/6	25	>20			
24	porous 4/8	25	>20			
31	porous 8/11	45	>20			

4.2.3 Poro-Elastic Road Surfaces (PERS)

The Poro-Elastic Road Surface (PERS) is a material which is designed and prefabricated in Japan. The dimension of the slab is 1 m × 1 m × 30 mm. Pictures of the PERS slab used in this study are shown in Figure 4-4. It can be seen that

there are perpendicular grooves on the bottom of the slab and these grooves divide the bottom side into blocks with the size of 20 cm × 20 cm. The depth of the groove is 1 cm.

The PERS slabs were only used in this research to explore the effectiveness of measuring sound absorption coefficients with the Microflown surface impedance device. They are not included in other measurements. Details related to the measurement on PERS can be found in Section 4.4.2.

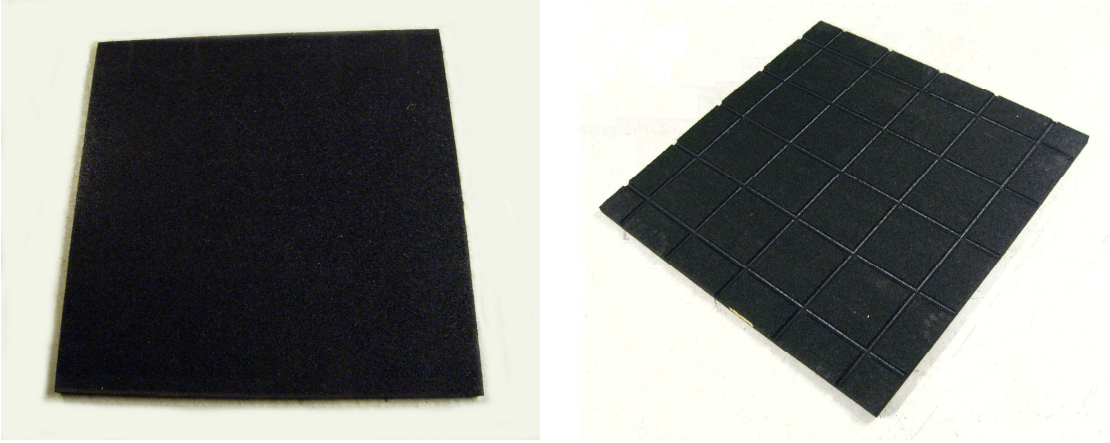

(a) Top surface (b) Bottom surface

Figure 4-4 PERS slab used in the test

4.3 Texture Measurement Method

4.3.1 Test device

For the surface texture measurements, high precision and accuracy are essential because of the rather small aggregate size which is used for thin surface layers. In this research program, a stationary laser profilometer was designed and developed based on the texture measurement regulation ISO 13473 [2]. The company Comax bv in The Netherlands was consigned to design and manufacture the device.

The laser profilometer is composed of three main parts, i.e. a laser sensor, a beam and a track which also works as the base for the device. A picture of the complete laser profilometer and the laser sensor are shown in Figure 4-5. The laser sensor, which contains a laser source and an optical sensor, is mounted on the steel beam for measuring the height of the surface profile. The vertical resolution of the laser sensor is 0.01 mm. The beam can move back and forth along the track. Data of the surface profile is collected by the laser with an interval of 0.1 mm in the moving direction. The laser sensor is also able to move in the transverse direction along the beam. The smallest distance between two neighboring measuring lanes is 1 mm. For an effective reception of the signal, the distance between the laser source and the sample surface needs to be between 90 cm and 130 mm. This can be realized by adjusting the vertical position of the censor.

The device is suitable for in-situ measurements of in service roads and in the laboratory on asphalt mixture samples. To start the test, the device is placed on the pavement or the sample. The measurement is controlled by a computer program. For starting a test, the sensor is firstly moved to the starting point. The number of test tracks, track length, and distance between two neighboring tracks need to be set on the control software. In a measurement, the beam moves forward along the track while the laser sensor is collecting the surface profile data. When the test on one track is finished, the data are transferred into the computer. Then the beam moves back to the starting point of the next track and the next test is started. The measuring process is computer controlled and is accomplished automatically. As the operating speed of the data collection is smaller than 60 km/h, the device is, according to the classification in ISO 13473-3 [2], treated as a stationary and slow type profilometer.

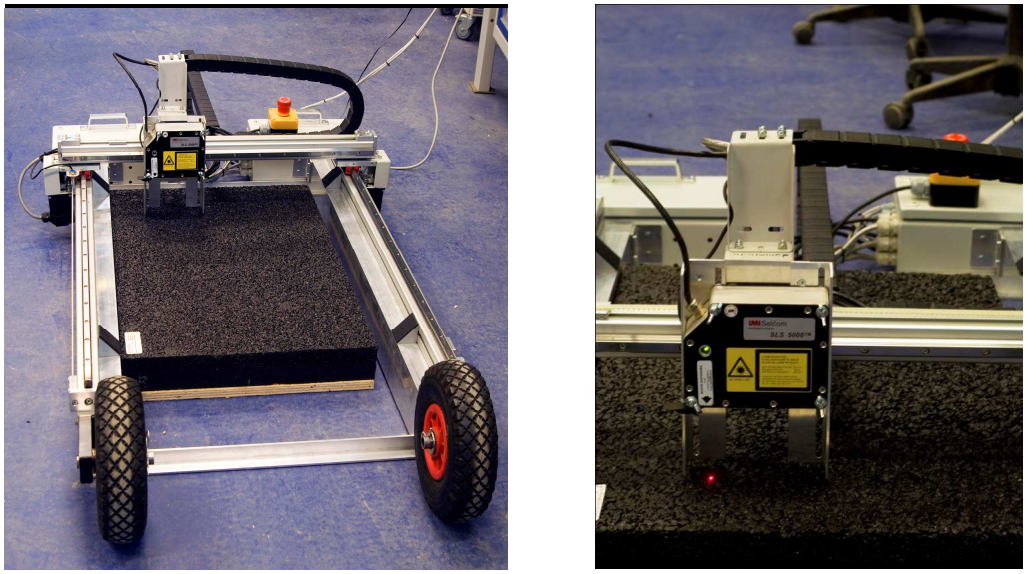

(a) Laser Profilometer (b) LMI SLS 5000 Selcom laser sensor

Figure 4-5 Laser profilometer and the laser sensor

4.3.2 Data proceeding methods

As shown in Figure 2-13, the Mean Profile Depth (MPD), Estimated Texture Depth (ETD), and effective root mean square value (RMS) can be calculated based on the collected data. Expressions of these indexes are given in Figure 2-13. Determination of the MPD is also written as follows:

$$MPD = (1^{st} \text{ peak level} + 2^{nd} \text{ peak level})/2\text{-average level} \qquad (4\text{-}1)$$

Based on signal processing theories, spectral analysis can also be performed for characterizing the surface profile. The profile (texture) spectrum is obtained by either digital or analogue filtering techniques. The results are expressed as the magnitudes of spectral components at different wavelengths. In this case, the resulting amplitudes within a certain frequency band can be transformed into a

unique indicator defined as texture profile level *TL*. Mathematically, *TL* is expressed by a logarithmic transformation of an amplitude representation of a profile:

$$TL_i = 10 \cdot \lg\left(\frac{\alpha_{t,i}^2}{\alpha_{t,ref}^2}\right) = 20 \lg \frac{\alpha_{t,i}}{\alpha_{t,ref}} \quad (4\text{-}2)$$

Where

TL_i – the texture profile level at octave band with wavelength λ_i (ref. 10^{-6}m), dB;

λ_i – the center wavelength of the octave band, mm;

$\alpha_{t,i}$ – the root mean square (RMS) value of the vertical displacement of the surface profile, m;

$\alpha_{t,ref}$ – the reference value (= 10^{-6} m).

Details of the MPD calculation and the spectral analysis of surface texture based on the laser tested data are given in the ISO Standard 13473 part 1 [3] and part 4 [4] respectively.

4.3.3 Influence of sample dimension

Laboratory samples of asphalt mixtures are generally cylindrical cores or rectangular slabs. In the specification [3], it is suggested to use the largest samples available and each profile measured should be at least 100 mm long. In terms of the size, both the slab and core samples in this research meet these requirements.

In the spectral analysis, the required evaluation length l depends on the longest octave-band-center wavelength λ_{max}. For a stationary and slow type profilometer, the relationship is $l \geq 5\ \lambda_{max}$ [4]. For core samples, the maximum measuring length is 150 mm (the diameter). According to the relationship, the longest wavelength that can be evaluated is 32 mm on the 1/3 octave band. This indicates that the cores cannot provide texture level information for longer wavelengths. Therefore, the spectral analysis is not conducted on core samples. Only the MPD is calculated for scaling the surface texture of a core.

The length of the slab is 700 mm, which is larger than the upper limit of the distance that can be scanned by the device in the longitudinal direction (500 mm). So the evaluation length for the slab is 500 mm. The maximum octave-band-center wavelength λ_{max} is approximately 125 mm in the 1/3 octave band. This implies that the measurements performed on the slabs also provide information about the longer wavelengths. Therefore the spectral analysis is performed on the slab measurements. Also the MPD is calculated.

4.4 Sound Absorption

4.4.1 Measurement device

Two standard methods for testing the sound absorption of road surface materials are the impedance tube and the Extended Surface Method (ESM) according to ISO 10534-1 and ISO 13472-1 respectively. In this research, a new measurement approach is applied which is based on the so called P-U free field technology [5]. The device used is the Surface Impedance Setup developed by Microflown Technologies. The principle and an image of the setup are shown in Figure 2-22.

As the measurement is based on free field technology, the reverberant room or the impedance tube is no longer required. So the device can be used for non-destructive tests on road surfaces as well as on samples in the lab. Compared with the impedance tube measurements, there is also no upper frequency limitation. With the tube measurements the upper frequency limitation is proportional to the inverse of the tube diameter [6]. The applicable frequency range of the free field test is up to 20 kHz. Moreover, the acoustic behavior of the material under oblique incident waves can be measured.

During the test, the loudspeaker emits a continuous sound signal. The sound pressure (P) and the acoustical particle velocity (U) at the same position are measured by the P-U probe simultaneously [7]. The acoustical impedance for the free field Z_{ff} is calculated using:

$$Z_{ff} = \frac{P\left(h_s - h_p\right)}{U\left(h_s - h_p\right)} = \frac{i\rho_0 c_0 k \dfrac{Q}{4\pi\left(h_s - h_p\right)} e^{-ik\left(h_s - h_p\right)}}{\dfrac{Q}{4\pi}\dfrac{ik\left(h_s - h_p\right)+1}{\left(h_s - h_p\right)^2} e^{-ik\left(h_s - h_p\right)}} = \frac{ik\left(h_s - h_p\right)}{ik\left(h_s - h_p\right)+1}\rho_0 c_0 \quad (4\text{-}3)$$

With

Q – sound strength from the source, m^3/s;
k – the wavenumber, m^{-1};
h_s – distance from the point source to the sample, m;
h_p – distance from the probe to the sample, m;
ρ_0 – the density of air;
c_0 – speed of sound in air.

Similarly, the acoustical impedance measured close to the sample surface $Z_{measure}$ is given by:

$$Z_{measure} = \frac{i\rho_0 c_0 k \frac{Q}{4\pi\left(h_s - h_p\right)} e^{-ik\left(h_s - h_p\right)} + i\rho_0 c_0 k \frac{Q}{4\pi\left(h_s + h_p\right)} e^{-ik\left(h_s + h_p\right)} R_p}{\frac{Q}{4\pi} \frac{ik\left(h_s - h_p\right)+1}{\left(h_s - h_p\right)^2} e^{-ik\left(h_s - h_p\right)} - R_p \frac{Q}{4\pi} \frac{ik\left(h_s + h_p\right)+1}{\left(h_s + h_p\right)^2} e^{-ik\left(h_s + h_p\right)}} \tag{4-4}$$

$$= \frac{\frac{e^{-ik\left(h_s - h_p\right)}}{\left(h_s - h_p\right)} + R_p \frac{e^{-ik\left(h_s + h_p\right)}}{\left(h_s + h_p\right)}}{\left(\frac{ik\left(h_s - h_p\right)+1}{ik\left(h_s - h_p\right)}\right)\frac{e^{-ik\left(h_s - h_p\right)}}{\left(h_s - h_p\right)} - R_p\left(\frac{ik\left(h_s + h_p\right)+1}{ik\left(h_s + h_p\right)}\right)\frac{e^{-ik\left(h_s + h_p\right)}}{\left(h_s + h_p\right)}} \rho_0 c_0$$

With the ratio of measured impedance and the free field impedance, the reflection coefficient R_p can be derived:

$$R_p = \frac{\frac{Z_{measure}}{Z_{ff}} - 1}{\frac{Z_{measure}}{Z_{ff}}\left(\frac{h_s - h_p}{h_s + h_p}\right)\left(\frac{ik\left(h_s + h_p\right)+1}{ik\left(h_s - h_p\right)+1}\right)+1} \frac{h_s + h_p}{h_s - h_p} e^{ik\,2h_p} \tag{4-5}$$

Consequently, the sound absorption coefficient α is obtained by:

$$\alpha = 1 - \left|R_p\right|^2 \tag{4-6}$$

When testing in a normal room, the room reflection influences the measurement which gives a noisy result. In order to get rid of the room reflection, a moving average filter is used to smooth the data. In this study, the moving averaged result in a normal room was found to be similar to the result obtained in an anechoic room at frequencies higher than 150 Hz [8]. The moving average filter was used in all sound absorption tests performed in this study.

The surface impedance measurement is a new technology, and there is no specification how this test should be performed on a road surfaces or asphalt mixture samples. In order to obtain a better understanding about how to use the device, a series of exploration tests was undertaken. Measurements were carried out on different types of road surfaces in various conditions, including in situ pavements, core samples and slab samples. The influence of measurement distance and sample size was investigated. The results of the exploration tests are described in the remaining sub-sections of 4.4.

4.4.2 Study on the effects of the distance of the probe to the measured surface

The distance between the probe and the sample surface is one of the most important factors affecting the results of the measurement. According to the

manufacturer, the distance should be as small as possible. In order to unify the measurement distance in the tests, the influence of the distance was investigated first.

In the laboratory, the test was performed on the 1 m × 1 m PERS slab. The surface area is large enough for eliminating the influence of the sample dimension. The measurements were taken at a distance of 5 mm, 15 mm, 20 mm, 30 mm, 50 mm and 150 mm. As a distance smaller than 5 mm is difficult to control, the smallest distance was set as 5 mm. A tripod was used to fix the device and keep the probe in a stable position during the test. The test position was above the center of the slab. Figure 4-6 illustrates the test position on the PERS slab. The sound absorption curves from the tests are plotted in Figure 4-7. It can be seen that the results achieved below (≤) 20 mm distance from the slab are comparable except for certain deviations at low and high frequencies. With the increase of the measurement distance, the absorption curves show greater fluctuations. It is thus recommended to keep the measurement distance less than 20 mm and as small as possible. In all the laboratory measurements in this research, the distance between the probe and sample surface is set at 5 mm.

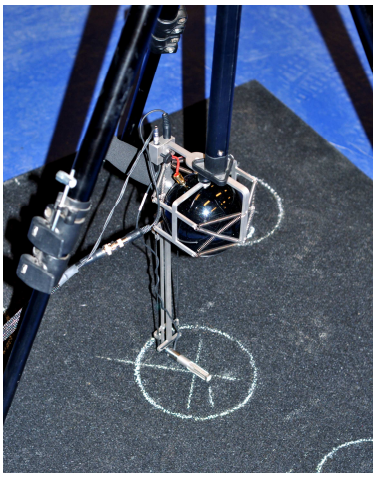

Figure 4-6 Absorption measurement on the PERS slab

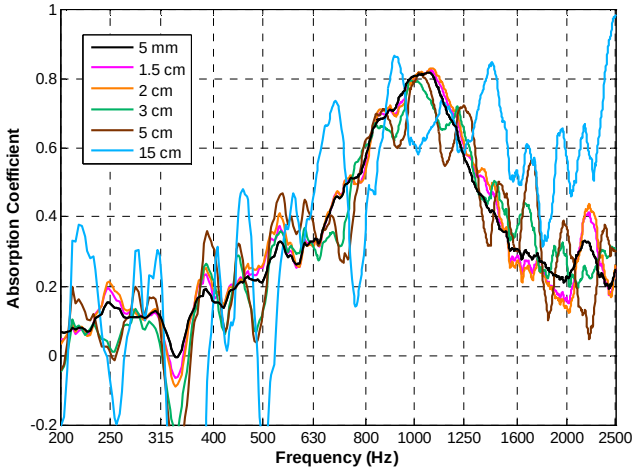

Figure 4-7 Absorption measurements on a PERS slab at several probe-surface distances

4.4.3 Measurement on core samples

4.4.3.1 Measurements on original cores

Sound absorption measurements were performed both on the core samples and the sections where the cores were drilled. The tests are illustrated in Figure 4-8. The in-situ test was done at three points around the coring position. A wind cap was placed on the probe to reduce the influence of the wind noise in the lower frequency ranges (see Figure 4-8 (a)). As the wind cap has a certain thickness, the distance from the probe to the surface could not be as small as in the laboratory test. The smallest distance in the field test was set at 30 mm. According to the former study on the setup, the distance between the P-U probe and the test surface was set at 5 mm for the test in the lab. A tripod was used to fix the setup during the measurements.

(a) Measurement on field (b) Measurement on the core

Figure 4-8 Sound absorption measurement in the field and on original cores

In this study, core samples were kept in the same state as they were collected in field. So the cores kept their original heights and no cleaning took place. The measured absorption coefficients from the original cores were compared with those obtained in-situ. In Figure 4-9, examples of the test results are given. In this chapter, porous asphalt samples are mostly used to show the results. As the sound absorption curve for porous asphalt generally has an obvious peak, it provides convenience for readers to observe the curves and make comparisons. The selected curves are representative for all the measured ones. Data acquired in the measurements were smoothed by the moving average linear method and the absorption coefficients are presented in 1/12 octave band.

The in-situ test results show one clear peak on each absorption curve. The positions of the peaks are different from each other because of the different thicknesses and tortuosities of the porous asphalt surfaces [9]. For the original core samples, the coefficients in the low frequency range (generally below 400 Hz) are quite high. The locations and the heights of the second peaks are also not always consistent with the in-situ measurements. It should therefore be

concluded that the test results on the cores are not comparable with those obtained from the in-situ measurements. Therefore it is concluded that using the surface impedance setup directly on core samples is not advisable. Special precautions should be taken.

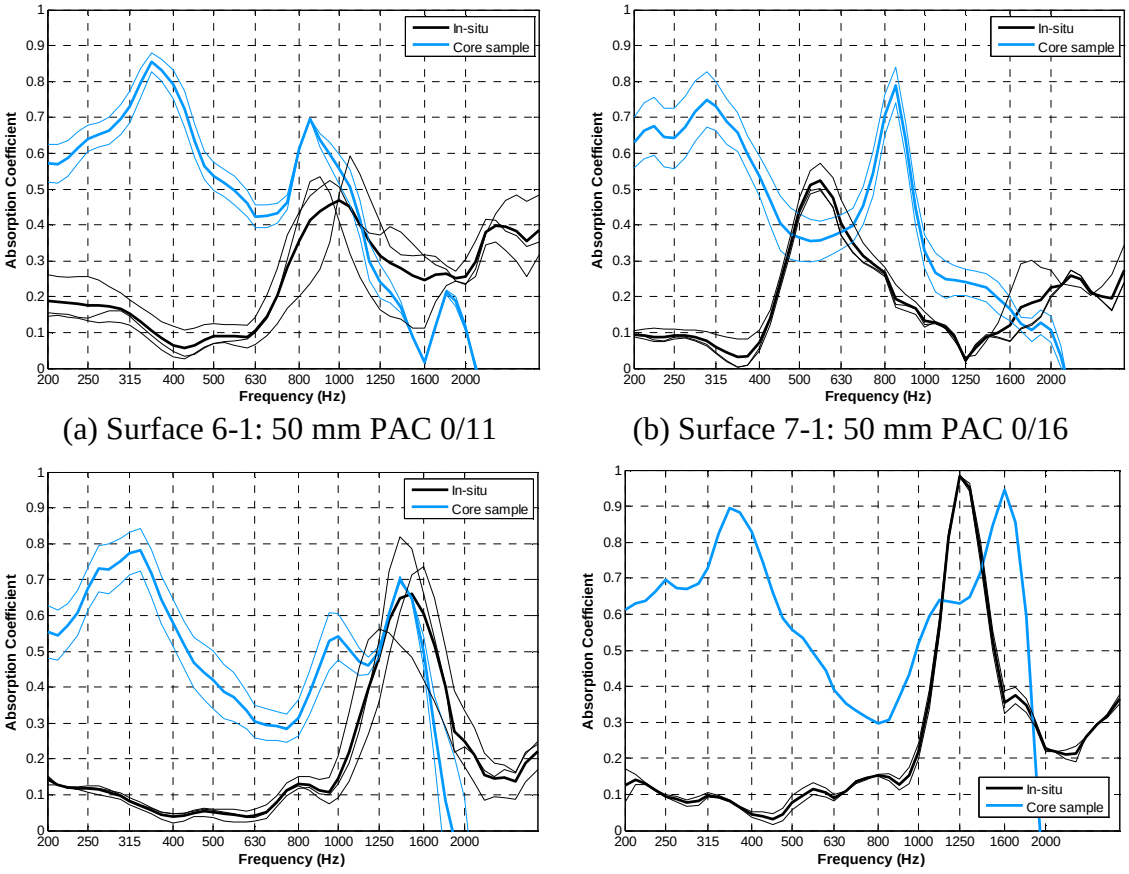

(a) Surface 6-1: 50 mm PAC 0/11

(b) Surface 7-1: 50 mm PAC 0/16

(c) Surface 9-1: 25 mm PAC 4/8

(d) Surface 31-1: 45 mm PAC 8/11

Figure 4-9 Absorption measurement results on field and original core samples

Figure 4-10 is a schematic diagram showing the sound wave propagation in a road surface and a core sample. The ground floor and the layer below the porous layer are considered as rigid. It is speculated that the disagreement in absorption measurement done on slabs/surface layers and cores is mainly caused by (as marked in Figure 4-10): 1) the fact that part of the sound waves are spread into the space around the core, and the device records these waves as being absorbed; 2) the sound leaks through the voids which are interconnecting the core surface and its sides.

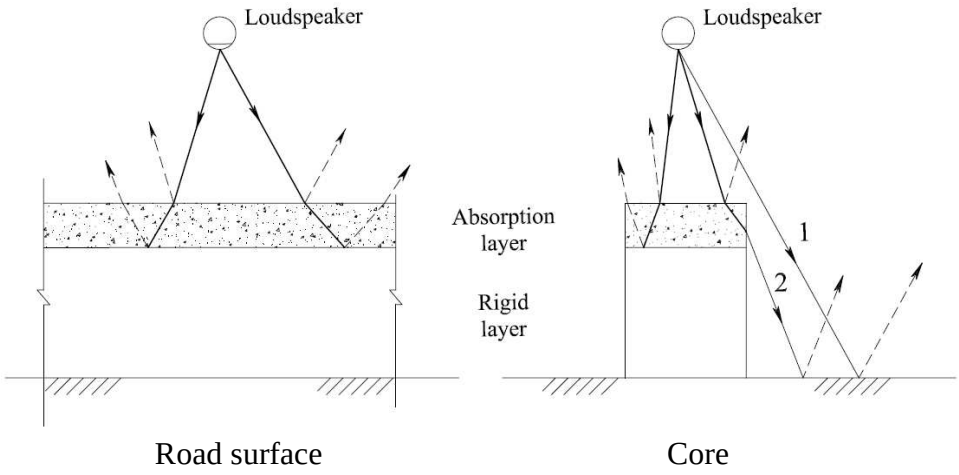

Figure 4-10 Sound impedance test on a slab/road surface and a core

For a better understanding of the factors influencing the acoustic measurements on cores, experiments were performed on cores prepared in the following two ways.

1) Wrapped cores: The core was firstly wrapped in a plastic film over its full height and then sealed with scotch tape outside. This preparation aims at preventing the sound leak from the exposed voids in the sides. It should be noted that the smearing in the coring process could cause close of the pores in the side walls. However, for porous asphalt samples with high air voids, the influence is not big. Exposed pores can be seen on the side wall of the core.

2) Cut cores: The surface layer including 10 mm of the underlying base course was cut from the core in order to reduce the height of the core without damaging the porous layer. The influence of the height can be investigated by comparing the results obtained on the cut cores with those obtained on original cores with the full height.

Figure 4-11 shows the wrapped cores and cut cores used in the tests. The absorption results obtained on the wrapped and cut cores are shown in Figure 4-12. As the tendency observed from all the core samples is similar, only the result of one representative measurement is given for both types of samples. It can be seen from Figure 4-12(a) that the peak values and the location of peaks do not change when the core is wrapped. Only small changes occur in the medium frequency range. So the interconnected pores between the core surface and the side do not have a major influence on the sound absorption measurement on a core sample.

In Figure 4-12 (b), it is found that the absorption coefficients decrease strongly at low frequencies and the values are close to the results of the in-situ test when the core is shortened. However, the coefficients rise between 800-1000 Hz. From the shapes of the curves before and after cutting, it seems that the high values in the

low frequency range “move” towards the higher frequencies when the height of the core becomes smaller.

(a) Wrapped core (b) Original and cut cores

Figure 4-11 Examples of the wrapped core and cut cores

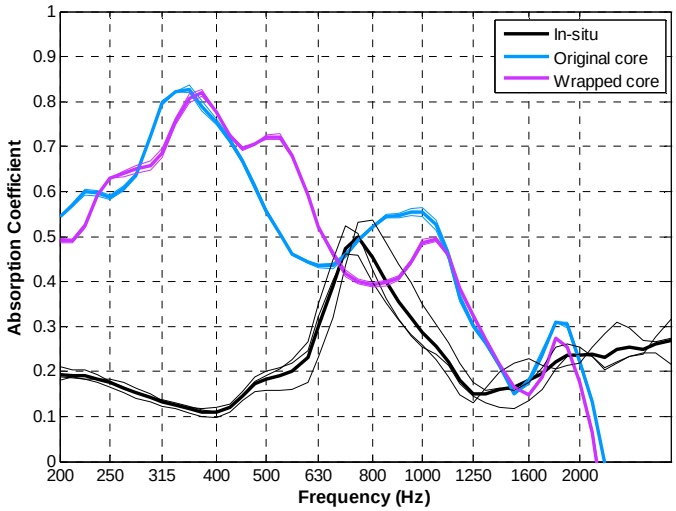

(a) on wrapped core 8-2

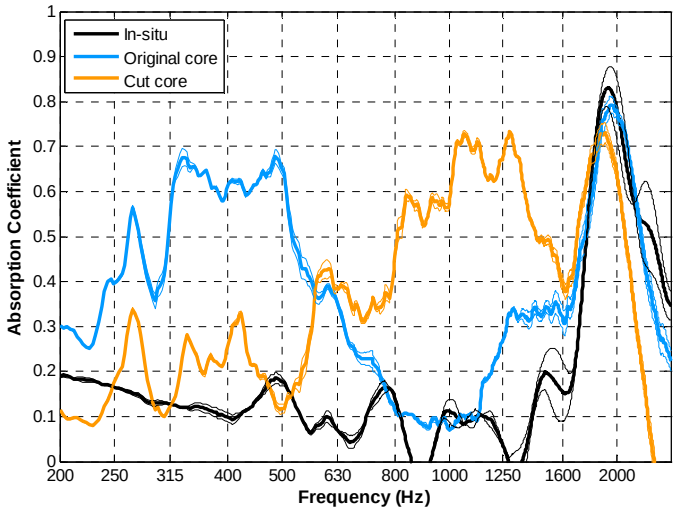

(b) on cut core 9-2

Figure 4-12 Sound absorption results obtained on a wrapped and cut core

4.4.3.2 Improvement of the measurement method

Based on the analysis presented above, it is concluded that the height and the surface size of a sample strongly influence the sound absorption test results with the surface impedance setup. Consideration should be paid to these two factors for improving the laboratory test with the P-U free field technology:

Core height: From comparison between the tests on cut cores and original cores, as given in Figure 4-12 (b), the height of the core influences the frequency where the peak absorption coefficient occurs. When the height of the core is smaller, the peak position is closer to the in-situ test. In order to diminish the influence, the height should be as small as possible. In other words, there should be little altitude difference of the surface in the testing field.

Surface area: According to a former study by Microflown, the P-U probe works well on a surface with dimensions larger than 150 mm × 150 mm [5]. As a consequence, the size of a road surface sample should be at least 300 mm × 300 mm for a slab sample and cylindrical samples should have a diameter of at least 300 mm. However, the diameter of a core sample commonly used in road engineering test is 100 mm or 150 mm. Cores with a diameter of 300 mm are not easy to achieve in the lab or from the field. These observations imply that slab samples with a surface size larger than 300 mm × 300 mm are to be preferred for laboratory test. This type of sample can also conveniently be produced in most road research labs.

For a core sample, the surface size of which is fixed by the mold, an effective way to improve the measurement is to enlarge the testing surface area and diminishing the influence of the height of the core. An auxiliary platform was designed to address this objective. The platform therefore consists of a wooden table with a hole in the center and an iron tube with a circular edge support. The surface area of the table is 1 m×1 m. Details of the design parameters for the table and the tube are shown in Table 4-5 and Table 4-6 respectively.

Table 4-5 Design parameters for the wooden table

Parameter	Value
Material	dense wood (okoume multiplex)
Dimension of the table top	1 m × 1 m × 30 mm
Height of the table	250 mm from top surface to the ground
Position of the hole	center of the table
Diameter of the hole	156 mm

Table 4-6 Design parameters for the iron tube

Parameter	Value
Material	iron
Height	80 mm
Interior diameter of the tube	150 mm
Thickness of the sidewall	3 mm
Outside diameter of the tube	156 mm
Outside diameter of the edge support	200 mm
Thickness of the edge support	1 mm

When utilizing the platform, the core is firstly wrapped with tape on the sidewall. With this treatment, the side wall of the core is considered to be fully sealed. The wrapped cores are placed in the tube which is then settled into the hole of the table. This mounting can be considered as a simulation of Kundt's tube. Similar measures were also taken in the tests done by the Microflown company. In their study, a simple wooden structure was used as boundary to simulate the mounting of the impedance tube [8]. The gap between the sample and the tube sidewall is filled by wrapping the core with plastic film and duct tape to prevent leaking of the sound wave. This also helps to seal the exposed pores in the sides of the core. During a measurement, the surface of the core is kept on the same horizontal level as the table. The platform and the position of the core during the test are shown in Figure 4-13.

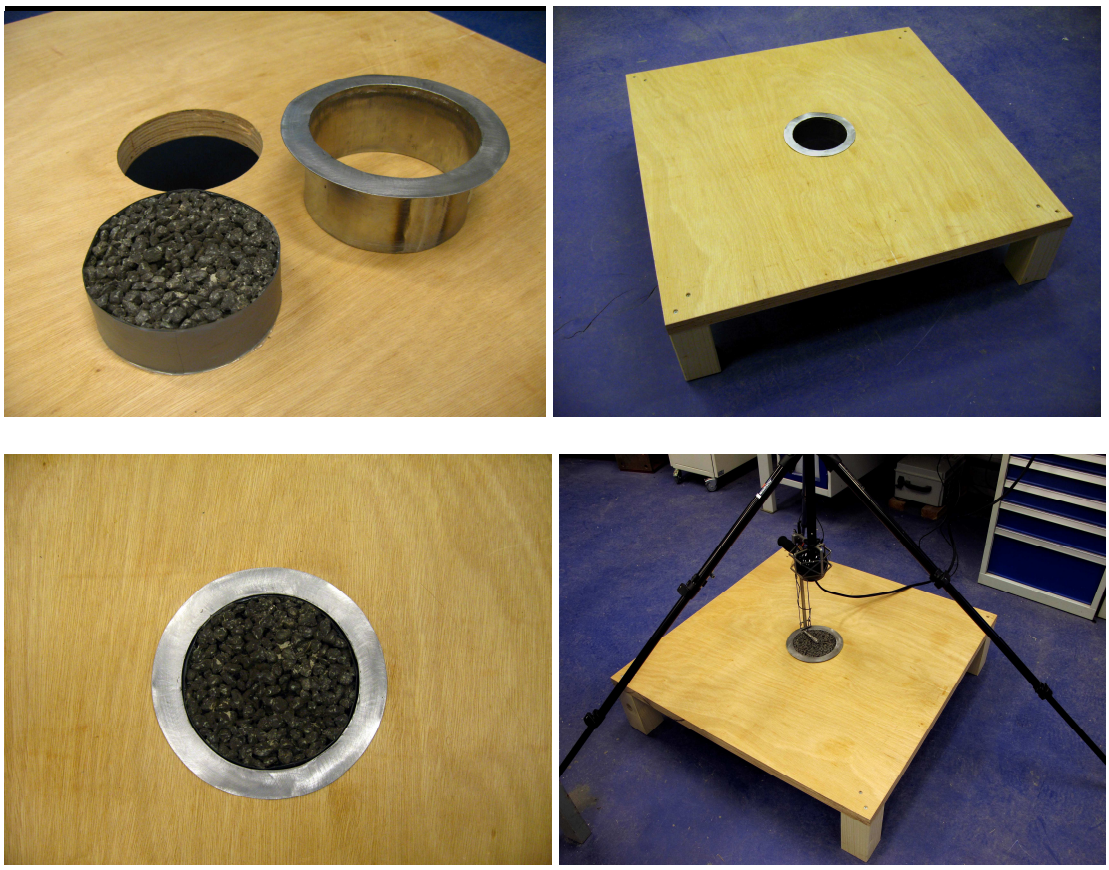

Figure 4-13 Platform supporting the absorption measurement on core samples

A number of sound absorption measurements on cores were taken with the platform set-up. Results from some samples are given in Figure 4-14. In order to study the influence of the surface of the platform, a dense steel plate, the sound absorption of which is regarded as 0, was also placed in the tube for testing. A picture of the steel plate placed in the platform is shown in Figure 4-15. The measurement result is shown in Figure 4-16. In this case, the sound absorption can totally be attributed to the wooden surface of the platform, as the steel part is not considered to absorb sound waves. The analyses described here-after are performed by reviewing all the test results; they are not only limited to the charts shown here. Other test results can be found in the CD attached to this thesis.

For cores 7-1, 9-1 and 31-1, see Figure 4-14 (b), (c) and (d), the maximum absorption coefficients and the positions of the peaks measured on cores in the platform are in good agreement with the in-situ tests. However, there are also differences between the tests on cores with platform and the in-situ measurements for some surfaces. For example, in Figure 4-14 (a), the maximum absorption coefficient occurs at a lower frequency range compared to the in-situ measurement for surface 6-1. Theoretically, the position of the maximum absorption coefficient is related to the thickness of the absorber and the tortuosity of the porous structure [9]. As there is no change of the thickness or the structure of the porous surface in the process, the reason of this peak “shifting” is most likely caused by the test method with the platform.

There is a small peak around 360 Hz for each absorption curve by testing with the platform, which can be seen in Figure 4-14 (c) and (d). By comparing with Figure 4-16, a similar peak around 0.2 is also observed at the same frequency. As the steel core does not absorb the sound waves, the peaks are recognized to be caused by the wooden surface surrounding the core. For a more exact description of the sound absorption coefficient of the core sample, this influence of the surrounding surface needs to be removed from the curve. Nevertheless, measurements using cores and the platform are in general in reasonable good agreement with the field measurements (see Figure 4-14).

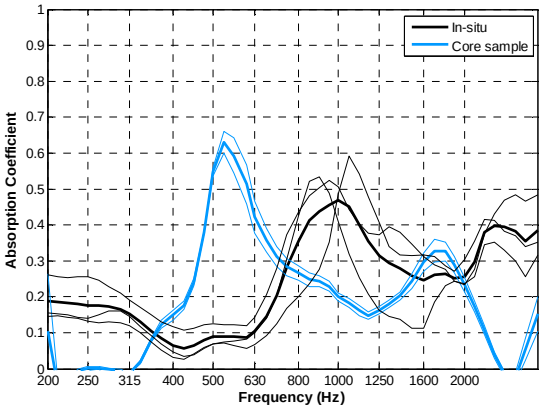

(a) Surface 6-1: 50 mm PAC 0/11

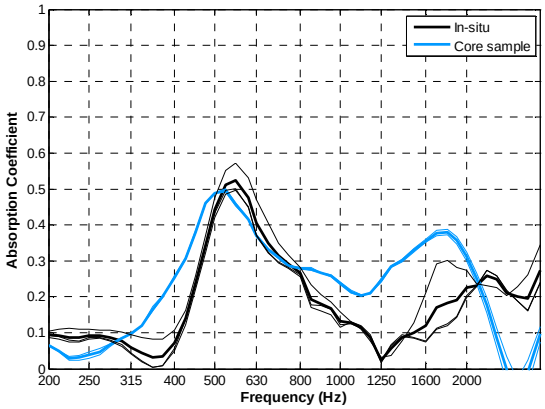

(b) Surface 7-1: 50 mm PAC 0/16

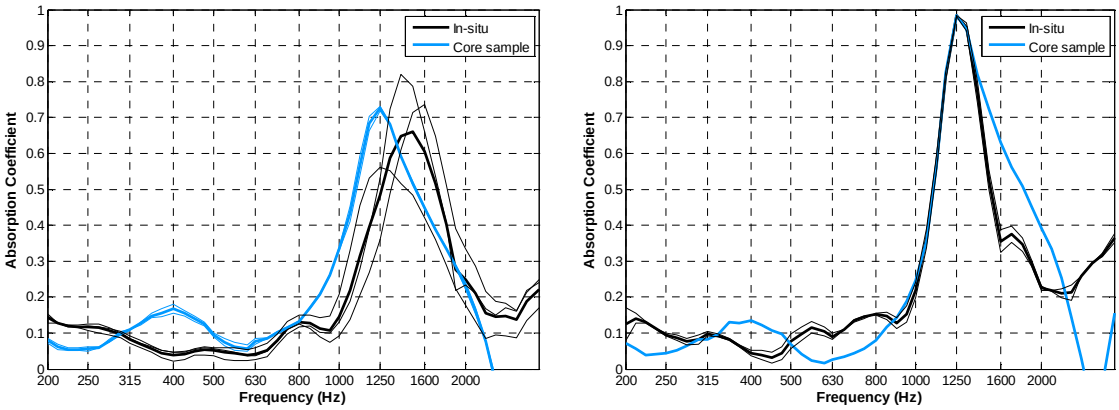

(c) Surface 9-1: 25 mm PAC 4/8 (d) Surface 31-1: 45 mm PAC 8/11

Figure 4-14 Absorption measurement results on field and original core samples

Figure 4-15 Steel plate placing in the platform

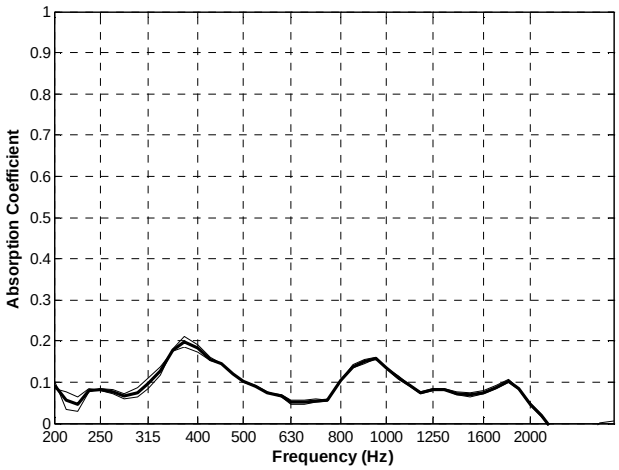

Figure 4-16 Absorption measurements on steel plate placing in the platform

4.4.3.3 Comparison with impedance tube test

For verifying the test method with the platform, further investigations were made by comparing the measurement results obtained with the Microflow equipment and using the platform with those obtained from the standard method by using the impedance tube. Several cores were selected for testing with the impedance tube; the measurements were carried out in the acoustical lab at Hogeschool

Windesheim in the Netherlands. The device used in the test is shown in Figure 4-17. The samples used in this test are cores with a diameter of 100 mm. Those cores were drilled from 150 mm diameter core samples used in the platform test. In this study, the thin layer surfacing slabs were also involved. After absorption measurements on the slab, cores with a diameter of 150 mm were drilled from the slab samples and used in the sound absorption test with the platform. 100 mm diameter cores were then drilled from the 150 mm cores for the impedance tube measurements.

In an impedance tube measurement, the core sample is mounted at the rigid end of the tube. The incident plane sound wave signals are generated by the loudspeaker at the other end of the tube. The maximum and minimum sound pressure amplitudes at different frequencies are recorded. The sound absorption coefficients are calculated from those pressure amplitudes. According to the length of the tube, the sound absorption can be measured precisely up to a frequency 1250 Hz. The results for frequencies higher than 1250 Hz are not reliable. The sound absorption coefficients from the field test, test with the platform and impedance tube test are compared in Figure 4-18. As the sound absorption coefficients from the impedance tube test are generated on the one third octave band, all the three curves in the figure are illustrated in the one third octave band.

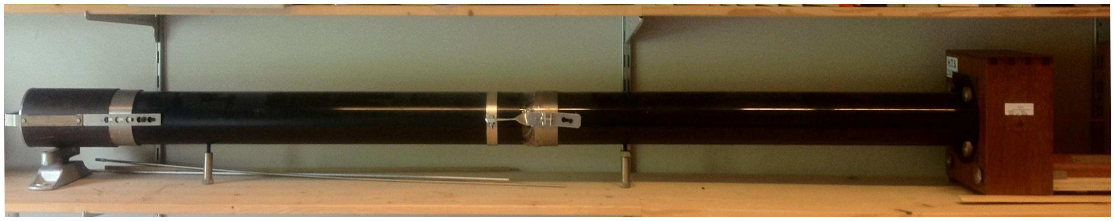

Figure 4-17 Impedance tube for sound absorption measurement

From existing studies on elastic porous material [10] and foams [8], it is known that the sound absorption property may change when samples are cut from the free field samples and mounted in a tube. As shown in Figure 4-18, the investigation performed in this research also shows that the sound absorption determined by the P-U probe on cores placed in the platform does not always match the response determined by means of tests on a large surface (being the surface of a real pavement) or the response determined by means of the impedance tube. The test result is affected by both the size and the mounting method of the sample. It can be stated that the measurement results obtained on core samples, by means of the surface impedance setup or the impedance tube, reflect the sound absorption ability of the cores, but not always the sound absorption ability of the practical road surface made of the same material.

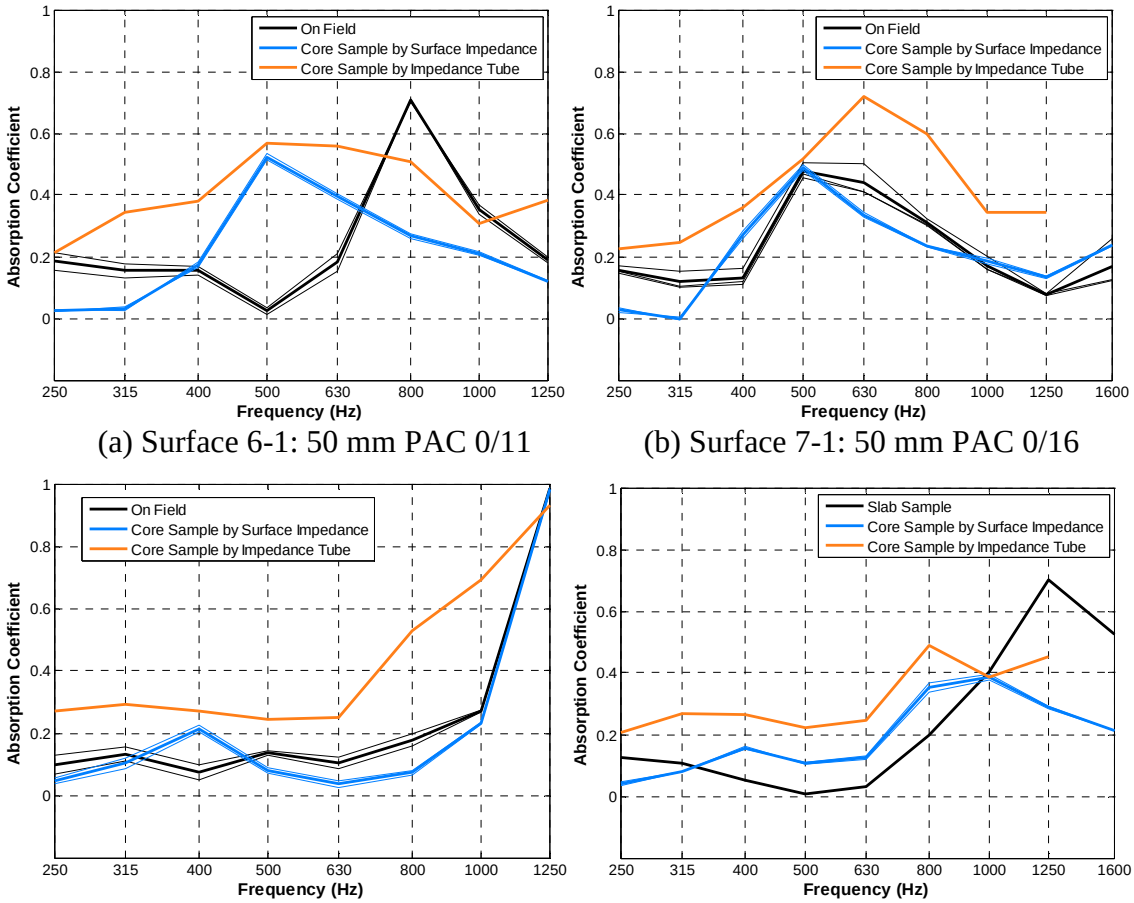

(a) Surface 6-1: 50 mm PAC 0/11

(b) Surface 7-1: 50 mm PAC 0/16

(c) Surface 31-1: 45 mm PAC 8/11

(d) Slab P02

Figure 4-18 Sound absorption as determined by three different methods

From all the test results and the analysis described above, it is suggested that the core samples should not be used in a laboratory measurement of sound absorption of road surface. Slabs have to be produced. Only when slabs cannot be produced, measurements with the surface impedance setup and platform might be considered. For the pavement in service, the tests are preferred to be carried out directly on the road surface.

4.4.4 Measurement on slab samples

Experiments were carried out on slab samples for exploring appropriate operations for using the surface impedance setup. According to Microflown, slab samples with a size larger than 300 mm × 300 mm are preferred for an accurate absorption measurement with the surface impedance setup. The slab samples used in this research are 700 mm × 500 mm, which provides a sufficiently surface area for the test. Aiming for a refined observation, the absorption measurements were taken at 77 points on each slab. The test positions and the numbering of the positions are illustrated in Figure 4-19. As shown in Figure 4-19, the distance between two neighboring points in either the longitudinal or transverse direction is 50 mm. The closest distance from the point to the edge of the slab is 100 mm. The influence of the test positions, in particular the distance to the edge of the slab, was investigated by placing the slabs in different

surroundings. As shown in Figure 4-20, tests were carried out by placing the slab on a wooden pallet and on the concrete floor of the laboratory respectively.

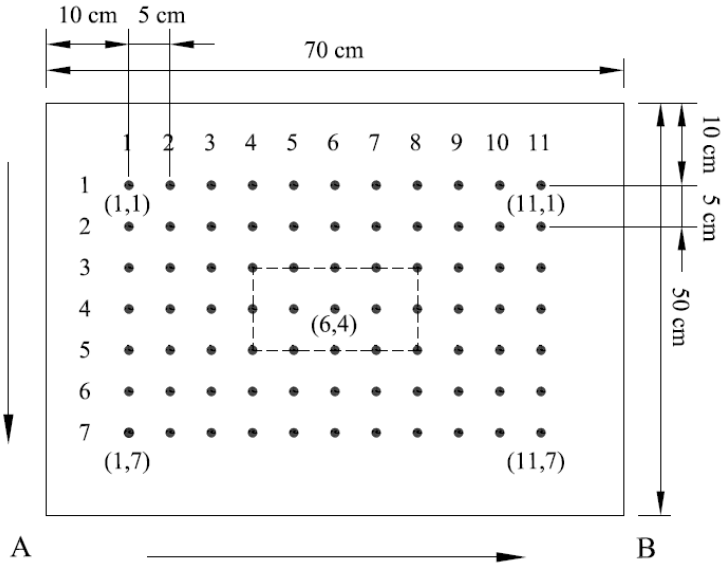

Figure 4-19 Measurement positions on the slab samples

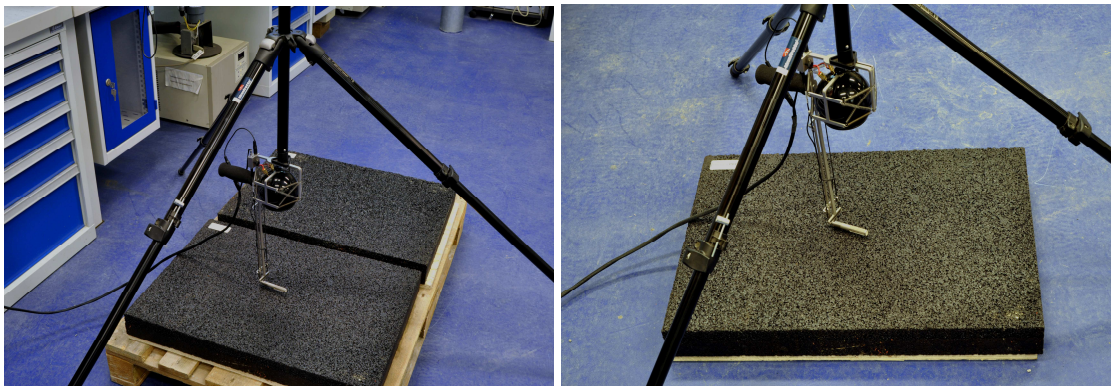

(a) on a wooden pallet (b) on the concrete lab floor

Figure 4-20 Sound absorption measurement on slabs

Examples of the test results are displayed in Figure 4-21. The sound absorption curves in Figure 4-21 are from the measurements on slab P02, the air voids content of which is 18%. Results from a quarter of the testing surface are displayed. For the figures in the first row, it can be seen that there is a large peak located between 630 Hz and 800 Hz from the test on the pallet. However, there is no such a peak on curves measured on the slab settling on the ground. The agreement becomes better when the test points are away from the edge. This indicates that the test position does influence the measurement results. When the test position is close to the edge, the measurement results tend to be influenced by the surroundings outside the sample.

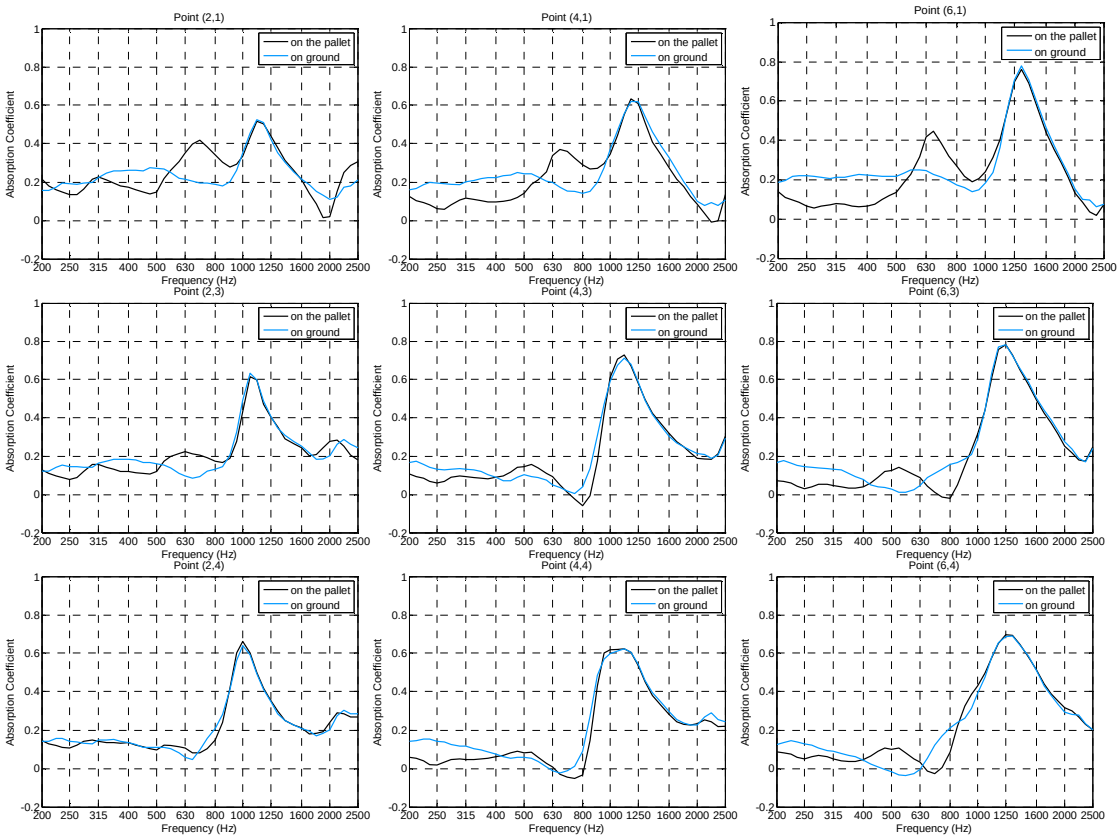

Figure 4-21 Sound absorption curves measured from different positions on slab P02

By comparing the results from different slabs, it was decided that only the results obtained on the 15 points around the central area could be taken into account for calculating a representative absorption coefficient of the slab. In other words, the distance from the testing point to the edge of the slab is suggested to be no smaller than 200 mm; the impact from the surrounding area can be neglected in this way. The selected area is illustrated as a rectangle with dashed line in Figure 4-19.

4.4.5 Summary of using the surface impedance setup

The surface impedance setup based on P-U technology was applied in the noise absorption measurements. Tests were carried out both on the trial sections in Kloosterzande and different types of samples in the lab, including PERS, thin layer surfacing slabs, and cores drilled from the Kloosterzande sections and cores drilled from the thin layer surface slabs. Based on the results that were obtained, the following conclusions are drawn for using the device for sound absorption measurements of road surfaces.

(1) With respect to the size of the surface area, the following is concluded: Measurements on large areas (road surface, 1 m × 1 m PERS slab, 700 mm × 500 mm slab samples) provide reliable results. Field measurements are always to be preferred. In the laboratory experiments, the test surface should be large enough to eliminate the influence of the surroundings

outside the slab. It is found that the influence is slight when the distance from the test point to the edge is larger than 20 cm. Thus it is suggested that the size of the slab sample should be not smaller than 40 cm × 40 cm. Results achieved from the central area are considered valid for presenting the sound absorption ability of the material.

(2) With respect to the probe-surface distance the following is concluded. From the current test results and previous studies by Microflown, it is known that the test results are less accurate when the distance is larger than 20 mm. Therefore, the probe should be kept as close as possible to the test surface, especially when the surface area is small. 5 mm is suggested in the lab measurement. A tripod has to be used for stable positioning of the probe. When a wind cap is used in field tests, the maximum distance should be around 30 mm.

(3) It is suggested that core samples should not be used in the measurement. Only in case slabs cannot be produced, the test might be done by using the platform to evaluate the sound absorption coefficients of road surface.

4.5 Mechanical Impedance Measurement

Because the mechanical impedance is considered influential parameter on tyre - road noise only recently, there is no standardized test yet to measure this parameter. Generally speaking, the mechanical impedance can thus be estimated by applying an impact to the road surface and recording the response of the material in terms of vibrations [11]. In this research, an impedance hammer system is applied as a simple method for evaluating the mechanical impedance of surface samples.

Stiffness is an important mechanical property of the road surface which can be measured with various test methods in the lab. It is of interest to study the relationship between the stiffness and the mechanical impedance of the road surface materials. With this relation, the mechanical impedance of the road surface can thus be estimated from the measured stiffness. Therefore, in this research, the stiffness of the materials is also to be tested and the cyclic indirect tension test (ITT) is used for this purpose.

4.5.1 Mechanical impedance measurement with impedance hammer

A hammer excitation device is used for measuring the mechanical impedance of the materials investigated in this research, see Figure 4-22. The device consists of a hammer for applying the impact load, one sensor in the head of the hammer for recording the force and three accelerometers measuring the acceleration of the sample surface. This technology has been extensively used for testing the dynamic properties of railway structures [12, 13]. For measurement on road surface materials, it is suggested to be used on samples with a large surface area [14]. In this study, the test was carried out on the Kloosterzande test sections and on the laboratory slab samples. As the size of core samples is small, it cannot

simulate the response of the real road surface subjected to a blow of the impact hammer. Thus the cores were not involved in the measurement with this method. The measurement procedure is as follows [15].

1) Three accelerometers are placed on the surface of the slab samples for measuring the vibration due to the impact load generated by the hammer. For achieving an even response at each sensor position, the sensors are placed at 120 degrees intervals around the hitting point. The placement of the sensors is illustrated in Figure 4-22 (a). In the test, three 4 cm × 2 cm steel sheets are firstly glued onto the surface of the top layer, and the sensors are fixed on the steel sheets. In order to get an as good as possible measurement of the surface reaction to the impact load, the sensors were placed as close as possible to the point of impact. However, enough space is also needed for applying the impact load. For balancing both requirements, the center to center distances between each two sensors is set at 65 mm.

2) As the slabs were used for other measurements as well, the surface needed to be kept as much as possible in its original condition. Therefore bitumen is used for sticking the steel sheets on the sample. Using an epoxy type of glue, might cause damage and pollution of the surface.

3) The floor of the lab is not perfectly flat, and gaps could exist between the bottom surface of the slab and the floor of the lab. A carpet was placed underneath the slab, with the aim to provide uniform contact between the slab and the laboratory floor.

4) A hammer with a plastic tip is chosen to increase the contact time of the load pulse with the surface. The material is also more similar to that of vehicle tires than a metal hammer tip.

The mechanical impedance test is performed at a room temperature (around 20^{o}C). During a measurement, five hits are applied on the central position of the small area surrounded by the sheets in 8 seconds. A picture of the hitting can be seen in Figure 4-22 (b). The force is measured by the sensor in the hammer, and the motion of the surface is recorded by the accelerometers.

For calculating the mechanical impedance, the data processing is performed according to the following steps:

1) Unit conversion and peak selection
As the original results are in the form of electrical signals, the data is firstly transferred into force and acceleration expressions using SI units. Examples of the load and acceleration versus time curves are shown in Figure 4-23 (first hit on the center of slab P01). It can be seen that the force acts on the sample during a very short time, less than 1 ms. Vibrations at the surface where the sensors are located last for 0.01 to 0.015 second.

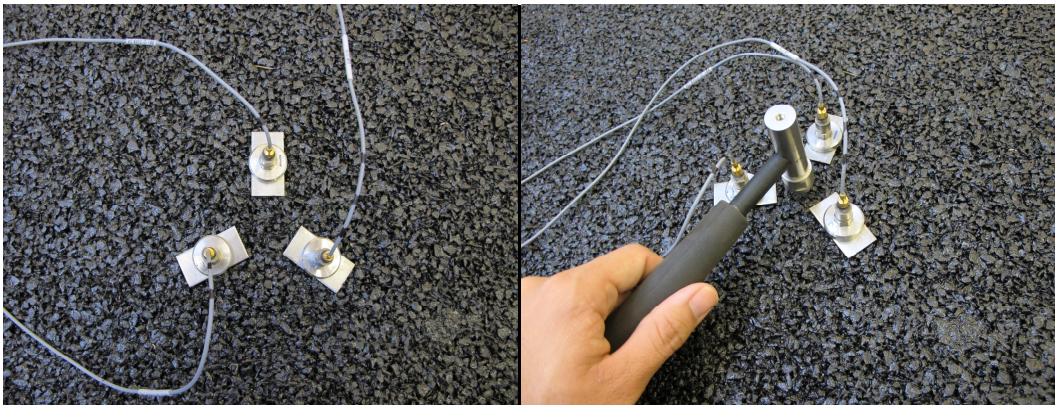

(a) Placement of the sensors (b) Hammer hitting the slab surface

Figure 4-22 Impedance hammer measurement on slab samples

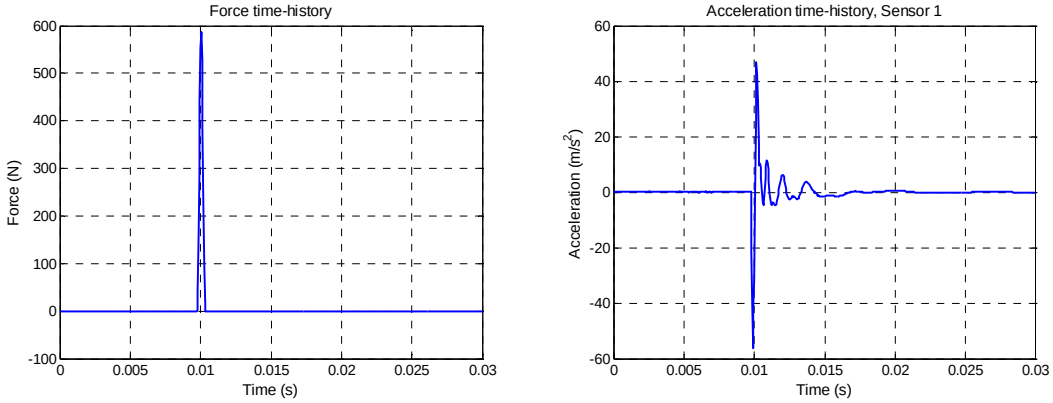

Figure 4-23 Example of force and acceleration time-history

2) Velocity calculation

The velocity of the vibration is obtained by integration of the acceleration. In this study, the Trapezoidal rule is employed for the numerical integration [16]. The velocity v_i in the hitting period is calculated using the following equation:

$$v_i = \int_{t_1}^{t_2} a_c(t)dt \approx (t_2 - t_1)\frac{a_c(t_1) + a_c(t_2)}{2} \quad (4\text{-}7)$$

Where a_c is the acceleration at time t, and t_1 and t_2 are two neighboring moments at which the accelerations are recorded. In this study, the integration period t_2 - t_1=0.00005 s.

3) Mechanical impedance calculation

The mechanical impedance is calculated by its definition, as given in Eq. (2-28). Since the driving force acts shortly on the surface, only acceleration data measured during the same period are taken into account. Acceleration data outside this period are all set to 0 in the calculation. As the velocity is at different positions to where the driving force is applied, the calculated results are therefore considered as mechanical transfer impedance. These mechanical impedance

values are then transferred into the frequency domain by doing a fast Fourier transformation (FFT) and expressed in decibels using the following formula:

$$L_z = 10 \cdot \lg(Z / Z_{ref}) \tag{4-8}$$

where L_Z is the decibel expression of mechanical impedance in the frequency domain, Z is the measured impedance and Z_{ref} is the reference impedance Z_{ref} =1 Ns/m.

4.5.2 Resilient modulus measurements

In this study, the stiffness test is carried out for relating the stiffness with mechanical impedance. Several standardized laboratory test methods are available for measuring the dynamic modulus of asphalt mixes such as bending, direct tension-compression and cyclic indirect tension tests (ITT) [17].

The cyclic 5 pulse ITT method is used for determining the resilient modulus of the thin layer surfacing cores. The equipment used is a Universal Testing Machine (UTM). All samples had a diameter of 100 mm. The device with mounted sample is shown in Figure 4-24.

The tests are conducted at 5 temperatures being 5, 10, 15, 20, 25^{o}C. A typical plot of the applied load and the resulting displacement is given in Figure 4-25. Part a shows the instantaneous elastic response (deformation), part b shows the delayed elastic response, and part c shows the total recoverable deformation which is the sum of instantaneous and recoverable deformation.

Prior to the test, the specimens are conditioned for at least four hours at the test temperature. Then the specimens were placed into the loading apparatus. The mounting of the specimen was done according to the specification NEN-EN 12697-26 [17]. In the test, a pulse load is applied along the vertical diameter of the specimen via the loading platens. The horizontal deformation of the sample is measured by means of two linear variable differential transformers (LVDT).

The measurement is done in a load-controlled mode. The pulse load is selected sufficiently low to avoid permanent deformation and avoid fatigue damage during testing.

The tests were carried out from a lowest temperature 5^{o}C to a highest temperature 25^{o}C, with 5^{o}C increase at each time. Based on measurement results at these temperatures and load frequencies, master curves of the stiffness modulus of the mixtures were constructed.

At each temperature, the test was performed at loading frequencies of 8Hz, 4 Hz, 2 Hz, 1 Hz, 0.5 Hz and 8 Hz. The test at 8 Hz at the end is done to determine whether any damage develops in the sample. For this purpose the obtained modulus values are compared with the values obtained in the first measurement at the same frequency.

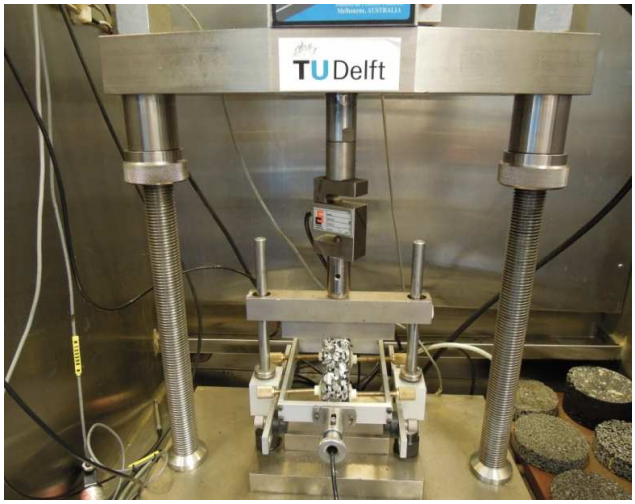

Figure 4-24 Setup of the cyclic ITT in the laboratory

The resilient modulus is calculated by using the equation:

$$M_R = \frac{F\left(v+0.27\right)}{h\,\Delta d} \tag{4-10}$$

Where
F – maximum applied force (repeated load), N;
v – Poisson's ratio;
h – thickness of the specimen, mm;
Δd – total recoverable horizontal deformation, mm.

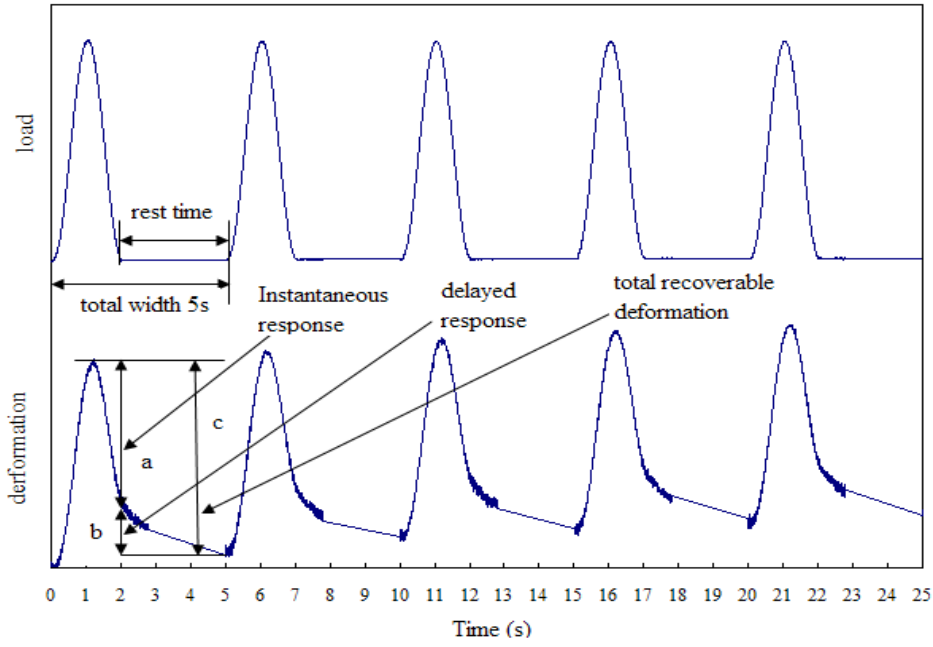

Figure 4-25 The load signal applied in the five pulses ITT and the resulting deformation

The result of mechanical impedance covers a large frequency (0 Hz-3000 Hz), while the stiffness in this test set-up can only be achieved at low frequencies, no higher than 8 Hz. In order to be able to make a comparison between the mechanical impedance and the stiffness at the same frequency, the time-temperature superposition principle was used to construct a master curve for the stiffness over a wide frequency range. This was done with the data collected at different temperatures. By shifting the stiffness modulus versus loading frequency for various temperatures horizontally with respect to the curve chosen as the reference, a complete master curve at a chosen reference temperature T_R can be assembled [18]. The shift factor a_T is defined as:

$$a_T = \frac{f_{red}}{f} \tag{4-11}$$

where f_{red} is the loading frequency where the master curve to be read, f is the loading frequency at which the modulus is obtained. The shifting factor can be determined by different methods. In this study, the Williams – Landel – Ferry (WLF) model was employed:

$$\log a_T(T) = \frac{a(T - T_R)}{b + T - T_R} \tag{4-12}$$

with constants a and b.

A sigmoidal model which similar to the one developed by Pellinen and Witczak [19] was then used for obtaining the master curves for all mixtures in this study. The model can be expressed as follow:

$$\log(M_{mix}) = \log(M_{min}) + \left[\log(M_{max}) - \log(M_{min})\right] \cdot M_t \tag{4-13}$$

with

$$M_t = 1 - \exp\left[-\left(\frac{10 + \log f_{red}}{\eta}\right)\right]^{\gamma} \tag{4-14}$$

where

M_{mix} – resilient modulus of mixture, MPa;
M_{min} – minimum modulus, MPa;
M_{max} – maximum modulus, MPa;
η, γ – shape parameters which are related to the curvature of the S-shaped function and the horizontal distance from the turning point to the origin, respectively.

As the mechanical impedance is measured around 20^{o}C, a reference temperature of 20^{o}C is selected to construct the master curves of the resilient modulus. All of the model parameters or constants were obtained by fitting the sigmoidal model to the experimental data. This was realized by minimizing the sum of squares of the errors using the Solver Function in the Excel.

4.6 CT-Scanning

The mixture composition of the sample is to be investigated by using X-ray Computerized Tomography (CT). This is a non-destructive three dimensional imaging tool originally developed for medical diagnosis. In recent years, the CT method has gained increasing application in research of civil engineering materials [20-22].

The principle of a CT-scanner is based on the extinction of X-ray radiation. In the test, the X-ray source and detectors rotate around the sample and determine the extinction of X-rays of the entire sample under a variety of angles. Thereafter, the computer can calculate the extinction value of a particular volume element within the sample. The density of the material in the scanned cross section is subsequently calculated and a two-dimensional image is created. The different grey scales in the image reflect the different densities of the objects.

The scanner used in this study is the Siemens SOMATOM Plus4 Volume Zoom medical scanner available at the Delft University of Technology. A picture of the machine is shown in Figure 4-26, in which the mounting of the sample is also displayed. The samples used in the test are cores with a diameter of 100 mm. The scanning is done in slices which are 1 mm apart. For a 30 mm thick sample, a total of 30 slices are scanned.

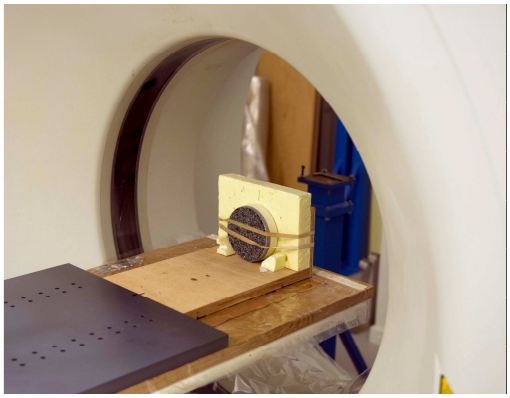

Figure 4-26 Mounting of the sample for CT scanning

The digital processing technique is then used to identify the mixture compositions based on the image from CT-scanning. For asphalt mixture samples, the volumetric composition of the material is represented in terms of air voids, mortar (defined here as bitumen, additives, filler, sand and aggregates <2 mm) and coarse aggregates (≥ 2 mm). The distinction between air voids, mortar and aggregate is made by the choice of the Hounsfield units (HU). Based on the density of the different components, the air voids have the lowest HU value, followed by the mastic, and then the aggregates. In order to determine the bulk volume of these three separate groups, threshold HU values need to be set. In the scanned image, everything below the first threshold is assumed the air voids, all between the two boundaries is the mortar, and everything above the second threshold is regarded as coarse aggregate. Determination of the threshold values

is implemented by using the volume sample analyzer in the software VGStudio MAX 2.0. Figure 4-27 shows an example of the results after the introduction of 500 HU as a border between the air voids and mortar and 1400 HU as a threshold value between the mortar and coarse aggregate. The yellow fields indicate the volume of air voids and coarse aggregates respectively in Figure 4-27 (a) and (b).

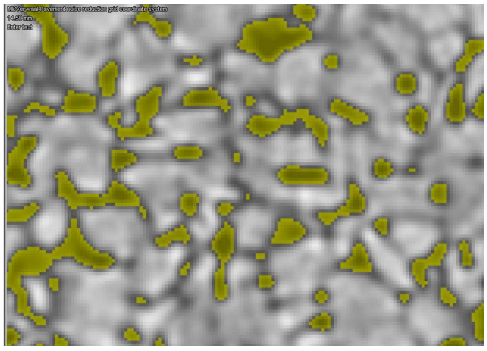

(a) Air voids content

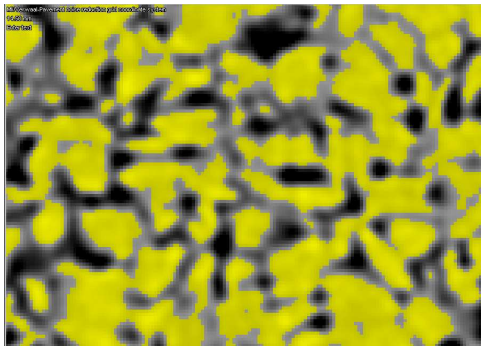

(b) Coarse aggregate content

Figure 4-27 Sectional view of the scanned core with 500 HU and 1450 HU as threshold values

With the border values set, the volume of the three separate groups per slice can be obtained. The calculation is executed with the assistance program in the software package Avizo. The area to be analyzed is first determined as shown in Figure 4-28. In order to eliminate possible disturbing effects of the core edges and the outside area, the analysis is performed in a cylindrical space cut out in the core, as illustrated in Figure 4-28 (a). All the scanned slices of the core are contained in the cylindrical space as shown in Figure 4-28 (b). Percentages of air voids, mortar and coarse aggregate are computed for each slice in the space. The average percentages of voids, mortar and coarse aggregate are calculated from a representative part of the sample being a few millimeters below the top surface to a few millimeters above the bottom of the sample. More details about using CT scanning image to determine the mixture compositions can also be seen in Chapter 5.

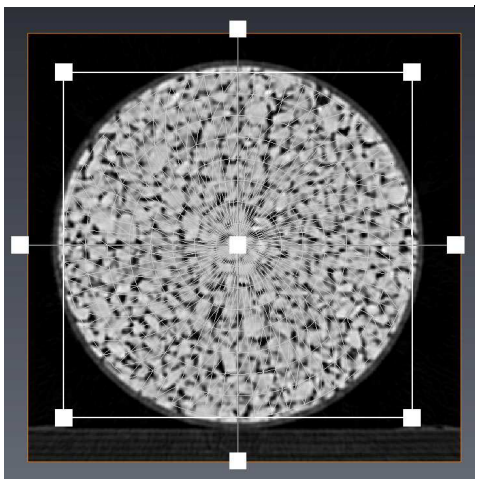

(a) Sectional view of the space

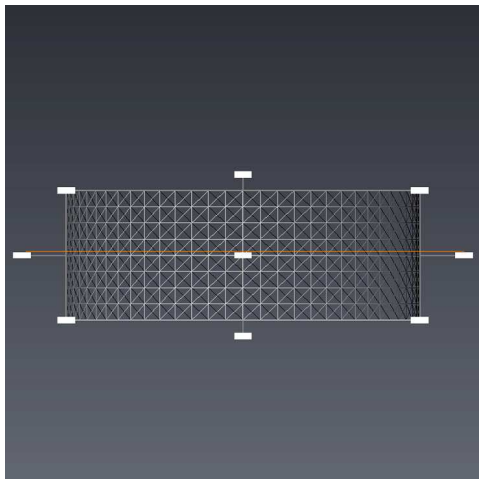

(b) Side view of the space

Figure 4-28 Space used for determination of the bulk volume percentages

References

1. van Blokland, G.J., Reinink, H.F., and Kropp, W., *Acoustic optimization tool. RE3: Measurement data Kloosterzande test track*, in *M+P Report DWW.06.04.8*. 2007, M+P Raadgevende Ingenieurs bv: Vught, the Netherlands.
2. ISO13473-3, *Characterization of pavement texture by use of surface profiles -- Part 3: Specification and classification of profilometers*. 2002, International Organisation for Standardization (ISO): Geneva, Switzerland.
3. ISO13473-1, *Characterization of pavement texture by use of surface profiles -- Part 1: Determination of Mean Profile Depth*. 1997, International Organisation for Standardization (ISO): Geneva, Switzerland.
4. ISO/TS13473-4, *Characterization of pavement texture by use of surface profiles -- Part 4: Spectral analysis of surface profiles*. 2008, International Organisation for Standardization (ISO): Geneva, Switzerland.
5. de Bree, H.-E., Leussink, P., Korthorst, T., Jansen, H., Lammerink, T.S.J., and Elwenspoek, M., *The μ-flown: a novel device for measuring acoustic flows.* Sensors and Actuators A: Physical, 1996. **54**(1–3): p. 552-557.
6. ISO10534-1, *Determination of sound absorption coefficient and impedance in impedance tubes - Part 1: Method using standing wave ratio*. 1996.
7. Lanoye, R., de Bree, H.-E., Lauriks, W., and Vermeir, G. *A practical device to determine the reflection coefficient of acoustic materials in-situ based on a Microflown and microphone sensor*. in *ISMA-International Conference on Noise and Vibration Engineering*. 2004. Leuven, Belgium.
8. de Bree, H.-E., Nosko, M., and Tijs, E. *A handheld device to measure the acoustic absorption in situ*. in *NVH GRAZ*. 2008.
9. James T. Nelson, E.K., Aybike Öngel, Bruce Rymer *Acoustical Absorption of Porous Pavement.* Transportation Research Record: Journal of the Transportation Research Board, 2008. **2058**: p. 125-132.
10. Vigran, T.E., Kelders, L., Lauriks, W., Leclaire, P., and Johansen, T.F., *Prediction and Measurements of the Influence of Boundary Conditions in a Standing Wave Tube.* Acta Acustica united with Acustica, 1997. **83**(3): p. 419-423.
11. Harris, C.M. and Piersol, A.G., *Harris' shock and vibration handbook*. 2002, New York: McGraw-Hill.
12. Remennikov, A. and Kaewunruen, S., *Determination of dynamic properties of rail pads using instrumented hammer impact technique.* Acoustics Australia, 2005. **33**(2): p. 63-67.
13. De Man, A.P., *Dynatrack: A survey of dynamic railway track properties and their quality*. 2002, Delft University of Technology: Delft, The Netherlands.
14. Schwanen, W. and Kuijpers, A.H.W.M., *Development of a measurement system for mechanical impedance*, in *SILVIA Project Report SILVIA-M+P-013-01-WP2-230605*. 2005.

15. Li, M., Molenaar, A.A.A., van de Ven, M.F.C., and van Keulen, W., *Mechanical Impedance Measurement on Thin Layer Surface With Impedance Hammer Device.* Journal of Testing and Evaluation, 2012. **40**(5).
16. Atkinson, K., *An Introduction to Numerical Analysis (2nd Edition)*. 1989, New York: John Wiley & Sons.
17. NEN-EN12697-26, *Bituminous mixtures –Test methods for hot mix asphalt – Part 26: Stiffness*. 2004, European Committee for Standardisation: Brussel.
18. Medani, T.O. and Huurman, M., *Constructing the Stiffness Master Curves for Asphaltic Mixes*. 2003, Faculty of Civil Engineering and GeoSciences, Delft University of Technology.
19. Pellinen, T.K. and Witczak, M.W., *Stress Dependent Master Curve Construction for Dynamic (Complex) Modulus.* Journal of the Association of Asphalt Paving Technologists, 2002. **71**: p. 281-309.
20. Emin Kutaya, M., Arambulab, E., Gibsonc, N., and Youtcheffc, J., *Three-dimensional image processing methods to identify and characterise aggregates in compacted asphalt mixtures*. International Journal of Pavement Engineering, 2010. **11**(6): p. 511-528.
21. You, Z., Adhikari, S., and Emin Kutay, M., *Dynamic modulus simulation of the asphalt concrete using the X-ray computed tomography images.* Materials and Structures, 2009. **42**(5): p. 617-630.
22. Gopalakrishnan, K., Ceylan, H., and Inanc, F. *Using X-ray computed tomography to study paving materials*. Proceedings of the ICE - Construction Materials, 2007. **160**, 15-23.

CHAPTER 5

MEASUREMENTS AND INVESTIGATIONS

5.1 Measurement Program

To investigate the surface characteristics and mixture compositions of thin layer surfacings, measurements were performed on thin layer surfacing samples. With these test results, the relationship between different surface characteristics and the material properties were investigated. The samples used in this study are the slabs produced in the lab of Ballast Nedam and the cores with thin layer surfacing on top taken from the Kloosterzande sections. For information about the slabs the reader is referred to Table 4-2. The mixture compositions of the cores from the Kloosterzande sections are shown in Table 4-4.

The important surface characteristics related to tyre - road noise, including surface texture, sound absorption, mechanical impedance and stiffness, were measured. The measurement methods are described in Chapter 4. CT scanning is used to determine the mixture compositions of the samples. The measurement programs for the slabs and the Kloosterzande samples are illustrated in Figure 5-1 and 5-2 respectively. The numbers in the figure indicate the order of testing. Outcomes from the different measurements are also shown in the figures. Specific information about the measurement programs are given here-after.

Texture and sound absorption tests can be performed directly on the slabs; no special precautions need to be taken. Furthermore these measurements do not affect the surface. Like the texture and absorption measurements, mechanical impedance tests by means of the impedance hammer also requires a large surface area. Due to the hammer impact on the sample, there could be slight damage of the surface after the test. Moreover, a small amount of bitumen is used to glue the steel bars on which the sensors are located to the pavement surface. Some of the bitumen inevitably remains on the surface, and it changes the original state of the surface. Considering these influences, the mechanical impedance test has to be carried out on the slab after the surface texture and sound absorption measurements.

One hundred fifty (150) mm diameter cores were drilled from three positions of each slab. They were used for comparing the sound absorption test results performed on slab and cores. The coring positions and numbering of the cores are shown in Figure 5-3. The 150 mm diameter cores from the slabs are not involved in the measurements mentioned in this chapter. The measurements on the Ø150 mm cores indicated in Figure 5-1 are discussed in section 4.4.3.3.

Core samples with a diameter of 100 mm were required for the stiffness tests. They were drilled from the 150 mm diameter cores after the sound absorption tests were performed. Then also the 40 mm dense bottom layer surface was cut off. The final sample is a thin layer cylindrical sample with 100 mm diameter and 30 mm thickness. Examples of the 100 mm cores and the samples used for stiffness testing are shown in Figure 5-3. CT scanning was also performed on these 100 mm diameter samples used for stiffness testing. The samples provide enough space for detecting the internal structure and mixture composition. As the bottom layer was removed, the CT scanning focused on the top layer, and no redundant data was collected. Because the stiffness test by using the ITT method could result in small deformation in the radial direction, the CT scanning was performed before the stiffness measurements.

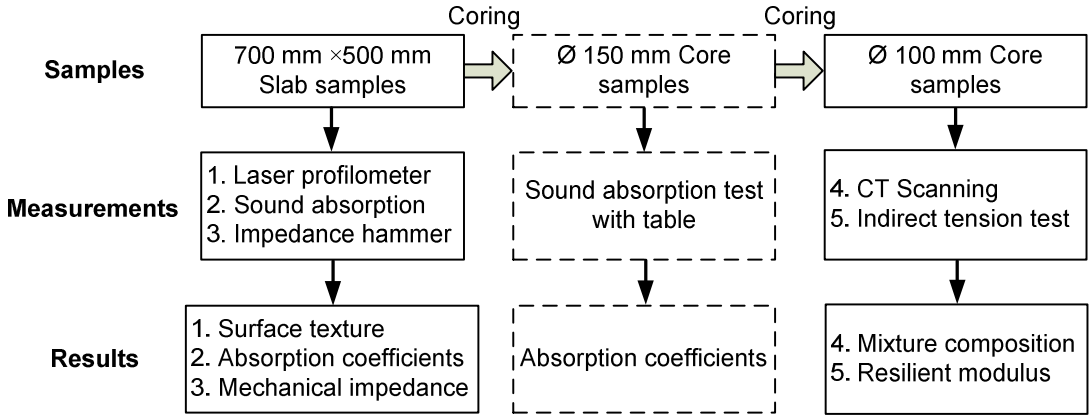

Figure 5-1 Measurement program on slab samples

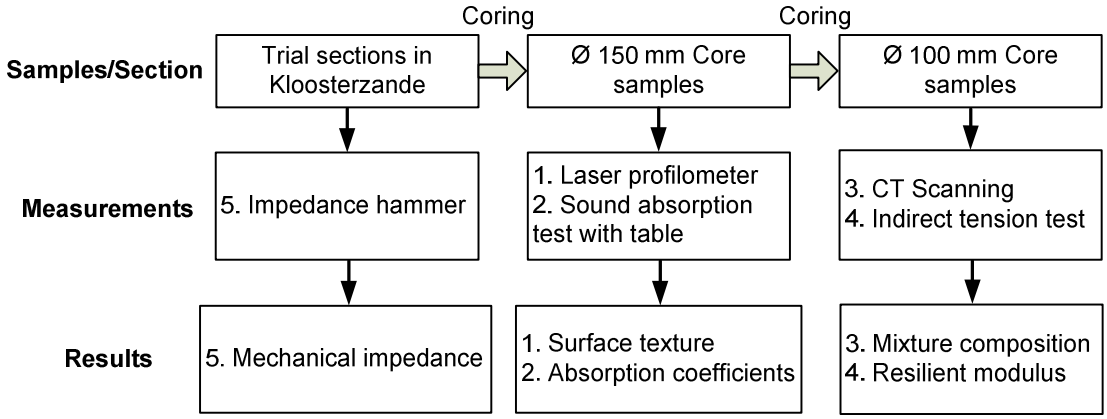

Figure 5-2 Measurement program on cores from the Kloosterzande sections

For the core samples from the Kloosterzande trial sections, similar considerations hold as for the slabs. The surface texture and sound absorption tests are performed on the Ø150 mm cores. As the surface of the cores is small, they cannot be used for impedance hammer testing. These tests were thus carried out directly on the surfaces of the Kloosterzande sections.

In this chapter, the measurement results obtained on the thin layer surfacing samples are reported and relationships between surface characteristics and material properties are explored. The CT scanning results are presented in Section 5.2. The surface texture, sound absorption and mechanical impedance and stiffness measurements are discussed in Sections 5.3 to 5.5.

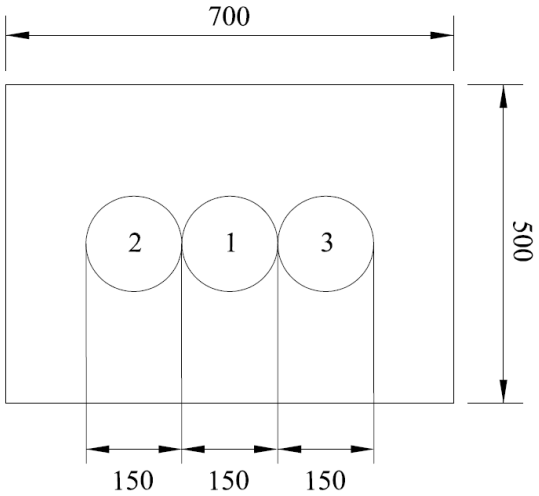

(a) Coring positions and numbers

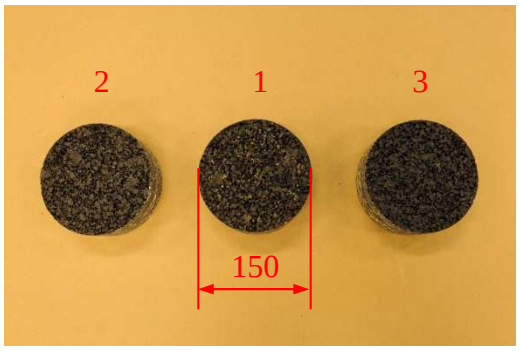

(b) 150 mm diameter cores from slab

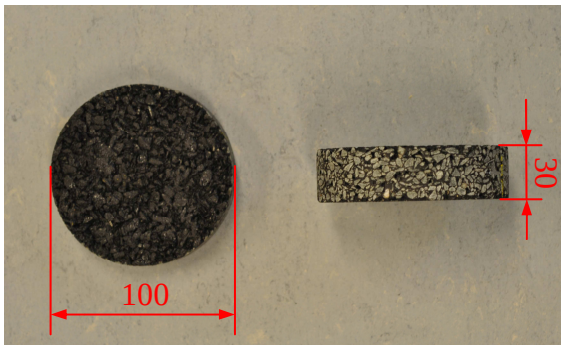

(c) Top view and side view of 100 mm diameter cores from slab

Figure 5-3 Cores from slabs and stiffness samples

5.2 Mixture Compositions

With the CT scanning measurement a reasonable indication of the mixture composition of the samples was obtained. The mixture composition, including air voids content, coarse aggregate and mortar content, represents some basic material properties and is taken into account for investigation of the surface characteristics. In this section, CT scanning data are presented; special attention is given to the amount of connected air voids in the porous structure since this is an essential parameter related to sound absorption of the road surface. This was evaluated using a cluster-labeling algorithm [1].

5.2.1 Selection of cores

Tests were performed on cores from both the slabs and the Kloosterzande sections. As there were 61 cores in total from these two sources (27 from slabs and 34 from sections), it was necessary to select the cores which are of interest for the research and to eliminate redundant work caused by scanning cores with the same surface properties.

The research focuses on single thin layer surfaces, so all the cores with a thin layer surface were considered as options for CT scanning. Certain porous asphalt samples were also chosen for comparing the properties with the thin layer surfaces; the related samples are from Kloosterzande sections numbered as 6, 7, 8 and 31. Four cores, namely Ref-1, P02-1, 4-1 and 9-1 were used in an initial trial with CT scanning. The selection is actually made using the following rules.

1) At least one core for each type of material needs to be scanned;

2) The porous asphalt samples are only used as references in this study, and therefore there was no need to scan all the samples. In this case, one core for each type of porous asphalt was selected. Cores 6-1, 7-1, 8-1 and 31-1 are chosen for CT scanning.

3) For slab samples, the cores drilled from the center of the slabs were all selected. They are marked as No.1 as shown in Figure 5-3. Some other cores, such as Ref-2, P02-2 and P07-3, were also included for comparison purposes. The resulting mixture composition of a certain slab is the average of all the cores drilled from it.

4) For thin layer surfacing samples from the Kloosterzande sections, the cores form the west lane were all selected. In addition, the measurement results of texture and sound absorption were also compared. Cores with different measured surface characteristics but identical designed material indexes needed to be scanned separately.

Based on the rules given above the cores shown in Table 5-1 were subjected to CT scanning. The total number of selected cores is 31.

Table 5-1 Core selection for CT scanning

Source of the Core	Selected ores for CT scanning	Amount
Ballast Nedam slabs	Ref-1, Ref-2, P01-1, P01-1, P02-2, P03-1, P04-1, P05-1, P06-1, P06-2, P06-3, P07-1, P07-3, P08-1, P08-2	15
Kloosterzande sections	2-1, 2-2, 3-1, 4-1, 4-2, 5-1, 5-2, 6-1, 7-1, 8-1, 9-1, 9-2, 15-1, 15-2, 24-1, 31-1	16

5.2.2 Investigation on mixture compositions

The 3D internal structure of the asphalt mixtures was acquired by using the X-ray CT scanning technique. Based on the grey images created from the CT scanning,

the spatial distributions of aggregate, mortar and air voids of the sample were determined. More details about CT scanning are given in Section 4.6. The air voids, mortar and coarse aggregate distribution at different depths of the samples are shown in Figure 5-4 and Figure 5-5. In the figures, examples from cores taken from the Ballast Nedam slabs and the Kloosterzande sections are given. CT scanning results for all the tests can be found in the CD, which is attached to this dissertation.

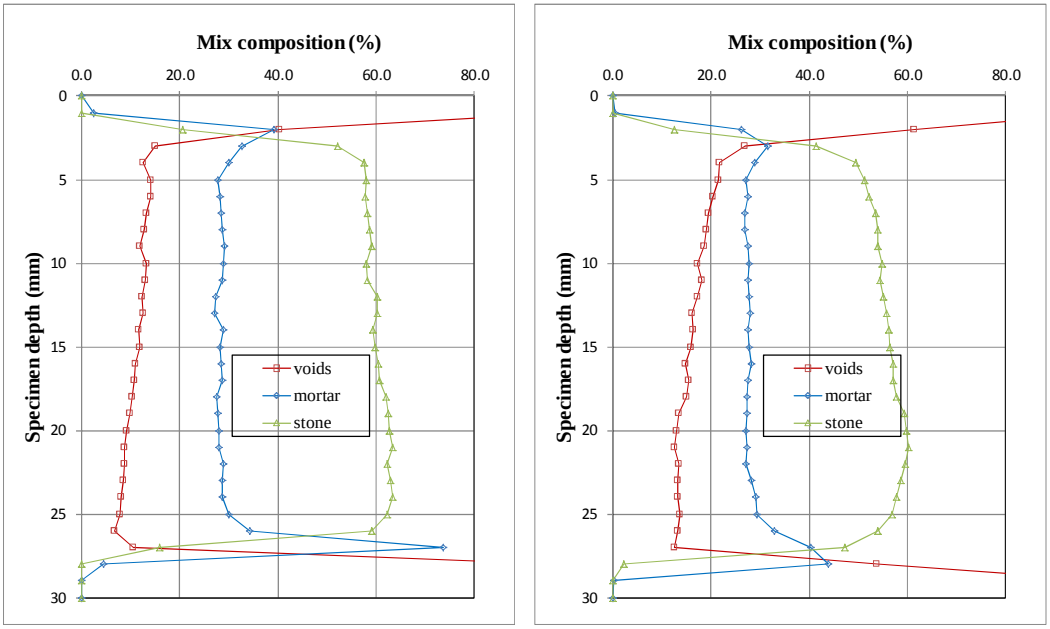

(a) Ref-2, 12% air voids content (b) P02-2, 18% air voids content

Figure 5-4 Mixture compositions of slab samples

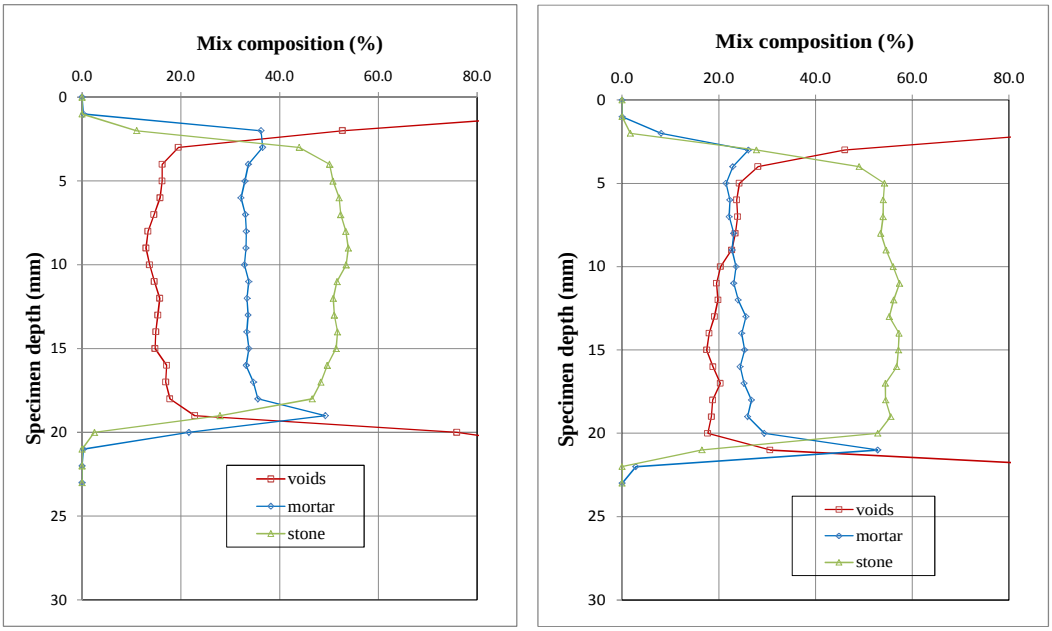

(a) 4-2, 12% air voids content (b) 9-2, >20% air voids content

Figure 5-5 Mixture compositions of core samples from sections

The following can be concluded from the measurements. The cores from the slabs show that the air voids content close to the surface is much higher than the designed value, and decreases with the depth. The air voids content generally meets the designed value at the half its thickness, and smaller values are found in the lower part of the sample. For example, as shown in Figure 5-4 (a), the air voids content at the surface of sample Ref-2 is 15%, and it decreases to 11.9% in the middle part of the core, which is approximately equal to the design value of 12%. At the bottom of the layer, the air voids content is 6.7%. The figure also shows that the mortar content is almost constant over the whole depth, and the coarse aggregate content increases somewhat with depth. Similar distributions of the mixture composition are observed on all the cores taken from the slabs.

The mixture composition over the height of the cores from the Kloosterzande sections appeared to be rather homogeneous. In certain cores, there is slight increase of the air voids content with depth (with a decrease of the coarse aggregate content correspondingly).

For each sample, the average mixture composition was calculated from the results of the different slices. Determination of the first and last images for calculating the average is based on investigating the component distribution and the scanned images. Figure 5-4 and Figure 5-5 show that the top and bottom slices have extreme high or low values for the void and aggregates content respectively, and they should be left out in the calculation. The calculation generally starts from the slice at a depth of: maximum aggregate size +1 mm. For example, for the mixture with maximum stone size 6 mm, the first slice used for the determination of the voids content at 6 mm+1 mm= 7 mm. It is thought that no aggregates are exposed at this position to the air. Blank images and partly scanned images due to small tilt or imperfect sawing of the samples at the bottom are excluded.

The rough mixture compositions obtained from the CT scans are expressed by volume fraction. The results for slabs and the cores can be seen in Table 5-2. The content of aggregate and mortar by mass can be evaluated when the densities of the specimen and aggregate are provided. Table 5-3 shows the bulk density of the mixture and the density of the aggregate for the different samples. The data were provided by the producer of the slabs, Ballast Nedam. The mass percentage of coarse aggregate and the mortar can be achieved by the equation:

$$P_{Ag} = \frac{V_{Ag} \cdot D_{Ag}}{D_S}, \qquad P_M = 1 - P_{Ag} \tag{5-1}$$

Where, P_{Ag} and P_M are respectively the content of coarse aggregate and mortar by mass, V_{Ag} and V_M are the volume fraction of coarse aggregate and mortar, D_{Ag} is the density of the stone, and D_s is the specimen density.

Table 5-2 Mixture composition by volume fraction

	Air voids content, % by volume	Designed air voids content, % by volume	Aggregate content, % by volume	Mortar content, % by volume
Ref	11.8	12.0	60.8	27.5
P01	10.7	8.0	63.0	26.3
P02	17.8	18.0	58.6	23.8
P03	8.8	8.0	59.8	31.2
P04	7.6	8.0	57.8	33.8
P05	12.6	12.0	65.9	21.5
P06	11.0	12.0	61.1	27.9
P07	12.1	12.0	62.2	25.7
P08	11.1	12.0	62.2	26.7
2-1	11.0	12.0	46.7	42.2
2-2	4.8	12.0	58.6	36.7
3-1	8.0	8.0	55.0	37.0
4-1	18.0	12.0	51.0	31.1
4-2	15.0	12.0	51.7	33.3
5-1	14.3	12.0	55.0	30.8
5-2	13.1	12.0	55.6	31.3
9-1	24.0	>20	52.3	23.7
9-2	20.3	>20	55.8	23.9
15-1	18.9	>20	44.3	36.8
15-2	18.4	>20	44.4	37.2
24-1	27.4	>20	50.6	22.0

Table 5-3 Density of mixture and aggregate for slab samples

	Density of the specimen, kg/m^3	Aggregate type	Aggregate density, g/m^3
Ref	2116	Bestone	2.705
P01	2215	Bestone	2.705
P02	1974	Bestone	2.705
P03	2211	Bestone	2.705
P04	2207	Bestone	2.705
P05	2116	Bestone	2.705
P06	2116	Tillred	2.62
P07	2116	Irish Greywacke	2.7
P08	2094	Bestone	2.705

The results of average content of air voids, coarse aggregate and mortar for the slab samples are shown in Table 5-4. The design value for each parameter is also listed It can be seen from the table that for a specimen with a designed air voids content of 12% respectively 18 %, the measured void content is around ± 1% off the target value. For samples with a designed air voids content of 8%, the measured void content is generally higher than the target. By comparing the results obtained for mixtures P01, P03 and P04, it is found that the air voids content is smaller for a mixture with a lower coarse aggregate content. Slab P04

with the smallest coarse aggregate content shows the lowest air voids content 8.37%, which is closest to the design value of 8%. This indicates that the target air voids content tends to be reached by using a smaller amount of coarse aggregate.

In this study, thin layer surfacings are defined by the air voids content Ω: dense ($\Omega \leq 9\%$), semi-dense ($9\% < \Omega \leq 14\%$), semi-open ($14\% < \Omega \leq 19\%$) and porous ($\Omega > 19\%$). According to the classification and the measured air voids content, sample P02 is a semi-open surface and all the other surfaces are considered as semi-dense or dense surface (This is only for P04).

For the measured coarse aggregate contents, the deviations from the design value are no more than 2.5% for all the samples. From the results, mixture P06 shows to have the smallest coarse aggregate content among the mixtures with a design coarse aggregate content value of 78%. The highest coarse aggregate contents are observed for samples P02 and P08.

It should be noticed that the calculation of the mixture composition based on CT images is influenced by the selection of the boundary values between the three groups in the grey image. The boundaries are distinguished by visual inspection and determination of the boundary values is to some extent arbitrary. However, the measurement results achieved in this study are generally in accordance with the designs and they are considered to be reasonable. The measured volumetric material properties are used for investigating surface characteristics as described in the following sections.

Table 5-4 Mixture composition of thin layer surfacing slabs

	Air voids content, % by volume	Designed air voids content, % by volume	Coarse aggregate content, % by mass	Designed coarse aggregate content, % by mass	Mortar content, % by mass	Mortar content from design values, % by mass
Ref	11.8	12.0	77.7	78.0	22.3	22.0
P01	10.7	8.0	77.8	78.0	22.2	22.0
P02	17.8	18.0	80.3	78.0	19.7	22.0
P03	8.8	8.0	73.1	72.0	26.9	28.0
P04	7.6	8.0	70.9	68.0	29.1	32.0
P05	12.6	12.0	80.0	78.0	20.1	22.0
P06	11.0	12.0	75.9	78.0	24.1	22.0
P07	12.1	12.0	79.3	78.0	20.7	22.0
P08	11.1	12.0	80.3	78.0	19.7	22.0

The surfaces of the Kloosterzande sections were designed and built by different contractors. The author does not have complete information of all the materials used. So the aggregate and mortar content of the samples from the Kloosterzande sections are not evaluated in this study. However, in general there are large differences in volumetric properties between cores from the Kloosterzande sections. In this study, it was decided to use the mixture composition data as determined by the contractors during their quality control.

The air voids and the corresponding design values for the cores taken from the sections are shown in Table 5-5. From the table, it can be seen that for cores with a design air voids content of 12%, the variation in the results is quite large. The air voids content of cores from section 4 is much higher than the target. In this case, the surface of section 4 can be regarded as semi-open type, which is designed as semi-dense type. Core 2-2 shows a very low porosity and it is thus regarded as dense surface. For the porous thin surfacings, the air voids content of cores from section No.15 is below 20%. It indicates that the air voids content does not meet the design value of porous asphalt, and they should therefore be treated as a semi-open surface. The fact that the actual material properties are different from the design could be due to construction or environmental influences. Nevertheless, the air voids contents determined by CT scanning are considered to reflect the status of the material properties of the core. They will be related to the surface characteristics in the following chapters.

Table 5-5 Air voids content of thin layer surfacing samples from Kloosterzande sections

	Air voids content, % by volume	Designed air voids content, % by volume	Coarse aggregate content measured on site, % by mass	Mortar content (100-coarse aggregate content), % by mass
2-1	11.0	12.0	50.8	49.2
2-2	4.8	12.0	50.8	49.2
3-1	8.0	8.0	66.2	33.8
4-1	17.0	12.0	75.9	24.1
4-2	15.0	12.0	75.9	24.1
5-1	14.3	12.0	69.0	31
5-2	13.1	12.0	69.0	31
9-1	24.0	>20	86.9	13.1
9-2	20.3	>20	86.9	13.1
15-1	18.9	>20	79.9	20.1
15-2	18.4	>20	79.9	20.1
24-1	27.4	>20	91.5	8.5

5.2.3 Degree of connectivity

Absorption of the sound wave occurs due to the porous structure of the road surface. In theory, only air voids which are interconnected and connected to the open surface of the road are considered to be effective for sound absorption. Connected pores are essential for the sound waves to pass through and dissipate in the system [2]. Acoustical models for evaluating the sound absorption are also developed based on a layer with interconnected pores over the full height [3, 4]. In road engineering, the commonly used bulk parameter air voids content takes into account both the interconnected and closed pores. The connected air voids are not considered as a separate indicator for describing the material properties. However, in practice not all the pores are connected. Knowledge about the connectivity of the pores is important to understand the sound absorbing capability of road surfaces, and it also helps to explain the influence of material properties on sound absorption. In this section, the percentage of connected pores

in the overall air voids system is calculated based on the CT scanning results. A relationship between the connected and overall air voids content is determined.

Figure 5-6 shows the 3D distribution of the air voids content in a sample generated by the software Avizo. In Figure 5-6 (a), the distribution of all the air voids in one core is illustrated. Figure 5-6 (b) presents the distribution of the connected pores. Clusters with different colours are isolated from each other. The objective of the study is to calculate the amount of interconnected pores which are connecting both the top and bottom surface of the sample.

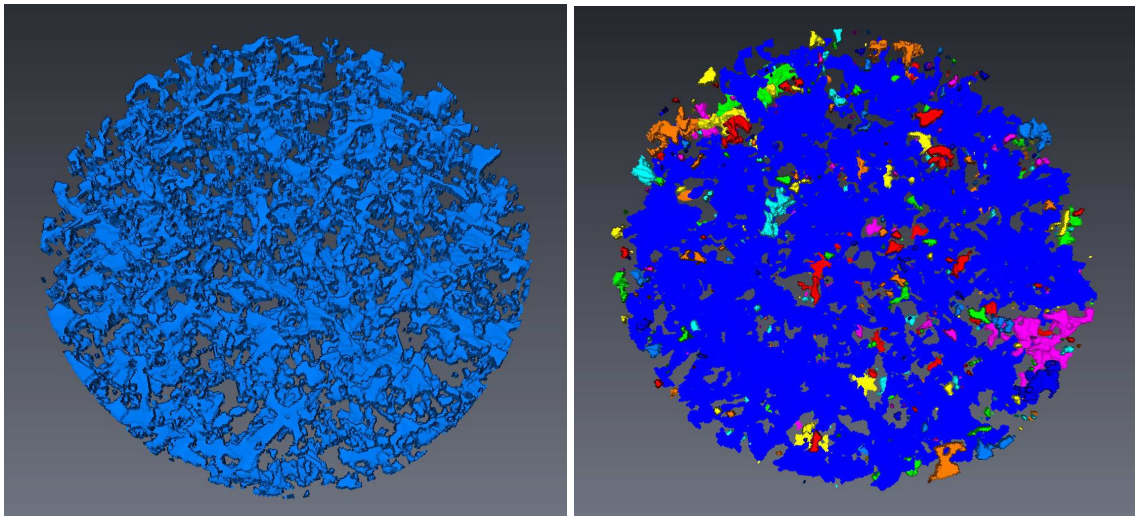

(a) Overall air voids (b) Connected air voids

Figure 5-6 3D distribution of air voids and connected air voids in a sample

In this study, the cluster-labeling algorithm proposed by Hoshen and Kopelman [1] is applied to study the connectivity of pores based on the grey scale image from the CT scanning. The method has been used for investigating the connectivity of Portland cement paste [5]. In this study it is also employed for analyzing asphalt mixtures. The algorithm is described here-after.

For the CT scanning image, the gray value of each pixel is proportional to the density of the corresponding material at the same point. To distinguish different components of the mixture (air voids, mortar and aggregate), threshold values are to be determined. From a previous study, it is known that the 500 HU and 1400 HU can be selected as border values to determine which grey scale separates the aggregates and mortar and which grey scale separates the mortar and voids. In this case, as only the air voids content is of interest, the mortar and aggregate can both be treated as “solid”. All the pixels with a gray value below the threshold 500 HU are regarded as air voids, and those above 500 HU as solid. As a result, the air voids and solid pixels can be presented with ‘‘1’’ and ‘‘0’’ respectively in a binary image.

In a 3D space, the CT scanned image is composed of series of slices and each volume element is presented by a voxel. The positional relationship of a voxel

with neighboring voxels is shown in Figure 5-7. The criterion to judge the connectivity is that only adjacent voxels which share a common surface are judged as connected, as shown by the first configuration in Figure 5-7. Voxels contacting each other by a vertex or an edge are considered not connected.

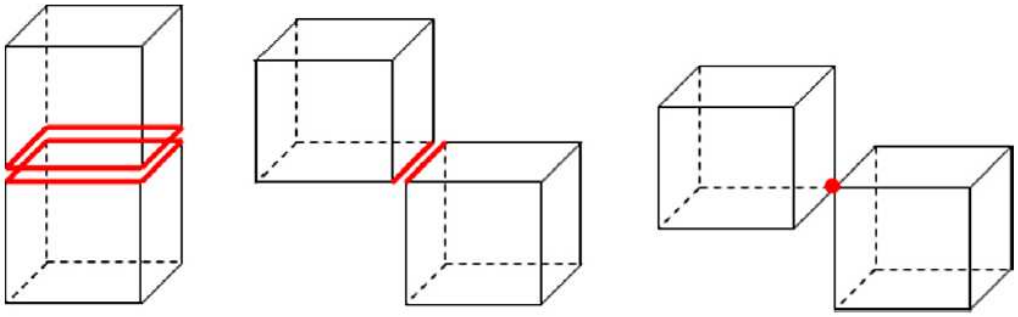

Figure 5-7 Configuration of adjacent voxels in a 3D image space

An example of detecting connected air voids on a 2D image is shown in Figure 5-8. In the Figure 5-8 (a), "1" presents the air voids and "0" the solid. The computer program is used to scan the binary image twice. The connected pixels as judged by the criterion specified in Figure 5-7 are labeled with the same cluster number. In the 3D space, the scanning and numbering process is similar, and the contact in the vertical direction needs to be taken into account.

When the cluster-numbering process is completed, clusters which are connected to both the top and bottom layer of the sample present the connected air voids. The degree of connectivity is qualified by dividing the connected air voids content by the overall porosity.

0	1	1	0	0	0	0
0	1	1	0	0	0	0
0	1	0	1	1	0	0
0	1	0	1	1	0	0
1	1	0	0	0	1	0
1	0	0	0	1	1	1
1	0	0	0	1	0	1

(a) 2D binary image

0	1	1	0	0	0	0
0	1	1	0	0	0	0
0	1	0	2	2	0	0
0	1	0	2	2	0	0
3	1	0	0	0	4	0
3	0	0	0	5	4	4
3	0	0	0	5	0	4

(b) Labeled clusters after first step

0	1	1	0	0	0	0
0	1	1	0	0	0	0
0	1	0	2	2	0	0
0	1	0	2	2	0	0
1	1	0	0	0	4	0
1	0	0	0	4	4	4
1	0	0	0	4	0	4

(c) Labeled clusters after second step

Figure 5-8 A 2D example of the implementation of the cluster-labeling program

The degree of connectivity calculated for the slab samples and cores from the trial sections are summarized in Table 5-6. In addition to the thin layer surfacinigs, the measurement results for the four porous asphalt samples are also given.

For the slab samples, it can be seen that the degree of connectivity for semi-dense samples is generally lower than 0.1 and even close to 0. The only exception is slab P05, with a degree of connectivity 0.42. This could be because of the larger sized coarse aggregates. A high connectivity degree of 0.68 is found for the semi-open type slab P02.

The cores from the trial sections show that the amount of connected voids generally increases with increasing overall air voids content. The porous thin layer surfacings 9-1, 9-2 and 24-1 and the four porous asphalt samples all show a high connectivity of the pores, with a ratio close to or higher than 0.9. For cores from section 15, the total air voids is similar with that of 6-1 and 7-1, but the amount of connected voids is much lower. This is thought to be caused by the smaller aggregates used in section 15. However, the current measurement results provide not enough data to confirm the dependence of connected air voids on the aggregate size.

Table 5-6 Degree of connectivity for different samples

Slab samples	Degree of connectivity	Air voids content, %	Maximum aggregate size, mm	Cores from trial sections	Degree of connectivity	Air voids content, %	Maximum aggregate size, mm
Ref	0.04	11.8	6	2-1	0.01	11.0	4
P01	0.09	10.7	6	2-2	0.00	4.8	4
P02	0.68	17.8	6	3-1	0.00	8.0	6
P03	0.03	8.8	6	4-1	0.77	18.0	6
P04	0.01	7.6	6	4-2	0.02	15.0	6
P05	0.42	12.6	8	5-1	0.51	14.3	8
P06	0.02	11.0	6	5-2	0.12	13.1	8
P07	0.00	12.1	6	9-1	0.89	24.0	8
P08	0.02	11.1	6	9-2	0.93	20.3	8
				15-1	0.23	18.9	6
				15-2	0.55	18.4	6
				24-1	0.98	27.4	8
				6-1	0.93	19.4	11
				7-1	0.90	19.1	16
				8-1	0.88	21.3	8
				31-1	0.99	31.3	11

Also visual inspections were done on the cores from the Kloosterzande sections. From the inspection, it was found that the surface of core 15-1 was seriously clogged by fine soil. A picture of the surface of section 15-1 is shown in Figure 5-9; the surface of section 9-1 is also shown for contrast. It can be seen that there is nearly no open area in the surface of the core 15-1.

It should be noted that the calculation of the air voids content and connectivity is concentrated on the internal parts of the core, and the exposed surface is not taken into account. The actual connectivity degree could therefore even be lower than the value shown in Table 5-6. For other cores, the influence of clogging on connectivity is neglected, as exposed pores were clearly visible at the surface. The surface of section 9-1 in Figure 5-9 (b) is used as an example of a surface with little influence of clogging. In this study, core 15-1 is thus considered as a special sample which is affected by clogging.

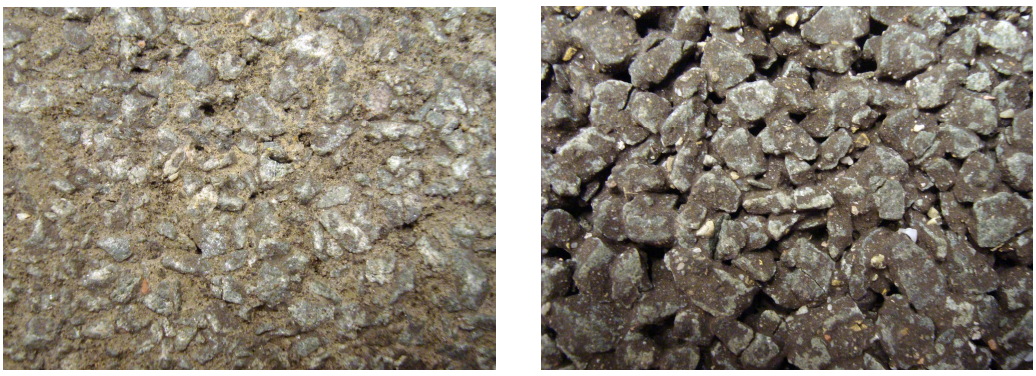

(a) Core 15-1 (b) Core 9-1

Figure 5-9 Surface of cores from trial sections

The scatter plot of the connectivity degree versus the overall air voids content of the sample is given in Figure 5-8. Based on the distribution of the test results, the relation between the connectivity degree and air voids content can be characterized by three groups. In Figure 5-8, different colours are used for illustrating the groups, and trend lines are plotted to show the relation between the connectivity and the air voids content.

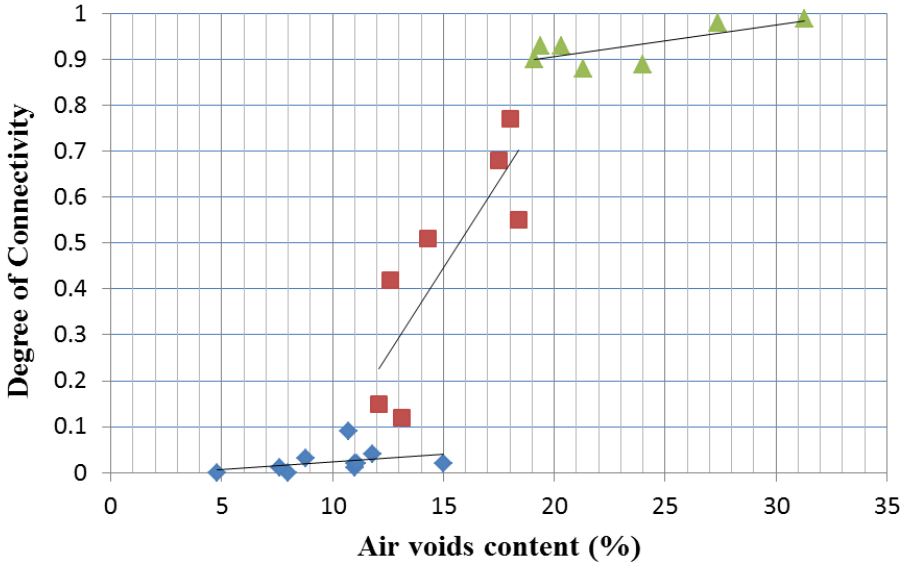

Figure 5-10 Degree of connectivity versus air voids content of road surfaces

The three groups are:
1) Cores with air voids content below 12% (except one point at 15%). The degrees of connectivity of the sample are around or lower than 0.1, and some are close to 0. It means there are nearly no pores connecting from top to bottom.

2) Cores with air voids content between 12% and 19%. The connectivity degree ranges from 0.1 to 0.8. In general, the connectivity degree increases rapidly with increasing air voids content.

3) Surface with air voids content higher than 19%. The commonly used porous asphalt surfaces (with design air voids content higher than 20%) belong to this group. The observed connectivity degree is close to or exceeding 0.9, which reflects that the road surface layer is a very permeable porous structure. This indicates the layer is effective in absorbing sound over the whole depth.

The influence of connectivity on the sound absorption will be determined by investigating the sound absorption coefficients of the different surfaces.

5.3 Investigations on Surface Texture

Surface texture measurements were performed on slab and core samples by scanning them with the laser profilometer. The measurement traces for the surface texture test on the slabs are illustrated in Figure 5-11. The surface profiles are measured on 13 traces along the longitudinal direction. The length of

each trace is 50 cm, and the distance between two neighboring traces is 2.5 cm. As mentioned in Chapter 4, the texture level on the octave band and the mean profile depth (MPD) were determined.

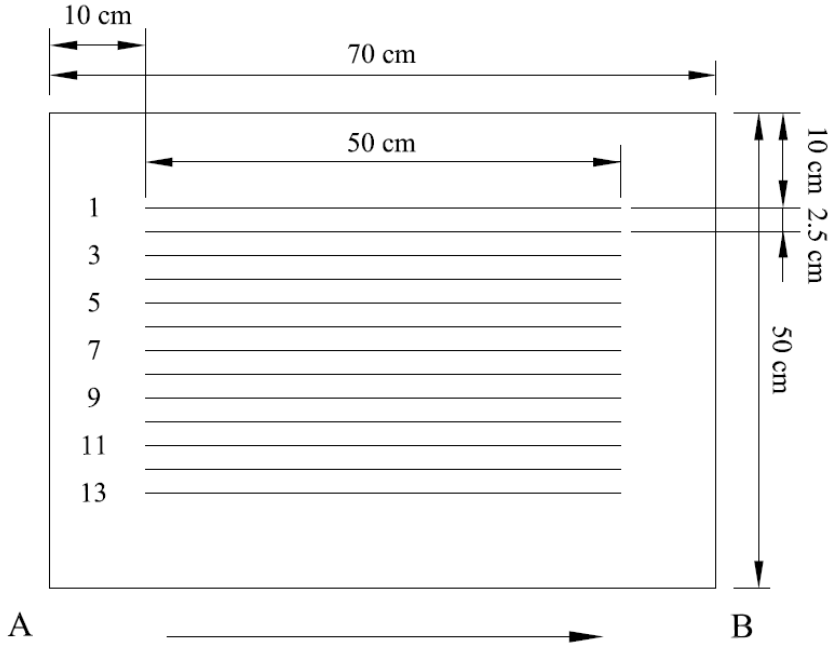

Figure 5-11 Measurement traces on slab sample

On core samples, surface profile data are collected on ten traces in two perpendicular directions. The positions of the traces are shown in Figure 5-12. The distance between two neighbouring traces is 10 mm. As the dimension of the core is limited (150 mm diameter), the spectral analysis is not appropriate [6]. Therefore only the MPD is calculated for scaling the surface texture of core samples.

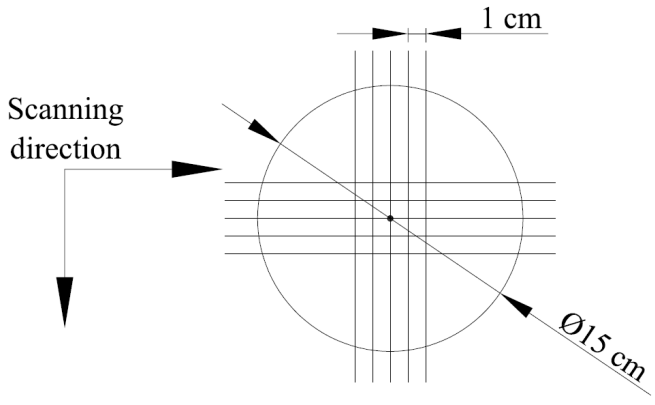

Figure 5-12 Measurement traces on core sample

5.3.1 Investigation on surface texture level

The texture levels tested from the 13 traces on each slab are shown in Figure 5-13. In the figure, measurements on slabs Ref and P08 are given as examples (The rest figures are given in the CD attached to the thesis). The thick line in the

figures denotes the average texture level from the 13 traces. In both cases, it can be seen that the peak values of the texture level is generally located at the 8 mm wavelength. Below 8 mm, the variation in texture level is relatively smaller in comparison with the variances of the curves above 8 mm. The variation of the measurements from different traces should be considered when comparing the average of the test data.

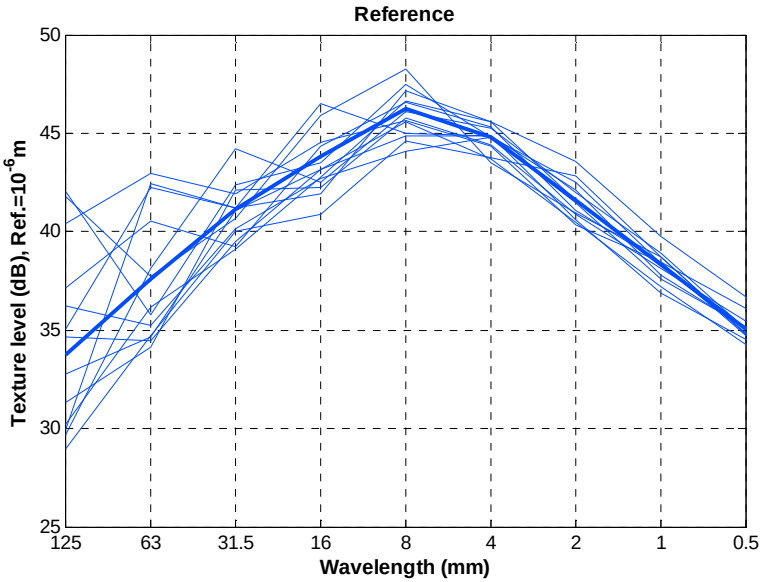

(a) Measurements on Ref

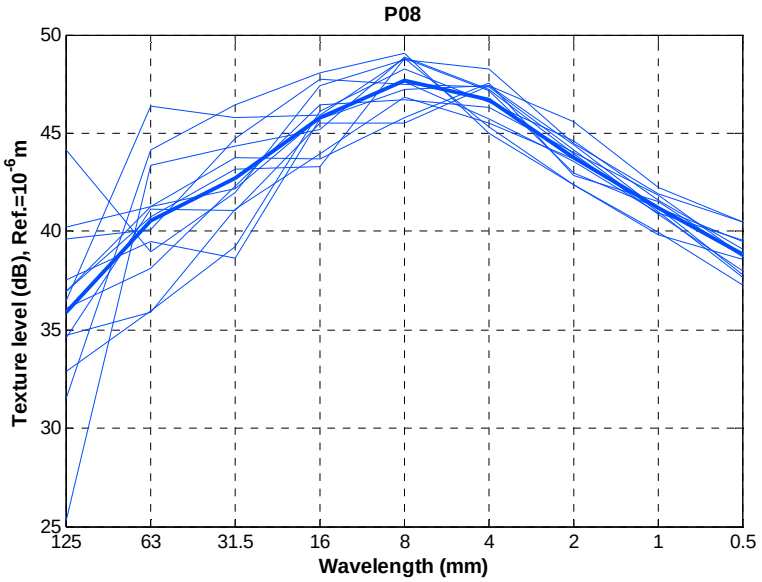

(b) Measurements on P08

Figure 5-13 Texture levels from different traces on the slab

The surface texture levels on the octave band of the wavelength for all the slabs are summarized in Figure 5-14. In addition, the texture levels for Kloosterzande sections 2-1 and 7-1 are also plotted as references. The texture levels for these two sections are from the in-situ tests on the sections in a previous project [7]. As listed in Table 4-4, section 2-1 is the thin layer surfacing with a maximum

aggregate size of 4 mm, and section 7-1 is the porous asphalt 0/16 section. They are shown to allow comparisons between surfaces with large material differences to be made.

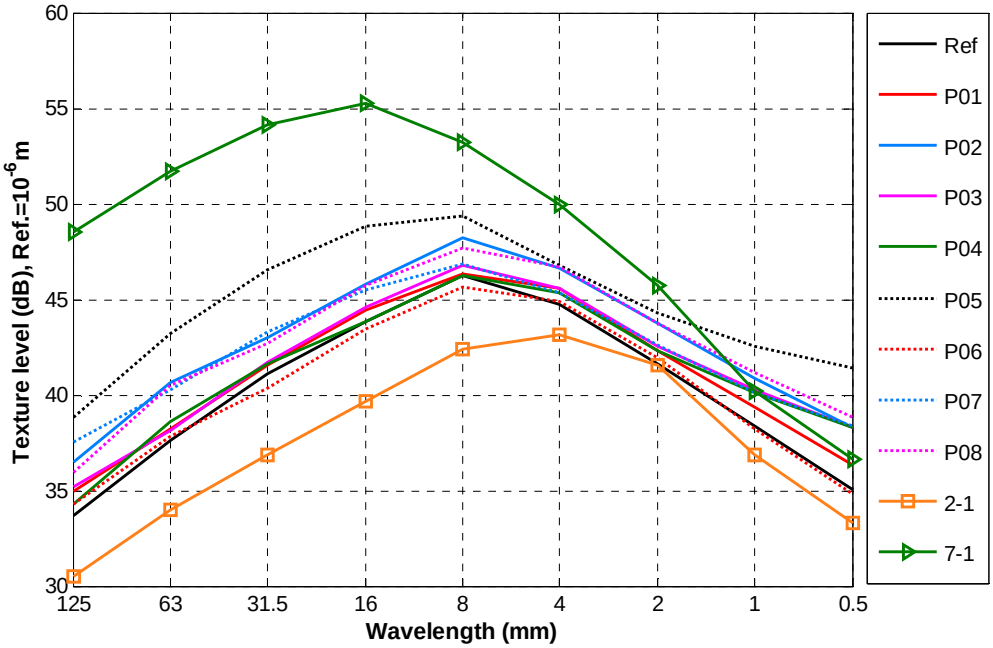

Figure 5-14 Texture levels of slab samples

From Figure 5-14, it can be seen that the texture level generally reaches a maximum at the wavelength equal (or close) to the maximum aggregate size of the mixture. For example, the maximum texture level for 0/16 porous asphalt 7-1 is at 16 mm, and for thin surfacings with a maximum aggregate size of 6 or 8 mm, the peak value of texture level appears at 8 mm wavelength. The figure also shows that there are relatively small differences in texture levels at wavelengths below 2 mm between samples. Above wavelength of 2 mm, obvious differences can be observed. The porous asphalt 0/16 and thin layer with coarse aggregate size 2/4 mm show the highest and lowest texture levels respectively. The texture levels of the slab samples are in-between. Sample P05, with coarse aggregate size 4/8 mm, has a larger texture level than those with a coarse aggregate size of 2/6 mm. From this overview, it is concluded that the coarse aggregate size is one of the most important factors affecting the surface texture level. A larger aggregate size leads to a higher texture level at wavelengths above 2 mm.

Specific investigations are made for thin layer slab samples. In Figure 5-15, comparisons of texture levels between the reference sample and samples with different material properties are shown.

From Figure 5-15 (a), it can be seen that texture levels for sample Ref, P01, P03 and P04 are close to each other at wavelengths $\geq$ 2 mm. It indicates that the influence of air voids on the texture is small in this wavelength range. Below 2 mm, P03 and P04 show higher texture levels compared with Ref and P01. This is mainly due to the larger content of the fine aggregate and sand which cause the

increase of the texture level at short wavelengths (< 2 mm). The sample P02 is considered as a semi-open type of thin layer surface with a design air voids content of 18%. As presented in Figure 5-15 (a), the texture level from 0.5 mm to 125 mm of P02 is higher than that of all the other surfaces. Therefore, the air voids content is also considered to be an important factor; it results in a higher texture level of semi-open thin surfaces compared with the semi-dense type.
In Figure 5-15 (b), a higher texture level is observed for P05, which is made of a larger maximum aggregate size 4/8, compared with the reference stone size 2/6. This shows that using larger size stones leads to a higher surface texture.

The effect of aggregate types is investigated in Figure 5-15 (c). The three mixtures are made of different types of aggregates with all the other design parameters kept equal. From the figure, it is seen that the measured texture levels are similar for the reference slab and sample P06. P07, which is made of aggregate type Irish Greywacke, shows a higher texture than the other two surfaces. The possible reasons for this observation are as follows: although the gradations are nominally the same (with aggregate size 2/6 mm), this does not necessarily mean that the gradation within the 2-6 mm gradation band were exactly the same. According to the producer of the slabs, the Irish Greywacke is more sharply broken than Bestone which tends to have more rounded edges. Therefore, in this case, shape of aggregates plays a role in surface texture level.

Figure 5-15 (d) shows that a higher texture level is achieved by increasing the binder content by 1%. This could be because the drainage of the mortar took place in the compaction process of the slab. It will result in larger amount of pores on the top of the sample and increases the texture level in turn.

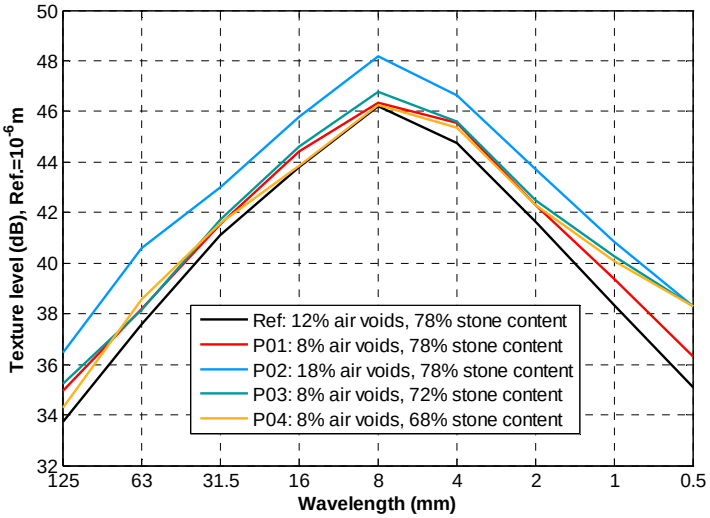

(a) Different air void contents and gradation

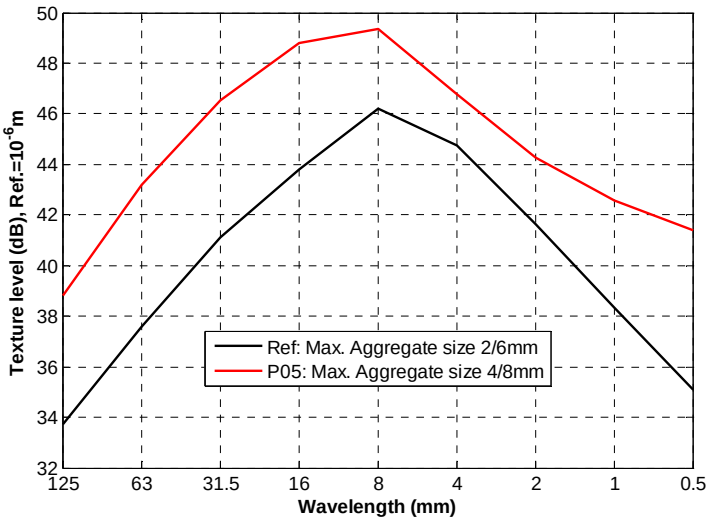

(b) Larger maximum aggregate size

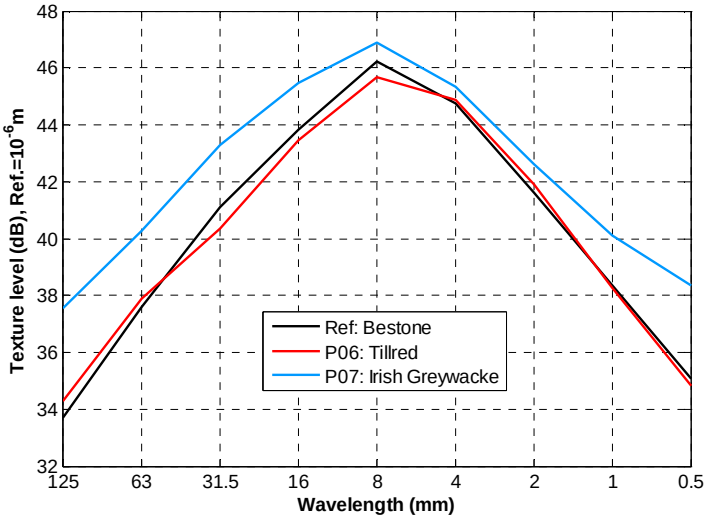

(c) Different aggregate types

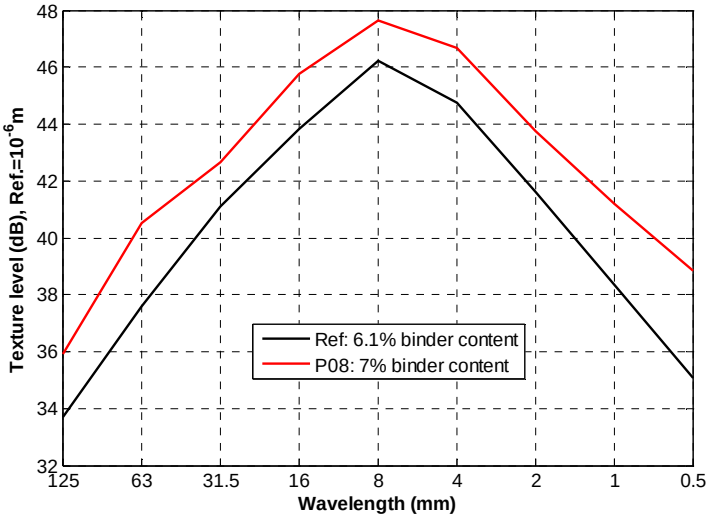

(d) Different binder contents

Figure 5-15 Comparison of surface texture levels between different slabs

5.3.2 Investigation on MPD

Another indicator for describing the road surface texture is the MPD. Experimental results of the MPD from the laser scanning measurements on the slab samples are given in Figure 5-16. The figure shows the averaged MPD from all the traces and the error bars which present the standard deviations of the test results. It can be seen that the tendency of changes in MPD with different slabs almost coincides with what was observed for the texture levels on the octave band. P05, with the larger maximum aggregate size, has the largest MPD. Samples with larger air voids contents, aggregate type Irish Greywacke and 1% more binder content (namely P02, P07 and P08) all display a higher MPD compared with the reference slab. Slab P01, P03, P04 and P06 have similar MPD's compared to the Reference.

As shown in Figure 5-16, there are variations between the test results from different traces for a certain slab. It is important to examine whether the differences of MPD values between samples are statistically significant. In the tests, the surface profile data were collected on a number of traces on each slab, and the tests are performed independently between slabs. Therefore, the T-test is used to determine if there are significant differences of MPD values between the reference slab and slabs with different material compositions. The T-test is performed between the slab Ref and one other slab each time. The null hypothesis is that the means of data from the two slabs are equal. The commonly used significance level 0.05 is considered as threshold. If the resulting significance (*Sig.*) is less than 0.05, the null hypothesis is rejected, and it means that a significant difference exists between the averaged MPD of the two slabs. The t-value and the statistical significance from all the tests are given in Table 5-7. It can be seen that MPD from slabs P02, P05, P07 and P08 are different from that of slab Ref. Other slabs show similar MPD values. From the test, it can be confirmed that the differences of the average MPD values which are shown in Figure 5-16 are mainly due to the properties of the slab. The interpretation of the variation of the MPD for slabs with different material properties is the same as was used to explain the differences in texture levels (see section 5.3.1).

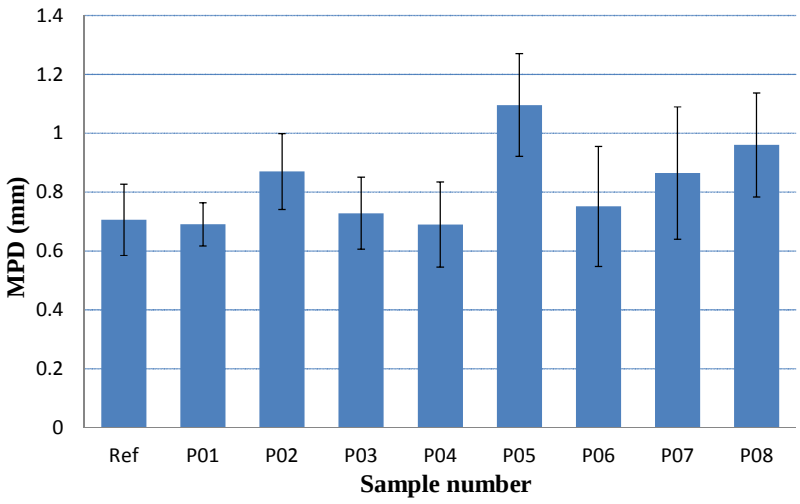

Figure 5-16 MPD of slab samples

Table 5-7 T-test results between Ref and samples with material adjustments

	P01	P02	P03	P04	P05	P06	P07	P08
t-value	0.460	-5.014	-0.705	0.406	-8.250	-1.107	-4.647	-5.476
Sig. (2-tailed)	0.649	0.000	0.484	0.687	0.000	0.275	0.000	0.000

The measurement results from the cores of the Kloosterzande sections are shown in Figure 5-17. The MPD's which were obtained from on-field tests on the newly built sections are also illustrated. The in-situ test data were collected in the year 2006 and refer to the database provided by DVS. The figure shows that surfaces with a larger aggregate size and a higher air voids content generally show a higher MPD, i.e. a higher MPD was measured on cores from section 9 and 24 in which 4/8 mm aggregate size was used and which had a voids content of more than 20%. Also the in-situ measurements on section 5 as well as the cores taken from that section exhibit a higher MPD due to the use of coarse aggregate with size 4/8 mm. The voids content in these cores was around 12%. The mixtures with aggregate size 2/4 and 2/6 mm all show a much lower MPD value.

When comparing the results of the in-situ measurements with those obtained from the cores, the following points should be taken into consideration. The in-situ measurements were done in 2006 and 2007 while the cores were taken in 2010 and measured in 2011. Since no traffic was applied on the sections, it might very well be that same clogging did occur because of dust and soil being blown over the sections. Figure 5-9 (a) gives clear evidence for that. Furthermore, the in-situ measurements were taken over a much longer length than the measurements on the core. The measurements on the core can be considered as spot measurements while the in-situ measurements give a better representative of the overall section.

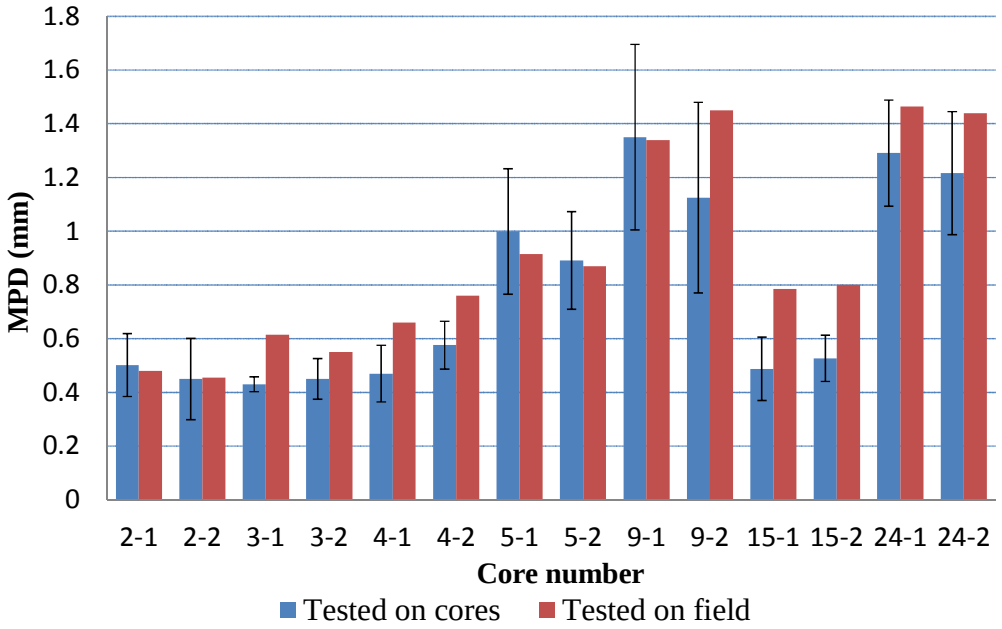

Figure 5-17 MPD of core samples from trial sections

The relations between the MPD and different material properties are illustrated in Figure 5-18. The MPD tested from all the slabs and cores are plotted against the air voids content, maximum aggregate size and coarse aggregate content respectively. From the distribution of the MPD, it can be seen that the MPD generally increases with increasing air voids content, increasing maximum aggregate size and increasing coarse aggregate content. The trend lines determined by means of linear regression are also given in the figures. A reasonable good linear relationship is found between the MPD and maximum aggregate size, as the coefficient of determination R^2 is 0.64. For the air voids content and coarse aggregate content, no clear linear relation is found with the MPD. However, the surface structure is determined by the combination of different material properties [8]. A multivariate linear regression will be more appropriate for expressing the relationship between MPD and material properties. The development of the multivariate regression equation will be discussed in Chapter 7.

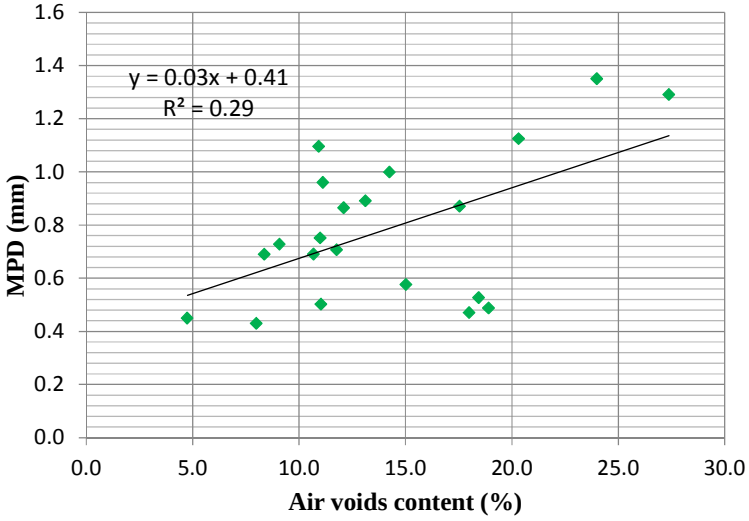

(a) with air voids content

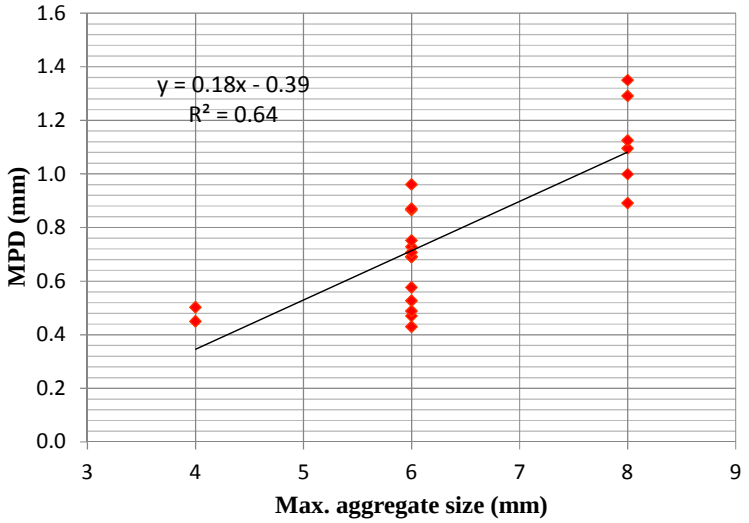

(b) with maximum aggregate size

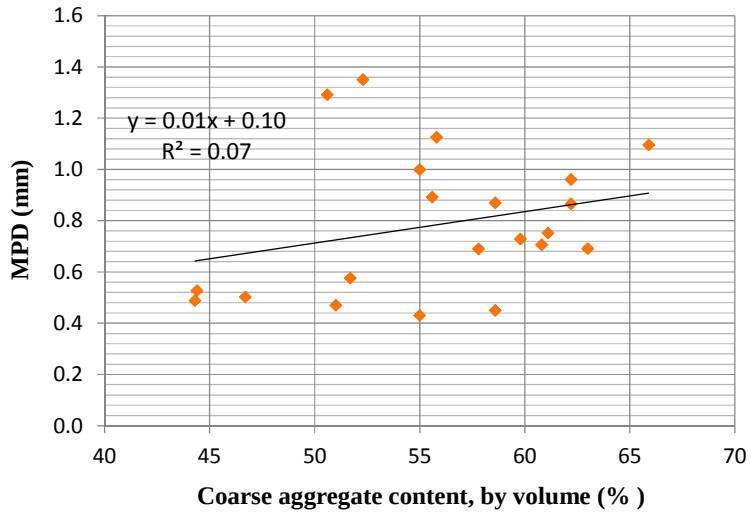

(c) with coarse aggregate volume content

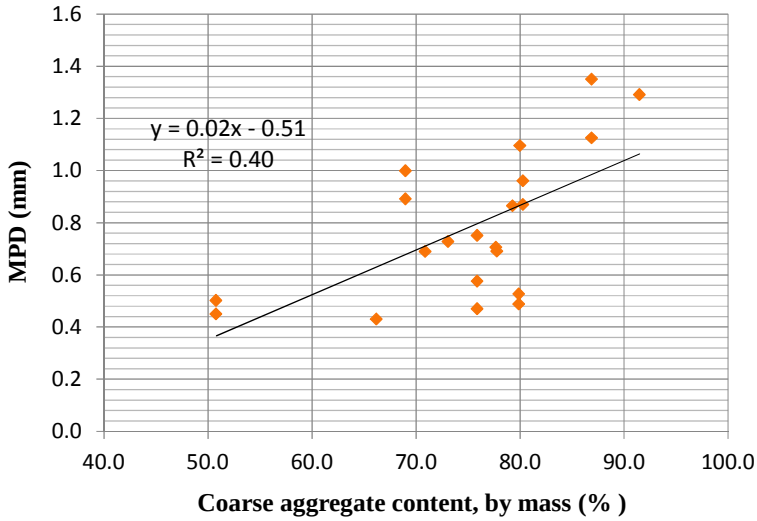

(d) with coarse aggregate mass content

Figure 5-18 Relations between MPD and material properties

5.4 Investigation on Sound Absorption

5.4.1 Investigation on measurement results

The sound absorption measurements were carried out on the thin layer surfacing slabs and the core samples from the Kloosterzande sections with the P-U surface impedance setup. The test setup used on both the slab and core samples has been described in Chapter 4. In this section, the test results are shown and further analyzed to investigate the relationship between the sound absorption and the basic material properties. Theoretical models are also developed for simulating the sound absorption curve for thin layer road surfacings.

As discussed in Chapter 4, the sound absorption was measured on each slab at different positions. The 15 test results obtained in the central area of the slabs, see Figure 4-20, are used in the investigation. Figure 5-19 gives examples of the

absorption coefficients obtained at 5 different positions. The results in the figure are from the Ref and P02 slabs respectively. According to the literature review, the peak absorption coefficient and the frequency at which the peak absorption occurs are the two important parameters to be observed.

Acoustical properties depend on the characteristics of the tested surface [9]. Because the air voids do not distribute uniformly in the surface layer, the sound absorption curves vary between different positions. Figure 5-19 shows that in both slabs variations exist between sound absorption curves obtained at the different locations. However, Figure 5-19 (b) shows that on the surface with a high porosity, P02, an obvious peak can be seen around 1250 Hz on each curve. The variations between the test results are small and therefore the representative sound absorption coefficient for slab P02 can be calculated directly by averaging the results from the different positions.

With respect to the semi-dense sample, such as the Ref shown in Figure 5-19 (a), the absorption coefficients are small in the whole frequency range. In this case, two methods are taken for calculating the representative sound absorption of a certain surface. The first method is to directly calculate the average of the absorption coefficients on the frequency band from different measurements. As the peak absorption coefficients locate at various frequencies for different measurements, the peak values may be eliminated to some extent. The second method is used to provide only the averaged peak absorption coefficient and the peak frequency. For a certain slab, the peak absorption coefficient and the peak frequency tested at each position are firstly extracted. The average of these peak absorption coefficients and the average of the peak frequencies are then calculated respectively.

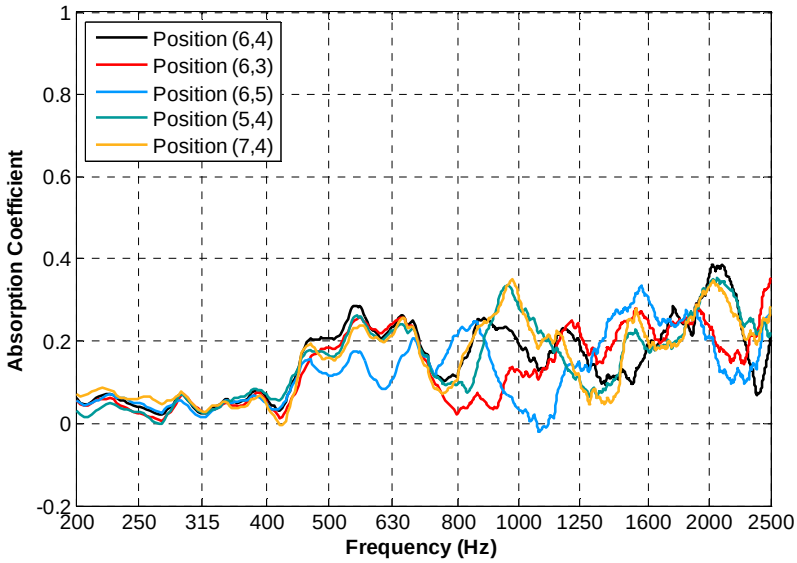

(a) Measurements on Ref

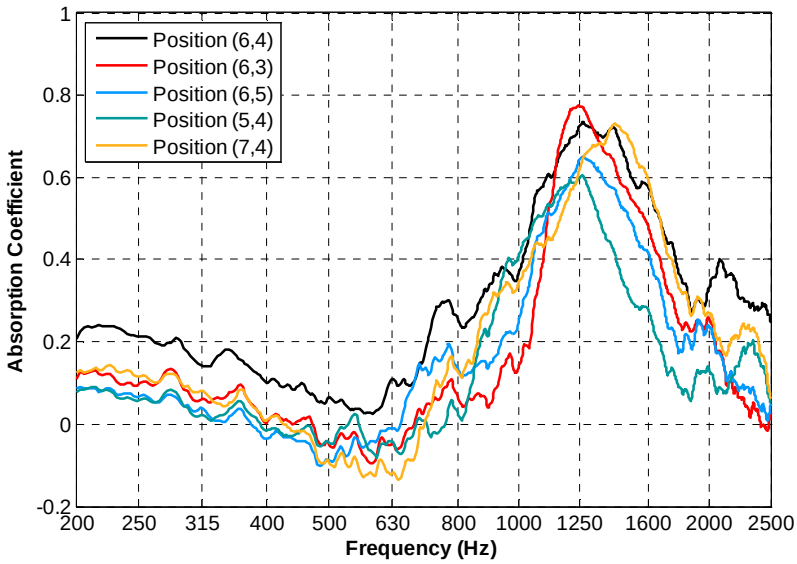

(b) Measurements on P02

Figure 5-19 Sound absorption coefficients at different positions on the slab

The averaged absorption coefficients from method 1 are shown in Figure 5-20. The averages for semi-dense slabs are from the 9 points on and around the center of the slab. It can be seen from the figure that there is an absorption peak of about 0.7 around 1250 Hz for slab P02. For all the other samples, the peak values are much lower. Those peak values are between 0.2 and 0.3, and appear at frequencies ranging between 700 Hz to 1100 Hz. By investigating the averaged sound absorption curves, it can be concluded that the porous type thin layer surfacing provides a high and broad absorption peak in contrast to the semi-dense surfacings. For semi-dense surfaces, the absorption peaks are small, and the differences between the various samples are not higher than 0.1. So they are considered to have similar sound absorption properties.

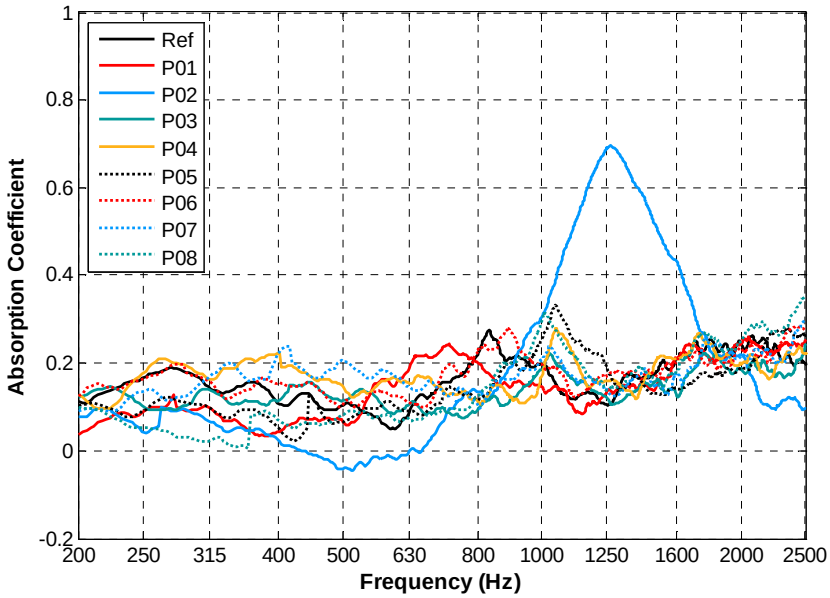

Figure 5-20 Sound absorption coefficients of slabs

When using method 2, the average is calculated from the test results of the 15 positions located in the central part of the slabs, see Figure 4-20. From Figure 5-19 (a) or Figure 5-20, it can be seen that the peak absorptions for a semi-dense surface generally occur in two frequency ranges. The first peak is between 700 Hz and 1250 Hz, while the second peak is located between 1600 Hz and 2500 Hz. In each frequency range, the peak values and the corresponding peak frequencies from different tests are collected and averaged. The results are summarized in Table 5-8.

As shown in Table 5-8, slab P02 shows the highest first peak value, with an average of 0.70, located at 1215. 8 Hz. Slab P05 has the second highest peak absorption coefficient. Slab P05 has a larger aggregate size and higher air voids connectivity compared with the other semi-dense surfaces. P01 shows the lowest absorption peak with an average value of 0.23. For the other samples, the peak absorption coefficients are quite close, ranging from 0.27 to 0.31. The averaged peak frequencies for these semi-dense slabs are from 869.5 Hz to 1040 Hz. The standard deviation for the mean peak frequencies is higher than 95, and is up to 169.2 Hz on slab P08. For semi-dense surfaces, the second peak absorption coefficient ranges from 0.29 to 0.39, with the averaged location ranging from 2065.6 Hz to 2353.3 Hz.

From the above, it can be seen that there are large differences in maximum sound absorption between porous type thin surfacings and semi-dense (or dense) types of surfacings. This is considered to be dominated by the air voids content of the material. For samples with a designed air voids content between 8% and 12%, the absorption coefficients are small and there are very small differences between the samples. This shows that the small changes in the mixture composition do not have a big influence on the sound absorption of semi-dense thin surfacings. If one aims for a general investigation on the influence of material properties on sound absorption, samples with larger differences in mixture composition need to be taken into account. This investigation can be accomplished by combining the measurement results from the Kloosterzande cores with the measurements done on the slabs.

Table 5-8 Peak absorption coefficients and the corresponding frequencies

	Peak 1	Std	Frequency (Hz)	Std (Hz)	Peak 2	Std	Frequency (Hz)	Std (Hz)
Ref	0.30	0.08	970.3	114.6	0.38	0.04	2301.8	279.5
P01	0.23	0.04	925.0	159.3	0.33	0.04	2353.3	188.2
P02	0.70	0.07	1215.8	97.4				
P03	0.27	0.03	972.3	160.2	0.29	0.05	2105.9	344.6
P04	0.31	0.06	1034.4	129.0	0.32	0.05	2065.6	342.0
P05	0.33	0.07	958.0	133.1	0.30	0.07	2102.5	332.2
P06	0.31	0.07	869.5	148.7	0.34	0.06	2242.0	316.1
P07	0.29	0.06	885.5	95.5	0.33	0.05	2235.9	288.8
P08	0.31	0.05	1040.0	169.2	0.39	0.06	2194.3	298.3

Sound absorption measurements were performed on Kloosterzande core samples by using the platform described in Chapter 4. Since the surface area of a core is

small, the measurement is taken on one position, which is the center of the core. The effect of different testing positions is therefore not taken into account. In order to facilitate the investigation, test results for cores with large differences in designed air voids content are shown separately. Sound absorption coefficients for cores with a designed air voids content equal to or less than 12% are illustrated in Figure 5-21, and absorption curves for samples with a designed air voids content above 20% are presented in Figure 5-22. All absorption curves show a common small peak around 400 Hz and a dramatic drop of the absorption coefficient above 2000 Hz. They proved to be caused by the platform system as discussed in Chapter 4. Therefore, the absorption coefficients below 500 Hz and above 2000 Hz are left out from the investigation on the core samples.

As shown in Figure 5-21, the peak absorption coefficients for the core samples locate between 800 Hz and 1000 Hz, which is in agreement with the test results obtained on the slabs. The value of the maximum absorption coefficient ranges from 0.18 to 0.37. By taking into account the air voids content determined with CT scanning (as shown in Table 5-5), the peak value generally increases with increasing air voids content. For example, the maximum peak value is observed on sample 4-1, which has an air voids content of 17%. Sample 2-2 shows a lowest peak absorption coefficient, as the air voids content is just 4.8%.

In Figure 5-22, the sound absorption coefficients for the porous type thin layer surfacings are shown. The bottom part of core 24-2 was damaged in the cutting process, and it was not suitable for the sound absorption measurement. Thus the result for 24-2 is not shown. Figure 5-22 shows that high peak absorption coefficients were found on cores from sections 9 and 24, with values greater than 0.7. The peaks locate at different frequencies ranging from 1250 Hz to 1900 Hz. Based on the CT scanning results shown in Table 5-6, the high absorption coefficients for such surfaces are considered to be caused by the high air voids content (>20%) and the highly connected pore structures. For sample 15-2, a peak absorption coefficient slightly higher than 0.4 was obtained, which occurs between 800 Hz and 1000 Hz. The absorption coefficients of core 15-1 are quite low in the whole frequency range, with a peak value around 0.25. This is mainly because the open pores at the surface of 15-1 were seriously clogged by fine soil as shown in Figure 5-9. Because of the influence of clogging, the data obtained on core 15-1 were not used in further analyses of sound absorption.

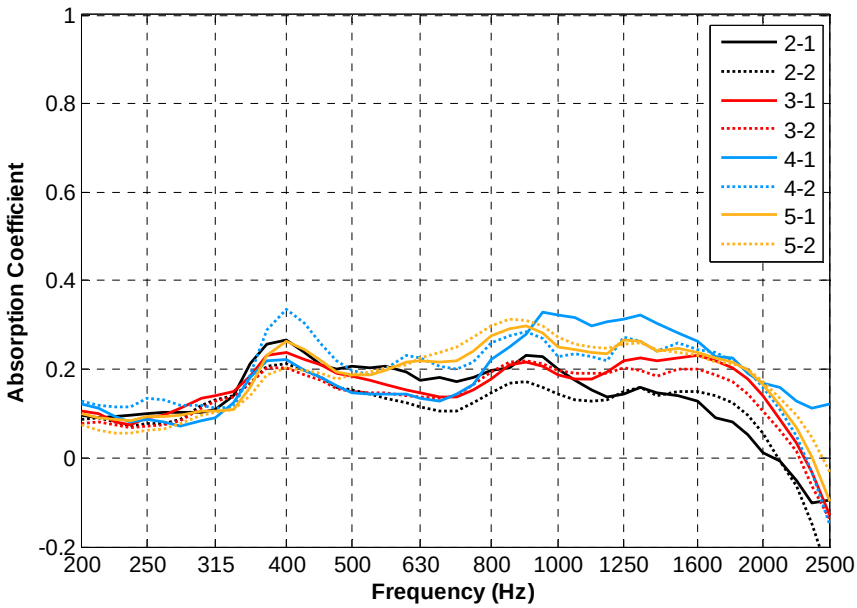

Figure 5-21 Sound absorption coefficients of thin layer surfacing cores

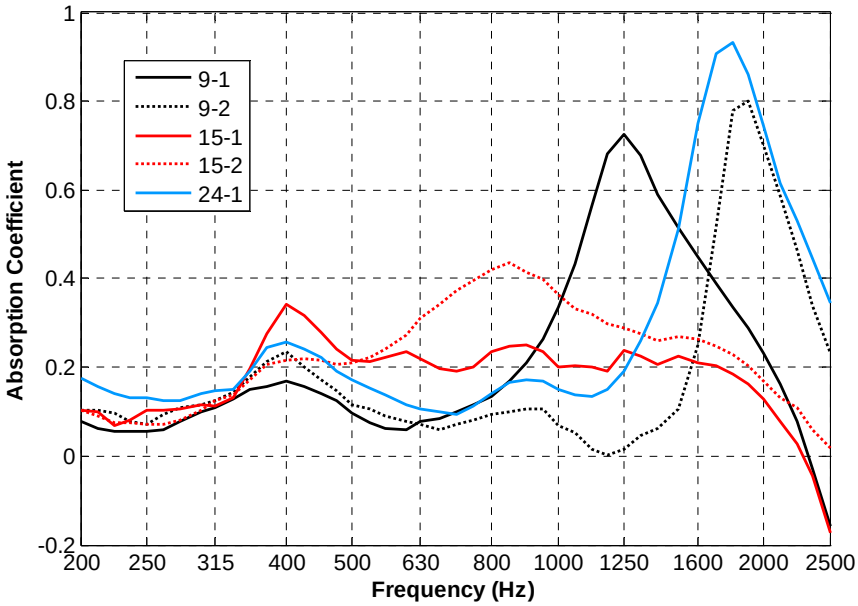

Figure 5-22 Sound absorption coefficients of porous thin layer surfacing cores

5.4.2 Statistical analysis

In this section a relationship is developed between sound absorption and material properties. Measurement results from both the slab and cores from thin layer surfacings were used. In this study, most of the thin layer surfacings are of the semi-dense type, and only small differences in material properties between the samples are investigated. The sound absorption measurements showed that the sound absorption properties for these semi-dense surfaces are quite similar. In order to enlarge the scope of the investigation, the four porous asphalt cores, namely 6-1, 7-1, 8-1 and 31-1 from the Kloosterzande sections were also used in the analysis.

Figure 5-23 shows the relation between the first peak absorption coefficients for different material properties. The data are from the measurement results of all the thin layer surfacing samples and the four porous asphalt cores as mentioned above. The regression equations and the trend lines are shown in the figures.

Figure 5-23 (a) and (b) show that the peak absorption coefficient increases with increasing air voids content and increasing degree of connectivity respectively. Good linear relationships are found between the peak absorption coefficient and the two parameters.

The amount of connected air voids is calculated by multiplying the air voids content with the degree of connectivity. Its relation with the absorption coefficient is shown in Figure 5-23 (c). It can be seen that quite a good linear relationship between the peak absorption coefficient and the connected air voids content is found. Comparing Figure 5-23(c) with Figure 5-23 (a) shows that R^2 is increasing when connected air voids are taken into account in the regression though both equations provide good linear relationships. Given its higher R^2, the equation based on the connected air voids content is preferred for predicting the sound absorption in practice.

The influence of the maximum aggregate size is shown in Figure 5-23 (d). A power regression is used in this analysis because it results in a higher R^2 compared with linear regression. The peak absorption coefficient tends to increase with increasing maximum aggregate size when the size is equal or below 11 mm. However, the predictive power of the relationship is still low given the small R^2.

In Figure 5-23 (e) and (f), the influence of the coarse aggregate content and mortar content are presented. The coarse aggregate content and mortar content are expressed by mass fractions. In general, the peak absorption coefficient increases when the coarse aggregate content increases, while it decreases with an increasing mortar content.

The Influence of the coarse aggregate content and mortar content is also given for volume fractions, as shown in Figure 5-23 (g) and (h). Low R^2 values are found in the regression analysis, especially for coarse aggregate content. However, the distributions of the measurement data show that, the peak absorption generally decreases with increasing volume content of coarse aggregate and mortar. This is thought to be roughly related with the air voids content, as a higher coarse aggregate and mortar volume means a lower air voids in some cases. Consequently, there is a lower absorption ability of the material according to the relations in Figure 5-23 (a) and (c).

This section provided general observations on the influence of basic material properties on the sound absorption of the road surface material. It is found that the connected air voids content is an essential parameter affecting the maximum

absorption coefficient. The regression equations are useful for road designers to relate the mixture compositions with the acoustical properties. Nevertheless, the road surface characteristic is determined by the combined effect of various material properties. For a better evaluation of the sound absorption of the surface, multivariate regression needs to be performed by taking into account a group of influencing parameters.

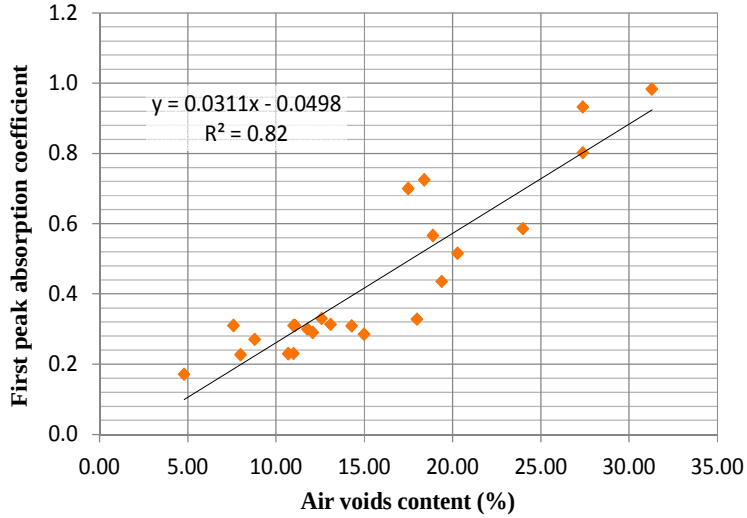

(a) with air voids content

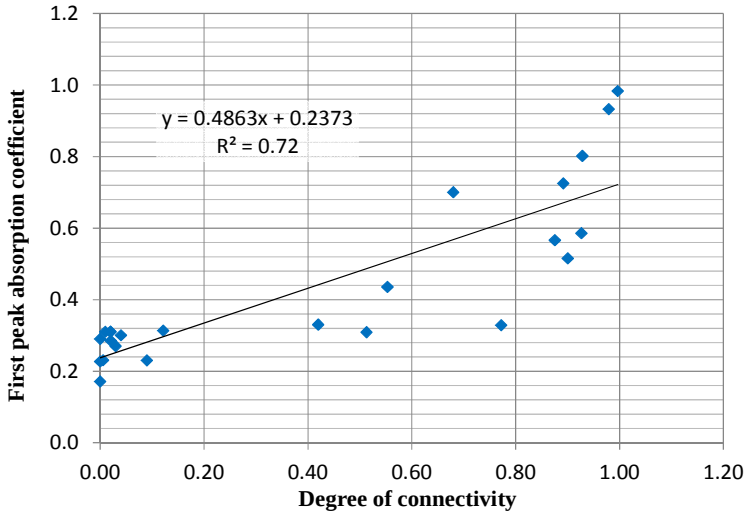

(b) with degree of connectivity

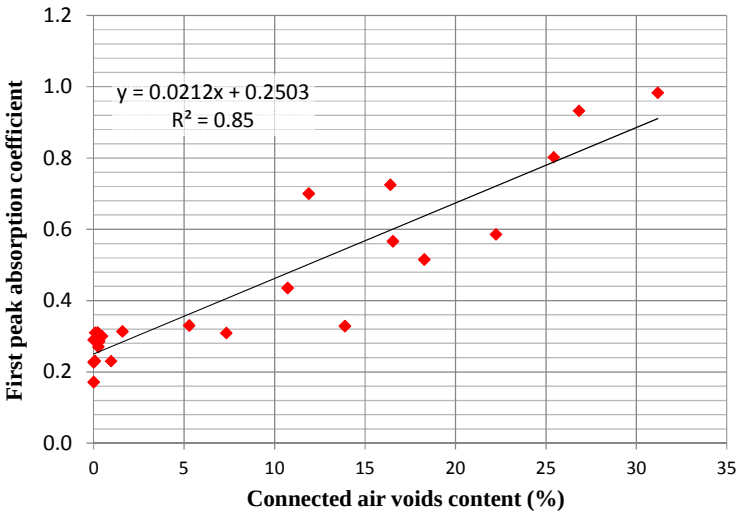

(c) with connected air voids content

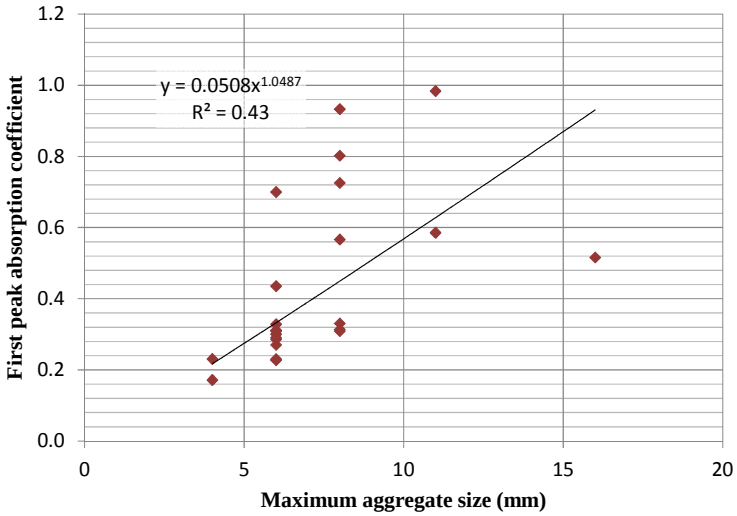

(d) with maximum aggregate size

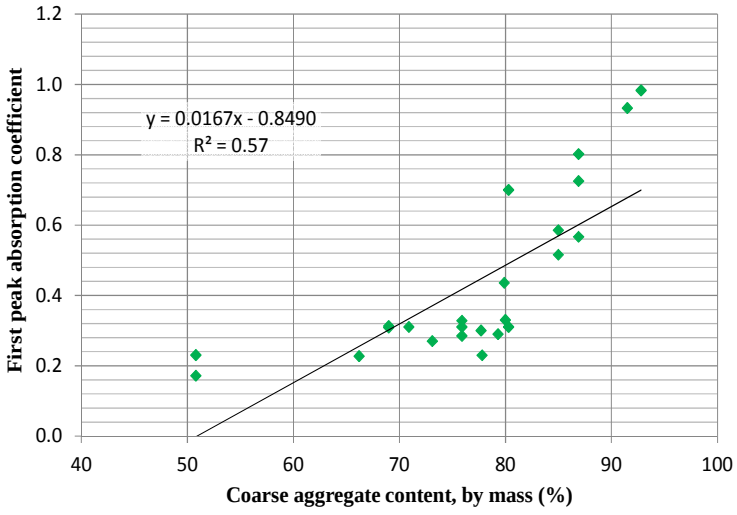

(e) with coarse aggregate content by mass

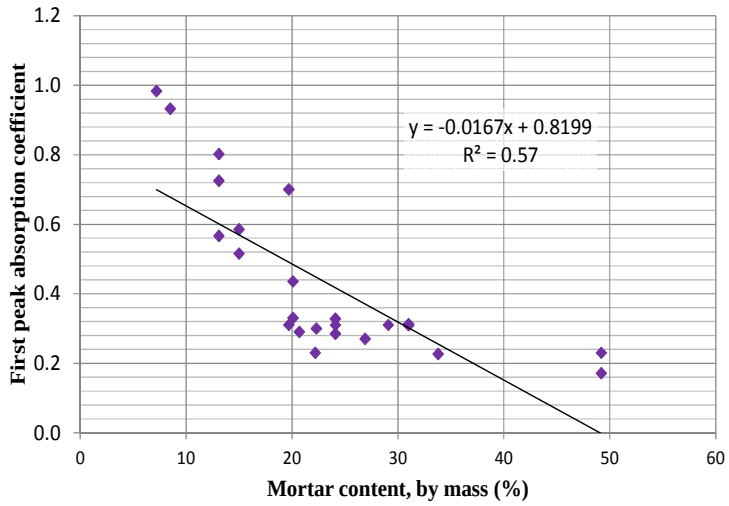

(f) with mortar content by mass

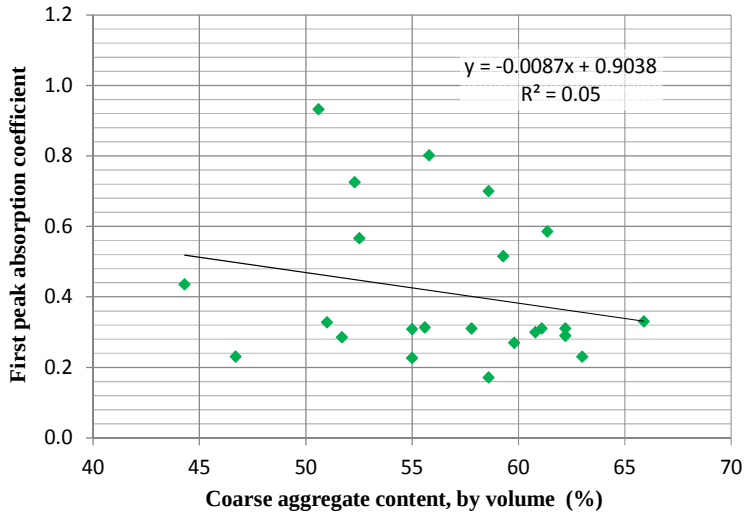

(g) with coarse aggregate content by volume

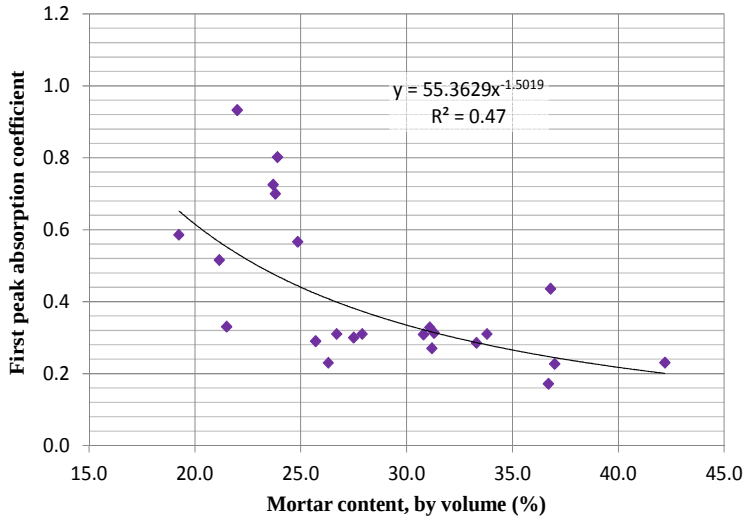

(h) with mortar content by volume

Figure 5-23 Relations between maximum sound absorption coefficient and material properties

5.4.3 Physical model of sound absorption

In the last two sections, sound absorption coefficients for thin layer surfacing samples were investigated based on the laboratory measurements, and relationships between the peak absorption coefficient and material properties were studied using regression analysis. It was found that the sound absorption curve for semi-dense thin surfacings generally has a first peak located between 800 Hz and 1250 Hz, with a magnitude lower than 0.35. For most of the porous thin surfacings, peak absorption coefficients higher than 0.7 were observed, and the peaks occur between 1250 Hz and 2000 Hz. The regression analysis showed that the peak absorption coefficient is linearly related with the connected air voids content. These studies are based on investigations of the test results, but no theoretical explanation for the measurement results are given yet.

In this section, theoretical models are developed for simulating the sound absorption properties of thin layer surfacings. The influencing parameters on sound absorption are also discussed in consideration with the material properties of a road surfacing. At the end, suggestions are given for improvement and usage of the acoustical model for thin layer surfacings.

Various models are used for describing acoustical properties of rigid porous media. In this study, the microstructural model developed by Attenborough is employed, as the model proves to fit well for porous asphalt [10]. The thin layer surfacings are treated as a special type of porous asphalt, so the model is considered to be applicable. From the literature review in Section 2.3.2.3, the complex wave number k and the characteristic impedance Z_c at a certain frequency f need to be known for modeling the sound absorption, and they can be determined from the material and environmental parameters. Generally, the two characteristics can be determined by the dynamic density ρ_g and bulk modulus K_g via the relationships:

$$k = \omega\left[\rho_g(\omega)/K_g(\omega)\right]^{1/2} \tag{5-2}$$

$$Z_c = \left[\rho_g(\omega)\bullet K_g(\omega)\right]^{1/2}/\Omega \tag{5-3}$$

where ω is the angular frequency, Ω is the air voids content.

In this study, a medium containing identical tortuous slit-like pores is used for modeling the thin layer surface. According to the microstructural model, the expressions for ρ_g and K_g can be written as [11]:

$$\rho_g(\omega) = \frac{q^2\rho_0}{\Omega}\left[1-\tanh\left(\lambda(\omega)\sqrt{-i}\right)/\left(\lambda(\omega)\sqrt{-i}\right)\right]^{-1} \tag{5-4}$$

$$K_g(\omega) = \frac{\rho_0 c_0^2}{\Omega}\left[1+(\gamma-1)\tanh\left(\lambda(\omega)\sqrt{-N_{pr}i}\right)/\left(\lambda(\omega)\sqrt{-N_{pr}i}\right)\right]^{-1} \tag{5-5}$$

$$\lambda(\omega) = \sqrt{\frac{3\rho_0 \omega q^2}{\Omega R_s}} \tag{5-6}$$

$$\gamma = c_0^2 \frac{\rho_0}{p_0} \tag{5-7}$$

with

R_s – flow resistivity, Pa·s/m^2;

q^2 – tortuosity;

N_{pr} – Prandtl number; It is a dimensionless number; in physics, it defines the ratio of momentum diffusivity (kinematic viscosity) to thermal diffusivity.

ρ_0 – the density of air, 1.225 kg/m^3;

c_0 – speed of sound in atmosphere, 343.2 m/s;

p_0 – Ambient atmospheric pressure, 100 kPa.

Eqs. (2-20) to (2-23) in Chapter 2 are used for calculating the absorption coefficients from the complex wave number k and the characteristic impedance Z_c.

As introduced in the literature study (see section 2.3.2.2), the four important parameters influencing the sound absorption of a road surface are the air voids content, the thickness of the layer, the airflow resistivity and tortuosity. These parameters need to be quantified for developing the model. A discussion of the input parameters is given hereafter, and the influence of the four parameters on sound absorption is discussed by considering the material properties of a road surface.

Layer thickness. The thickness of the layer which contains interconnected air paths through the material has a great effect on the position of the peak absorption frequency. Generally, the thicker the porous layer is, the lower the peak frequency. The degree of connectivity tests showed that there are nearly no connected air paths over the entire thickness for most of the semi-dense surfaces. This indicates that the effective thickness for absorption of the surface is actually smaller than the overall layer thickness. As the effective thickness is not determined, the samples without pores which are connected over the entire thickness are not taken into account in this study. From Table 5-6, only slabs P02 and P05 are selected for modeling.

Air voids content. The interconnected air voids are effective for the sound absorption of porous media [9]; the interconnected voids are also related to the flow resistivity and tortuosity [12]. In this study, both the overall air voids content and the degree of connectivity are measured. In the modeling, the overall air voids content and connected air voids are considered as input parameters separately. Sound absorption simulations by using these two different inputs are to be compared.

Flow resistivity. Flow resistivity is the flow resistance per unit thickness. It is an important factor influencing the magnitude of the sound absorption coefficient of the porous layer. If a material has a high flow resistivity, it is difficult for air to transport through the surface, and a low absorption coefficient of the material is generally measured. The parameter is related to the geometry of the pores which is determined by the material composition and the construction of the surface. Based on the measurements performed by M+P on the Kloosterzande sections, it is concluded that the flow resistivity for a road surface generally decreases with increasing air voids content [7].

For almost all granular materials, the flow resistivity cannot be predicted analytically [12]. Only for a few idealized absorbing materials, such as materials made of identical spheres or parallel identical fibers, such predictions can be made. So it is necessary to measure the parameter. However, most of the samples are not pervious over the whole thickness according to the CT scanning tests, and they are not suitable for the flow resistance measurements with the direct airflow method [13]. Therefore, the flow resistance (or flow resistivity) measurements are not done in this study. Flow resistivity used in the modeling refers to the database of AOT [7]. In the database, flow resistance measurements are recorded for different surfaces from the Kloosterzande sections. In the modeling, the slab samples are considered to have the same flow resistance as surfaces with similar material properties in the database. For example, P02 has similar material properties as section No.15. Therefore, the flow resistance data of section No.15 is used in the modeling of P02. Likewise, the flow resistance of section No.5 is adopted for modeling for P05, as P05 and section No.5 have the same material composition. In this study, the surface layers are assumed to be homogenous, and the flow resistivity is derived by dividing the measured resistance with the thickness.

Tortuosity. Tortuosity is a measure for the irregularity of the air-flow paths through the material. It mainly influences the peak frequency of the sound absorption. When the tortuosity is higher, the peak absorption appears at a lower frequency. The tortuosity q^2 can be deduced from the air voids content Ω with the following formula [14]:

$$q^2 = \Omega^{-n'} \tag{5-8}$$

where *n'* is the grain shape factor. For spherical grains the grain shape factor is 0.5, and it increases as the grains become flatter.

From Eq. (5-8), it can also be seen that the tortuosity decreases as the air voids content increases. There are several suggestions on the value of grain shape factor *n'* for porous asphalt [10], but no value is specified for thin layer surfacings. The tortuosity is thus to be obtained by fitting the modeled absorption curve with the measured one. The method is also used in the study by Bérengier [15].

Values of all the parameters for the model are summarized in Table 5-9. For each sample, two models were developed. The only difference between Model 1 and Model 2 is that Model 1 is built by using the connected air voids content, while model 2 uses the overall air voids content.

The absorption curves simulated with the models are shown in Figure 5-24 and Figure 5-25 respectively. The average measured absorption curve which is also shown in Figure 5-20 is used for comparison with the modeling results. Figure 5-24 gives the modeling curve for slab P02. The analysis shows that using a value of 3.5 for the tortuosity resulted in the best fit. From the result, it can be seen that both Model 1 and Model 2 fit the average absorption data well. Model 2, which is using the overall air voids content, is even closer to the experimental data. The peak of the curve from Model 1 is narrower than the measured one and has a lower peak value. From this study, it is thus concluded that the overall air voids content can be used directly for modeling the semi-open (or porous as assumed) type of thin layer surfacing.

Table 5-9 Values of parameters in modeling the sound absorption

	P02		P05	
	Model 1	Model 2	Model 1	Model 2
Air voids content, %	12.1	17.8	5.3	12.6
Thickness, mm	30		30	
Flow resistivity, kPa·s/m^2	60		153	
Tortuosity	from the fitness		from the fitness	
Ambient atmospheric pressure, kPa	100			
Density of air, kg/m^3	1.225			
Sound speed, m/s	343.2			
Prandtl number	0.71			
Grazing angel	90^o			

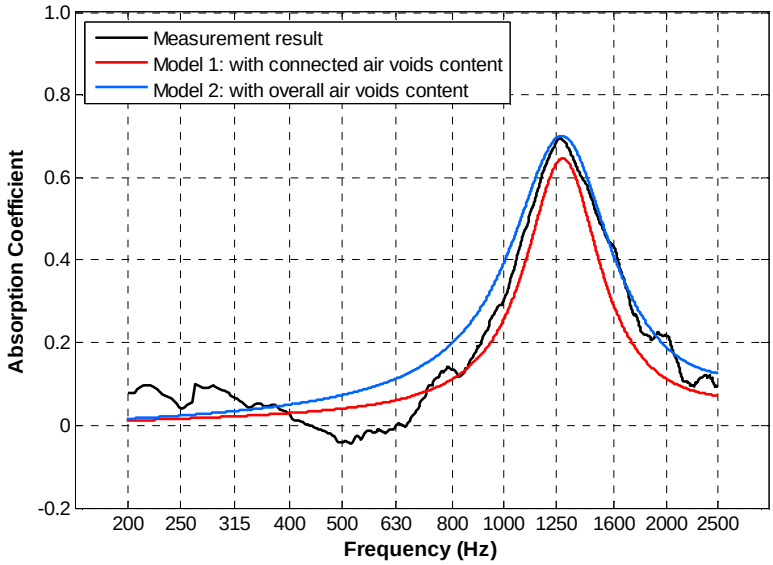

Figure 5-24 Modeling of sound absorption coefficients for slab P02

The simulation result for P05 is shown in Figure 5-25. Using a tortuosity value of 5.5 resulted in the best fit. It is recalled that 15 absorption measurements were taken on each slab. The absorption curves derived from each location differed somewhat with respect to each other. Analyses of results from different test positions showed that the tortuosity ranges from 5.5 to 8. This could be caused by the varying air voids content at different spots. Model 1 shows a good agreement with the first peak of the measured data, while model 2 overestimates the absorption coefficient of the first peak. It is thus concluded from the results that using the connected air voids is preferred to be used than the overall air voids content as input parameter for modeling the sound absorption of semi-dense thin layer surfacings. For the second peak at high frequencies no good simulation is obtained from either model.

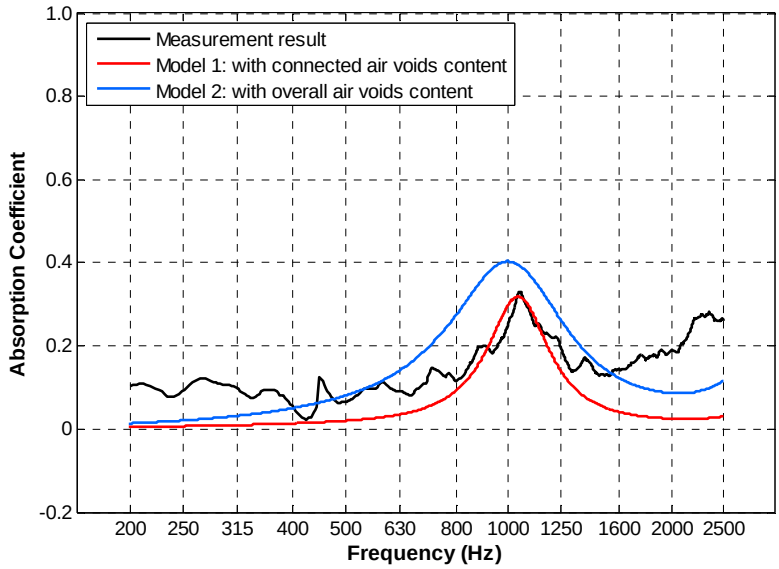

Figure 5-25 Modeling of sound absorption coefficients for slab P05

From the theoretical sound absorption model and the discussion on the influencing parameters it is clear that sound absorption of a road surface is related to the combined effect of different material properties. The air voids content is considered to be the most important factor influencing both the magnitude and the position of the absorption peak. For a porous thin layer surfaces, the overall air voids can be used for evaluating the sound absorption, while for a semi-dense surface, the connected air voids content is preferred as the input parameter. In practice, the degree of connectivity can be estimated from Figure 5-10.

Tortuosity influences the location of the first peak absorption. By fitting the experimental data, the tortuosity for a porous thin layer surfacing is estimated at 3.5. For a semi-dense surface, it ranges from 5.5 to 8. This is considered to be caused by the variation of air voids and grain shape of the specific surface. This tortuosity range could be used as a first estimate in the future work of modeling. In addition, the effective thickness and the flow resistivity are also suggested to

be measured in order to improve the present model. In addition to the theoretical sound absorption model, also statistical models are developed for predicting the maximum sound absorption of thin layer surfacings. This is discussed in Chapter 7.

5.5 Mechanical Impedance and Stiffness

5.5.1 Mechanical impedance

On each slab, impedance hammer tests were performed at three positions as shown in Figure 5-27. The numbering of the three sensors is also given. On each position, two tests were carried out. From Section 4.5.1, it is known that five strikes are applied on the slab in each test.

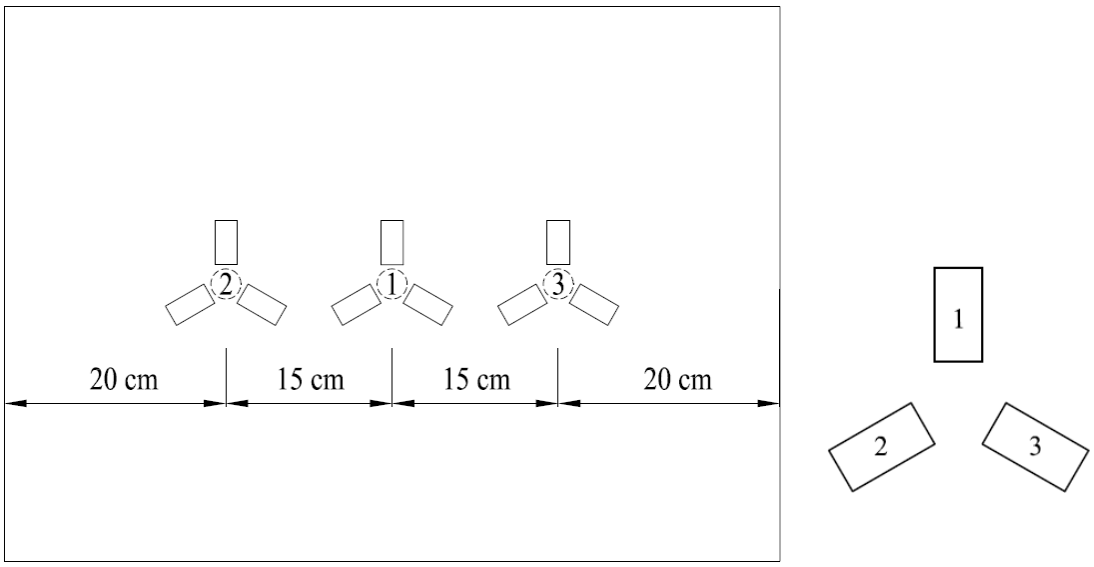

Figure 5-26 Test positions on the slab and numbering of the sensors

Figure 5-27 gives an example of the mechanical impedance in the frequency domain from the two tests on three different positions. The data used are from slab P05. The curve from each test is the average mechanical impedance calculated from the five strikes. For example, Position 1-1 in the figure means the first test at the position 1 shown in Figure 5-26. Results are shown for the individual sensors respectively. From the figure, it can be seen that the shapes of the impedance curve achieved on the same sensor are approximately the same, but are different between sensors. A resonance frequency is generally observed between 1500 Hz and 2000 Hz. In some cases, there are large differences of resonance among the tests, as shown in Figure 5-27 (c). Sometimes the results from the tests on the same position differ, like the two tests on position 1 given in Figure 5-27 (c). All the investigations denote that there are variations between different tests, and these variations need to be taken into account in further analyses.

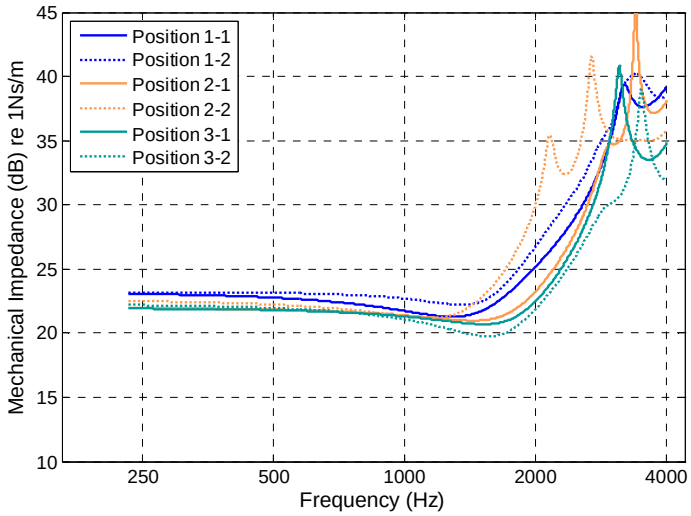

(a) Results from sensor 1

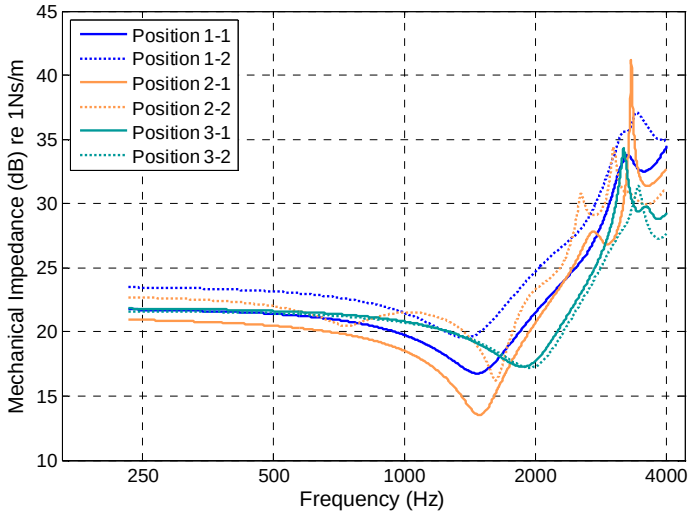

(b) Results from sensor 2

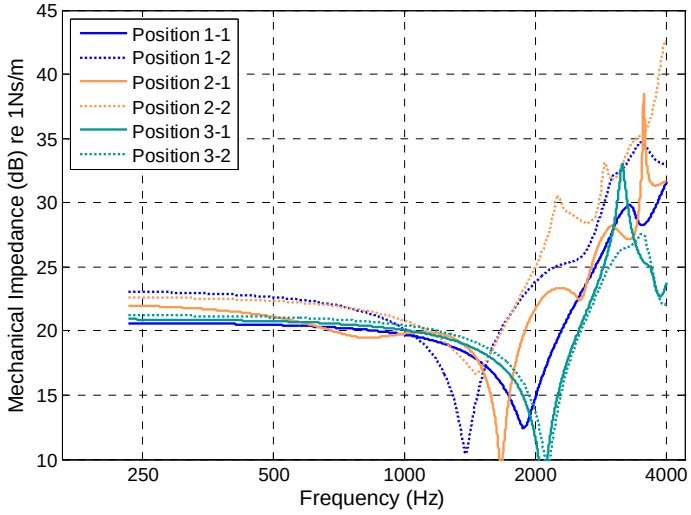

(c) Results from sensor 3

Figure 5-27 Mechanical impedance calculated on different sensors of P05

The final results of the mechanical impedance tests for each slab are the average values of the test results from the three test positions, three sensors, two measurements and five strikes. A summary of the mechanical impedance of all the slabs is illustrated in Figure 5-28. It can be seen from the figure that the mechanical impedance for the different mixtures is close to each other below 1000 Hz, while the curves become very noisy at frequencies above 3000 Hz. The resonance frequency is between 1500 Hz and 2000 Hz. The resonance is related with damping of the system and not considered as valid mechanical impedance information [16]. So the differences of the results are mainly found between 2000 Hz and 3000 Hz. However, when the variations between the separate tests are considered, the differences between 2000 Hz and 3000 Hz can also be regarded as insignificant. As a result, it can be concluded that the mechanical impedance in the frequency domain for all the thin layer surfacing samples is comparable.

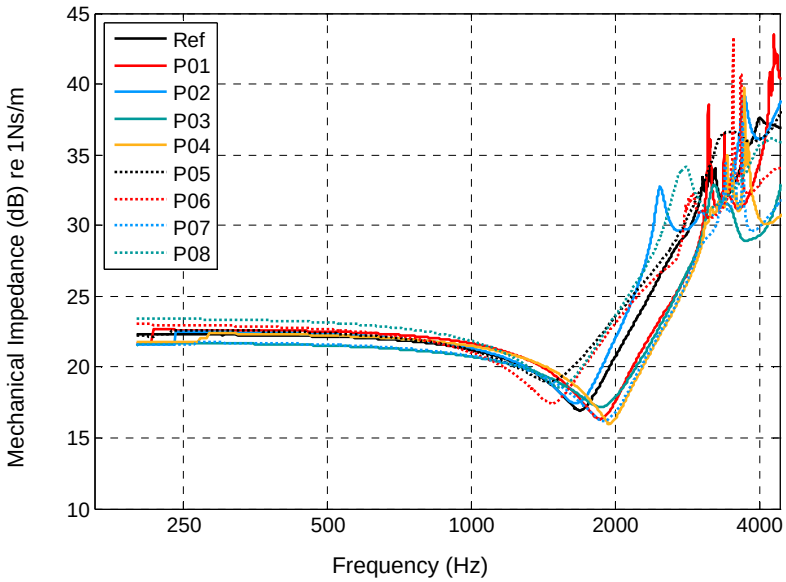

Figure 5-28 Mechanical impedance of slab samples

It should be noted that the resonance between 1500 Hz and 2000 Hz does not reflect the mechanical impedance of the slab. According to a previous study [16], the frequency band which is of interest for tyre - road noise lies between 500 Hz and 2000 Hz. This means there is lack of information on the important frequencies in the spectral analysis. Therefore, a new indicator for the mechanical impedance is proposed in this study.

As known the stiffness is the ratio between maximum force applied and the resulting maximum displacement. In analogy with the stiffness, the new indicator of mechanical impedance (MI') is defined as the ratio of maximum force to the maximum resulting velocity. Figure 5-29 shows the curves of the force and the velocity which is obtained by integration of the acceleration signal. The maximum force and the maximum velocity can be achieved from the curves. MI' is thus calculated by:

$$MI' = Max.Force/Max.Velocity \quad (5\text{-}9)$$

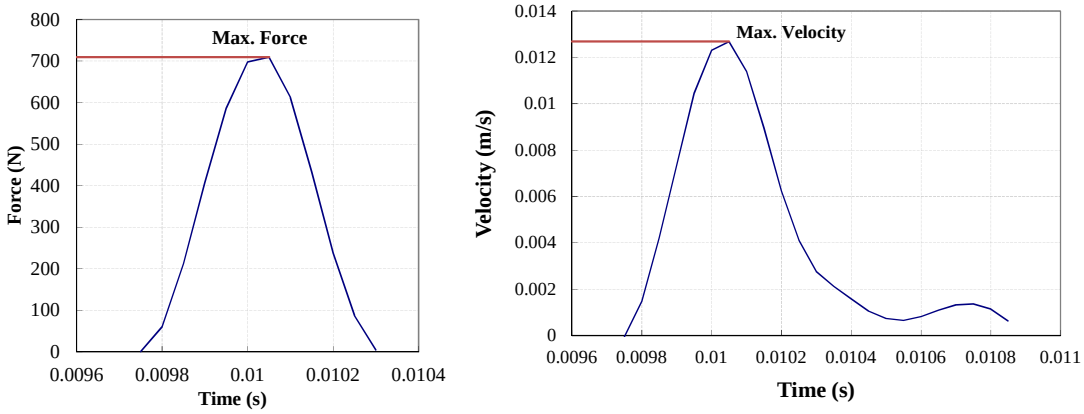

(a) Force (b) Velocity

Figure 5-29 Curves of fore and velocity in an impedance hammer test

The mechanical impedance expressed by MI' is calculated for the slab samples and the Kloosterzande sections. As the cores are small, they cannot be used for the impedance hammer measurements. The tests were thus carried out directly on the surfaces of the Kloosterzande sections. A measurement on the section is illustrated in Figure 5-30. On each section, two measurements were taken on one position. Thin layer surfacing sections numbered 2, 3, 4, 5, 9 and 15 were tested. Since section 24 had been removed, no data could be collected on it. In addition, the tests were carried out on section 1 with a dense asphalt surface layer and on section 12 which had a poro-elastic surface (Roll Pave). These two surfaces have material properties which are quite different from the thin layer surfacings and are used for comparison purposes. The dense layer is a standard ISO surface with a coarse aggregate size of 0/8 mm and a designed thickness of 30 mm. The poro-elastic surface is a Roll Pave type, which was developed in the Netherlands [17]. This surface has been presented in section 2.2.4.4. A picture of the Roll Pave pavement on the Kloosterzande sections is shown in Figure 5-31.

Figure 5-30 Impedance hammer test on the Kloosterzande sections

(a) Roll Pave surface (b) Roll Pave and the 8/11 porous asphalt

Figure 5-31 Roll Pave on Kloosterzande section 12

The MI' values for the slab samples and Kloosterzande sections are plotted in Figure 5-32. For comparison purposes also data that was collected from the concrete floor of the lab are given in Figure 5-32.

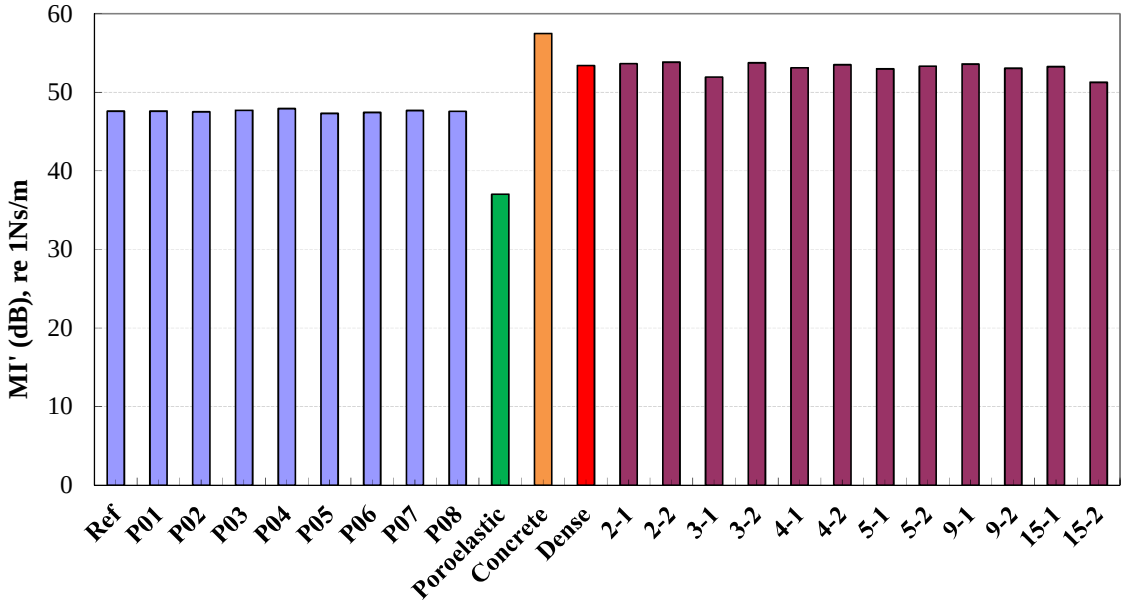

Figure 5-32: Mechanical impedance for different surfaces

For each surface, the MI' in the figure is the average of the tests performed on this surface. By comparing the results obtained on the different surfaces, it can be seen that the mechanical impedance of the concrete floor is the highest, while the lowest value is found on the poro-elastic surface. The slab samples show very similar MI' values. This observation is in agreement with the conclusion from the investigation on the impedance in the frequency band.

The MI' values of all the Kloosterzande sections, including the thin layer surfacings and the dense surface, are comparable. However, the mechanical

impedance of asphalt surfaces on Kloosterzande sections is higher than those of slab samples. It indicates that the in-situ road surface has a higher resistance to motion compared to the slabs produced in the lab. A possible explanation can be that the surfaces in practice are well compacted by a roller compactor and consequently have a more stable structure. Also, the surface area of the in-situ sections is much larger than that of the slab. Furthermore the real road has a multi-layer structure composed of a top layer, base layer and a sub-grade. For the slab samples, the surface area is limited and the boundaries are different. The slab is not glued to the ground underneath. These placement conditions of the slabs might make them more easily to vibrate than the real road surface.

5.5.2 Stiffness

The stiffness test was performed by means of the ITT method as discussed in Section 4.5.2. The master curves of the resilient modulus were generated based on the test results obtained at different temperatures and loading frequencies. As the mechanical impedance is measured at 20^{o}C, a reference temperature of 20^{o}C is chosen to construct the resilient modulus master curves. As three cores were extracted from each slab, the master curve for the slab is based on the average modulus of the three cores. The frequency range for the curves is from 0.1 Hz to 2000 Hz. The resilient modulus in relation to mixtures composition is illustrated in Figure 5-33. The master curves for samples with different material properties are in general close to each other.

Figure 5-33 (a) shows the influence of the air voids content on the resilient modulus. It can be seen that the master curves of Ref and P02 almost overlap each other in the whole frequency range. The modulus of P01 is lower at frequencies below 10 Hz, but it is higher above 10 Hz compared to Ref and P02. This indicates that the influence of the air voids content on the stiffness is not obvious for materials with a high air voids content, in this case higher than 12% in this case. The stiffness above 10 Hz increases when the air voids content decreases to a certain level, e.g. 8%.

Figure 5-33 (b) compares the resilient modulus of samples with various coarse aggregate contents. The volumetric content of the aggregate is considered in the analysis. The designed air voids of the samples are all equal to 8%. It shows that the stiffness increases with increasing coarse aggregate content. This is probably caused by a more stable skeleton with a large percentage of aggregates resulting in smaller deformations caused by the loads.

Figure 5-33 (c) shows that the modulus of two specimens with a different maximum aggregate size is almost the same in the frequency range above 100 Hz. At frequencies lower than 100 Hz, the resilient modulus of the cores with a coarse aggregate size of 2/6 mm is higher than that of the cores with 4/8 mm as maximum aggregate size. This is because the lower frequency corresponds to a high temperature in the stiffness test. The bitumen works less at high temperature. The 2/6 mm aggregates in the mixture are better connected than 4/8 mm

aggregates because of the smaller size. Thus the 2/6 mm aggregates are considered better interlocked and has more resistance to deformation.
The effect of aggregate types is shown in Figure 5-33 (d). Ref and P07 show almost the same resilient modulus which is higher than that for P06. It seems that the aggregate type has influence on the stiffness. However, it is much more likely the bitumen has more influence because of the difference in bitumen type used. As known from Section 4.2.1, a type of colorless bitumen (Sealoflex) with addition of color pigments is used as binder for P06. In other slabs, Cariphalt DA bitumen is used. As shown in Table 4-3, both types of bitumen do not have the same penetration and softening point, so the stiffness is also different.

Figure 5-33 (e) shows that a lower stiffness is obtained by increasing the binder content by 1%; this is in agreement with common knowledge.

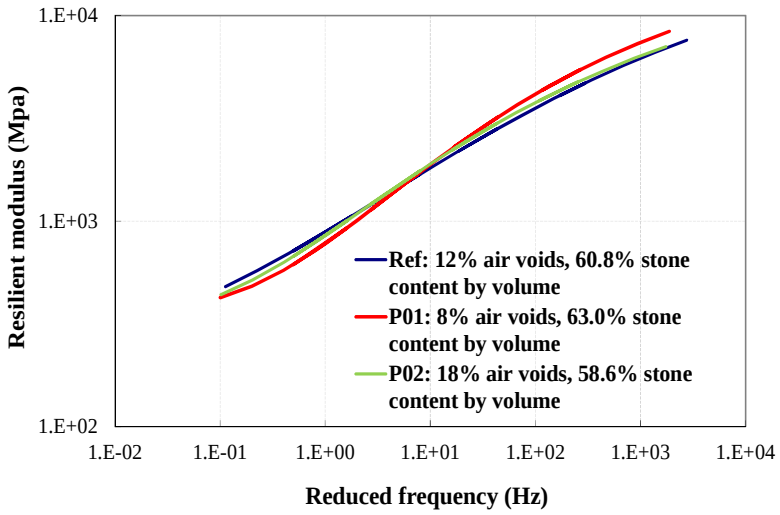

(a) Different air voids contents

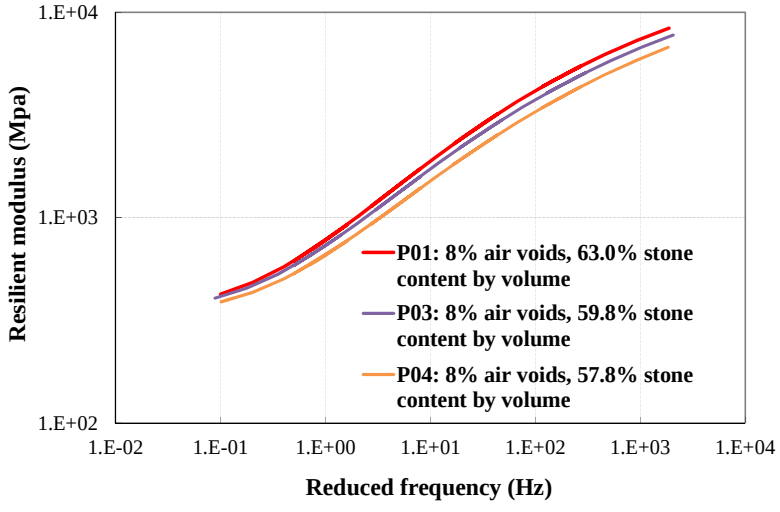

(b) Different coarse aggregate contents by volume

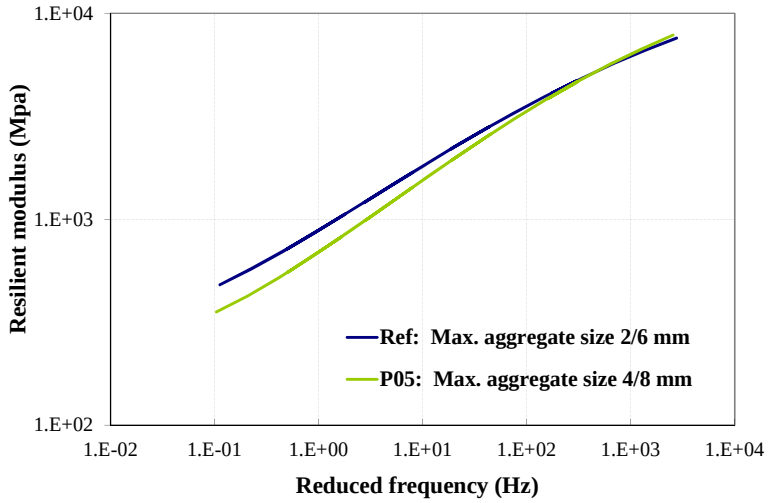

(c) Different maximum aggregate sizes

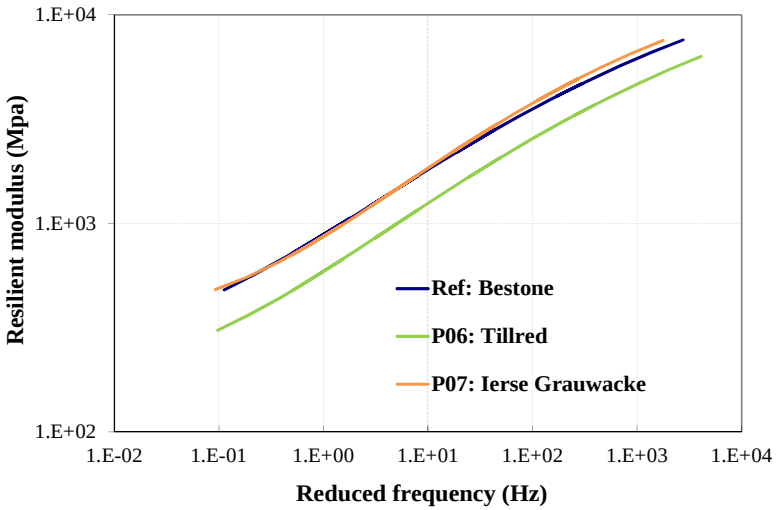

(d) Different aggregate types

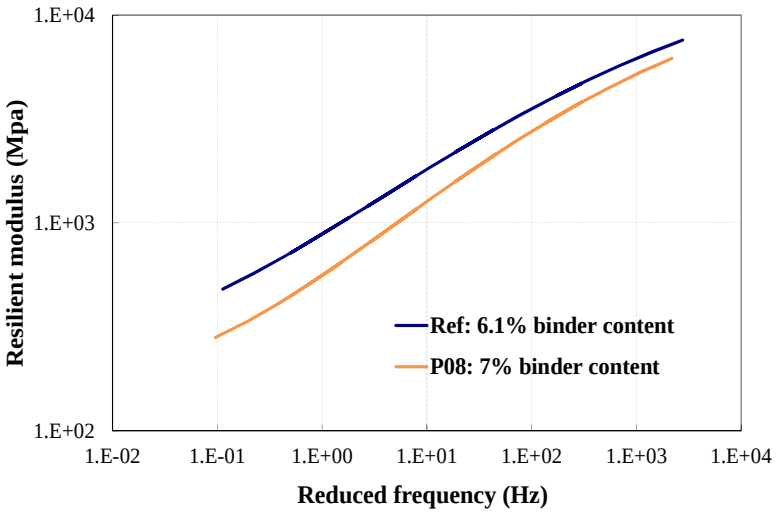

(e) Different binder contents

Figure 5-33 Master curves of the resilient modulus of slab samples (20°C)

Figure 5-34 illustrates the resilient modulus master curves of the thin layer surfacings from the Kloosterzande trial sections. The cores from section 3 and 4 are very thin, close to 20 mm. It was difficult to apply the load along the radial direction of the core, and results from these cores are therefore considered to be invalid. Thus, the master curves for cores from section 3 and 4 are not shown. The figure shows that all the master curves are close to each other, with a variation within 10%. As the cores were drilled from the four years old sections, there are many factors influencing the mechanical properties, such as the construction process, environmental effects causing ageing of the bitumen, etc. Moreover, only one core was taken from each section, and the result of that one sample cannot really be considered as representative for an entire section. Therefore the relation between stiffness and the material properties are not investigated for the cores from the trial sections. The resilient modulus data shown in Figure 5-34 are only used for detecting the relationship between mechanical impedance and stiffness.

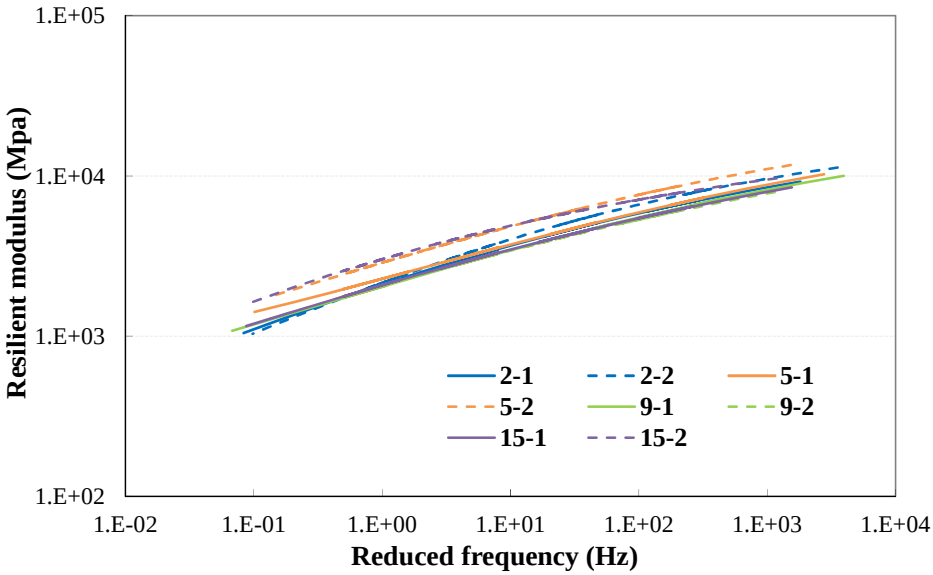

Figure 5-34 Resilient modulus master curves of the Kloosterzande cores (20^{o}C)

As discussed previously, in addition to the thin layer surfacings, other types of road materials were also involved in the study, i.e. the dense asphalt mixture, cement concrete and a poro-elastic surface. Figure 5-35 compares the master curves of the thin layer surfacing slabs, the thin layer surfacings from Kloosterzandes, a dense asphalt concrete surface, a poro-elastic surface and cement concrete at 20^{o}C. The dense mixture used in the laboratory test is actually not the same as the dense surface section No.1 in Kloosterzande. It is a dense mixture made in the lab. The mixture composition of this material is shown in Table 5-10. The binder used in the mixture is bitumen 40/60. The properties of the bitumen are given in Table 5-11.

Table 5-10 Material properties of the dense mixture used in stiffness test

Aggregate type and gradation					Maximum aggregate size, mm	Binder, % by mass	Air voids content, % by volume
Aggregate type	Scottish crushed granite		Norwegian Bestone	Crushed sand			
Sieve, mm	8-5.6	5.6-4	6-2	2-0.063			
Content, % by mass	11.2	19.6	21.5	33.2	8	6.5	2.75

Table 5-11 Properties of bitumen 40/60

Penetration at 25 ºC, 0.1 mm	Softening point, ºC
45	53.6

The figure clearly shows the differences in stiffness between concrete, asphalt and poro-elastic surfaces. The cement concrete shows the highest resilient modulus in the whole frequency range, followed by the surfaces from Kloosterzande, the thin layer surfacing slabs and the poro-elastic surface, in a descending order. The curves for asphalt mixtures from the same source (e.g. Kloosterzande or slabs) are close to each other. More specifically, thin layer surfacings from the Kloosterzande sections have almost the same resilient modulus. The stiffness values of the slab samples are also close but they are lower than those from the Kloosterzande sections. The trends coincide with the observations made on the mechanical impedance data.

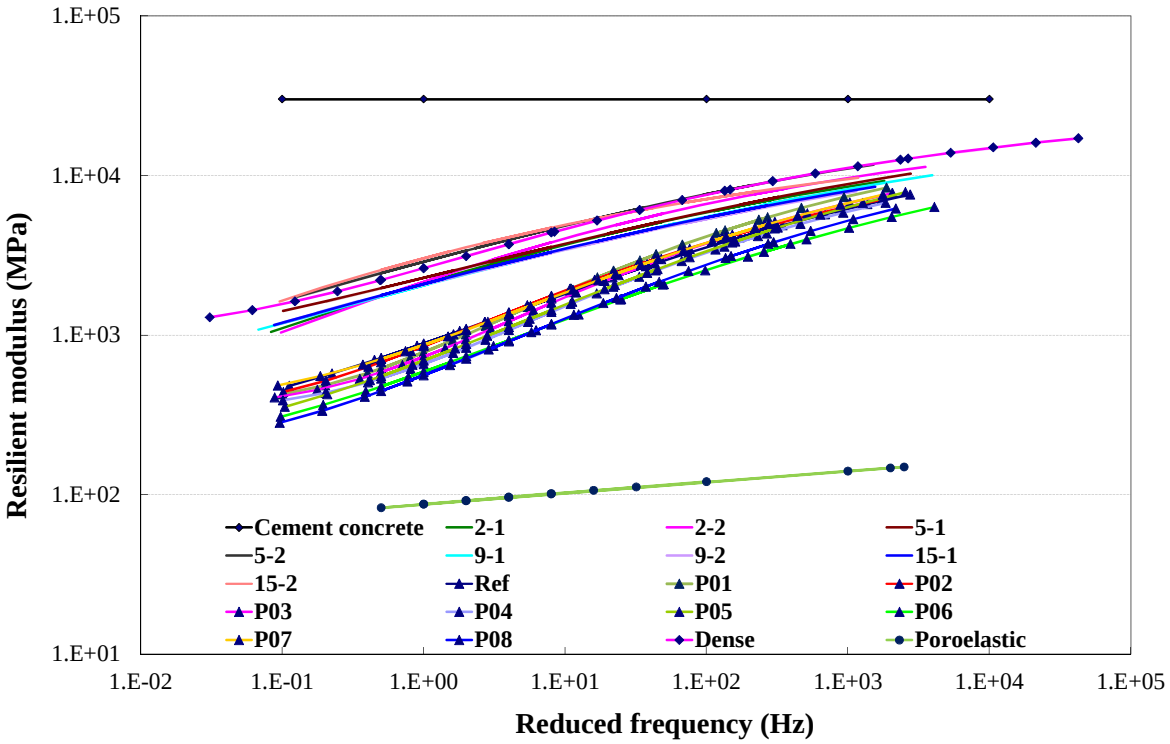

Figure 5-35 Master curves of resilient modulus for different types of road surface samples (20^{o}C)

5.5.3 Relationship between mechanical impedance and stiffness

According to the definition, the stiffness is the frequency dependent ratio between a dynamic force and the resulting dynamic displacement while mechanical impedance is the ratio between the force and the velocity. It is assumed that a relationship exist between the stiffness and mechanical impedance because of the relation between the displacement and the velocity [18, 19]. In this sub-section, this relationship is determined by using the measurement results from the resilient modulus and the mechanical impedance tests on thin layer surfacing samples. It is known that there is currently no standard for measuring the mechanical impedance of a road surface, but there are standardized methods for testing the stiffness. With the relationship, the mechanical impedance can be deduced from the stiffness measurements. It also means that the tyre - road noise reduction by considering mechanical impedance can be studied by using the stiffness of the material.

By comparing the MI' values and the resilient modulus shown in Figure 5-32 and Figure 5-35 respectively, significant differences of mechanical impedance are only observed between materials with a large difference in stiffness. In this section, the specific relationship between the mechanical impedance and stiffness is explored based on the data from both the impedance hammer and resilient modulus tests. The MI' is used as a representative parameter for the mechanical impedance. In terms of stiffness, the resilient modulus at certain frequencies is selected in the analysis. As the mechanical impedance ranging from 500 Hz to 2000 Hz mainly influences the tyre - road noise, in this study, the resilient modulus values at 500 Hz and 2000 Hz are used for denoting the stiffness at medium and high frequency respectively.

Figure 5-36 shows the MI' values against the resilient modulus. Regression analysis is performed for determining the relationship. The regression equation and the trend line are also shown in the figure. It can be seen that the MI' value is linear related with the logarithm of the resilient modulus at 500 Hz and 2000 Hz respectively. According to the regression trend line, the MI' value is sensitive to the stiffness when the stiffness of the material is low. This can be observed by comparing the trend below and above 5000 MPa. As shown in the figures, when the resilient modulus is below 5000 MPa, MI' dramatically decreases with reducing resilient modulus. From 5000 MPa to 30000 MPa, MI' slowly increases.

According to existing research, a larger mechanical impedance tends to result in a higher tyre - road noise level [20]. From a noise reduction point of view, a road surface with low mechanical impedance is appreciated. This study shows that a low mechanical impedance coincides with a very low stiffness. For an asphalt road surface, it is difficult to improve the noise reduction based on the mechanical impedance. The good relation between mechanical impedance and stiffness however shows that an effective way to obtain a low mechanical impedance is to use materials with a very low stiffness, such as poro-elastic materials, with stiffness value lower than 150 MPa in the whole frequency range

being investigated. As the mechanical impedance is not a parameter that is regularly used, the regression equations derived in this study can be used to estimate the mechanical impedance from the stiffness of a material.

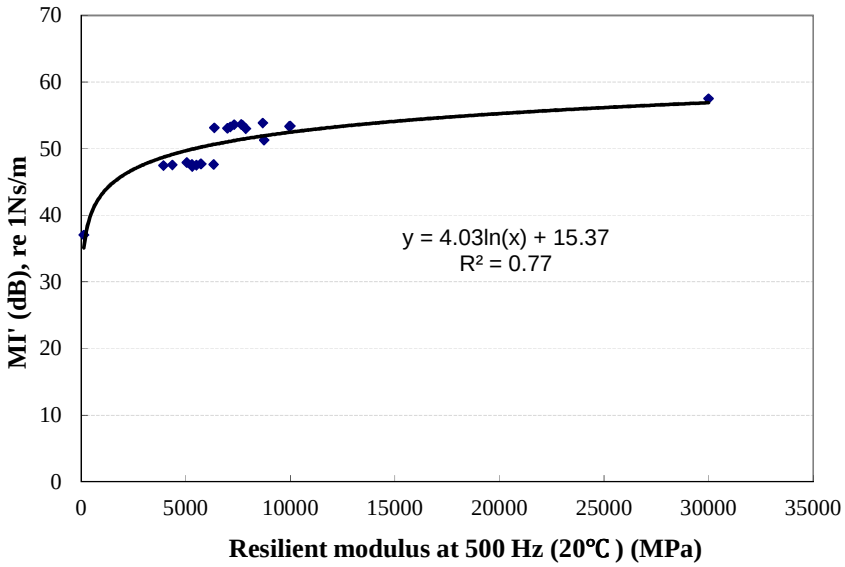

(a) Resilient modulus at 500 Hz

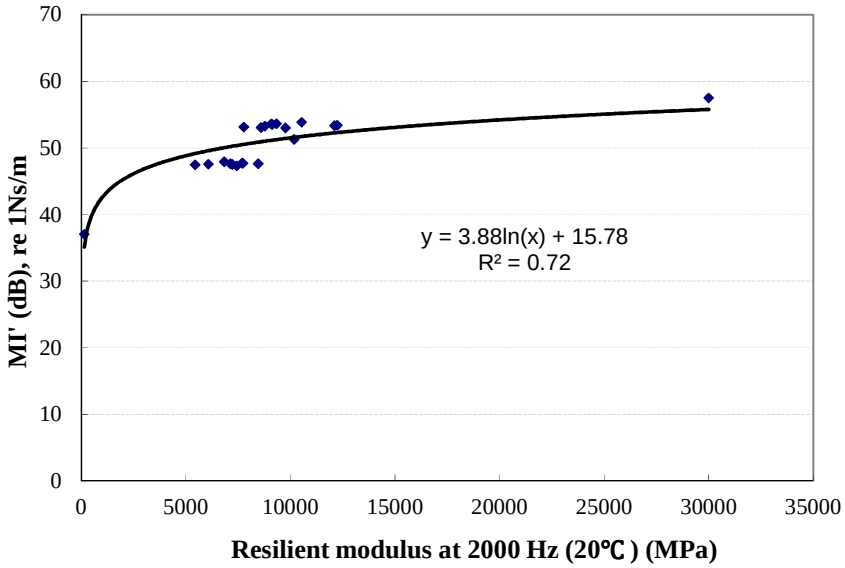

(b) Resilient modulus at 2000 Hz

Figure 5-36: Relationship between mechanical impedance and resilient modulus

5.6 Summary and Conclusions

Experiments were carried out for measuring the mixture composition and the surface characteristics of thin layer surfacing samples. Surface characteristics measured in this study included surface texture, sound absorption, mechanical impedance and stiffness. Both the slab samples produced in the lab and the cores from the Kloosterzande trial sections were involved in the measurements. The test results of the different surface characteristics were investigated, and influence of the material properties on different surface characteristics were

analyzed. A summary of the investigations performed as well as conclusions are presented in this section.

Mixture compositions:
CT scanning provided the mixture compositions of the samples. CT scanning showed that in general the measured voids content of the slabs was in agreement with the design air voids content of 12% and 18%. For samples with a design air voids content of 8%, the target air voids content was approached when the mixture contained less coarse aggregates. The cores from the trial sections showed a large variation in air voids content for samples with a design value of 12%. This was considered to be caused by the construction process.
The degree of connectivity for core samples was obtained by means of a cluster-labeling algorithm. It was shown that the connectivity highly depends on the air voids content. For samples with an air voids content less than 12%, the degree of connectivity was generally below 0.1 and close to 0. For cores with a porosity higher than 19%, the degree of connectivity was close to or exceeding 0.9; this denoted a large amount of connected air voids. The relation between the connectivity degree and the air voids content that was developed in this study can be used in future work for estimating the degree of connectivity from the air voids content.

Surface texture:
Surface profile data were collected by means of a laser profilometer. For the slabs, the surface texture level was expressed in terms of wavelengths in the octave band. For both the slab and core samples, the MPD was calculated from the measured texture profiles. The investigations showed that the maximum aggregate size is the most important factor influencing the surface texture. A material with a larger stone size showed higher peak value of the texture level. In the spectral analysis, the peak texture level generally occurs at a wavelength which is equal or close to the maximum aggregate size. A linear relationship was developed between the maximum aggregate size and the MPD. It is also found that the surface texture increases with increasing air voids content and increasing coarse aggregate content.

Sound absorption:
The sound absorption was measured with the P-U surface impedance setup. The results obtained on thin layer surfacing samples showed high absorption coefficient peaks, equal to or higher than 0.7, for surfaces with an air voids content higher than 17% and with exposed pores at the surface. Small variations in peak frequency were observed between tests on different positions. For a surface layer with a designed air voids content no higher than 12%, or with a clogged surface, a first peak of the absorption coefficient is generally observed between 800 Hz and 1250 Hz; its magnitude is smaller than 0.35. This first peak of the absorption coefficient is correlated with different material properties by means of regression analysis. Regression analysis showed that the absorption coefficient increases linearly with the connected air voids content and the overall

air voids content. The connected air voids content is considered to be an essential parameter determining the maximum absorption. The influence of the coarse aggregate content and mortar content are both attributing to the connected air voids content in the surface layer. Acoustical models were developed for simulating the sound absorption curves of the thin layer surfacing slabs. From the models, it can be seen that the overall air voids content can be used directly to simulate the sound absorption of a semi-open surface like P02. For a semi-dense type of thin layer surfacing, better fit is achieved when the connected air voids content is used as explanatory variable.

Mechanical impedance:
Mechanical impedance tests with the impedance hammer setup were carried out on the slabs and the Kloosterzande sections. Furthermore the resilient modulus of the mixtures was measured on 100 mm cores with the repeated load ITT test. In addition to thin layer surfacings, also a dense asphalt concrete mixture, cement concrete and a poro-elastic surface layer were involved in the measurements. The test results showed that the cores from the road sections have comparable mechanical impedance while slab samples made in the lab also have a similar mechanical impedance. But there are differences between samples from these two sources. The difference in mechanical impedance of materials is only significant when there is a significant difference in stiffness. The regression analysis showed that MI', representing the mechanical impedance, is linearly related to the logarithm of the resilient modulus. An effective way to reduce the mechanical impedance is by using very low stiffness materials, such as poro-elastic materials, with stiffness value lower than 150 MPa in the whole frequency range being investigated. It will not be possible to produce low mechanical impedance layers using standard asphalt concrete mixtures.

References

1. Hoshen, J. and Kopelman, R., *Percolation and cluster distribution. I. Cluster multiple labeling technique and critical concentration algorithm.* Physical Review B, 1976. **14**(8): p. 3438-3445.
2. Sandberg, U. and Ejsmont, J., *Tyre/Road Noise Reference Book*. 2002, Kisa, Sweden: Informex.
3. Hamet, J.F., *Reduction of tire road noise by acoustic absorption: Numerical evaluation of the pass-by noise level reduction using the normal incidence acoustic absorption coefficient*. 2004, Laboratoire Transports et Environnement.
4. Hamet, J.F. and Be´rengier, M., *Acoustical characteristics of porous pavements: A new phenomenological model*, in *Internoise 93*. 1993: Leuven, Belgium. p. 641–646
5. Zhang, M., et al., *Computational investigation on mass diffusivity in Portland cement paste based on X-ray computed microtomography (μCT) image.* Construction and Building Materials, 2012. **27**(1): p. 472-481.

6. ISO/TS13473-4, *Characterization of pavement texture by use of surface profiles -- Part 4: Spectral analysis of surface profiles*. 2008, International Organisation for Standardization (ISO): Geneva, Switzerland.
7. van Blokland, G.J., Reinink, H.F., and Kropp, W., *Acoustic optimization tool. RE3: Measurement data Kloosterzande test track*, in *M+P Report DWW.06.04.8*. 2007, M+P Raadgevende Ingenieurs bv: Vught, the Netherlands.
8. Gerretsen, E., *Model for tyre-road sound emission Part B, phase 1: relation between road properties and material data (in Dutch: Model geluidemissie band-wegdek Deel B, fase 1: relaties wegdekeigenschappen met materiaalgegevens)*, in *TPD-HAG-RPT-970118 for CROW*. 1997.
9. Crocker, M., et al., *Measurement of Acoustical and Mechanical Properties of Porous Road Surfaces and Tire and Road Noise.* Transportation Research Record: Journal of the Transportation Research Board, 2004. **1891**(-1): p. 16-22.
10. Attenborough, K., Bashir, I., and Taherzadeh, S., *Outdoor ground impedance models.* The Journal of the Acoustical Society of America, 2011. **129**(5): p. 2806-2819.
11. Stinson, Y.C.a.M.R., *On acoustical models for sound propagation in rigid frame porous materials and the influence of shape factors.* Journal of the Acoustical Society of America, 1992. **92**: p. 1120–1131.
12. Vér, I.L. and Beranek, L.L., *Noise and Vibration Control Engineering - Principles and Applications (2nd Edition)*. 2006: John Wiley & Sons.
13. ISO9053, *Acoustics — Materials for acoustical applications — Determination of airflow resistance.* 1991.
14. Berryman, J.G., *Long-wavelength propagation in composite elastic media II. Ellipsoidal inclusions.* Journal of the Acoustical Society of America, 1980. **68**(6): p. 1820-1831.
15. Berengier, M.C., Stinson, M.R., Daigle, G.A., and Hamet, J.F., *Porous road pavements: Acoustical characterization and propagation effects.* Journal of the Acoustical Society of America, 1997. **101**(1): p. 155–162.
16. Schwanen, W. and Kuijpers, A.H.W.M., *Development of a measurement system for mechanical impedance*, in *SILVIA Project Report SILVIA-M+P-013-01-WP2-230605*. 2005.
17. Morgan, P.A., *IPG Research Report - Innovative mitigation measures for road traffic noise*, in *Report DVS-2008-018*. 2008, Road and Hydraulic Engineering Division of Rijkswaterstaat: Delft, the Netherlands.
18. Nilsson, N. and Sylwan, O., *New vibro-acoustical measurement tools for characterization of poro-elastic road surfaces with respect to tire/road noise*, in *Tenth international congress on sound and absorption*. 2003: Stockholm, Sweden.
19. Vigran, T.E., *Building Acoustics*. 2008, London and New York: Taylor & Francis.
20. Müller-BBM & M+P, *Influence of surface texture on the tyre-road noise (in German: Einfluss der Fahrbahntextur auf das Reifen-Fahrbahn-Geräusch)*, in *FE 03.293/1995/MRB*. 2001.

CHAPTER 6

INFLUENCE OF SURFACE CHARACTERISTICS

6.1 Introduction

The relationship between road surface characteristics and tyre - road noise is investigated in this chapter. It is the most important topic in the field of tyre - road noise research. From existing research, it is known that the surface texture and sound absorption are the two most important road surface characteristics related to noise generation. In addition, mechanical impedance is also a medium influential factor, which plays a role in explaining the noise reducing function of poro-elastic surfaces [1, 2].

A great deal of work has been undertaken on determining the influence of the surface texture and sound absorption on tyre - road noise. Also modeling of the relationship between texture and adsorption on one hand and noise on the other has been extensively researched [3, 4]. In early work of Sandberg [5], the relationship between the noise spectrum and the texture spectrum was investigated. It was found that increasing texture levels lead to an increase of the noise level at frequencies below 1.5 kHz, and result in a decrease of noise levels above 1.5 kHz. Similar results were reported by Anfosso-Lédée who introduced geometric indenters to characterize the road surface texture [6].

Texture levels expressed in a wavelength spectrum were standard used as predictors for evaluating tyre - road noise in the models developed by these researchers. Regression analysis of tyre - road noise was conducted by the California Department of Transportation [7, 8]. In the study, MPD was employed for describing the surface texture. Other influencing parameters, such as age, layer thickness and number of days with air temperature higher than 30 ^{o}C, etc, were also included in the regression and showed to have impact on the noise levels. Sound absorption is another important factor contributing to noise reduction of porous asphalt. Sound energy can partly be absorbed by the road surface due to its porosity. This helps to reduce the tyre - road noise by eliminating the horn effect and absorbing sound waves in the propagation path. The maximum noise reduction caused by road surface absorption generally occurs at frequencies around the maximum absorption coefficient, but with a small frequency shift [9, 10]. In the study of Hamet [11], the attenuation of pass-

by noise at a certain frequency was linearly related to the sound absorption coefficient at a shifted frequency. Peeters [12] improved the linear relationship by taking into account the horn effect of surfaces with low and medium (between 0.2 and 0.6) absorption coefficient. In some studies, the air voids content is also used directly as a parameter for describing the influence of the porous pavement structure [2].

In this chapter, the investigation concentrates on the influence of the surface characteristics on the tyre - road noise production on thin layer surfacings. It is based on a statistical analysis of the data collected from the trial sections in Kloosterzande. The surface texture and sound absorption are the main characteristics taken into account. Besides, the influence of air flow resistance, vehicle speed, and tyre type are also discussed in the research program. Compared to previous work, highlights of the analysis in this study are:

1) The study focuses on thin layer surfacings. They are commonly used as noise reducing surface layer in urban and provincial areas in the Netherlands. As mentioned in previous chapters, there are great interests for studying this type of surface. It is important and of interest to predict the noise reducing effects of thin layer surfacings.
2) In addition to correlation analysis as commonly used in previous studies, linear regression is also performed to express the relationship between the noise level and the surface characteristics. For the thin layer surfacing investigated in this study, the variations of the surface characteristics are limited and are in a relatively small range. Within this small range, linear regression relationships with a high precision can be developed.
3) Different combinations of surface characteristics are used in the investigation. In the study, the MPD and texture levels are used respectively for describing the surface texture; the absorption curve on 1/3 octave band of the frequency and the maximum absorption coefficients represent the sound absorption of the surface respectively.
4) In the regression analysis, the multicollinearity exists between the input texture levels and absorption coefficients on the 1/3 octave band of the frequency. In this study, different statistical methods are employed to eliminate the influence of the multicollinearity. The combined effect of the spectrum levels of texture and sound absorption is displayed by the regression equations as obtained.
5) A new type of model is developed. This model focuses on the change of the tyre - road noise caused by changes of the road surface properties [13]. Only the difference values of noise and surface characteristics are considered in the analysis, and not the global values. With this method, the regression function is able to calculate the increase and reduction of the noise level directly and it is convenient for investigation of the noise reduction effect of different surfaces.

The organization of this chapter is as follows:

6.2 gives an overview of the database and discusses the extraction of data from the database for using them in this study; 6.3 describes the whole progress of the analysis, and the methods used in each step are also presented; 6.4 shows the investigation of the influence of surface characteristics from thin layer surfacings on noise. The analysis progress is demonstrated in detail. Examples are given by using different regression methods. The influences of vehicle speed and use of truck tyres are also discussed; 6.5 presents the analysis based on the difference values of noise levels caused by changes of the surface characteristics; A summary and recommendations are given in 6.6.

Figure 6-1 gives a schematic presentation of the investigation, including pretreatment of the extracted data, the variable selection and data analysis. The analyses in this chapter refer to this scheme. Details about each item in the chart are explained in the following sections.

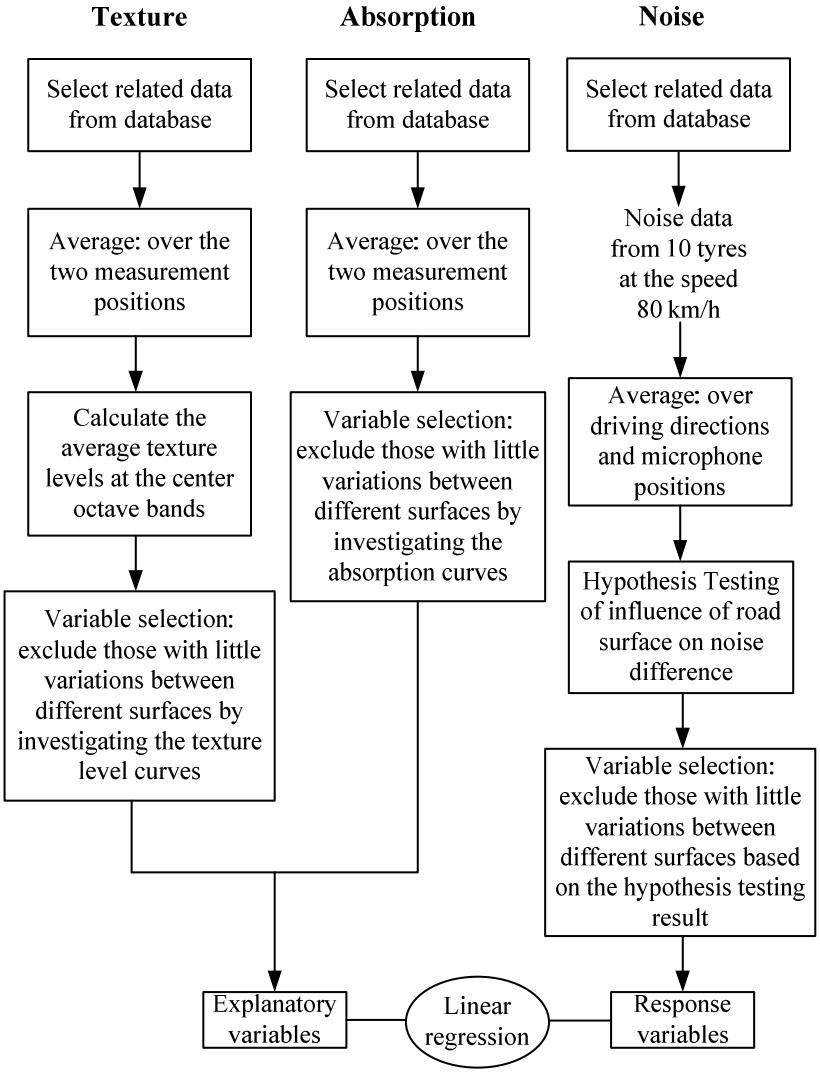

Figure 6-1 Diagram of the analysis

6.2 Data Extraction and Pretreatment

As introduced in section 4.2, a database was set up based on the measurements on 40 trial sections in Kloosterzande in the Netherlands. It contains comprehensive information of noise related properties for different types of road surfaces and tyres [14]. The database used in this investigation was provided by the Centre for Transport and Navigation (DVS) in the Netherlands.

Parameters describing tyre - road noise and surface characteristics highly related to noise generation are listed in Table 6-1. The record forms of the data for different items are also shown. It is known that road surface texture and sound absorption are two main factors affecting the tyre - road noise levels. They are recorded by different indexes in the database. For the sound absorption, the sealed tube method was only applied on several road sections, and results from this method are not included in the analysis. Air flow resistance is another parameter reflecting the effect of porosity and used as a predictor in the model SPERoN. As it is not a commonly used factor and since it is correlated with both texture (which is influenced by stone size in the mixture) and sound absorption, this parameter is not included as an independent variable in the regression analysis. From Chapter 5, it is known that the mechanical impedance is not much different for different thin layer surfacings. Hence, this parameter is also not used in the investigation.

In the database, tyre - road noise levels were measured by both the near field (CPX) and far field (CB) method. However, CB tests were only done on a number of selected sections, and the data are not sufficient for a complete investigation. Therefore, the CB level data are excluded. Nevertheless, the far field noise level can be deduced from its relationship with near field test results. A study on the relation between the far field and near field method is presented in Chapter 2. The noise levels concerned in the following study are the near field noise levels measured by the CPX method.

Data for all the selected surface characteristics and noise levels, namely texture, sound absorption tested by means of ESM, air flow resistance and noise level from CPX test, were then extracted from the database. Figure 6-2 illustrates the different testing positions of the surface characteristics and the tracks for the CPX tests. As shown in the figure, the east and west lane for each surface were built based on the same design. However, because of the variation in the construction process, the surface characteristics and the sound emission properties are different for lanes with the same nominal design. Therefore, they can be treated as different surfacings [14]. For texture, sound absorption and flow resistance, the data from measurements at the positions B and C are extracted. The average of values from B and C are used for presenting the surface characteristics of each lane in this research.

Table 6-1 Record form of influencing parameters and noise level

Parameter	Data store form	
Surface texture	Average MPD, ETD and RMS values and the standard deviation (mm); Texture levels in 1/3rd band spectrum from 0.5 till 500 mm octave (mm)	
Sound absorption	Extended surface method (ESM)	Data of acoustic absorption measurements, in1/3rd octave band spectrum from 250 till 4000 Hz
	Sealed tube method	*Data of acoustic absorption measurements, in1/3rd octave band spectrum from 250 till 2000 Hz*
Air flow resistance	Specific air flow resistance R_s, measured by on site test methods developed by M+P, (Pa s/m)	
Noise level	Close Proximity (CPX) method	Vehicle speed and corresponding standard deviation (km/h); A-weighted equivalent sound level $L_{A,eq}$: overall level and its standard deviation, the 1/3rd octave band spectrum from 50 till 5000 Hz (dB)
	Coast-By (CB) method	*Vehicle speed (km/h);* *Maximum A-weighted sound level $L_{A,max}$: overall level and the 1/3rd octave band spectrum from 50 till 5000 Hz (dB);* *Sound exposure level (SEL): overall level and the 1/3rd octave band spectrum from 50 till 5000 Hz (dB);* *Microphone position: 1.2 m, 3 m and 5 m*

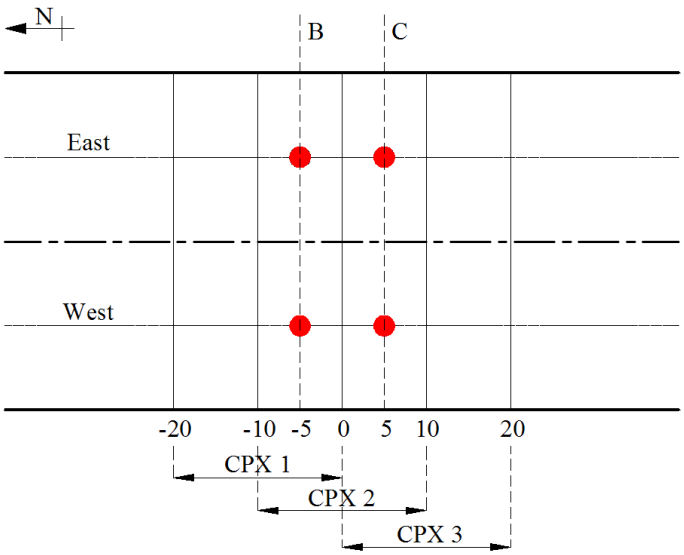

Figure 6-2 Test positions on the trial section, Unit: m

In terms of CPX measurements, the following facts have to be taken into consideration with respect to data extraction of passenger car tyres measurements:

1) Segment

For the CPX test, the measurements were taken from 20 m before the center of the section to 20 m after the center on each section where the surface was assumed to be homogenous. As shown in Figure 6-2, three segments were measured. Both CPX segment 1 and segment 3 are overlapping with segment 2.

In this study, data collected from the central part, CPX 2 as show in Figure 6-2, are used for analysis.

2) Direction
The measurements were performed in both directions along each track, i.e. from north to south and from south to north. They are both taken into account.

3) Microphones
On each side of the trailer, 11 microphones were placed around the test tyre when testing the Kloosterzande sections. According to the specification [15] for the CPX method, the noise is generally measured at two standard inner positions. Therefore only noise levels measured at these two positions are adopted in this study. This selection also facilitates comparison with other measurements in the future, as most of the noise collections are made using the standard positions.

4) Speed
For the passenger car tyre measurements, 8 test speed intervals are used in this research being: 40 – 45, 45 – 50, 50 – 55, 55 – 65, 65 – 75, 75 – 85, 85 – 100 and 100 – 120 km/h. A linear relationship between the sound pressure levels of tyre - road noise and the logarithm of the speed has already been identified, and it is possible to predict the noise level caused at different speeds [2]. In this study, the analyses will mainly focus on condition when the speed is between 75 and 85 km/h. The influence of vehicle speed will be discussed seperately in section 6.4.6.

5) Tyres
The CPX measurements were taken by employing different types of car (and truck) tyres. Table 6-2 lists the 11 types of passenger car tyres with similar dimensions. As the slick tyre is not applied in normal traffic, it is excluded from the study. Since the current research only aims to make a general observation on the tyre type effects, the tyres are not further categorized by specific properties, such as width, diameter and material.

Table 6-2 Passenger car tyre types used in current study

Tyre No.	Type	Size	Tyre Type	Tyre No.	Type	Size	Tyre Type
1	Michelin Energy	175/65R14*	Summer tyre	7	Continental ContiPremiContact	195/65R15	Summer tyre
2	Goodyear GT3	175/65R14	Summer tyre	8	Continental Slick	195/65R15	Slick
3	Pirelli P3000 Energy	175/65R14	Summer tyre	9	Goodyear Ultragrip 7	175/65R14	Winter tyre
4	Continental ContiEcoContact EP	175/65R14	Summer tyre	10	Vredestein Snowtrac2	195/65R15	Winter tyre
5	Michelin Energy	195/65R15	Summer tyre	11	Avon ZV1	185/65R15	CPX A
6	Vredestein Hi-Trac	195/65R15	Summer tyre				

*175=Tyre width in mm; 65=Aspect ratio (height is 65% of width); R = Tyres with a radial construction; 14=Diameter of rim (in inch).

Examples of the profiles of the passenger car tyres are shown in Figure 6-3. Other tyres can be seen in the CD attached to this thesis.

(a) Passenger car tyre 05:
Michelin Energy 195/65R15

(b) Passenger car tyre 09:
Goodyear Ultragrip 7 175/65R14

Figure 6-3 Examples of profiles of passenger car tyres

6) Invalid data

Tests by means of a CPX-trailer are possibly disturbed by external noise. The two main sources of disturbance are driving noise and wind noise. From inspection of the measured 1/3rd octave band spectra it is shown that wind noise is mainly dominant in the lower frequency ranges. Data collected during great disturbance caused by wind are considered as 'invalid' and marked in the database. These invalid data are not used in the investigation. Table 6-3 shows the factors related to the CPX measurements. The average values of the sound level are calculated over the two directions and the two microphone positions. Tyre types and speed will be treated in different ways according to the investigation.

Table 6-3 Parameters related to CPX measurements

Item	Tyre	Direction	Microphone Position	Speed
Number	10	2	2	1 of 8
Name	see Table 6-2	North and North	standard CPX inner positions	75-85 km/h

The above discussion is based on tests done with passenger car tyres. The data extraction process for truck tyres is similar. A specific investigation on noise from truck tyres is presented in section 6.4.7.

6.3 Analysis Program and Methods

Data of the selected parameters are extracted from the DVS database, and they are used for investigating the influence of surface characteristics on tyre - road noise. The analysis can be accomplished in two steps being:
a. variable selection and
b. data analysis.

6.3.1 Initial variable selection

In the regression analysis, parameters for road surface characteristics are selected as explanatory variables and the noise levels are used as response variables. From Table 6-1, it can be seen that the number of texture levels and the sound absorption coefficients on the 1/3 octave band is large. If all these levels are considered as explanatory variables for the regression, a total of 44 input variables need to be used. In that case, the resulting function could be very complex. Moreover, introducing as many as possible candidate variables may lead to confusion, because some of the variables are redundant or irrelevant, and they would negatively influence the regression analysis. Therefore, it is essential to reduce the number of input variables as much as possible [16].

The response variables, being noise, can also be presented by sound pressure levels at different frequencies. In this research, the noise levels which are significantly influenced by the surface characteristics are of interest and they are collected for the study. Hence, a choice of the noise levels is also carried out. Specific methods used in this selection process are as follows:

1) Texture level

In order to reduce the number of the texture levels as explanatory variables in the regression, the average of the texture level at each three adjacent wavelengths is calculated by means of the following equation [2]:

$$TL = 10\lg\left(\frac{1}{3}\sum_{i=1}^{3}10^{0.1TL_i}\right) \tag{6-1}$$

TL_i means the texture level at one of the three adjacent wavelengths. The calculation of the average is illustrated by the scheme in Figure 6-4. The figure shows how the texture levels TL_{63}, TL_{32} and TL_1 are achieved. The derived texture level TL is named by the texture level at the centre wavelength of the three. For example, when the average is calculated from texture levels with wavelengths 50 mm, 63 mm and 80 mm, the result is named as TL_{63}. An example of the comparison between the original and average texture level is shown in Figure 6-5. The data are from section 4-1. From the figure, it can be seen that the averaged texture level can precisely describe the texture spectrum from the measurement. Therefore it is reasonable to use the averaged texture levels in the analysis hereafter.

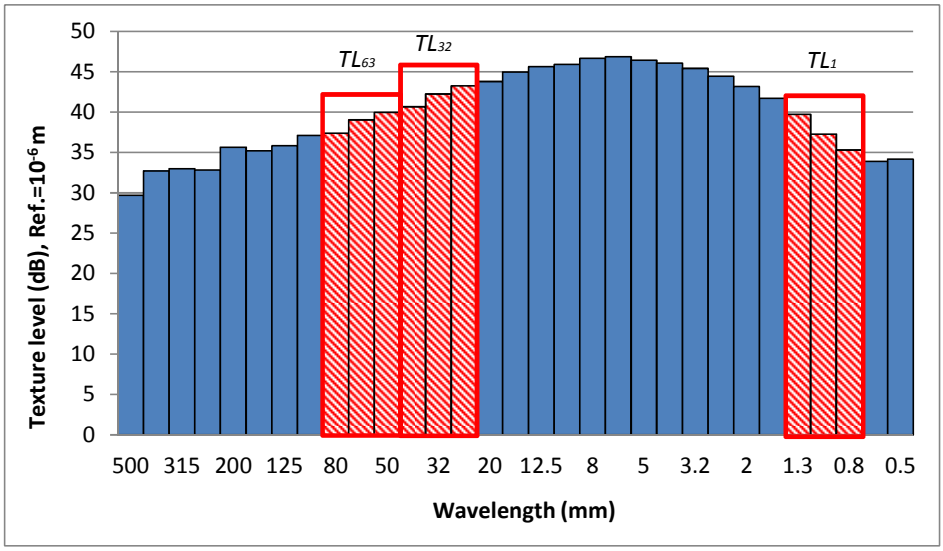

Figure 6-4 Example of averaging of the texture level

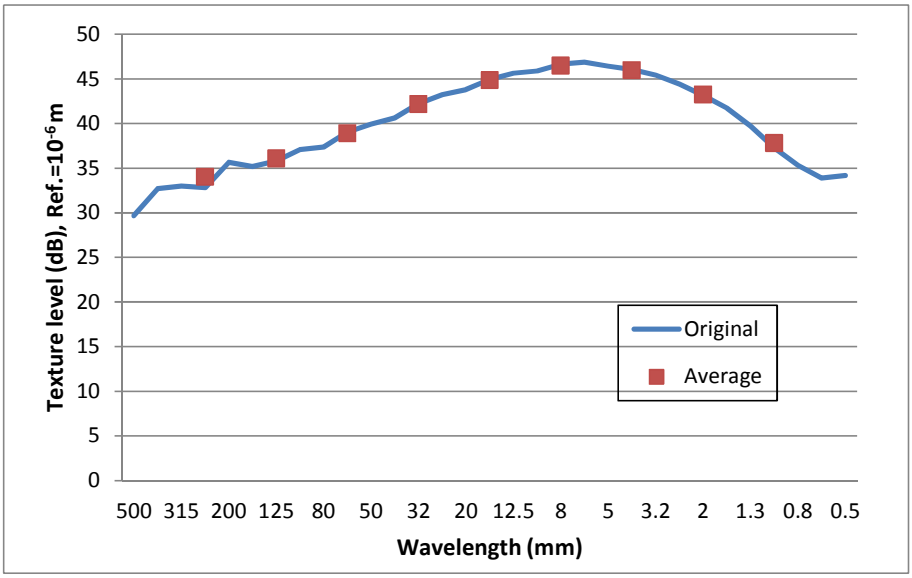

Figure 6-5 Comparison between the original and averaged texture level on section 4-1

An investigation was then made on the spectrum of averaged texture level. At certain wavelengths, the differences in texture levels between various road surfaces are small and therefore these texture levels will have only a small influence on the noise level. Therefore such data are removed from the input variable set.

2) Sound absorption

The sound absorption curves from the different road surfaces are plotted. Variable selection is decided based on observation of the curves. At a certain frequency, the differences in absorption coefficient of different road surfaces are small and they are considered to have such a small influence on the noise level. Therefore they need not to be taken into account.

3) Noise
A hypothesis test is performed to investigate the influence of the road surface on noise generation. The null hypothesis is that there is no effect of the difference of the road surfaces on the tyre - road noise levels. The significance level is set at 0.05. *F* tests are performed on the noise data from different sections. The null hypothesis is rejected when the observed significance from the *F* test is less than 0.05. It means that the differences between various road sections affect the noise level.

Before the hypothesis testing, a test of normality is performed to examine the distribution of the data at a certain frequency for different road surfaces. If the data followed the normal distribution, the one way analysis of variance (ANOVA) was used for the hypothesis test. Otherwise the non-parametric test method was employed. When using the non-parametric test, there is no precondition that the population fits any distribution. So it is also referred to as a distribution-free test. All these statistical tests are executed by using the statistical software SPSS.

From literature it is known that besides the spectrum, the surface texture can also be represented by the MPD, while the sound absorption can be described by the maximum absorption coefficient. In this study, these parameters are therefore also taken into account in the investigation. By using different combinations of indenters of surface texture and sound absorption, four groups are set up to present the road surface characteristics. These four combinations are listed in Table 6-4.

Table 6-4 Combination of surface texture and sound absorption

Combination	Explanatory variables	
	Surface texture	Sound absorption
1	Texture levels at selected wavelengths	Absorption coefficients at selected frequencies
2	MPD	Absorption coefficients at selected frequencies
3	Texture levels at selected wavelengths	Maximum absorption coefficient
4	MPD	Maximum absorption coefficient

6.3.2 Data analysis

As shown in Figure 6-1, the regression analyses are performed based on the data from combinations of surface characteristics and selected noise levels. Details about the analysis program and the related methods are discussed in this section.

6.3.2.1 Basic model

The research focuses on thin layer surfacings. The variations in surface characteristics are considered limited, because the difference in material properties between sections is relatively small. It is assumed that the tyre - road noise level is linearly related to the surface characteristics. The relationship between the noise levels and the surface characteristics can thus be developed by multivariate linear regression.

The standard regression model is defined as:

$$\mathbf{y} = \mathbf{X}\boldsymbol{\beta} + \boldsymbol{\varepsilon} \tag{6-2}$$

where **y** is the response variable representing a certain noise level. It is a vector containing n observations, $\boldsymbol{X}$ is an $n \times p$ matrix, in which the (i, j)th element is the value of the jth indenter of the surface characteristic (i.e. the texture or sound absorption) for the ith observation, $\boldsymbol{\beta}$ is a vector of the p regression coefficients and ε is a vector of error terms. The coefficient of determination R^2 is considered as the index for judging the effect of the prediction. R^2 closer to 1 denotes a better fit of the model.

6.3.2.2 Correlation analysis

The correlation coefficients between each two variables, including all the explanatory variables ($\boldsymbol{X}$) and response variables ($\boldsymbol{y}$), are calculated. Investigation of the correlation between noise level and texture level and sound absorption coefficient is based on the contour lines of the correlation coefficient. This method is commonly used by researchers [5, 6].

The correlation matrix between each of the explanatory variables is also built. If the correlation coefficient value is high, it means that the explanatory variables are not independent from each other. This matrix can thus be used for examining the multicollinearity between the variables.

6.3.2.3 Multicollinearity

Multicollinearity [17] refers to the statistical phenomenon that two or more predicting variables in a multiple regression model are highly correlated. With normally used least square regression analysis methods, the multicollinearity is hidden in the regression coefficients. It does not influence the prediction ability of the model as a whole, but the contribution of the individual predictor X_i to the response y cannot truly be reflected by these regression coefficients. It means that the influence of single input parameters cannot be investigated with such a regression function.

Mathematically, a set of variables is collinear if one or more linear relationships exist among the variables, for example:

$$\kappa_1 X_{1i} + \kappa_2 X_{2i} + \cdots + \kappa_k X_{ki} = 0 \tag{6-3}$$

where κ_j are coefficients and X_{ji} are explanatory variables.

The simplest method for judging multicollinearity is the correlation matrix, which can be used to detect whether there are large correlations between pairs of explanatory variables.

In a regression analysis, the phenomenon of multicollinearity can also be diagnosed by the variance inflation factor (VIF) and the tolerance. The VIF and tolerance can be calculated by the following equations:

$$\text{VIF} = \frac{1}{1-R^2_i}, \qquad \text{Tolerance} = \frac{1}{\text{VIF}} \tag{6-4}$$

where R^2_i is the coefficient of determination of the regression equation for each X_i. A VIF higher than 5 or 10 (this is to be determined by the user in different cases) and a tolerance of less than 0.20 or 0.10 indicate a multicollinearity problem.

The sign of the regression coefficient β in Eq. (6-2) is another symptom of multicollinearity. If the sign of β is not consistent with that of the partial correlation coefficient between the predictor and the dependent variables, it reveals the presence of multicollinearity. All these methods for judging the multicollinearity are used in the regression analyses described in the following sections.

6.3.2.4 Regression Methods

Normally the least square method is used for regression when multicollinearity does not exist among the explanatory variables. However, in this study, the multicollinearity commonly occurs between the explanatory variables (a case study is given in section 6.4). In order to minimize the influence of multicollinearity, many regression methods have been developed and generally they can be categorized into three types:

1) Variable selection: the redundant explanatory variables are removed from the model by mathematical methods, such as forward, backward, stepwise regression and all the subsets methods [18];
2) Suppression Type: the dimension of the explanatory variable matrix is reduced by choosing a small number of principal components which are formed by combinations of the original explanatory variables. These components maintain most of the information of the original data. The regression includes Principal Component Regression (PCR) [19] and Partial Least Squares (PLS) [20];
3) Shrinkage estimators: the coefficients for the predictor variables are shrunk systematically, which makes the regression stable, e.g. ridge regression [21], and Lasso (least absolute shrinkage and selection operator) method [22].

In this chapter, it was preferred to include all the selected parameters in the regression function. This preference was based on the fact that by doing so an overview of the influence of the texture level and sound absorption on the tyre - road noise level can be given. Thus method 1 is not used in this chapter. The investigation is conducted by means of the suppression type regression. Both the PCR and PLS are used. Hereafter brief introductions of the two approaches are given.

1) Principal component regression (PCR)
The principal component analysis gathers highly correlated variables into new orthogonal and independent variables, which are called principal components (PC). The principal component PC_j is presented as a linear function of all the standardized original variables X_i:

$$PC_j = \sum_{i=1}^{p} c_{ij} X_i \tag{6-5}$$

where c_{ij} is the eigenvector corresponding to the *j*th principal component and the *i*th explanatory variable. After choosing the first significant PCs, the standardized principal component regression equation is built with the selected principal components:

$$\hat{y}' = \sum_{j=1}^{p'} B_j' PC_j \tag{6-6}$$

where $\hat{y}_j'$ is the estimate of the standardized principal component regression equation, B_j' the *j*th standardized partial regression coefficient of the standardized principal component regression equation, and *p'* the selected number of the PCs. The modeling process is then finalized by transforming the standardized principal component regression equation into a general linear regression equation [23].

2) PLS (Partial Least Squares)
From the introduction given above, it is known that the drawback of the PCR technique in regression analysis is that it only captures the maximum variance in $\boldsymbol{X}$, without considering the relationship with the dependent variable $\boldsymbol{y}$. By contrast, the partial PLS method creates orthogonal combinations of predictors by maximizing the covariance between elements in $\boldsymbol{X}$ and $\boldsymbol{y}$. It is particularly suited when the matrix of predictors has more variables than observations, and when multicollinearity exists among the *X* values.

Assume predictor $\boldsymbol{X}$ is an $n \times p$ matrix and response $\boldsymbol{y}$ an $n \times q$ matrix, in which *n* is the number of the observations. The PLS methods tries to find a linear decomposition of $\boldsymbol{X}$ and $\boldsymbol{y}$,

$$X = U_X Q_X{}^{\mathrm{T}} + \varepsilon_X, \; Y = U_Y Q_Y{}^{\mathrm{T}} + \varepsilon_Y \tag{6-7}$$

where U_X and U_Y are an $n \times l_s$ matrix, containing the l_s number of extracted latent vectors, Q_X and Q_Y are, respectively, $q_X \times l_s$ and $q_Y \times l_s$ orthogonal loading matrices, and the matrices ε_X and ε_Y represent the residuals. Different algorithms, such as Non-linear Iterative Partial Least Squares (NIPALS) and simple partial least squares regression (SIMPLS), can be used to extract the latent factors. The final input number of latent vectors is selected when $\boldsymbol{X}$ and $\boldsymbol{y}$ are highly explained by the l_s latent vectors and a good regression is achieved. A small number of inputs is preferred, as increasing the input numbers of the latent vectors means possible introduction of multicollinearity.

6.4 Investigation on Thin Layer Surfacings

In this study, the investigation focuses on thin layer surfaces. According to the general definition, the thickness of a thin layer surface varies between 20 and 30 mm [1]. The designed mixture composition of each selected thin layer surface is given in Table 6-5. The number of the section refers to the number used in the report of the Kloosterzande sections [14]. A total of 9 surfaces could be rated as a thin layer surface, including semi-dense thin layers (No.2 to No.5), porous asphalt (No.9, 15 and 24) and SMA (No.19 and No.20). Except for section No.19, the thickness of the surfaces was in all cases 25 mm; they do however have different material compositions. For each design, two trial tracks were constructed. Because of the variation in the construction process, the resulting mixture compositions for the two sections with the same nominal design are different. It means that 18 tracks are used for the regression. A detailed description of the investigations performed on the thin layer surfacings is presented in this section.

Table 6-5 Designed mixture compositions of different thin layer surfacings

Section Number	No.2	No.3	No.4	No.5	No.9	No.15	No.24	No.19	No.20
Max. aggregate size, mm	4	6	6	8	8	6	8	6	8
Aggregate size, mm	2/4	2/6	2/6	4/8	4/8	2/6	4/8	0/6	0/8
Binder content, %	7.2	7.8	7.5	6.6	6.0	6.6	6.0	7.8	7.2
Air voids content, %	12	8	12	12	>20	>20	>20	4	5
Thickness, mm	25	25	25	25	25	25	25	20	25

6.4.1 Investigation of the test results

6.4.1.1 Investigation of the surface characteristics

The averaged texture levels for the 9 thin layer surfaces are calculated based on Eq. (6-1) and they are illustrated in Figure 6-6 in a 1/3rd octave band spectrum with wavelengths ranging from 1 till 250 mm. For each section, the texture level of the west lane is plotted. From Figure 6-6, one can observe that surfaces with large sized aggregates and high air voids content, such as section 9 and 24, show a greater texture level. For those with smaller maximum aggregate sizes, the texture level is lower. It can also be seen that the wavelength corresponding to the maximum texture level depends on the maximum aggregate size of the mixture. For mixtures with a maximum aggregate size of 8 mm (Section 5, 9, 20 and 24), the maximum levels appear at 16 mm wavelength, for the 6 mm maximum aggregate size mixtures (Section 3, 4, 15, 19), the maximum is at the 8 mm wavelength, and for the 4 mm maximum aggregate size mixtures (Section 2), the maximum locates at the 4 mm wavelength. Moreover, the differences in texture level between the sections are small when the wavelength is below 4 mm. In order to be able to make a comprehensive investigation of the influence of the texture spectrum, the texture levels with wavelengths from 1 to 250 mm are all used as explanatory variables in the regression analysis.

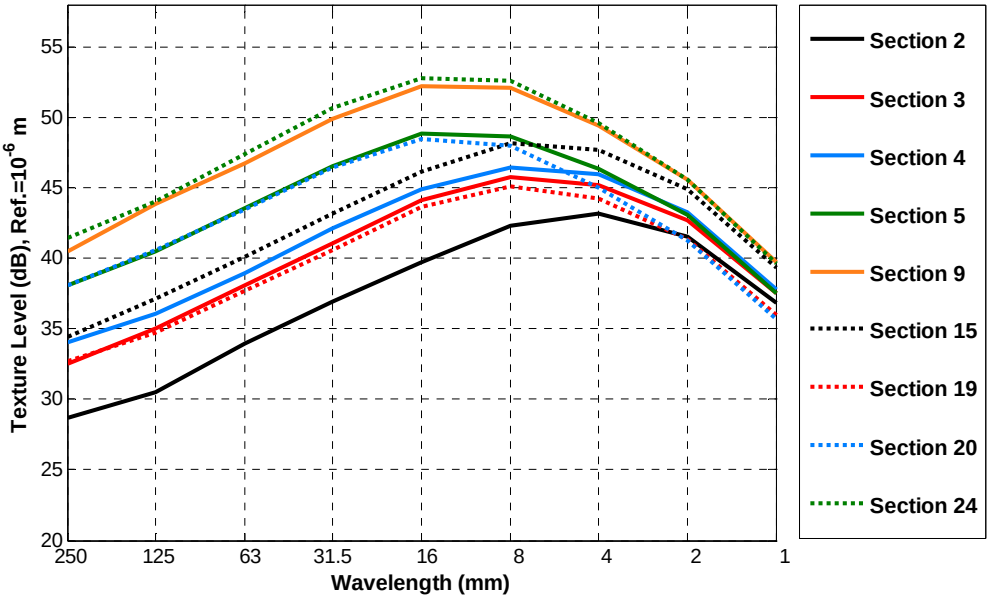

Figure 6-6 Surface texture level for the thin layer surfacing sections

In this study, the absorption coefficient is used as the measure for describing the sound absorbing ability of the road surface. The sound absorption coefficients for the 9 thin layer surfaces are shown in Figure 6-7. The data used are also from the west lane of each section. It can be seen from the figure that the maximum absorption coefficients of the porous type (air voids content >20%) thin layer surface are much higher compared to the others, and the values are around 0.7. The peak values locate at 1600 Hz and 2000 Hz for different mixtures respectively. For the surface with a designed air voids content of 12%, the first peak value of the absorption curve generally occurs at 1250 Hz, the values range from 0.25 to 0.35. For the dense surfaces, sections 19 and 20, the absorption coefficients are small and not higher than 0.2 in the whole octave band. It can be seen that considerable differences between the absorption curves are at frequencies $f \geq$ 1000Hz. Below 1000 Hz, the sound absorption coefficients are smaller than 0.2, and the differences of absorption coefficients between sections are generally within 0.1. The influence of these small absorption coefficients below 1000 Hz is considered to have an insignificant influence on the change of noise and therefore these particular coefficients are neglected in the study.

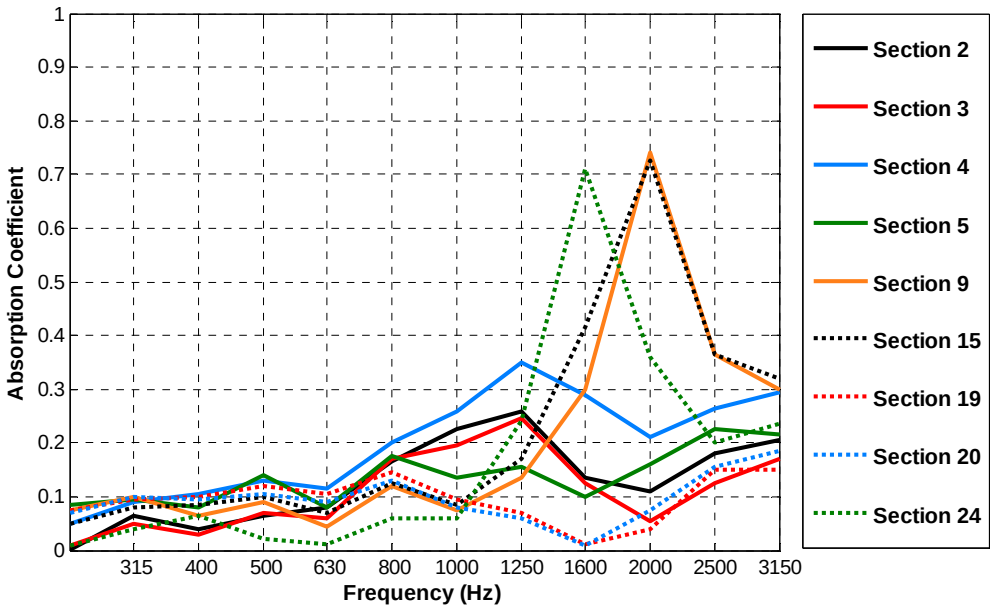

Figure 6-7 Sound absorption coefficients for the thin layer surfacing sections

6.4.1.2 Investigation on tyre - road noise

The sound pressure levels obtained by means of the CPX tests are, for each trial section, plotted in the 1/3rd octave band. Examples are given in Figure 6-8. They are from the CPX measurements with the 05 Michelin Energy 195/65R15 tyre and the averaged values from the 10 tyre types (as shown in Table 6-2). A complete overview of the noise levels from the different passenger car tyres is given in Appendix A.

Figure 6-8 (a) illustrates a typical distribution of the noise level in the frequency domain. The maximum noise levels are generally located at 800 Hz or 1000 Hz. The highest peak values are from the sections with the largest texture level (as shown in Figure 6-6). In the low and medium frequency range (≤1000Hz), the sequence of the noise level generally follows the order of the value of texture level. This indicates that at those frequencies, the tyre - road noise is mainly related to the surface texture and considered to be caused by the tyre vibration mechanism. In the high frequency range, larger drops of the noise levels for surfaces with higher absorption coefficients can be observed, i.e. section 9 and 24. The influence of the sound absorption is considered to be significant at higher frequencies. Figure 6-9 shows the noise curves from different tyres on a certain section. In the figure, the noise levels measured on section 4 are displayed.

By comparing the noise curves from different tyres (see Figure 6-8 and Appendix A), it can be seen that the distribution of the noise level on the frequency axis for all sections are comparable. The averaged noise level from the 10 passenger car tyres is calculated and used as a representative of the CPX noise levels on the thin layer surfacings. These averaged noise levels are also used in the regression analysis.

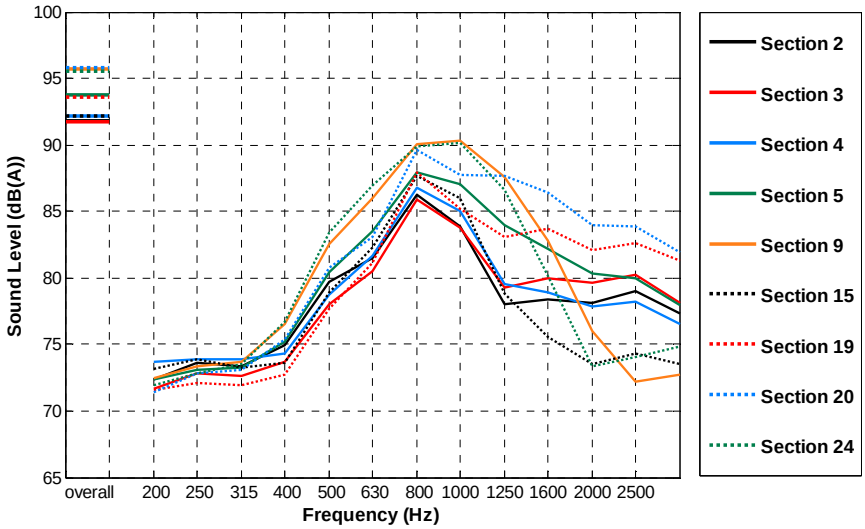

(a) Noise level tested by tyre 05: Michelin Energy 195/65R15

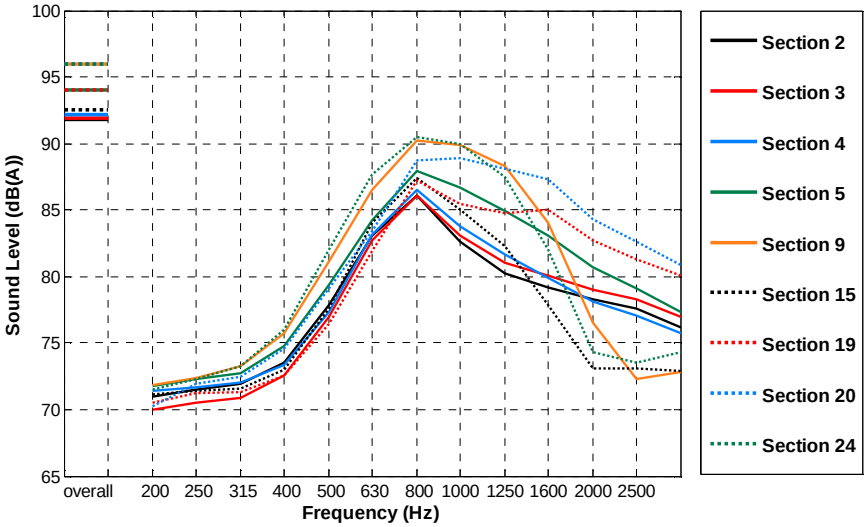

(b) Averaged noise level from 10 types of passenger car tyres

Figure 6-8 Tyre - road noise levels for the thin layer surfacing sections

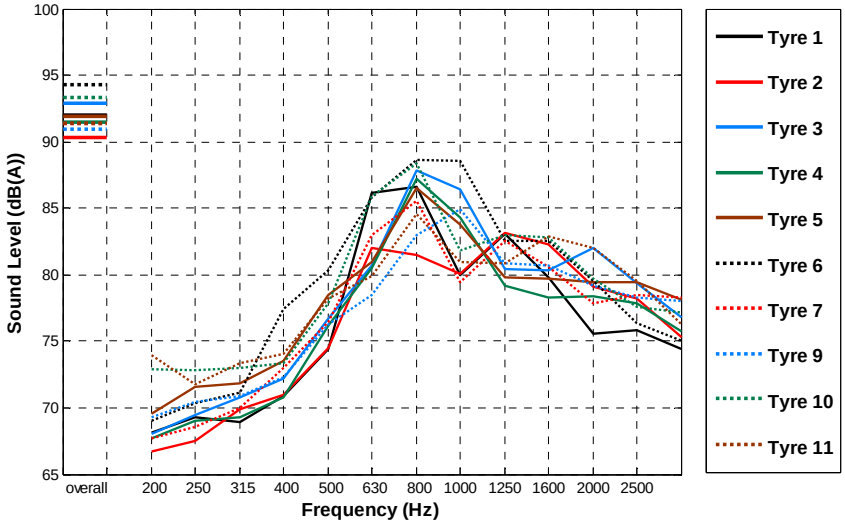

Figure 6-9 Tyre - road noise levels on section 2-2 for different tyres

6.4.2 Hypothesis test

Prior to the hypothesis test, the test of normality is performed to examine the distribution of the data at certain frequencies for different road surfaces. The examination is carried out on every section with data from the 10 tyres. The procedure is performed by using the statistical software package SPSS. Results of the significance values for the thin layer sections are given in Table 6-6. Considering a significance level of 0.05, it can be seen that the data set of the overall noise level and the noise levels at the frequency larger than 630 Hz are all well modelled by a normal distribution for nearly all the surfaces. Most of the data sets of the noise levels below 630 Hz also obey the normal distribution, except some cases, such as data from surface 4-2 at 200, 315, and 400 Hz. However, when considering a significance level of 0.01, nearly all data sets can be rated as normally distributed. Therefore, in this study, it is assumed that all the data sets, corresponding to certain frequency and road surface, follow the normal distribution.

Table 6-6 Tests of normality on thin layer surfacings

Surface No.	Significance from Shapiro-Wilk test													
	$L_{A,\,eq}$	L_{200}	L_{250}	L_{315}	L_{400}	L_{500}	L_{630}	L_{800}	L_{1000}	L_{1250}	L_{1600}	L_{2000}	L_{2500}	L_{3150}
2-1	0.77	0.23	0.30	0.60	0.10	0.05	0.54	0.32	0.33	0.12	0.58	0.82	0.80	0.57
2-2	0.82	0.00	0.01	0.18	0.04	0.02	0.55	0.11	0.37	0.18	0.18	0.73	0.85	0.34
3-1	0.94	0.72	0.51	0.76	0.02	0.03	0.74	0.34	0.61	0.09	0.28	0.93	0.26	0.43
3-2	0.71	0.34	0.34	0.17	0.08	0.34	0.48	0.55	0.26	0.70	0.68	0.79	0.70	0.33
4-1	0.36	0.08	0.04	0.12	0.62	0.64	0.40	0.04	0.40	0.39	0.75	0.09	0.67	0.22
4-2	0.84	0.01	0.06	0.04	0.04	0.18	0.19	0.03	0.23	0.88	0.56	0.53	0.63	0.22
5-1	0.31	0.09	0.06	0.07	0.00	0.03	0.66	0.84	0.78	0.89	0.46	0.67	0.62	0.22
5-2	0.81	0.01	0.01	0.10	0.50	0.16	0.58	0.91	0.73	0.61	0.17	0.94	0.62	0.31
9-1	0.29	0.08	0.35	0.63	0.78	0.50	0.37	0.26	0.89	0.61	0.60	0.45	0.13	0.74
9-2	0.64	0.05	0.94	0.66	0.11	0.71	0.20	0.38	0.47	0.14	0.30	0.36	0.37	0.56
15-1	0.82	0.17	0.24	0.21	0.56	0.60	0.23	0.20	0.33	0.20	0.33	0.81	0.25	0.37
15-2	0.45	0.03	0.05	0.01	0.14	0.34	0.19	0.58	0.22	0.29	0.31	0.53	0.45	0.07
19-1	0.35	0.11	0.09	0.07	0.47	0.82	0.36	0.42	0.07	0.64	0.81	0.87	0.67	0.67
19-2	0.12	0.00	0.02	0.02	0.47	0.49	0.85	0.33	0.22	0.03	0.47	0.89	0.46	0.79
20-1	0.74	0.07	0.25	0.53	0.22	0.36	0.32	0.20	0.42	0.79	0.96	0.50	0.64	0.50
20-2	0.31	0.03	0.05	0.04	0.01	0.52	0.34	0.92	0.75	0.27	0.41	0.47	0.96	0.29
24-1	0.83	0.00	0.01	0.01	0.14	0.81	0.47	0.56	0.08	0.80	0.32	0.88	0.56	0.41
24-2	0.45	0.04	0.02	0.02	0.26	0.44	0.62	0.06	0.48	0.77	0.33	0.66	0.61	0.50

A hypothesis test was then conducted by using ANOVA. The null hypothesis was that there is no effect of the difference of the road surfaces on the noise levels. Noise data for all the tyre types were included in the hypothesis test, and the analysis is performed using the SPSS software package. The calculated significance for each noise level is listed in Table 6-7. A significance level of 0.05 was used. The null hypothesis is thus rejected when the obtained significance is less than 0.05, which indicates the road surface characteristics have a considerable effect on the tyre - road noise level. When the resulting

significance is higher than 0.05, the null hypothesis is accepted and it implies there is no influence of the road surface properties.

A variable selection was then made based on the results of the ANOVA tests. From the results in Table 6-7, it is concluded that the road surface variations account for the differences of overall noise level and noise levels at frequencies above 350 Hz. The influence of road surface on noise level below 350 Hz is trivial, and noise levels at these frequencies are therefore not considered in the further investigations.

Table 6-7 Significance values of different road surfaces on noise level from ANOVA

	$L_{A,eq}$	L_{200}	L_{250}	L_{315}	L_{400}	L_{500}	L_{630}	L_{800}	L_{1000}	L_{1250}	L_{1600}	L_{2000}	L_{2500}	L_{3150}
Sig.	0.00	0.56	0.30	0.00	0.00	0.00	0.00	0.00	0.00	0.00	0.00	0.00	0.00	0.00

6.4.3 Correlation analysis

Correlation coefficients for all possible combinations of the noise and the texture and sound absorption spectral bands were calculated. The correlation matrices are illustrated by contour diagrams as shown in Figure 6-10.

From Figure 6-10 (a), it can be seen that there is a high positive correlation between the noise level below 1250 Hz and the texture level with wavelengths larger than 8 mm. For short wavelengths (≤4 mm) texture, it shows a high negative correlation with the noise level at the high frequency range (>2000 Hz). These findings are similar with those from the studies of Sandberg and Anfosso-Lédée in which different types of road surfaces were investigated [5, 6]. However, the cross-over frequency is located between 1250 and 2000 Hz; this is higher in comparison with the study by Sandberg et.al.. For texture with wavelengths larger than 8 mm, the cross-over frequency is even between 1600 and 2000 Hz. According to Sandberg, the noise level in this medium frequency range (between 800 Hz and 1250 Hz or 1600 Hz) is due to the impact of the tyre tread on the road surface.

Figure 6-10 (b) shows the correlation between the noise level and sound absorption coefficients at different frequencies. The noise levels below 500 Hz are not significantly related with the sound absorption coefficient. Above 500 Hz, high negative correlations (generally higher than 0.6) are found around the diagonal line of the figure. It means that in general, the absorption coefficient has a high negative correlation with noise levels located in neighbouring frequencies. For example, the absorption coefficient at 1000 Hz is highly correlated with the noise level at 800 Hz, 1000Hz and 1250 Hz.

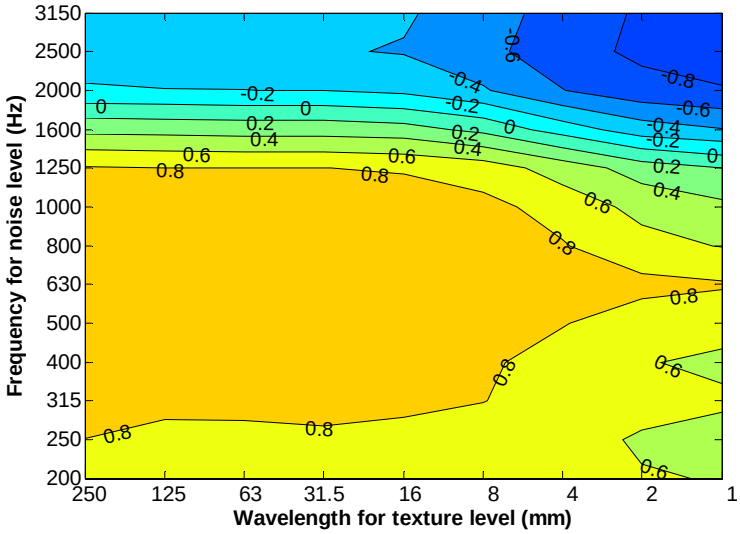

(a) Surface texture level

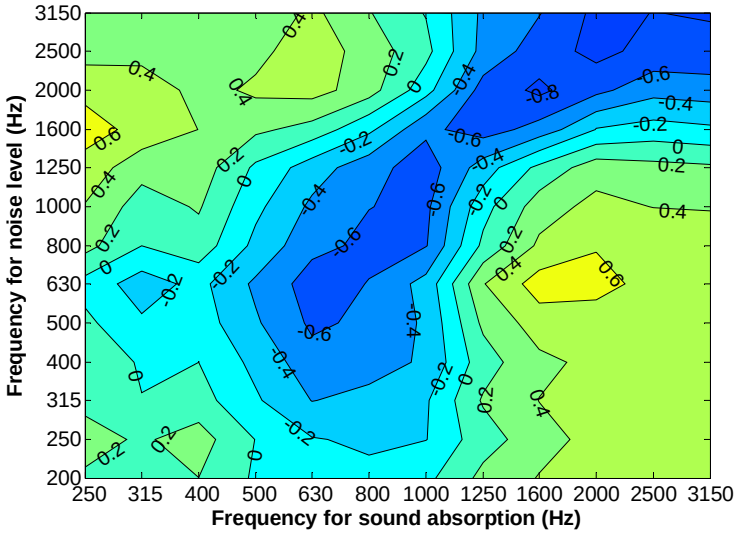

(b) Sound absorption coefficient

Figure 6-10 Contour lines of the correlation coefficient between noise level (at 80 km/h) and surface characteristics for passenger car tyre

The correlation matrix between each of the surface characteristic parameters was calculated and the results are shown in Table 6-8. In the table, TL_i indicates the texture level at wavelength λ_i, and AL_j the sound absorption coefficient at frequency f_j. For surface texture, a high degree of inter-correlation (or: "a high correlation") can be observed between each two variables, especially for texture levels with a wavelength larger than 4 mm. The MPD is highly correlated with the texture levels on the wavelength spectral band from 1 mm to 250 mm. From the measurement results presented in Chapter 5, it was already known that a surface with a larger MPD generally shows a higher texture level on the whole wavelength band. Sound absorption coefficients located at neighbouring frequency bands show significant correlation with each other. The maximum absorption coefficient is strongly correlated with the sound absorption above 1600 Hz.

It should be noted that the texture level with a short wavelength (≤ 4 mm) shows a strong correlation with the sound absorption coefficient at high frequency (≥2000 Hz). The reason for this is that the absorption coefficient is determined by the air voids content which in turn is highly related to the stone size and stone content. The stone size and content however are also determining the texture level with a small wavelength. This leads to a high correlation between short wavelength texture and the sound absorption coefficient. Similarly, a high correlation can also be seen between the MPD and the maximum absorption coefficient. Air flow resistance is highly related with small wavelength texture levels and maximum sound absorption.

Based on the analysis, one can also conclude that high multicollinearity exists between certain surface characteristic parameters. As discussed in sections 6.3.2.3 and 6.3.2.4, PCA and PLS methods are to be used when these inter-correlated parameters are involved in the regression analysis.

Table 6-8 Correlation coefficients between surface characteristics

	MPD	TL_{250}	TL_{63}	TL_{16}	TL_{4}	TL_{1}	AL_{1000}	AL_{1250}	AL_{1600}	AL_{2000}	AL_{2500}	Max. absorption	Flow resistance
MPD	1.00	0.93**	0.94**	0.95**	0.91**	0.76**	-0.43	0.27	0.59*	0.64*	0.54*	0.78**	-0.65**
TL_{250}		1.00	1.00**	0.99**	0.87**	0.64**	-0.41	0.15	0.44	0.52*	0.47*	0.61*	-0.61*
TL_{63}			1.00	1.00**	0.88**	0.66**	-0.41	0.16	0.45	0.53*	0.48*	0.63**	-0.63**
TL_{16}				1.00	0.91**	0.70**	-0.40	0.18	0.48*	0.57*	0.51*	0.66**	-0.65**
TL_{4}					1.00	0.92**	-0.25	0.40	0.68**	0.77**	0.70**	0.87**	-0.82**
TL_{1}						1.00	-0.04	0.53*	0.72**	0.81**	0.74**	0.89**	-0.91**
AL_{1000}							1.00	0.55*	-0.02	-0.34	-0.16	-0.25	-0.17
AL_{1250}								1.00	0.76**	0.15	0.12	0.49*	-0.52*
AL_{1600}									1.00	0.51*	0.29	0.82**	-0.58*
AL_{2000}										1.00	0.87**	0.87**	-0.65**
AL_{2500}											1.00	0.66**	-0.63**
Max. absorption												1.00	-0.69**
Flow resistance													1.00

**Correlation is significant at the 0.01 level.
* Correlation is significant at the 0.05 level.

6.4.4 Analyses using PCR

Regression analysis is performed to determine the impact of individual surface parameters on tyre - road noise. The explanatory variables refer to the 4 combinations which were shown in Table 6-4. The input and output variable selections are based on the results from 6.4.1 and 6.4.2. When the spectral band of texture level and sound absorption coefficient are used as input variables, the PCR method is employed to eliminate the multicollinearity. The way how PCR for regression was used in this study is shown in Figure 6-11. The flow chart is also appropriate for the PLS method. In this section, it will be shown how the PCR analysis is performed. Furthermore the results of the analyses, being the influence of surface characteristics on tyre - road noise, will be presented. A detailed example is given by using the input variable combination 1 shown in Table 6-4.

For variable combination 1, a total of 15 parameters were selected as explanatory variables. The complete set of explanatory and the response variables is listed in Table 6-9.

Table 6-9 Summary of explanatory variables and response variables

	Explanatory variables	Number of explanatory variables	Response variables	Number of response variables
Sound Absorption	Sound absorption coefficients at frequencies 1000, 1250, 1600, 2000, 2500 and 3150 Hz	15	Overall noise level and noise levels at 315, 400, 500,630, 800, 1000, 1250, 1600, 2000, 2500 and 3150 Hz	12
Surface Texture	Texture levels at wavelengths 250, 125, 63, 31.5, 16, 8, 4, 2 and 1 mm			

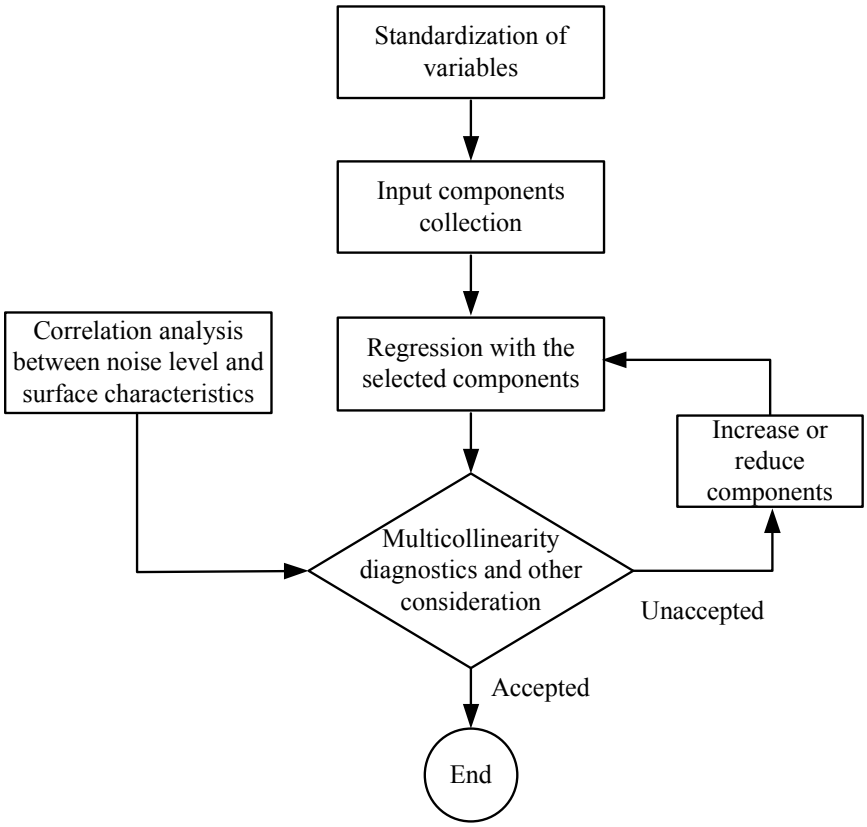

Figure 6-11 Process of the regression analysis with PCA or PLS

In the principal component analysis, new independent input variables (components) are firstly generated by linear combinations of the standardized original surface characteristics based on Eq. (6-5). The standardized variables X_i are achieved by the formula:

$$X_i = \frac{x_i - \overline{x}_i}{\sigma_i} \tag{6-8}$$

where $\overline{x}_i$ is the mean of each variable in the sample, σ_i is the standard deviation.

The values of the eigenvectors, namely the coefficients c_{ij} in Eq. (6-5), are shown in Table 6-10. The eigenvalues of the coefficients matrix of the new variables are extracted and given in Table 6-11. The first components, which contain most of the information of the input variables, are to be selected. A simple rule which has proven to be useful in practice is to select components with an eigenvalue greater than 1.0. Based on Table 6-11, the first three components, accounting for 93.8% of the cumulative variance, are selected as principal components and they are used as input variables for the multivariate regression.

With the selection of the principal components, the number of the input variables of the regression reduced to 3 from 15. The three components can be explained based on the eigenvalues given in Table 6-10:

In PC1, the coefficients for nearly all the surface parameters are positive. It means all these parameters will show a similar influence on the noise levels due to the same signs.

In PC2, the coefficients for texture level with wavelengths ≥8 mm are positive; the coefficients for texture levels at wavelength ≤ 4mm and sound absorption are negative. It reflects that the effect of long wavelength texture level (≥8 mm) on noise is opposite to short wavelength texture level (≤4 mm) and sound absorption. In addition, the coefficients for AL_{1000} and AL_{1250} are larger compared to others. It means the sound absorption at these two frequency bands is of great importance.

With respect to PC3, the effects of sound absorption at high frequency (≥2000 Hz) are essential.

Table 6-10 The eigenvalues for the components

	Components														
	1	2	3	4	5	6	7	8	9	10	11	12	13	14	15
TL_{250}	0.29	-0.22	-0.15	0.14	-0.10	0.09	-0.15	-0.23	-0.09	0.82	-0.07	0.10	-0.08	0.13	-0.09
TL_{125}	0.29	-0.21	-0.15	0.13	-0.06	0.13	0.10	0.03	-0.18	-0.18	0.64	-0.41	-0.33	0.22	0.05
TL_{63}	0.29	-0.21	-0.15	0.12	-0.03	0.08	0.05	0.01	-0.23	-0.29	0.14	0.79	-0.02	-0.18	-0.03
TL_{32}	0.29	-0.21	-0.14	0.12	-0.03	0.10	-0.02	-0.03	-0.22	-0.24	-0.39	-0.20	0.56	0.34	0.31
TL_{16}	0.30	-0.19	-0.14	0.10	-0.02	0.05	0.01	0.07	0.07	-0.12	-0.23	-0.34	0.08	-0.55	-0.59
TL_{8}	0.31	-0.10	-0.10	0.03	0.02	-0.05	-0.03	0.03	0.48	-0.03	-0.22	-0.04	-0.37	-0.30	0.61
TL_{4}	0.31	0.06	-0.03	-0.03	0.14	-0.15	-0.03	0.12	0.58	-0.12	-0.04	0.16	-0.03	0.56	-0.38
TL_{2}	0.29	0.20	0.03	-0.04	0.36	-0.29	-0.01	0.12	0.09	0.23	0.47	-0.01	0.53	-0.25	0.15
TL_{1}	0.28	0.26	0.06	-0.05	0.47	-0.37	0.15	-0.06	-0.48	-0.01	-0.30	-0.06	-0.36	0.07	-0.03
AL_{1000}	-0.10	0.47	-0.23	0.66	0.25	0.30	-0.35	-0.05	0.03	-0.07	0.01	0.00	-0.04	-0.01	0.00
AL_{1250}	0.10	0.50	-0.41	-0.02	-0.39	0.05	0.63	-0.01	0.04	0.09	-0.04	0.02	0.06	0.00	0.01
AL_{1600}	0.20	0.32	-0.28	-0.58	-0.21	0.11	-0.59	0.08	-0.15	-0.08	0.02	-0.02	-0.05	-0.02	-0.01
AL_{2000}	0.24	0.14	0.40	-0.26	0.25	0.69	0.19	-0.34	0.09	-0.01	0.00	0.01	0.03	-0.03	-0.01
AL_{2500}	0.22	0.16	0.49	0.19	-0.27	0.15	-0.02	0.71	-0.14	0.14	-0.08	0.02	-0.06	0.02	0.04
AL_{3150}	0.23	0.21	0.42	0.22	-0.47	-0.34	-0.17	-0.53	0.02	-0.16	0.07	-0.02	0.03	-0.05	-0.02

Table 6-11 The eigenvalue, % of variance for principal components

Component	Initial Eigenvalues		
	Total	% of Variance	Cumulative %
1	9.907	66.046	66.046
2	2.719	18.124	84.169
3	1.448	9.653	93.823
4	.619	4.130	97.952
5	.157	1.045	98.997
6	.076	.507	99.503
7	.038	.256	99.759
8	.017	.113	99.872
9	.014	.093	99.965
10	.004	.026	99.991
11	.001	.005	99.996
12	.000	.002	99.998
13	.000	.001	99.999
14	.000	.000	100.000
15	.000	.000	100.000

The linear regression is performed with the three PCs as explanatory variables. As an example, the equation obtained for noise level at 1000 Hz L_{1000} is shown as follow:

$$L_{1000} = 0.25PC1 - 0.36PC2 - 0.07PC3 \tag{6-9}$$

The standardized regression coefficients for different noise levels are summarized in Table 6-12. For all noise levels except for the noise level at 315 Hz, the R^2 are higher than 0.75. It is therefore concluded that the regression equations fit the data well. The tolerance and VIF values are calculated according to Eq. (6-4) and are used to detect multicollinearity. As the PCs are orthogonal to each other, the tolerance and VIF are equal to 1.00 for every regression equation.

Table 6-12 Regression coefficients on the principal components

Component	$L_{A,\,eq}$	L_{315}	L_{400}	L_{500}	L_{630}	L_{800}	L_{1000}	L_{1250}	L_{1600}	L_{2000}	L_{2500}	L_{3150}
1	0.20	0.25	0.25	0.27	0.29	0.27	0.25	0.19	0.00	-0.16	-0.21	-0.21
2	-0.45	-0.10	-0.21	-0.14	-0.01	-0.25	-0.36	-0.48	-0.60	-0.47	-0.36	-0.37
3	-0.07	-0.10	-0.13	-0.17	-0.12	-0.03	-0.07	-0.02	0.04	-0.01	-0.23	-0.30
R^2	0.87	0.68	0.76	0.82	0.87	0.90	0.92	0.89	0.82	0.77	0.84	0.90

In order to investigate the influence of surface characteristics, the standardized principal component regression equations are transformed into general linear equations expressed by the original surface characteristics. It is known that the units of texture level and absorption coefficient are different. For comparing the relative importance of different variables, the standardized regression coefficients are used in the analysis. They are identical to the regression coefficients achieved by using the standardized variables [24]. The standardized regression coefficients for all the surface parameters are shown in Table 6-13.

An example for the noise level at 1000 Hz is given as follow:

$$L_{1000} = 0.16TL_{250} + 0.16TL_{125} + 0.16TL_{63} + 0.16TL_{32} + 0.15TL_{16} + 0.12TL_{8} + 0.06TL_{4} - 0.03TL_{1} - 0.18AL_{1000} - 0.13AL_{1250} - 0.04\Delta AL_{1600} - 0.02AL_{2000} - 0.03AL_{2500} - 0.05AL_{3150} \quad (6\text{-}10)$$

The results shown in Table 6-13 are based on an adjustment of the regression by using the first 3 PCs. From the correlation analysis, it is known that the noise level at 2000 Hz is strongly correlated with the sound absorption coefficient at 1600 Hz. The contribution of the absorption coefficient at 1600 Hz is presented by the fourth component as shown in Table 6-10. Thus, a new regression is performed on L_{2000} by using the first four components. It can be seen that there is an increase of the R^2 of the regression for L_{2000} compared to the case when 3 PCs are selected as input (compared with Table 6-12). Moreover, the signs of the regression coefficients do not change after adding the fourth PC in the regression. It means that using this extra PC as input does not introduce multicollinearity to the results. So the regression equation using 4 PCs for L_{2000} is acceptable.

The influence of the surface texture level and sound absorption coefficients on the tyre - road noise levels can be observed from Table 6-13. In this research, a coefficient with a value ≥ 0.1 is arbitrarily selected as indication of the importance of the influence. It means that the influence is considered important when the regression coefficient is not smaller than 0.1. For facilitating the investigation, the background of the form is marked in blue for the item with an absolute regression coefficient ≥0.1. The surface characteristics are classified into three groups for investigation:

1) Texture level at long wavelength (≥8 mm)

In the wavelength range higher than 8 mm, a larger texture level results in higher noise level. The impact of the texture levels on the noise level below 2000 Hz is high. On each noise level, contributions from texture levels between 16 mm and 250 mm are almost the same. The importance of the 8 mm wavelength texture level is relatively small compared with others.

2) Texture level at short wavelength (≤4 mm)

The influence of short wavelength texture levels is small on the noise levels in the low and medium frequency range (<1600 Hz). At the high frequency, the noise level greatly decreases with an increasing short wavelength texture level. The influence of the texture level at 2 mm and 1 mm wavelength are higher than that at the 4 mm wavelength.

3) Sound absorption coefficients

There is almost no influence of sound absorption on low frequency noise. The impact on noise reduction appears at noise levels above 800 Hz. The noise level reduces with increasing absorption coefficients.

Table 6-13 Standardized coefficients from PCR with variable combination 1

	$L_{A,\,eq}$	L_{315}	L_{400}	L_{500}	L_{630}	L_{800}	L_{1000}	L_{1250}	L_{1600}	L_{2000}	L_{2500}	L_{3150}
TL_{250}	0.17	0.11	0.14	0.13	0.10	0.14	0.16	0.16	0.13	0.13	0.05	0.07
TL_{125}	0.16	0.11	0.14	0.13	0.10	0.14	0.16	0.16	0.12	0.12	0.05	0.06
TL_{63}	0.16	0.11	0.14	0.13	0.10	0.14	0.16	0.16	0.12	0.12	0.05	0.07
TL_{32}	0.16	0.11	0.14	0.13	0.10	0.14	0.16	0.16	0.12	0.11	0.04	0.06
TL_{16}	0.15	0.11	0.13	0.13	0.10	0.13	0.15	0.15	0.11	0.09	0.03	0.05
TL_{8}	0.12	0.10	0.11	0.11	0.10	0.11	0.12	0.11	0.06	0.02	0.00	0.01
TL_{4}	0.04	0.08	0.07	0.08	0.09	0.07	0.06	0.03	-0.04	-0.09	-0.08	-0.08
TL_{2}	-0.03	0.05	0.03	0.05	0.08	0.03	0.00	-0.04	-0.12	-0.16	-0.14	-0.14
TL_{1}	-0.07	0.04	0.01	0.03	0.07	0.01	-0.03	-0.07	-0.15	-0.20	-0.17	-0.17
AL_{1000}	-0.22	-0.05	-0.09	-0.06	0.00	-0.14	-0.18	-0.24	-0.29	0.13	-0.09	-0.08
AL_{1250}	-0.18	0.02	-0.03	0.02	0.08	-0.09	-0.13	-0.21	-0.32	-0.26	-0.11	-0.09
AL_{1600}	-0.08	0.05	0.02	0.05	0.09	-0.02	-0.04	-0.11	-0.20	-0.47	-0.09	-0.08
AL_{2000}	-0.04	0.01	-0.02	-0.02	0.02	0.02	-0.02	-0.03	-0.06	-0.24	-0.19	-0.22
AL_{2500}	-0.06	-0.01	-0.04	-0.04	0.00	0.01	-0.03	-0.04	-0.07	-0.02	-0.22	-0.25
AL_{3150}	-0.07	0.00	-0.04	-0.04	0.01	0.00	-0.05	-0.06	-0.10	-0.03	-0.22	-0.25
R^2	0.87	0.68	0.76	0.82	0.87	0.90	0.92	0.89	0.82	0.94	0.84	0.90
Number of PC selected	3	3	3	3	3	3	3	3	3	4	3	3

With respect to the noise levels, the following comments are made:

1) Overall A-weighted equivalent sound level $L_{A,\,eq}$

The long wavelength texture levels account for the increase of the overall noise level, and the higher sound absorption coefficients reduce the overall noise level. As large regression coefficients are obtained for the absorption coefficients at 1000 Hz and 1250 Hz, thin layer surfaces are effective in providing sound absorption for noise in the 1000 and 1250 Hz band. Texture levels of 2 mm and 1 mm also lead to a decrease of noise, but the influence is small in comparison with the sound absorption.

2) Low frequency noise level (below 800 Hz)

The noise level at low frequencies is predominantly caused by the long wavelength surface texture levels. This indicates that the low frequency noise is caused by the impact mechanism between the tyre tread and the road surface.

3) Medium frequency noise level (from 1000 Hz to 2000 Hz)

The noise level at these frequencies is positively related with long wavelength texture levels implying that the noise level at these frequencies will increase when the wavelength of the texture is increasing. Short wave surface texture and sound absorption both lead to a decrease of the noise, and the impact is more significant at the higher frequencies of the medium frequency noise level band, such as 1600 Hz and 2000 Hz. It can also be deduced that the noise generation in this frequency range is from the joint effect of tyre vibration and air pumping mechanism.

4) High frequency noise level (above 2000 Hz)

In this range, the noise production is due to the air pumping mechanism. The analysis results show that short wavelength surface texture and sound absorption reduce noise at high frequencies.

Multivariate regressions are also carried out on the other 3 variable combinations given in Table 6-4. The PCR method is employed for combinations 2 and 3. According to the general selection rule, the number of PCs used for these two combinations are 3 and 2 respectively. As to combination 4, it contains only two parameters, namely the MPD and maximum sound absorption coefficient, so a least square regression is used. The standardized coefficients for different combinations are displayed in Table 6-14 to Table 6-16.

Table 6-14 shows the regression results when replacing the texture level with MPD. The table shows that the R^2 for half of the regressions are lower than 0.7, which implies weak linear relationships. The problem is attributed to the selection rule of the principal component analysis. In the PCR method, the selection is only based on the correlation between the explanatory variables. The selected PCs carry the most important information of the input data, but they are not always the most suitable explanatory variable for linear regression. As explained in 6.3.2.4, the PLS method can overcome the problem and it is used to give the considerations on both the explanatory and response variables. Details of using PLS for regression are given in the next section.

Table 6-14 Standardized coefficients from PCR with variable combination 2

	$L_{A,eq}$	L_{315}	L_{400}	L_{500}	L_{630}	L_{800}	L_{1000}	L_{1250}	L_{1600}	L_{2000}	L_{2500}	L_{3150}
MPD	0.32	0.24	0.29	0.33	0.35	0.36	0.35	0.30	0.08	-0.15	-0.15	-0.09
AL_{1000}	-0.50	-0.18	-0.30	-0.30	-0.25	-0.42	-0.46	-0.50	-0.41	-0.12	-0.05	-0.12
AL_{1250}	-0.16	0.07	0.01	0.07	0.14	-0.04	-0.09	-0.20	-0.36	-0.31	-0.17	-0.15
AL_{1600}	0.16	0.21	0.23	0.30	0.34	0.24	0.21	0.11	-0.15	-0.29	-0.18	-0.10
AL_{2000}	0.11	0.15	0.13	0.14	0.16	0.17	0.14	0.11	0.00	-0.11	-0.20	-0.22
AL_{2500}	-0.06	0.07	0.01	-0.01	0.02	0.02	-0.02	-0.03	-0.06	-0.08	-0.21	-0.28
AL_{3150}	-0.07	0.07	0.01	0.00	0.04	0.01	-0.03	-0.05	-0.10	-0.12	-0.22	-0.28
R^2	0.66	0.49	0.53	0.66	0.85	0.82	0.72	0.65	0.59	0.71	0.78	0.81
Number of PC selected	3	3	3	3	3	3	3	3	3	3	3	3

When combination 3 is considered, see Table 6-15, a good relationships were found, as the R^2 for all these equations is higher than 0.7. The influence of texture and sound absorption on noise level is generally in agreement with those observed by using combination 1 (see Table 6-13). It shows that larger surface texture dramatically increases the noise level below 2000 Hz, while sound absorption significantly reduces noise levels at frequencies ≥ 1000 Hz.

Table 6-15 Standardized coefficients from PCR with variable combination 3

	$L_{A,\,eq}$	L_{315}	L_{400}	L_{500}	L_{630}	L_{800}	L_{1000}	L_{1250}	L_{1600}	L_{2000}	L_{2500}	L_{3150}
TL_{250}	0.23	0.13	0.17	0.14	0.08	0.16	0.21	0.24	0.24	0.18	0.14	0.14
TL_{125}	0.22	0.13	0.16	0.14	0.08	0.16	0.20	0.23	0.23	0.16	0.13	0.13
TL_{63}	0.22	0.13	0.16	0.14	0.08	0.16	0.20	0.22	0.22	0.16	0.12	0.13
TL_{32}	0.21	0.12	0.16	0.13	0.08	0.16	0.20	0.22	0.22	0.15	0.11	0.12
TL_{16}	0.19	0.12	0.15	0.13	0.08	0.15	0.18	0.20	0.19	0.12	0.09	0.09
TL_{8}	0.12	0.10	0.12	0.11	0.10	0.12	0.13	0.12	0.07	0.01	-0.01	-0.01
TL_{4}	-0.02	0.07	0.05	0.07	0.12	0.06	0.02	-0.03	-0.13	-0.19	-0.19	-0.19
TL_{2}	-0.14	0.03	-0.02	0.04	0.13	0.01	-0.07	-0.15	-0.31	-0.35	-0.34	-0.33
TL_{1}	-0.20	0.01	-0.05	0.01	0.13	-0.02	-0.12	-0.21	-0.39	-0.43	-0.40	-0.40
Max.absorption	-0.20	0.01	-0.05	0.01	0.13	-0.03	-0.12	-0.22	-0.39	-0.42	-0.40	-0.40
R^2	0.80	0.70	0.77	0.81	0.87	0.85	0.87	0.80	0.74	0.89	0.93	0.89
Number of PC selected	2	2	2	2	2	2	2	2	2	2	2	2

Table 6-16 shows that, except for noise level L_{1600}, good linear relationships were also obtained using variable combination 4 as input. From the previous analysis, it is learned that 1600 Hz is the point where the influence of long wavelength texture level diminishes and short wavelength texture and sound absorption become dominant. So the noise level at such a frequency cannot be described well by the two generalized parameters MPD and maximum sound absorption coefficient.

The influence of MPD and maximum sound absorption are similar to those of texture and sound absorption on the spectral band. However, it should be noted that according to Table 6-8, MPD and maximum absorption coefficient are highly correlated.

Table 6-16 Standardized coefficients from regression with variable combination 4*

	$L_{A,\,eq}$	L_{315}	L_{400}	L_{500}	L_{630}	L_{800}	L_{1000}	L_{1250}	L_{1600}	L_{2000}	L_{2500}	L_{3150}
MPD	1.30	0.99	1.23	1.12	0.82	1.10	1.25	1.30	1.13	0.65	0.33	0.31
Max. absorption	-0.66	-0.15	-0.40	-0.21	0.20	-0.19	-0.46	-0.71	-1.20	-1.31	-1.14	-1.06
R^2	0.78	0.76	0.90	0.94	0.96	0.92	0.87	0.75	0.59	0.80	0.82	0.71

*The least square regression method is used.

6.4.5 Analyses using PLS

The PLS method is used for regression analyses with the same variable combinations as those used in the PCR analysis. From the algorithm, it is known that the relations between the input matrix *X* and output matrix *Y* are to be found, and this is based on modeling the covariance structures in these two spaces by the latent variable approach. There are different computer algorithms for extracting the latent variable. In this study, the so called SIMPLS [25] method is used, and the calculation process is supported by the statistical toolbox in Matlab. The resulting latent variables are successive orthogonal components that maximize the covariance between each input *X* and the output *Y*. The first few

components capture important information of X as well as explain the variance of Y to a good extent and they are selected for the regression.

An example of the PLS regression is given for the noise level at 1000 Hz with variable combination 1. In Figure 6-12, the percent of variance which is explained by the PLS components are shown for $\boldsymbol{X}$ and $\boldsymbol{Y}$ respectively. In this case, $\boldsymbol{X}$ denotes the standardized variables of texture level and sound absorption on the spectral band, as shown in Table 6-9. $\boldsymbol{Y}$ is the standardized vector of the noise level at 1000 Hz. The mean squared error (MSE) is also shown since this plot helps in selecting the input PLS components. The MSE is a statistic which quantifies the difference between the estimated and true values of a quantity. An MSE value close to 0 indicates a good regression.

Figure 6-12 shows that the first two components explain 93% of the response variables and 83% of the predictor variables. Figure 6-13 shows that the MSE is close to 0.1 when 2 PLS components are used as input. Based on these considerations, the regression model with the first two components is selected. The regression coefficients for L_{1000} are given in Table 6-17. It can be seen that the regression results obtained by means of PLS regression are quite close to those obtained using the PCR method.

The PLS regression is conducted on all the variable combinations for different noise levels. The results from variable combination 1 and combination 3 are very similar to those obtained from the PCR method. Detailed information about the regression coefficients is given in Appendix B.

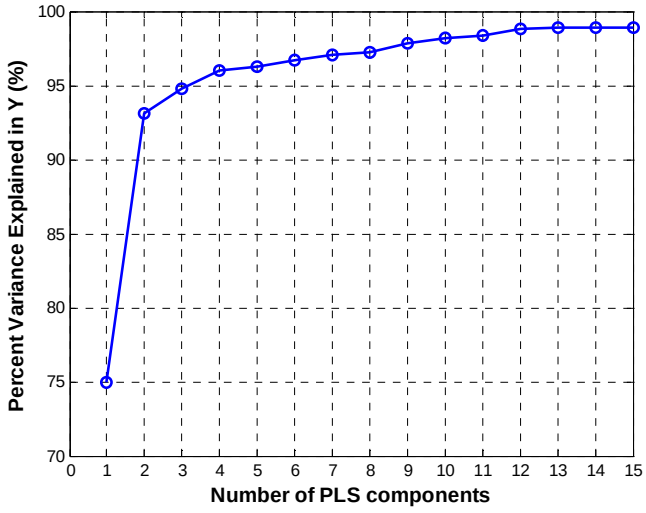

(a) Percent of variance explained in $\boldsymbol{Y}$

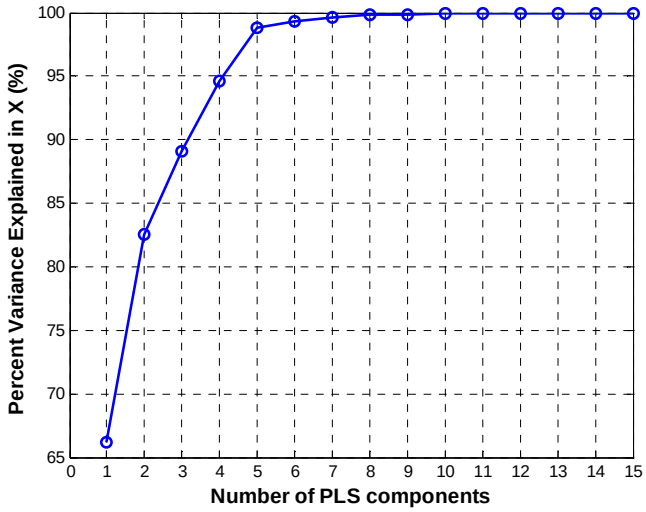

(b) Percent of variance explained in ***X***

Figure 6-12 Percent of variance explained in the variable

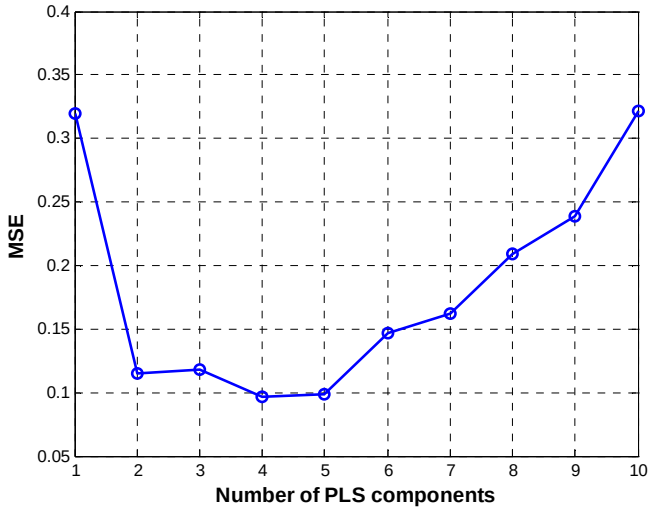

Figure 6-13 MSE of the PLS regression with different PLS components

Table 6-17 Regression coefficients for L_{1000} from PLS method

Noise level	TL_{250}	TL_{125}	TL_{63}	TL_{32}	TL_{16}	TL_{8}	TL_{4}	TL_{2}	TL_{1}
	0.16	0.16	0.16	0.16	0.15	0.12	0.05	-0.02	-0.05
L_{1000}	AL_{1000}	AL_{1250}	AL_{1600}	AL_{2000}	AL_{2500}	AL_{2000}		R^2	
	-0.20	-0.12	-0.03	-0.01	-0.02	-0.03		0.93	

Table 6-18 shows the results when combination 2 is used as input. By comparing Table 6-18 with Table 6-14, it is found that the R^2 for each equation increases. When the MPD is used to represent the surface texture, it combines the effect of both long and short wavelength texture level. As shown in Table 6-18, the noise levels below 2000 Hz increase with increasing MPD, and the noise levels above 2000 Hz reduce with the increasing MPD.

The coefficients for AL_{1000} in yhe low frequency noise levels (from 400 Hz to 630 Hz) are high. According to the correlation coefficients between the noise level and sound absorption as shown in Figure 6-10, the influence of sound absorption is not that high at these frequencies. It is thus considered that the multicollinearity between MPD and absorption coefficients is not completely eliminated. Therefore it is concluded that when using the PCR or PLS for regression, the multicollinearity cannot always be removed when certain generalized parameters, such as MPD or maximum sound absorption, are taken into account. PCR and PLS methods work well if the surface characteristics are expressed in spectral bands.

Table 6-18 Standardized coefficients from PLS with variable combination 2

	$L_{A,\,eq}$	L_{315}	L_{400}	L_{500}	L_{630}	L_{800}	L_{1000}	L_{1250}	L_{1600}	L_{2000}	L_{2500}	L_{3150}
MPD	0.52	0.82	0.77	0.72	0.56	0.54	0.55	0.47	0.27	0.01	-0.04	-0.02
AL_{1000}	-0.47	-0.08	-0.26	-0.25	-0.18	-0.40	-0.44	-0.46	-0.37	-0.13	-0.08	-0.13
AL_{1250}	-0.22	0.02	-0.05	0.05	0.15	-0.09	-0.15	-0.26	-0.38	-0.33	-0.19	-0.16
AL_{1600}	-0.03	0.01	0.02	0.15	0.28	0.10	0.04	-0.08	-0.29	-0.40	-0.27	-0.16
AL_{2000}	-0.01	-0.02	-0.03	0.00	0.09	0.07	0.04	0.01	-0.08	-0.22	-0.31	-0.28
AL_{2500}	-0.03	-0.02	-0.04	-0.06	-0.01	0.04	0.01	0.01	-0.01	-0.07	-0.18	-0.25
AL_{3150}	-0.03	0.01	-0.02	-0.03	0.01	0.05	0.00	-0.01	-0.03	-0.07	-0.18	-0.25
R^2	0.77	0.72	0.77	0.84	0.92	0.89	0.82	0.75	0.69	0.79	0.82	0.82
Number of components selected	2	2	2	2	2	2	2	2	2	2	2	2

6.4.6 Influence of the vehicle speed

As introduced in section 6.2, the CPX measurements were performed at 8 different speed intervals. According to the report from DVS, a relationship between the $L_{A,\,eq}$ and the logarithm of vehicle speed has been identified [14]. The linear relationship between the overall noise level and the logarithm of the speed was also validated in other studies. In this research, the investigation is especially focused on the influence of vehicle speed on the tyre - road noise from thin layer surfacings. The speed V is used as one of the influencing factors, and linear regression functions are developed with combinations of speed and surface characteristics as input variables. The analysis is not only made on the overall noise level $L_{A,\,eq}$, but also on noise levels at different frequency bands. PCR is used as the regression method.

The surface characteristics used as input are in accordance with the variable selection results shown in Table 6-9. In the principal component analysis, the first four components are extracted and listed in Table 6-19. It can be seen that the fourth component is equal to the vehicle speed and has no relation with any surface properties. In the first three PCs, the coefficients for surface characteristics are exactly the same as shown in Table 6-10, and there is no contribution from speed. Therefore, the speed is considered as an orthogonal component with surface characteristics, and it can be analyzed independently.

Table 6-19 The eigenvectors for the PCs considering the vehicle speed

PC	TL_{250}	TL_{125}	TL_{63}	TL_{32}	TL_{16}	TL_{8}	TL_{4}	TL_{2}	TL_{1}	AL_{1000}	AL_{1250}	AL_{1600}	AL_{2000}	AL_{2500}	AL_{3150}	V
1	0.29	0.29	0.29	0.29	0.30	0.31	0.31	0.29	0.28	-0.10	0.10	0.20	0.24	0.22	0.23	0.00
2	-0.22	-0.21	-0.21	-0.21	-0.19	-0.10	0.06	0.20	0.26	0.47	0.50	0.32	0.14	0.16	0.21	0.00
3	-0.15	-0.15	-0.15	-0.14	-0.14	-0.10	-0.03	0.03	0.06	-0.23	-0.41	-0.28	0.40	0.49	0.42	0.00
4	0.00	0.00	0.00	0.00	0.00	0.00	0.00	0.00	0.00	0.00	0.00	0.00	0.00	0.00	0.00	1.00

The regression coefficients achieved from PCR are given in Table 6-20. In the regression, the original speed data are used and no logarithmic values are used. As shown in the table, the standardized coefficients for speed are much higher than those for surface texture and sound absorption parameters. This means that vehicle speed plays the most important role in the noise level. The influencing trend of the individual roads surface parameter is consistent with the case without considering speed, as summarized in section 6.4.4 and 6.4.5.

The results show that R^2 increases in most cases when the driving speed is taken into account as independent variable. The driving speed has a significant effect on the overall noise level and the noise level at 315 Hz, compared with results in Table 6-13.

Table 6-20 Standardized coefficients from PCR with variable combination 1

	$L_{A,\,eq}$	L_{315}	L_{400}	L_{500}	L_{630}	L_{800}	L_{1000}	L_{1250}	L_{1600}	L_{2000}	L_{2500}	L_{3150}
TL_{250}	0.06	0.02	0.04	0.06	0.05	0.06	0.07	0.09	0.07	0.03	0.02	0.03
TL_{125}	0.06	0.02	0.04	0.06	0.05	0.06	0.07	0.09	0.07	0.03	0.02	0.03
TL_{63}	0.06	0.02	0.04	0.06	0.05	0.06	0.07	0.09	0.07	0.03	0.02	0.03
TL_{32}	0.06	0.02	0.04	0.06	0.05	0.06	0.07	0.09	0.07	0.03	0.02	0.03
TL_{16}	0.06	0.02	0.04	0.06	0.05	0.06	0.07	0.08	0.06	0.02	0.01	0.02
TL_{8}	0.04	0.02	0.03	0.05	0.05	0.05	0.06	0.06	0.04	0.00	-0.01	0.00
TL_{4}	0.02	0.01	0.02	0.04	0.04	0.03	0.03	0.02	-0.02	-0.04	-0.04	-0.04
TL_{2}	-0.01	0.01	0.01	0.03	0.03	0.01	0.00	-0.02	-0.06	-0.08	-0.07	-0.07
TL_{1}	-0.02	0.00	0.00	0.02	0.03	0.00	-0.01	-0.04	-0.08	-0.09	-0.09	-0.08
AL_{1000}	-0.08	-0.02	-0.02	-0.01	-0.01	-0.07	-0.08	-0.13	-0.16	-0.11	-0.05	-0.04
AL_{1250}	-0.06	0.00	0.00	0.03	0.03	-0.04	-0.06	-0.12	-0.17	-0.14	-0.05	-0.04
AL_{1600}	-0.03	0.01	0.01	0.04	0.04	-0.01	-0.02	-0.06	-0.11	-0.09	-0.04	-0.03
AL_{2000}	-0.01	0.00	-0.01	0.00	0.01	0.00	0.00	-0.01	-0.04	-0.06	-0.10	-0.10
AL_{2500}	-0.02	-0.01	-0.02	-0.02	0.00	-0.01	-0.01	-0.03	-0.05	-0.06	-0.11	-0.12
AL_{3150}	-0.03	-0.01	-0.02	-0.01	0.00	-0.01	-0.02	-0.04	-0.06	-0.08	-0.12	-0.12
V	0.92	0.96	0.83	0.65	0.72	0.85	0.88	0.83	0.81	0.82	0.84	0.88
R^2	0.96	0.95	0.76	0.62	0.72	0.90	0.97	0.96	0.92	0.91	0.94	0.96

Since the speed is independent of the surface characteristics, regression functions are developed with speed as the unique explanatory variable. Figure 6-14 shows the scatter diagram of the measured noise levels at different speeds and the trend line from the regression analysis. From the figure, it is concluded that the influence of speed on certain noise levels can be well presented by a linear equation. At each speed, the variability in the noise depends on the surface

characteristics; the influence of the surface characteristics has been discussed in the last two sections.

A comparison is also made on the predictive power of the equation using the speed and predictive power of the equation using the logarithm of the speed in the regression. The transformed speed V_T is expressed by

$$V_T = \log(\frac{V}{V_{ref}}) \tag{6-11}$$

Where V_{ref} is the reference speed of 70 km/h.

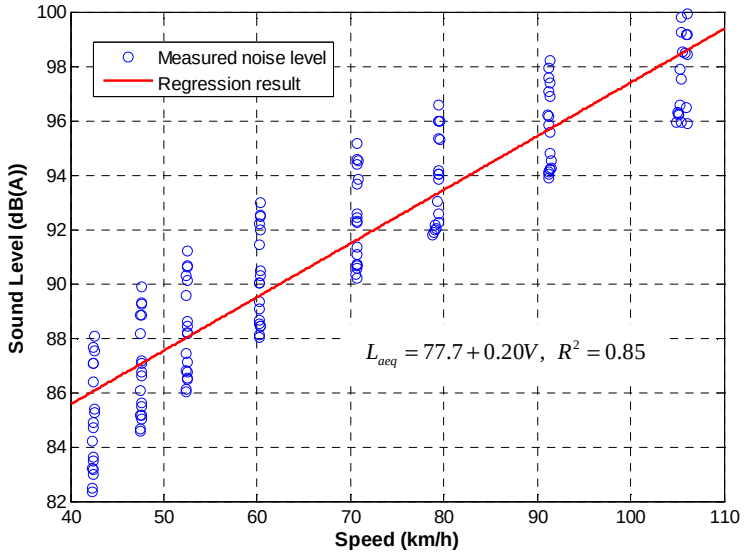

(a) Overall noise level

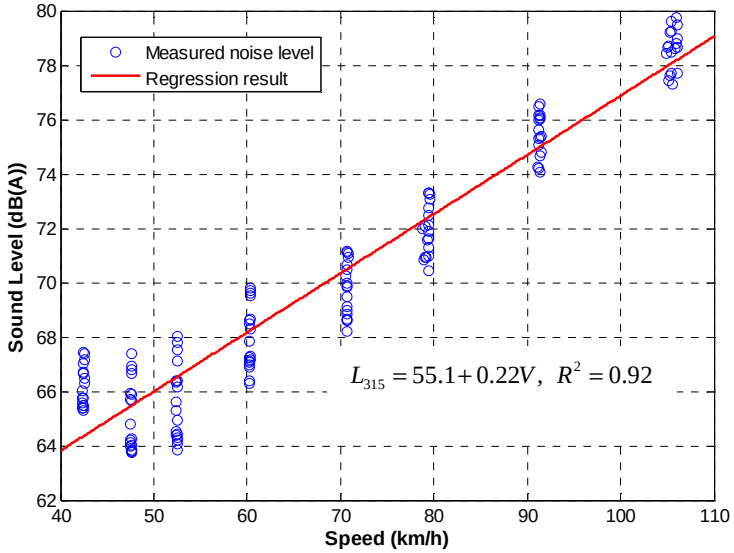

(b) Noise level at 315 Hz

Figure 6-14 Noise and speed relationship for passenger tyre

The results are shown in Table 6-21. For the noise level at most frequencies, R^2 increases a bit if the logarithm of the speed is used. Since the difference is only

small, the driving speed can be used directly for setting up a linear relation with the tyre - road noise on thin layer surfacings.

Table 6-21 PCR results with the logarithm of the speed

	$L_{A,eq}$	L_{315}	L_{400}	L_{500}	L_{630}	L_{800}	L_{1000}	L_{1250}	L_{1600}	L_{2000}	L_{2500}	L_{3150}
Surface characteristics	Refer to Table 6-20											
V_T	0.93	0.94	0.78	0.67	0.77	0.87	0.87	0.83	0.83	0.83	0.84	0.89
R^2	0.98	0.90	0.66	0.64	0.80	0.93	0.96	0.96	0.94	0.92	0.95	0.97

6.4.7 Study on truck tyres

In the previous sections, investigations were made on the noise produced from passenger car tyres. Since the properties of truck tyres are different from passenger car tyres, noise from these two types of tyre are generally studied separately [9]. In this section, the results of a special analysis on the influence of thin layer surfacings on noise levels from truck tyres are presented. The programs and methods used in this study are similar to those used in previous sections. The truck tyres involved in this study are listed in Table 6-22. According to the position used on a truck, the tyres can be classified into three groups, namely the tyre from the steering axle, drive axle and trailer axle. Some worn tyres are also taken into account in the study as marked in Table 6-22. All the tyres are new expect those marked in the table as worn.

Table 6-22 Truck tyre types used in current study

Tyre No.	Type	Size	Tyre Type	Tyre No.	Type	Size	Tyre Type
1	Continental HSR	315/80/22.5*	Steering axle	8	Michelin XDA2 Energy (worn)	315/80/22.5	Drive axle
2	Goodyear Marathon LHS	315/80/22.5	Steering axle	9	Michelin XDN Grip	315/80/22.5	Drive axle
3	Michelin XZA2 Energy (new)	315/80/22.5	Steering axle	10	Bridgestone M729	315/80/22.5	Drive axle
4	Michelin XZA2 Energy (worn)	315/80/22.5	Steering axle	11	Continental HTR	385/65/22.5	Trailer axle
5	Continental HDR	315/80/22.5	Drive axle	12	Goodyear Marathon LHT	385/65/22.5	Trailer axle
6	Goodyear Marathon LHD	315/80/22.5	Drive axle	13	Michelin XTA2 Energy (new)	385/65/22.5	Trailer axle
7	Michelin XDA2 Energy (new)	315/80/22.5	Drive axle	14	Michelin XTA2 Energy (worn)	385/65/22.5	Trailer axle

*315=Tyre width in mm; 80=Aspect ratio (height is 90% of width); 22.5=Diameter code for rim (in inch)

Figure 6-15 gives examples for tread patterns of different types of truck tyres. A complete overview of the tread patterns of all the truck tyres can be found in the CD attached. It can be seen from the figure that the truck tyres have different tread patterns. The grooves and blocks on the worn tyres are not that obvious as those on a new one.

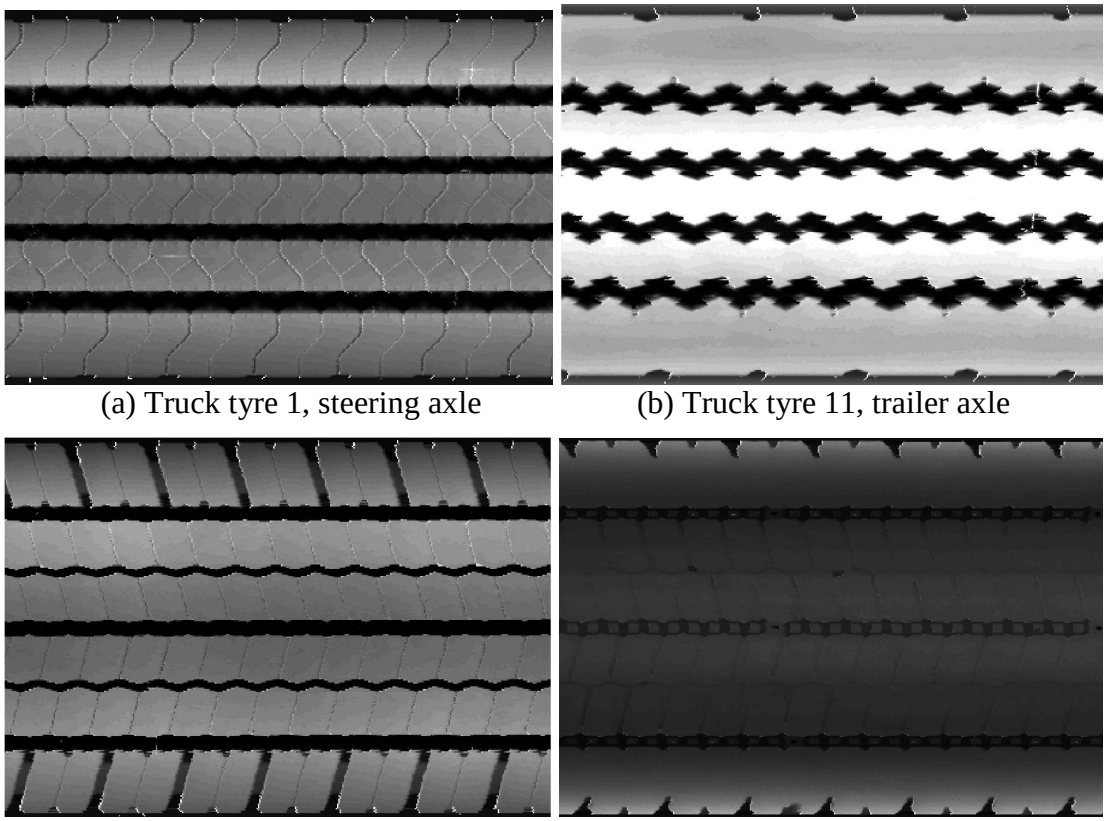

(a) Truck tyre 1, steering axle (b) Truck tyre 11, trailer axle

(c) Truck tyre 7, drive axle (new) (d) Truck tyre 8, drive axle (worn)

Figure 6-15 Examples of tread patterns of truck tyres

Noise levels measured on the different Kloosterzande sections as produced by the truck tyres in Figure 6-15 are shown in Figure 6-16. The driving speed during the tests was 75 - 85 km/h.

In general, the overall noise level and the maximum noise level on the 1/3rd octave band from a drive axle tyre are higher compared to those of the tyre on the steering axle or trailer axle. In most of the cases, new tyres also generate a higher noise level than worn tyres. This is because the impact noise between a rolling tyre and the road surface is smaller in case of worn tyres. For new axle tyres in good condition, the noise levels below 1000 Hz at different surfaces are very close to each other (the investigation is made on data from all the tyres, not only restricted to the curves in Figure 6-16. For other tyres, the readers are referred to the CD attached to this thesis). It indicates that in this frequency range, the noise levels are dominated by the tyre parameters and are not sensitive to the variation in the surface characteristics. For other types of truck tyres, the noise level is influenced by the combined effect of both the tyre and road surface. The increasing sound absorption coefficient leads to a reduced noise level above 1000 Hz. The surface with the lowest sound absorption ability and highest texture level, namely the thin SMA section 20, has the highest noise level in nearly all the cases.

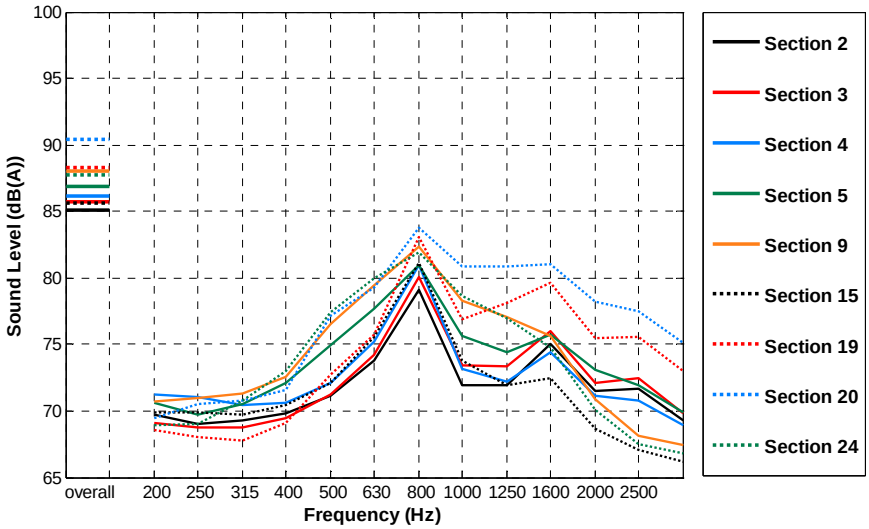

(a) Truck tyre 1, steering axle

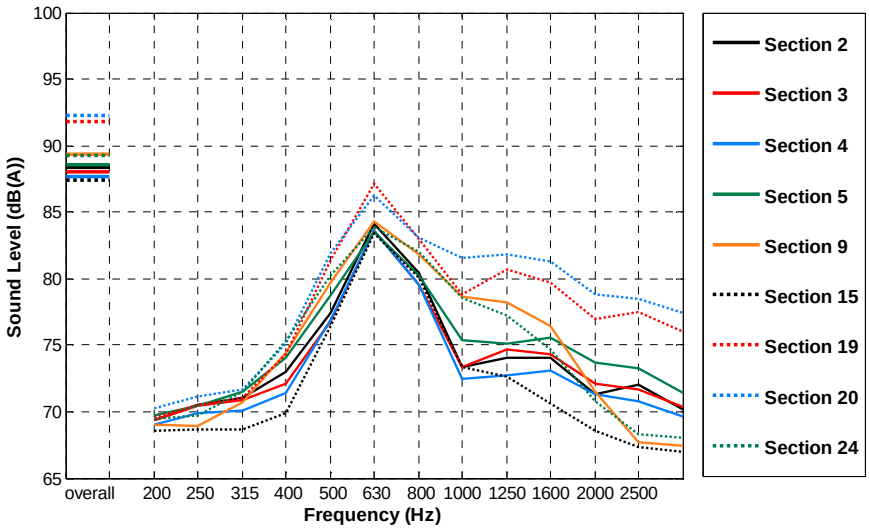

(b) Truck tyre 11, trailer axle

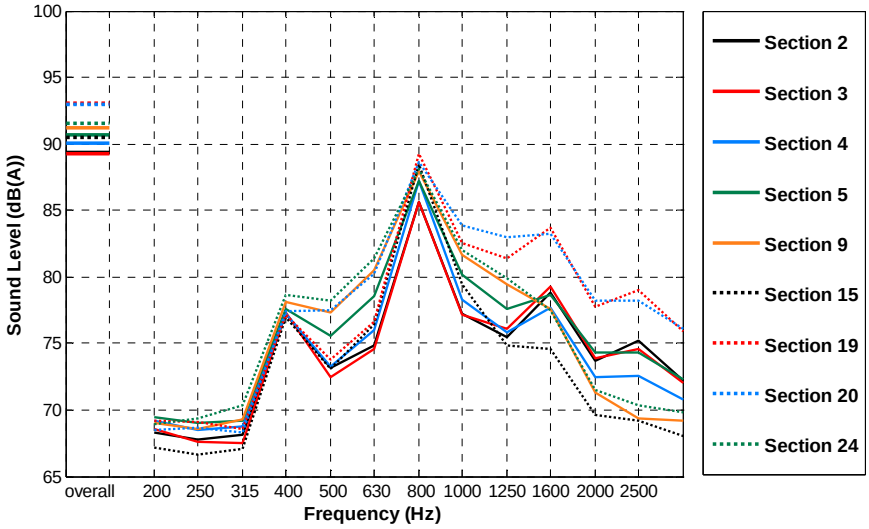

(c) Truck tyre 7, drive axle (new)

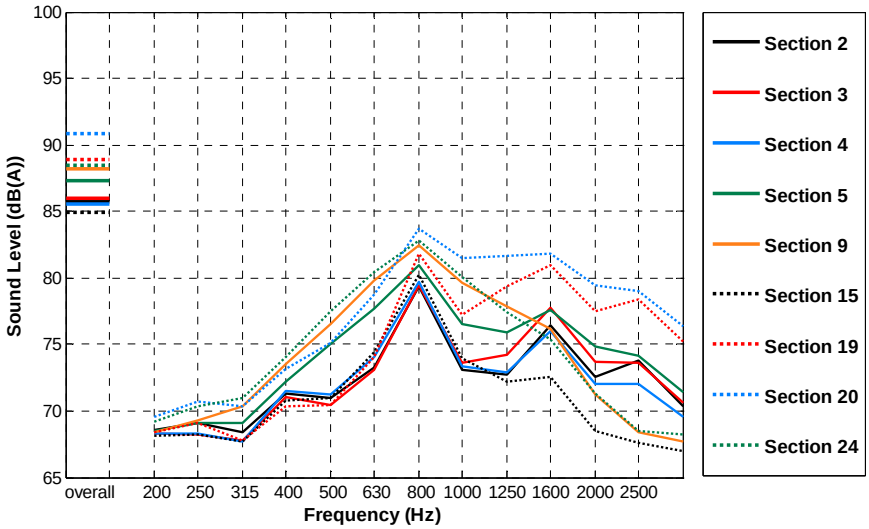

(d) Truck tyre 8, drive axle (worn)

Figure 6-16 Tyre - road noise levels for truck tyres at 75 - 85 km/h

For different types of truck tyres, large differences in noise level on the spectrum band of frequency are observed. It is not suitable to use the average value to present the noise from all the truck tyres. In this study, an investigation on the noise level is performed by using drive axle tyre No.7 as an example. The contour lines of the correlation coefficient between tyre road noise and surface characteristics are shown in Figure 6-17. In the lower frequency range, high correlations between long wavelength texture level and noise level are mainly found from 500 Hz to 630 Hz, see Figure 6-17(a). The correlation coefficients are lower than -0.6 between short wavelength texture levels (≤4 mm) and noise levels in the high frequency range (>1600 Hz). Compared with the results from passenger car tyres (shown in Figure 6-10), the cross-over frequency is lower, for truck tyres it is between 1000 Hz and 1500 Hz. The sound absorption, as shown in Figure 6-17(b), is negatively correlated with noise levels above 1000 Hz. The distribution of the contour line is similar to that for passenger car tyres.

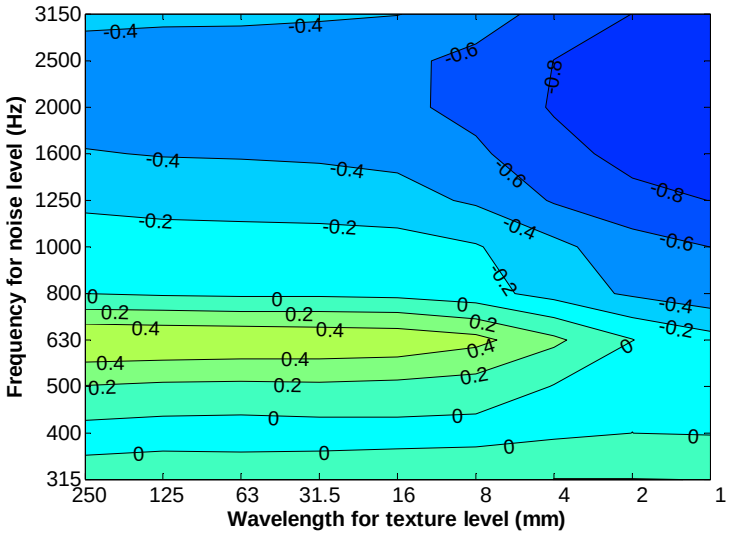

(a) Surface texture level

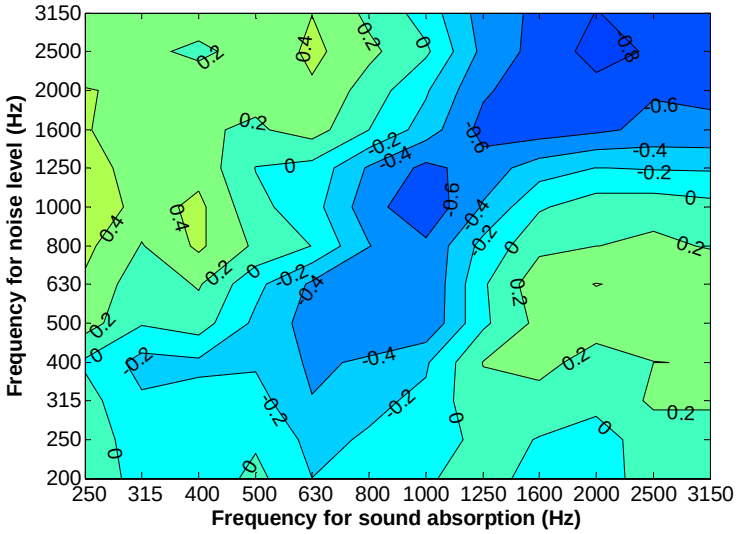

(b) Sound absorption coefficient

Figure 6-17 Contour lines of the correlation coefficient between noise level (at 80 km/h) and surface characteristics for truck tyre No.7

The regression analysis results are shown in Table 6-23. The coefficients listed are from the the PLS method, and the first two components are selected in the regression. For the overall noise level and the noise levels at 315 Hz, 400 Hz and 800 Hz, the linear relationships with the surface characteristics are weak.

Table 6-23 Standardized coefficients from PLS for truck tyre No. 7

	$L_{A,eq}$	L_{315}	L_{400}	L_{500}	L_{630}	L_{800}	L_{1000}	L_{1250}	L_{1600}	L_{2000}	L_{2500}	L_{3150}
TL_{250}	0.11	0.07	0.01	0.17	0.17	0.05	0.16	0.16	0.08	0.10	0.06	0.09
TL_{125}	0.12	0.11	0.08	0.17	0.17	0.07	0.15	0.15	0.07	0.09	0.05	0.08
TL_{63}	0.11	0.12	0.08	0.17	0.17	0.06	0.15	0.14	0.07	0.09	0.05	0.08
TL_{32}	0.10	0.10	0.06	0.17	0.17	0.05	0.14	0.14	0.07	0.08	0.04	0.07
TL_{16}	0.10	0.10	0.07	0.15	0.15	0.06	0.13	0.13	0.05	0.07	0.03	0.06
TL_{8}	0.07	0.07	0.06	0.11	0.12	0.05	0.09	0.07	0.01	0.02	-0.01	0.01
TL_{4}	-0.02	0.03	0.04	0.03	0.05	0.01	0.00	-0.04	-0.09	-0.09	-0.09	-0.09
TL_{2}	-0.12	-0.03	-0.02	-0.04	-0.02	-0.06	-0.10	-0.14	-0.17	-0.17	-0.16	-0.17
TL_{1}	-0.17	-0.04	-0.04	-0.06	-0.05	-0.12	-0.15	-0.19	-0.20	-0.21	-0.20	-0.21
AL_{1000}	-0.30	-0.04	-0.17	-0.18	-0.17	-0.30	-0.30	-0.28	-0.19	-0.13	-0.07	-0.10
AL_{1250}	-0.18	0.06	0.14	-0.09	-0.10	-0.12	-0.21	-0.23	-0.23	-0.19	-0.11	-0.14
AL_{1600}	-0.08	-0.07	0.09	-0.03	-0.02	0.01	-0.09	-0.14	-0.20	-0.21	-0.14	-0.16
AL_{2000}	-0.08	-0.16	-0.17	-0.06	-0.03	0.00	-0.06	-0.11	-0.15	-0.20	-0.21	-0.21
AL_{2500}	-0.04	0.01	-0.01	-0.07	-0.04	0.06	-0.05	-0.11	-0.11	-0.14	-0.17	-0.17
AL_{3150}	-0.06	0.00	-0.02	-0.06	-0.05	0.01	-0.07	-0.11	-0.11	-0.15	-0.17	-0.18
R^2	0.54	0.24	0.19	0.83	0.91	0.31	0.79	0.80	0.84	0.88	0.90	0.88
Number of components selected	2	2	2	2	2	2	2	2	2	2	2	2

For the other noise levels produced by truck tyre No. 7, the influence of long wavelength texture levels and sound absorption coefficient are close and this is also observed for the passenger car tyres. The effect of short wavelength texture

levels is more important. From 1000 Hz, the noise level starts to be reduced by increasing short wavelength texture levels. All this indicates that on drive axle tyres, the noise caused by tyre vibration is indifferent between various types of thin layer surfacings. Above 1000 Hz, the noise caused by air pumping is effectively reduced by the short wavelength texture and sound absorption coefficient. This phenomenon is also found for the truck tyres at other axles (examples can be seen in the CD). Therefore, it can be concluded that on the thin layer surfaces with a small variation of texture, the surface sound absorption is the primary factor in reducing noise from truck tyres.

6.5 Investigation into Change of Surface Characteristics

6.5.1 Model description

From the investigation of the thin layer surfacings, it is clear that variation of the mixture composition leads to differences of the surface characteristics, such as texture and absorption coefficient. Correspondingly, the tyre - road noise level changes with the changes in the surface characteristics. Models from existing studies all describe the relationship between the global noise level and the surface characteristics. In the previous sections of this chapter, the work was also focusing on relationships with global values. In this section, a new type of modeling approach is developed for evaluating the change of the tyre - road noise caused by the variation of the pavement material properties and the surface characteristics.

It is known that the generation of tyre - road noise is a complex and sensitive system, and there are a lot of factors influencing the noise levels. This is the main reason why existing models are unable to provide accurate predictions. In this study, the generation of tyre - road noise is treated as a ‘black box’. It is assumed that there are only changes of road surface properties, and all the other factors are considered stable. Under such condition, the change of the noise level is assumed to be caused completely by the variation of the road surface properties.

The framework of the target model is shown in Figure 6-18. The model does not attempt to relate the global noise level to a certain surface characteristic, but calculates the difference of tyre - road noise level caused by changing surface characteristics or material properties. Herein, the interpretation of the word “change” is at a general concept level. It can evaluate the effect of different designs made by road engineers, but also changes of road surface characteristics with time and difference in surface characteristics between different sections. As to tyre - road noise, the “change” indicates the increase or reduction of the noise level. It provides road engineers and authorities a direct index of the noise reduction or noise increasing effect of road surfaces, and can help guiding the design of the road surface. In most existing models, small changes of the material properties affecting the tyre - road noise are not taken into account. Actually, the changes of noise level between different types of road surfaces can be used as corrections to the prediction models. In some traffic noise models or out-door

sound propagation models, the use of the real functioning of the road surface as corrections to the model has proved to improve the prediction accuracy [2, 26]. In this study, the changes of noise level within the same type of surfaces are modelled. The target models can be used as corrections for existing models, and the prediction accuracy of these models is expected to improve by involving the influence of small differences between surfaces.

From Figure 6-18, it can be seen that the model computes the change of the noise level ΔL from the differences of the surface characteristics. Tyre related indices and environmental conditions are not involved because the model is mainly intended to be related with road engineering. The tyre and environmental influence factors are therefore considered as fixed in the analysis.

Since the study concentrates on thin layer surfacings with small variations of surface characteristics, it is assumed that the relation between the input and output is linear in this small range. The relationships were developed by means of linear regression. The statistical expression is as follow:

$$\Delta L(f) = \sum_{i=1}^{n} \beta_i \Delta \upsilon_i \tag{6-12}$$

Where $\Delta \upsilon_i$ denotes the change of a certain surface characteristic, including surface texture and sound absorption as mentioned in this study. β_i is the coefficient to be determined via a regression process.

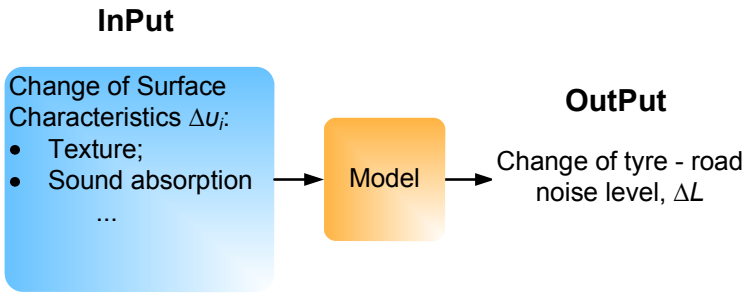

Figure 6-18 Framework of the model

The data used for the regression are from the 4 typical thin layer surfacings No.2 to No. 5 in Table 6-5. The analysis is only performed on these standard thin layer surfacings because it was aimed to restrict the change to a small interval. The SMA and PAC type of thin layer surfacings are not included. So a total of 8 sections is included, because two were built for each design.

From Section 6.4, it is known that the influence in the difference in surface characteristics is important on noise generated by passenger car tyres. Therefore, in this part, only data from car tyres are considered. The regression process is shown schematically in Table 6-14. From the chart, it can be seen that the different values of the noise level as well as variations of surface characteristics are calculated prior to the regression. Then these difference values are used for

developing the model. The initial variable selection method and regression methods are the same as used in the regression analysis with the global data. The details can be found in Section 6.3.

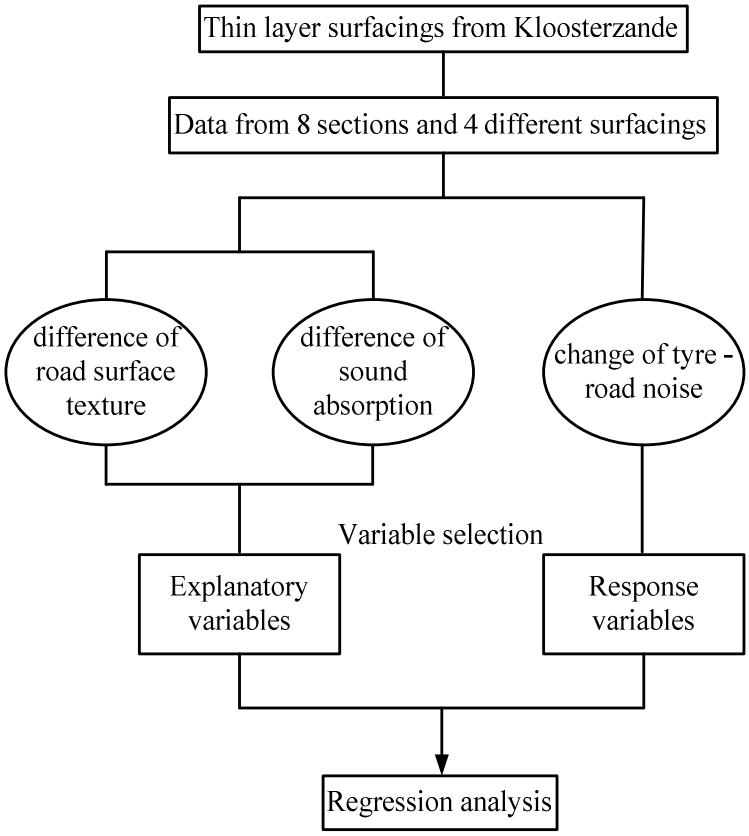

Figure 6-19 Development process of Model

6.5.2 Variable selection

The ANOVA method is used for selecting the noise levels to be taken into account in the analysis. The resulting significance values for each noise level are shown in Table 6-24. From the table, it can be concluded that the differences of overall noise level and noise levels at frequencies above 1000 Hz can be attributed to variations of the road surface. The road surface has little influence on noise levels below 1000 Hz. The only exception is the noise level at 500 Hz, for which the significance is smaller than 0.05 and therefore this noise level is considered to be affected by the road surface characteristics. The changes at those noise levels are thus chosen as response variables for the regression. In addition, the noise level generally reaches a maximum at 800 Hz as shown in Figure 6-8. The noise level at 800 Hz is also taken into account.

The selection of the parameters describing the surface characteristics is based on the investigation of the curves of texture level and sound absorption as shown in Figure 6-6 and Figure 6-7. However, only the first four sections are considered in this case. The selection is aiming to detect a relationship of the noise level differences with the change in texture level and sound absorption on the spectrum band. Thus texture levels with a wavelength below 4 mm and sound

absorption coefficients below 1000 Hz are not involved, because the differences are very small and are considered to have no effect on noise. The selected response variable and the two combinations of the explanatory variables are shown in Table 6-25.

Table 6-24 Significance of different road surfaces on noise level

	$L_{A,eq}$	L_{200}	L_{250}	L_{315}	L_{400}	L_{500}	L_{630}	L_{800}	L_{1000}	L_{1250}	L_{1600}	L_{2000}	L_{2500}	L_{3150}
Sig.	0.00	0.23	0.22	0.13	0.10	0.01	0.83	0.10	0.00	0.00	0.00	0.00	0.00	0.00

Table 6-25 Selection of explanatory variables and response variables

	Explanatory variables	Number of explanatory variables	Response variable	Number of responsible variables
Sound Absorption	Changes of sound absorption coefficient A at frequencies 1000, 1250, 1600, 2000 2500 and 3150 Hz	13	Change of the overall noise level and changes of noise levels at 500, 800, 1000, 1250, 1600, 2000, 2500 and 3150 Hz	9
Surface Texture	Changes of texture levels at wavelengths 250, 125, 63, 31.5, 16, 8, 4 mm			

6.5.3 Regression analysis

For the regression, the difference values of the noise level, texture level, and sound absorption coefficient between each two of the thin layer surfacing sections are calculated. The noise levels involved are also the averages from the 10 passenger car tyres as used in previous sections. The differences are calculated between every two sections. As there are 8 sections in total, the number of difference values obtained is 28. As the target model is just related to the change of the variables, no reference surface required.

Multivariate regressions are carried out on these calculated data based on Eq. (6-12). The PCR and PLS methods are employed to reduce the influence of multicollinearity between the explanatory variables. A set of regression equations is achieved. Regression coefficients for all the input parameters are given in Table 6-26.

From the regression results, it can be seen that R^2 for the equation of ΔL_{500} is low. Therefore the residual plot is checked and it is concluded that the relation between change of surface texture and ΔL_{500} is not completely linear. The plot indicates that these might be some non-linear trends which are not taken into account. An example of the residual plot for is given in Figure 6-20. For the noise levels at other frequencies, reasonable linear relationships with the variations of layer properties are found, as the R^2 are all higher than 0.65.

Table 6-26 Standardized regression coefficients by means of PCR

	$\Delta L_{A,\,eq}$	ΔL_{500}	ΔL_{800}	ΔL_{1000}	ΔL_{1250}	ΔL_{1600}	ΔL_{2000}	ΔL_{2500}	ΔL_{3150}
ΔTL_{250}	0.13	0.12	0.12	0.13	0.12	0.11	0.09	0.08	0.08
ΔTL_{125}	0.14	0.12	0.13	0.14	0.13	0.12	0.09	0.08	0.09
ΔTL_{63}	0.13	0.13	0.12	0.13	0.13	0.12	0.10	0.10	0.10
ΔTL_{32}	0.13	0.12	0.12	0.13	0.13	0.12	0.09	0.09	0.09
ΔTL_{16}	0.13	0.12	0.12	0.13	0.12	0.11	0.09	0.08	0.09
ΔTL_{8}	0.11	0.11	0.10	0.11	0.10	0.08	0.07	0.07	0.07
ΔTL_{4}	0.07	0.08	0.08	0.08	0.06	0.03	0.02	0.02	0.03
ΔAL_{1000}	-0.29	-0.05	-0.26	-0.28	-0.34	-0.33	-0.06	0.03	0.06
ΔAL_{1250}	-0.18	-0.08	-0.13	-0.16	-0.20	-0.24	-0.15	-0.12	-0.11
ΔAL_{1600}	-0.03	-0.07	0.03	0.00	-0.02	-0.10	-0.19	-0.21	-0.22
ΔAL_{2000}	0.11	-0.04	0.16	0.14	0.15	0.05	-0.17	-0.24	-0.26
ΔAL_{2500}	0.10	-0.03	0.15	0.13	0.14	0.04	-0.16	-0.22	-0.24
ΔAL_{3150}	0.02	-0.05	0.08	0.05	0.05	-0.04	-0.17	-0.21	-0.23
R^2	0.86	0.57	0.92	0.94	0.91	0.70	0.65	0.78	0.86
Number of PC selected	3	2	3	3	3	3	3	3	3

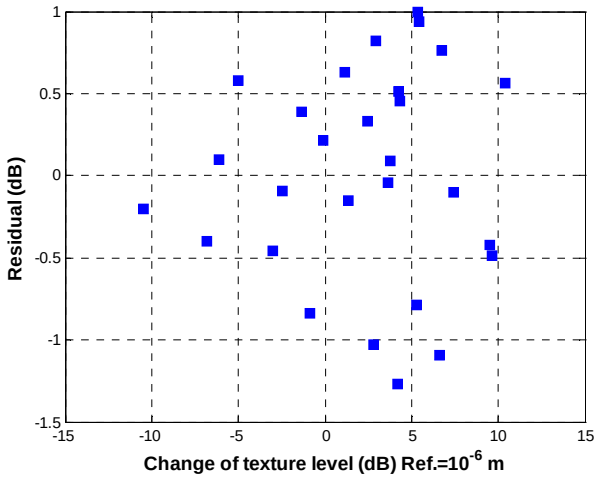

(a) With input variable ΔTL_{32}

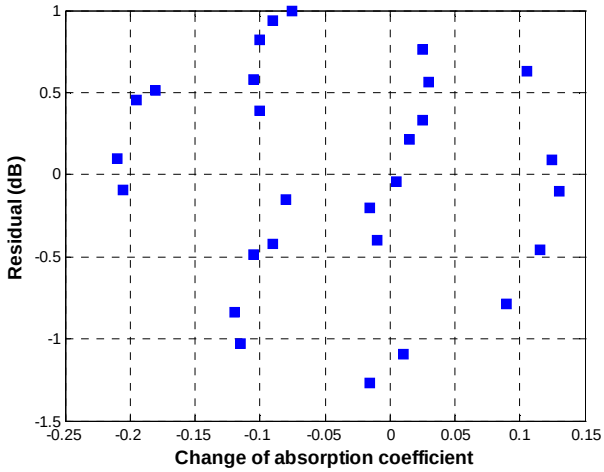

(b) With input variable ΔAL_{1250}

Figure 6-20 Resudial plot for regression equation of ΔL_{500}

For the change of overall noise level $\Delta L_{A,\,eq}$ and noise level from 800 Hz to 1600 Hz, the values and signs of the coefficients of the five equations are similar. This indicates that the influences of surface texture and sound absorption on noise levels at these frequencies and overall noise level are almost the same. On these levels, it can be seen that the difference of the texture level displays a positive influence on the change of noise. In other words, the noise increases when the texture level becomes larger. Major contributions are seen for the texture level with wavelength from 16 mm to 250 mm, because the regression coefficients for these texture levels are relatively higher. The influence of texture at 8 mm or 4 mm is smaller in contrast.

In terms of sound absorption, increase of the sound absorption at 1000 Hz and 1250 Hz leads to a reduction of the overall noise levels and noise levels between 800 Hz and 1600 Hz. The sound absorption coefficients around these two frequencies are thus found to be essential factors to characterize the noise reduction function of thin layer surfacings.

The change of the noise level at high frequencies (≥2000 Hz) decreases with increasing sound absorption coefficients, especially at sound absorption above 1250 Hz. The influence of the sound absorption at 1000 Hz is low. Therefore, increasing the sound absorption at frequencies higher than 1250 Hz is an efficient way to eliminate high frequency noise. The effect of the texture becomes smaller compared with that on the medium frequency noise (800 Hz to 1600 Hz). The reason is that the impact mechanism, which is highly related to the surface texture, is lower at high frequencies, while the air pumping mechanism appears to be dominant at these frequencies. The sign of the coefficient for the short wavelength texture level ΔTL_4 changes from positive to negative at frequency levels higher than 2000 Hz. This is because the texture level with small wavelength results in a lower noise production generated by air pumping.

Considering all the results, it is found that the relationships between the difference of tyre - road noise and variation of surface characteristics are similar with those that were determined for the global noise levels. This implies that it is rational to investigate the impact of surface characteristics on tyre - road noise by using either the global or the difference values.

A combination of the change of MPD and maximum sound absorption coefficient is also employed as input variable for the linear regression. The results by least square regression are summarized in Table 6-27. It can be seen from the table that the effect of the road surface can be investigated by providing two simple inputs. Therefore, the equations are also appropriate to be used as models to evaluate the change of the noise level for thin layer surfacings.

Table 6-27 Regression coefficients for ΔMPD and ΔAL_{max}

	$\Delta L_{A,\,eq}$	ΔL_{800}	ΔL_{1000}	ΔL_{1250}	ΔL_{1600}	ΔL_{2000}	ΔL_{2500}	ΔL_{3150}
Constant	0.10	0.22	0.50	0.37	-0.19	-0.90	-0.77	-0.52
ΔMPD	5.18	4.25	8.80	9.45	7.94	6.39	4.83	3.49
ΔAL_{max}	-2.32	0.78	-1.11	-3.92	-10.70	-16.57	-15.30	-11.21
R^2	0.91	0.89	0.92	0.89	0.83	0.76	0.76	0.76

6.6 Summary and Conclusions

The influence of road surface characteristics on the tyre - road noise was investigated for thin layer surfacings. A systematic analysis was carried out on the Kloosterzande trial sections database with different statistical methods. The original data were pre-treated and factors with non-negligible differences between trial sections were selected as variables in the regression. For solving the problem of multicollinearity between different explanatory variables, the PCR and PLS approaches were applied. As a result, a group of regression equations was developed for presenting the effect of surface texture and sound absorption on noise levels. A summary of the findings based on all the statistical analyses described in this chapter are given below.

Surface characteristics:
The texture levels and sound absorption coefficients can be categorized in three groups being: the long wavelength (≥8 mm) texture level, the short wavelength (≤4 mm) texture level and the sound absorption. In general, the long wavelength texture level increases the noise level below 2000 Hz, and the texture with short wavelength reduces the noise level higher than 1600 Hz. Increasing sound absorption will result in noise reduction above 800 Hz. Similar results can also found when using the MPD to represent surface texture or using the maximum absorption coefficient to characterize the sound absorption of the road surface.

Noise levels:
The overall noise level is mainly increased by higher texture levels at long wavelengths (≥8 mm) and effectively reduced by the sound absorption at 1000 Hz and 1250 Hz. Therefore, decreasing the long wavelength texture level and increasing the sound absorption at 1000 Hz and 1250 Hz are considered as two efficient ways to reduce the tyre - road noise production on thin layer surfacing.

The noise level at low frequencies (below 800 Hz) is highly related with the long wavelength surface texture level, and the noise is considered to be caused by the impact between tyre and road surface. Generation of noise in the medium frequency range (from 1000 Hz to 2000 Hz) is regarded as a combined consequence of the impact and air pumping mechanisms, because all the surface parameters show to have a strong influence on the noise levels.

At high frequencies, the tyre - road noise is mainly caused by the air pumping mechanisms. Increasing of the short wavelength (≤4 mm) texture level and

increasing the sound absorption leads to reduction of noise levels at high frequencies.

Vehicle speed:
Driving speed has a strong influence on tyre – road noise. The influence of speed is completely independent from the road surface characteristics. Noise levels are increasing linearly with increasing speed.

Truck tyre:
On thin layer surfacings, the surface texture is relatively small compared with other types of surface layers. The influence of texture is not that significant between different surfaces when truck tyres are used. In the low frequency band, only noise at 500 Hz and 630 Hz is strongly affected by the texture level. The short wavelength texture level and sound absorption effectively decrease the noise level at frequencies above 1000 Hz. Thus increasing the texture level at short wavelengths and sound absorption coefficients are considered as essential factors for reducing the noise from a rolling truck tyre on thin layer surfacings.

Analysis methods:
Two regression methods, namely PCR and PLS are introduced for eliminating the multicollinearity between the input parameters. When the combination of texture level and sound absorption per frequency band is utilized, the multicollinearity can be reduced very well. The standardized regression coefficients for the developed equations show the importance of individual variables.

The principal component analysis provides PCs which describe the most important properties of the surface characteristics and these PCs generalize the common features of different input variables. For the PLS method, the latent variables are highly related with both the input and output parameters. In this study, similar regression effects are achieved by using the PLS method with less components in comparison with the PCR method. It can be concluded that the PCR gives good explanations of the surface characteristics by the input PCs, while PLS generally helps to derive a linear relationship with a high fit by using a small amount of selected components.

Furthermore, a new type of modeling was developed which concentrates on the change of noise level caused by the variations of surface characteristics. The current results show that the influence of surface characteristics inspected by this method is in agreement with that by using the global values. However, the method provides a direct description of how noise reduces or increases due to changes of certain surface characteristics. This new method helps to correct existing models by taking into account the change of the noise level due to the small changes of road surface characteristics.

References

1. van Keulen, W. and Duškov, M., *Inventory study of basic knowledge on tyre/road noise*, in *IPG Report DWW-2005-022,*. 2005: Delft, the Netherlands.
2. Sandberg, U. and Ejsmont, J., *Tyre/Road Noise Reference Book*. 2002, Kisa, Sweden: Informex.
3. Wayson, R.L., *NCHRP Synthesis 268 - Relationship between pavement surface texture and highway traffic noise*, in *Transportation Research Board, National Academy Press*. 1998: Washington D.C.
4. Klein, P. and Hamet, J.F., *Texture and noise correlations using a dynamic rolling model*, in *SILVIA-INRETS-020-WP2, INRETS*. 2005.
5. Sandberg, U., *Road traffic noise—The influence of the road surface and its characterization.* Applied Acoustics, 1987. **21**(2): p. 97-118.
6. Anfosso-Lédée, F. and Do, M.-T., *Geometric Descriptors of Road Surface Texture in Relation to Tire-Road Noise.* Transportation Research Record: Journal of the Transportation Research Board, 2002. **1806**(Volume 1806 / 2002): p. 160-167.
7. Lu, Q., Fu, P.C., and Harvey, J.T., *Laboratory Evaluation of the Noise and Durability Properties of Asphalt Surface Mixes*. 2009, University of California Pavement Research Center: Berkeley and Davis.
8. Lu, Q., Harvey, J.T., and Wu, R., *Investigation of Noise and Durability Performance Trends for Asphaltic Pavement Surface Types: Four-Year Results*. 2011, University of California Pavement Research Center: Berkeley and Davis.
9. Kuijpers, A.H.W.M., Peeters, H.M., Kropp, W., and Beckenbauer, T., *Acoustic optimization tool, RE4 - Modelling refinements in the SPERoN framework*, in *M+P Report DWW.06.04.7*. 2007: Vught, the Netherlands.
10. Hamet, J.F., *Estimation of the attenuation of rolling noise by acoustic absorption*, in *SILVIA report SILVIA-INRETS-013-00-WP2-09/06/2004*. 2004: Bron Cedex, France.
11. Hamet, J.F., *Reduction of tire road noise by acoustic absorption: Numerical evaluation of the pass-by noise level reduction using the normal incidence acoustic absorption coefficient*. 2004, Laboratoire Transports et Environnement.
12. Peeters, B. and Kuijpers, A.H.W.M. *The effect of porous road surfaces on radiation and propagation of tyre noise*. in *Acoustics 08* 2008. Paris, France.
13. Li, M., van Keulen W., Molenaar, A.A.A., van de Ven, M. and Huurman, R., *New approach for modelling tyre/road noise*. in *Proceedings of INTER-NOISE Conference*. 2009. Ottawa, Canada.
14. van Blokland, G.J., Reinink, H.F., and Kropp, W., *Acoustic optimization tool. RE3: Measurement data Kloosterzande test track*, in *M+P Report DWW.06.04.8*. 2007, M+P Raadgevende Ingenieurs bv: Vught, the Netherlands.

15. ISO11819-2, *Acoustics - Method for measuring the influence of road surfaces on traffic noise -- Part 2: Close-proximity method*. 2000, International Organisation for Standardization (ISO): Geneva, Switzerland.
16. Miradi, M., *Knowledge Discovery and Pavement Performance - intelligent data mining*. 2009, Delft University of Technology: Delft, The Netherlands.
17. Belsey, D.A., Kuh, E., and Roy, E., *Regression Diagnostics: Identifying Influential Data and Sources of Collinearity*. 1980, New York: John Wiley and Sons.
18. Hocking, R.R., *The Analysis and Selection of Variables in Linear Regression.* Biometrics, 1976. **32**: p. 1-49.
19. Jolliffe, I.T., *Principal Component Analysis*. 2002, New York Springer.
20. Krämer, N., *An Overview on the Shrinkage Properties of Partial Least Squares Regression* Computational Statistics, 2007. **22**(2): p. 249 - 273.
21. Hoerl, A.E. and Kennard, R.W., *Ridge Regression: Biased Estimation for Nonorthogonal Problems.* Technometrics, 1970. **8**: p. 27-51.
22. Tibshirani, R., *Regression shrinkage and selection via the lasso: a retrospective.* Journal of the Royal Statistical Society: Series B (Statistical Methodology), 2011. **73**(3): p. 273-282.
23. Pires, J.C.M., et al., *Selection and validation of parameters in multiple linear and principal component regressions.* Environmental Modelling & Software, 2008. **23**(1): p. 50-55.
24. Bring, J., *How to Standardize Regression Coefficients.* The American Statistician, 1994. **48**(3): p. 209-213.
25. de Jong, S., *SIMPLS: An alternative approach to partial least squares regression.* Chemometrics and Intelligent Laboratory Systems, 1993. **18**(3): p. 251-263.
26. Jonasson, H.G. and Storeheier, S.Å., *Nord 2000. New Nordic prediction method for road traffic noise*. 2001, SP Swedish National Testing and Research Institute: Borås.

CHAPTER 7

MODELING OF TYRE - ROAD NOISE

7.1 Introduction

In Chapter 5 and Chapter 6, the influence of material properties on surface characteristics and the effect of surface characteristics on tyre - road noise produced on thin layer surfacings were investigated. In this chapter, models which relate the tyre - road noise to material parameters and surface characteristics are developed based on the knowledge achieved from the previous chapters. The models are proposed as practical tools for predicting the noise levels when designing or inspecting a pavement surface. The predictions help the road designers to determine optimal mixture composition given a wanted maximum noise level and consequently to optimize the mixture design of a noise reducing surface. The models are also useful for estimating the tyre - road noise when the surface characteristics are measured.

There are two important considerations for a model being effective for application in road engineering. The considerations and the corresponding modeling strategies are discussed below:

1) In practice, a model with a simple structure, small number of inputs as well as a high accuracy is preferred. Statistical models generally have simple structures and they are developed by regression on data collected from measurements [1-5]. In this way, the model provides a more practical approach to evaluate of tyre - road noise compared with the theoretically based physical models [6-8], which to some extent are based on an idealized situation.

   Statistical models however have difficulties in providing a general rule for all types of surfacings. For improving the accuracy of the prediction, this study therefore provides models for a certain type of road surface, but not one general model which is applicable for all types of surfacings. The accuracy of the prediction is expected to be improved in this way. In this chapter, tyre - road noise models for thin layer surfacings are developed. A similar method can also be adopted for other surface types.

2) The mixture properties are directly related to the design of the road surface and are of interest for road engineers [9]. In this study, both the surface characteristics and the basic mixture properties are considered as input variables for the model. It means that the evaluation of the tyre - road noise can be made either from the parameters of the surface layer, such as surface texture, absorption coefficient or mixture properties, such as aggregate size, aggregate gradation or air voids content, etc..

Based on these two considerations, a statistical model, using typical material parameters and surface characteristics as input variables are developed for thin layer surfacings. In this chapter, Section 7.2 gives a description of the target models and shows the modeling methods. Section 7.3 shows the regression results by using certain models as examples. Series of models are developed by using different combinations of input variables and regression methods. An initial selection is then made to collect candidate models with a higher prediction power. After that, validations are performed on the candidate models in 7.4. The models which give the best prediction results are proposed for use in practice.

7.2 Description of the model

7.2.1 Framework of the model

Figure 7-1 shows three possibilities to relate the tyre - road noise with the mixture composition and the surface characteristics. The figure shows that the noise levels can be predicted from the mixture composition, surface characteristics, or a combination of the two. Three types of models can thus be developed based on the choice linking the tyre - road noise to material properties. They are:

Type 1: Material properties are considered as independent variables, and the noise levels are computed directly from the material properties;

Type 2: The model has two parts. Type 2(a) links the surface characteristics to material properties while Type 2(b) deduces the noise level from surface characteristics. Models are developed independently for these two parts;

Type 3: Combinations of the material properties and the surface characteristics are used as predictors to evaluate the noise levels.

The diagram in Figure 7-1 is considered as the modeling framework. Table 7-1 gives a summary of the input and output for the different models.

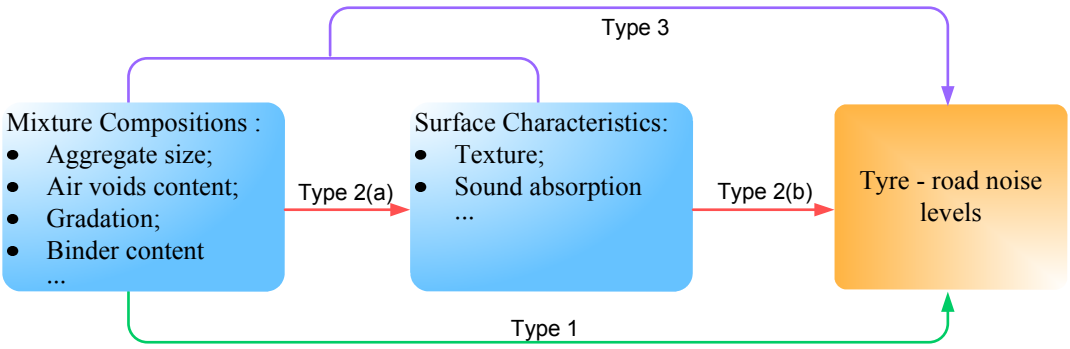

Figure 7-1 Three models for predicting tyre - road noise levels

Table 7-1 Inputs and outputs for different types of models

Model Type	Input	Output
Type 1	Mixture compositions	Tyre - road noise levels
Type 2(a)	Mixture compositions	Surface characteristics
Type 2(b)	Surface characteristics	Tyre - road noise levels
Type 3	Mixture Compositions and surface characteristics	Tyre - road noise levels

7.2.2 Data sources

In this study, three sources of data are available:

1) Database of Kloosterzande trial sections [10]. This database has been used in Chapter 6 for investigating the influence of surface characteristics on tyre - road noise levels. The material properties, surface characteristics and tyre - road noise are all provided in the database. It is involved in modeling of all the types shown in Figure 7-1.

2) Material properties and the surface characteristics measured on slabs. Specific measurement methods and measurement results obtained on laboratory produced slabs are shown in Chapter 4 and Chapter 5 respectively. Data on mixture compositions and surface characteristics were collected, but obviously no measurements on tyre - road noise could be collected. Thus the data from the laboratory tests can only be used in developing models of Type 2(a) as shown in Figure 7-1. For samples from Kloosterzande sections, though laboratory measurements were taken in this study, only the data from the database are used for modeling. This is because all these data (material properties, surface characteristics and noise levels) from the database were collected in the same time period.

3) Another database is supplied by DVS, which contains the measurement results from thin layer surfacing sections on highway A6 in the Netherlands. Those sections were built by different contractors in 2006 as part of the Dutch Noise Innovation Programme on noise mitigation (IPG, in Dutch: Innovatieprogramma Geluid) [11]. There are records on mixture

compositions, surface texture, sound absorption and the tyre - road noise of four sections. Data from these four sections are used in the validation of the models.

Table 7-2 summarizes how the data from the three sources are used.

Table 7-2 Data sources and the applications

Source	Data included	Use in this study
Database of Kloosterzande sections	Mixture compositions; Surface characteristics; Tyre - road noise.	All the modeling
Laboratory measurements on slabs	Mixture compositions; Surface characteristics.	Modeling Type 2(a)
Thin layer surfacings on highway A6	Mixture compositions; Surface characteristics; Tyre - road noise.	Validations

7.2.3 Initial variable selection

It is known that there are different indices to express the mixture composition, surface properties and tyre - road noise respectively. Figure 7-2 shows the specific indicators for the three groups based on the current data base. In the figure, six parameters are given to describe the mixture compositions. It should be noted that thickness is not a material property in a strict sense. The thickness mainly influences the positions of the peak sound absorption on frequency bands, and does not directly influence the level of tyre - road noise. Hence, layer thickness is considered as an indirect parameter and belongs to the same group as the material properties.

According to Table 7-1, tyre - road noise is considered as output of the model. The overall noise level and noise levels in the frequency range from 315 Hz up to 3150 Hz are all taken into account. The basic selection criteria for taking a specific parameter into account in this study were: the parameters are representative, related to the design of surface layer mixtures and can easily be tested or evaluated in practice. This will facilitate the application of the model in practice in the future.

The six parameters denoting the mixture compositions in Figure 7-2 are all initially selected as input variables. Further variable selections are performed in the modeling process. For surface characteristics, the two most important factors, namely surface texture and sound absorption coefficient are taken into account. In previous chapters, it is mentioned that the surface texture can be denoted by MPD or texture level with various wavelengths. The sound absorption can be expressed by either the maximum absorption coefficient or absorption coefficients at frequency bands. Thus there are different combinations of indicators for surface texture and sound absorption available for model development. In this study, three combinations of surface characteristics are adopted: 1) MPD and maximum absorption coefficient; 2) selected surface

texture levels and sound absorptions on the frequency band; 3) selected surface texture levels and maximum absorption coefficients. The variables from the initial selection are given in Table 7-3. It should be noted that the "noise levels" in this chapter refer to the noise levels from the CPX tests with passenger car tyres. Further selections of the input variables for different types of models will be explained in detail in Section 7.3.

Table 7-3 Initial selection of the input and output variables

Mixture composition	Unit	Surface characteristic combination		Unit	Noise level	Unit
Maximum aggregate size;	mm	Combination 1	MPD;	mm	Overall level (from CPX test with passenger tyre);	dB(A)
Coarse aggregate content;	% by mass		Maximum Absorption coefficient.	-		
Fine aggregate content;	% by mass	Combination 2	Selected texture levels with various wavelengths;	dB, ref 10^{-6} mm		
Air voids content;	% by volume		Absorption level on 1/3 octave band of frequency.	-	Noise levels on 1/3 octave band of frequency (from CPX test with passenger tyre).	
Binder content;	% by mass ratio with the mineral aggregate	Combination 3	Selected texture levels with various wavelengths;	dB, ref 10^{-6} mm		
Thickness.	mm		Maximum Absorption coefficient.	-		

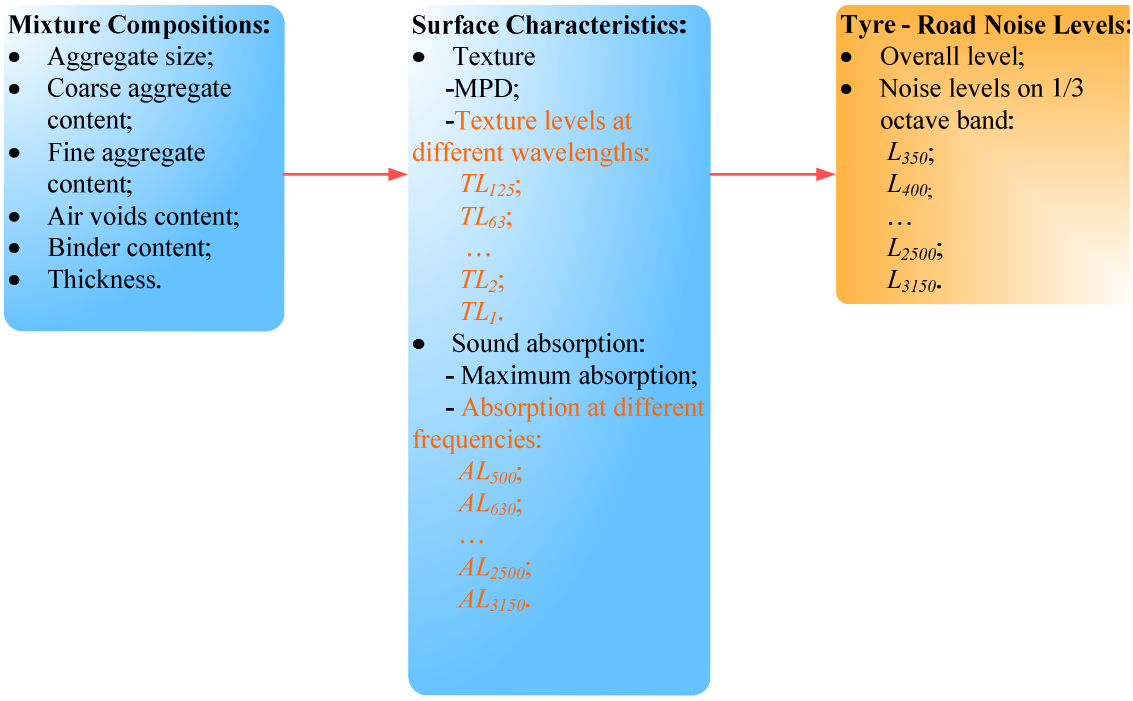

Figure 7-2 Expressions for material properties, surface characteristics and tyre - road noise levels

7.2.4 Regression methods

Overall noise levels and noise levels at each frequency band are modelled. The target model is a set of linear regression equations. Certain equations are developed corresponding to the overall noise level and the noise level at each

frequency band (350 Hz to 3150 Hz on 1/3 octave band). As there is more than one independent variable in the regression, multivariate linear equations are constructed. Multivariate regression estimates an equation with the form:

$$\mathbf{y} = a + \mathbf{X}\boldsymbol{b} \tag{7-1}$$

Where **y** is the vector of response variable; it presents a certain noise level or, in case of model Type 2(a), a certain surface characteristic. $\boldsymbol{X}$ is an $n \times p$ matrix, containing n observations of p predictor variables, which can be mixture composition, surface characteristics, or a combination of the two when different types of models are concerned. a is the constant, $\boldsymbol{b}$ is the vector of regression coefficients for the predictor variables. a and $\boldsymbol{b}$ are to be determined via the regression process.

The ordinary least squares approach is used to develop the linear regression models for each type of model with different variable input combinations. In addition, alternative models are also set up by means of variable selection methods. This aims to reduce the dimension of the independent variable vector and to simplify the structure of the model. The algorithms used in this study are backward elimination and the stepwise selection [12]. An introduction to both methods is given below:

(1) Backward elimination

The backward selection starts with the equation in which all variables are included. Based on a certain comparison criterion, the least useful variable (if any) is eliminated. The regression is then performed with the remaining variables and the selection is repeated until all the remaining explanatory variables satisfy the criterion stated hereafter. In this study, the elimination of variables is done according to the maximum probability of *F*-to-remove (POUT) [13]. At each step, the *F* value for a certain input variable is calculated from the *F*-test based on the hypothesis that the regression coefficient for this variable is 0, i.e. $b_i = 0$. The largest probability of the *F* value from all the variables is compared with the POUT. If the value is larger than POUT, it means the variable has indifferent influence on the response variable, and the variable is removed. The regression stops when no more variables are eligible for removal. In the study, the POUT is set as 0.1.

(2) Stepwise selection

The stepwise selection starts with no variable in the equation. The variables are selected into the equation one by one. At each time when a new variable enters the equation, the backward elimination is performed to check if there is one variable that should be deleted. If so, such a variable is removed. The procedure is a repetition of entering and backward eliminating of the input variables. The final regression equation is obtained when no variable is entered or removed. Probability of *F*-to-enter (PIN) is used to determine whether one variable should

be entered or not. The value of PIN is taken as 0.05. The elimination criterion is based on the POUT as mentioned above, and it is set as 0.1.

It should be noticed that multicollinearity may exist between the input parameters. As the input variables are not completely independent, the regression coefficients achieved in the model do not reflect the influence of a certain input parameter on the noise levels. However, the multicollinearity does not influence the prediction ability of the model as a whole [14]. In this chapter, the goal is to find the model with the best prediction accuracy. Therefore, the multicollinearity is not examined or eliminated on purpose. This implies that the models might not allow to determine the effect of changing the value of one parameter. From the previous chapter it is also known that the principal component regression (PCR) or partial least square regression (PLS) distributes the weights to the input variables based on the importance, but does not eliminate the variables. The study in this chapter prefers a model with a small amount of input variables. Therefore, the PCR and PLS methods are not used.

7.2.5 Surface groups

In the Kloosterzande trial sections database, there are various types of road surfaces. The surface types and the number of sections for each type of surface are shown in Figure 7-3. From Figure 7-3 and Chapter 6, it is clear that there are 18 thin layer surfacing sections based on 9 different designs. The research aims to find a prediction model of tyre - road noise for thin layer surfacings. The regression starts by using all the measured data from the 18 thin layer surfacing sections. In some regressions, there is a large number of input variables. In these cases, a large amount of observations are preferred. A bigger data set is constituted by adding data from other types of surfaces to the dataset of thin layer surfacings. As shown in Figure 7-3, the two data sets used in this study are: 1) data set of thin layer surfacings, including measurements from 18 thin layer surfacing sections; 2) dataset of all the surfaces, including both the single layer and two-layer porous asphalt surfaces as well as dense asphalt and SMA surfaces, this made the total number of sections 58. In this chapter, models are to be constructed separately by using the two data sets.

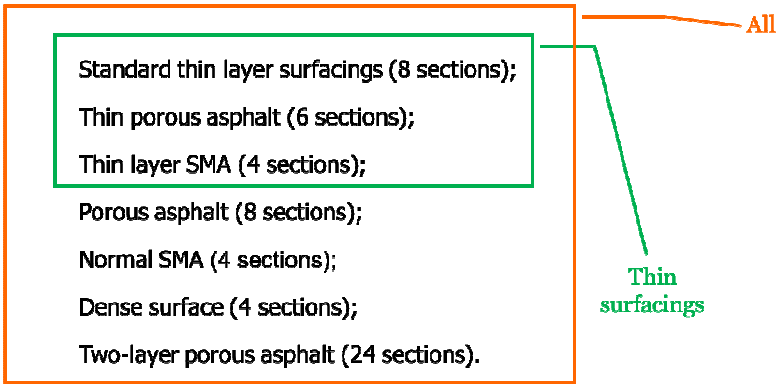

Figure 7-3 Road surface layer groups in the database of the Klooserzande sections

7.2.6 Other considerations

It has been shown in Chapter 6 that the influence of the driving speed of the vehicle on the noise levels is independent from the surface characteristics. The noise levels at different speeds can be deduced from the noise at a reference speed. In this research, the speed is not considered as an independent variable in the model. The noise levels used in the regression are all collected at a speed of 80 km/h.

Passenger car tyres are taken into account for the modeling. Information of the tyres is given in Table 6-2. In the modeling process, the author actually developed models for each type of tyre. The study in Chapter 6 showed that the average of the CPX noise levels from the 10 passenger cars can represent the near field tyre - road noise levels. In the traffic stream, there are different types of tyres. Hence using the average noise level is applicable for reflecting the general influence of various types of tyres. The averaged noise levels from the 10 passenger cars are used in the modeling. In other words, models developed in this study evaluate the average noise level at the standard CPX test positions [15].

Based on the discussions above, all the considerations for model development are summarized in Table 7-4. A complete overvies of the modeling process is given in Figure 7-4. By taking into account all the conditions, a total of 28 models were constructed. Each of these models is given a number which is shown in Figure 7-4. An initial selection is then performed on the 28 models to choose those with the best fit to the measured data. The selected models are validated using measurement data. The final models were determined based on the results of the validation.

Table 7-4 Considerations of the model development

Item	Material properties	Combination of surface characteristics	Tyre - road noise	Tyre type	Speed	Surface group	Model type	Regression method
Details	6 parameters as show in Table 7-3	1. MPD and maximum absorption coefficient; 2. Texture level and absorption coefficient on 1/3 octave band; 3. Texture level and maximum absorption coefficient.	Average of CPX noise levels from 10 passenger car tyres	Passenger car tyre	80 km/h	1. Thin layer surfacing; 2. All the asphalt surfaces.	3 types as shown in Figure 7-1	1. Ordinary least square; 2. Regression with variable selection.

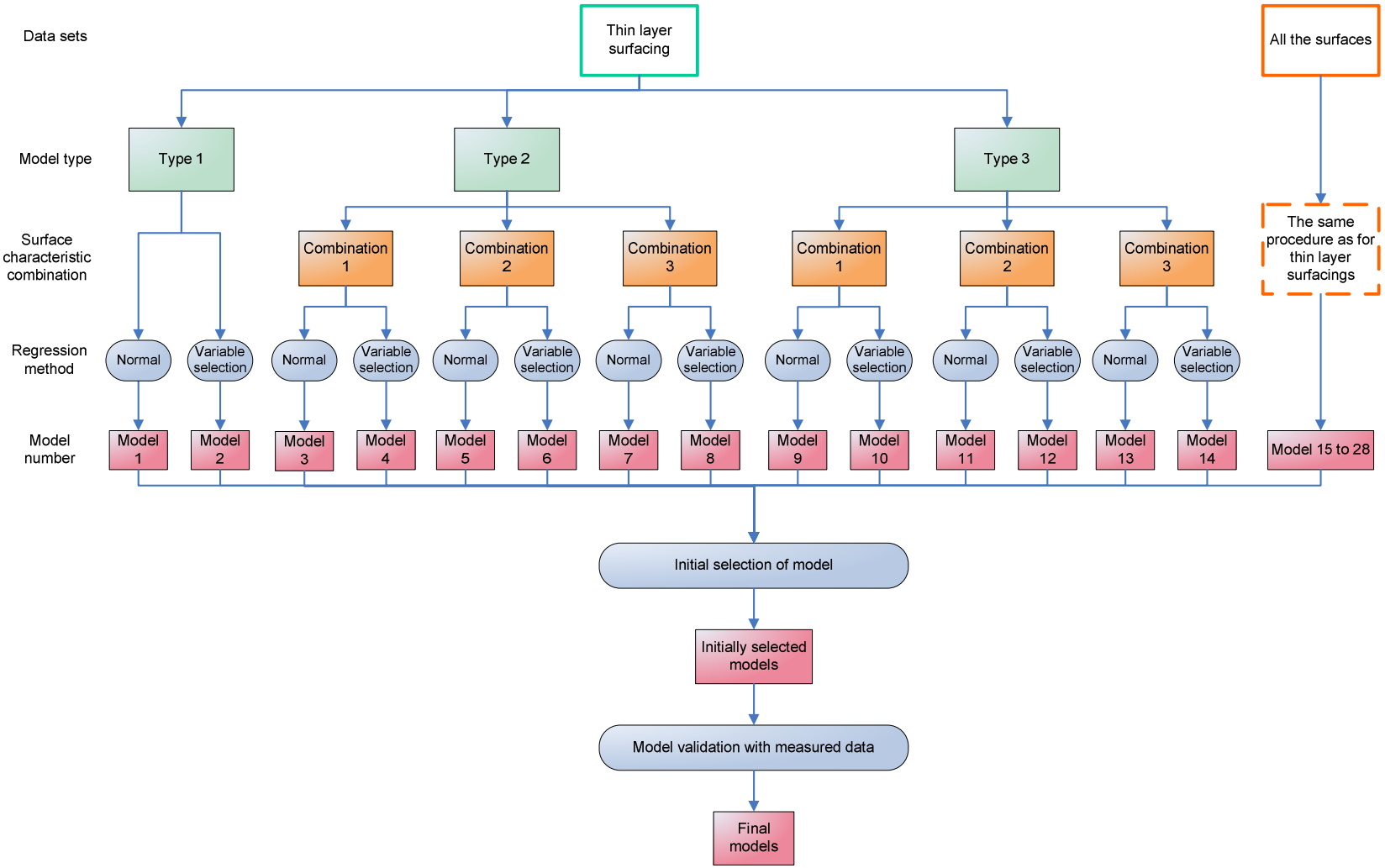

Figure 7-4 Complete model development process

7.3 Model Development

In this part the models, which are developed in different ways, are introduced. As there are 28 models in total, only the regression results of some of the models are shown as examples. For the specific expressions of all the models, the readers are referred to the CD attached to this thesis. In the end, candidate models are selected by investigating the quality of data fitting of the models. These candidates are then validated by means of field data.

7.3.1 Modeling using least square method

The regression results obtained with the standard least square method are shown in this sub-section. The modeling is based on the thin layer surfacing data set with surface characteristic combination 1 (see Table 7-3). It means that the three models given in Figure 7-5 were developed.

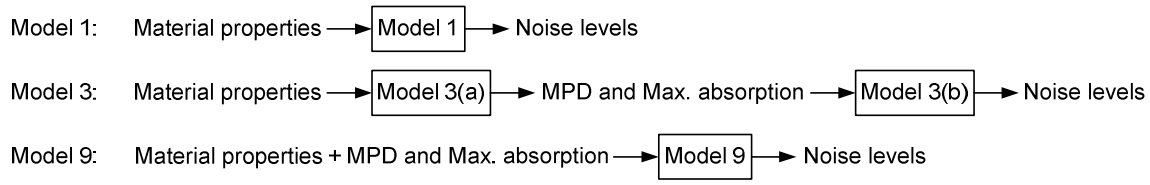

Figure 7-5 Examples of the noise models developed with least square regression method

The detailed results of the regression coefficients are given in Table 7-5 to Table 7-8. Table 7-5 shows a complete overview of the regression results. For each model, the regression results are stored in this form in excel files. It gives the regression coefficients for each input variable at different noise levels. In addition to R^2, there are also various statistics for indicating the fit of the model. Definitions of the statistics are as follows:

Adjusted R^2: It is a modification of R^2 that adjusts for the number of explanatory variables in a model. When more input variables are added to the regression model, the unadjusted R^2 generally increases. This even happens when the additional variables do little to explain the output variable. The adjusted R^2 helps to compensate this problem, as it is not sensitive to the number of the input variables. The adjusted R^2 increases only if the new term improves the prediction effect of the model. The adjusted R^2 is always less than or equal to that of $R^{2.}$

MSE: The mean squared error. This statistic quantifies the difference between the values estimated by means of the regression equation and the true value of the quantity being estimated. MSE is calculated by the equation:

$$\mathrm{MSE} = \frac{\sum_{i=1}^{n} (\hat{Y}_i - Y_i)^2}{n} \tag{7-2}$$

Where $\hat{Y}_i$ is the estimated value and Y_i is the true value, n is the number of observations. The smaller the MSE is, the closer the estimator is to the true value. As shown in Table 7-5, the MSE achieved on noise levels at 1250 Hz, 1600 Hz and 2000 Hz are larger compared to noise levels at other frequencies. This means the deviations of the predicted values from the actual data are greater at these three frequencies.

P value for the full model: This is the probability that the regression equation does not explain the variation in *y*, i.e. that any fit is purely by chance. This is based on the *F* probability distribution. An ANOVA analysis of the data is performed in order to determine whether the association between the variables is statistically significant. This is determined by the result of the *F*-test ("*F*"), and is indicated by "Significance *F*", the associated *P* value for the *F* test. The value of "Significance *F*" displayed depends on the results of the regression analysis and the confidence level chosen in the regression analysis dialog box. For a confidence level of 95%, if "Significance *F*" is <0.05, the null hypothesis is rejected (there is a statistically significant association between *X* and *y*). Conversely, if "Significance *F*" is >0.05, the null hypothesis is accepted (there is no statistically significant association between *X* and *y*). In Table 7-5, all *P* values are equal to 0.00, which denotes good explanations of the noise levels by the linear combinations of the material properties.

In this section, the fit of the regression models is mainly based on observing the R^2 and adjusted R^2. The MSE and *P* value are used as the optional measures. They are not decisive for the model selection in this section. In the following sub-sections, only the R^2 and adjusted R^2 are given in the tables showing the results of the regression analyses.

Some of the regression equations from Model 1 are listed below as examples, the acceptable ranges for input values for thin layer surfacing are also given:

$$L_{A,eq} = 56.77 + 0.60MS + 0.51CA + 0.35FA - 0.09BC - 0.13\Omega - 0.34h, \quad R^2 = 0.93 \tag{7-3}$$

$$L_{1000} = 28.09 + 1.28MS + 0.65CA + 0.45FA + 0.53BC - 0.07\Omega - 0.36h, \quad R^2 = 0.95 \tag{7-4}$$

where

$L_{A,eq}$ – the overall noise level, dB (A);
L_{1000} – noise level at 1000 Hz, dB (A);
MS – maximum aggregate size, mm, for thin layer surfacing, 4 mm≤*MS*≤8mm;
CA – coarse aggregate content, % by mass, in this study, 50.8%≤*CA*<91.5%;
FA – fine aggregate content, % by mass, in this study, 2.8%≤*FA*<49.2%;
BC – binder content, % by mass ratio with the aggregates, in this study, the input value of *BC* is between 5.4% and 7.8%;
Ω – air voids content, % by volume, for thin layer surfacing, 4%≤Ω<25%;

h – thickness of surface layer, mm, for thin layer surfacing, 20mm≤h≤30mm .

Table 7-5 shows the detailed results of the regression analysis for Model 1. The table, shows that a good linear relationship is obtained between the noise levels and the mixture compositions, as all the R^2 achieved are higher than 0.8 (adjusted R^2 higher than 0.7). This indicates that the noise levels can be reasonably predicted directly from the six mixture properties with a good accuracy.

Table 7-5 Regression results for Model 1

	$L_{A,eq}$	L_{315}	L_{400}	L_{500}	L_{630}	L_{800}	L_{1000}	L_{1250}	L_{1600}	L_{2000}	L_{2500}	L_{3150}
Constant	56.77	40.14	34.34	37.57	63.21	60.55	28.09	7.34	-2.51	25.23	92.87	104.87
Max. Aggregate size	0.60	0.98	1.21	1.19	0.53	0.47	1.28	1.62	1.96	1.89	0.00	-0.74
Coarse aggregate content	0.51	0.19	0.31	0.36	0.23	0.37	0.65	0.89	0.95	0.48	-0.09	-0.08
Fine aggregate content	0.35	0.19	0.28	0.31	0.17	0.25	0.45	0.63	0.73	0.45	-0.04	-0.09
Binder content	-0.09	1.21	1.00	0.51	-0.20	-0.13	0.53	1.07	2.05	2.23	-1.13	-2.34
Air voids content	-0.13	0.09	0.07	0.06	0.07	-0.03	-0.07	-0.14	-0.23	-0.25	-0.45	-0.51
Thickness	-0.34	-0.07	-0.15	-0.14	-0.08	-0.26	-0.36	-0.64	-0.91	-0.58	0.26	0.27
R^2	0.93	0.83	0.95	0.95	0.94	0.95	0.95	0.91	0.86	0.90	0.94	0.96
Adjusted R^2	0.89	0.74	0.92	0.92	0.91	0.93	0.92	0.85	0.78	0.84	0.91	0.94
MSE	0.30	0.23	0.14	0.28	0.30	0.17	0.58	1.21	2.05	1.83	0.94	0.45
P value for the full model	0.00	0.00	0.00	0.00	0.00	0.00	0.00	0.00	0.00	0.00	0.00	0.00

In developing the models of Type 2(a), thickness is considered to have no direct relation with the parameters in the three surface characteristic combinations. Thickness is thus not used as input variable for model Type 2(a), and only the other five material properties are included. Table 7-6 gives the regression results for Model 3(a), which computes the MPD and maximum absorption from the material properties. Linear relationships with a high R^2 are found between the surface characteristics and the material properties. It indicates that the MPD and maximum absorption can be predicted from the five material properties with a high accuracy. According to Table 7-7, Model 3(b) works well for predicting the overall noise level and noise level at most of the frequencies based on MPD and maximum absorption. The only exception is the model for the noise level at 1600 Hz.

Table 7-6 Regression results for Model 3(a)

	MPD	Max. Absorption
Constant	-4.72	-0.15
Max. Aggregate size	0.17	-0.01
Coarse aggregate content	0.04	0.01
Fine aggregate content	0.03	0.00
Binder content	0.08	-0.03
Air voids content	0.01	0.02
R^2	0.94	0.86
Adjusted R^2	0.93	0.83

Table 7-7 Regression results for Model 3(b)

	$L_{A,eq}$	L_{315}	L_{400}	L_{500}	L_{630}	L_{800}	L_{1000}	L_{1250}	L_{1600}	L_{2000}	L_{2500}	L_{3150}
Constant	90.08	69.89	70.77	74.07	80.01	84.08	79.96	78.08	78.88	79.86	80.29	78.62
MPD	6.32	2.65	4.70	6.06	4.22	5.01	9.47	10.85	9.92	6.36	3.11	2.44
Max. Absorption	-4.56	-0.59	-2.18	-1.59	1.46	-1.23	-4.93	-8.44	-14.97	-18.26	-15.26	-12.02
R^2	0.78	0.76	0.90	0.94	0.96	0.92	0.87	0.75	0.59	0.80	0.82	0.71
Adjusted R^2	0.75	0.72	0.89	0.93	0.96	0.91	0.86	0.72	0.53	0.77	0.80	0.67

As seen in Table 7-8, Model 9 has the best prediction of all three models shown in Figure 7-5. When the combination of the six mixture compositions and the two surface characteristics are used as predictors, the R^2 is above 0.88 for all noise levels. By comparing the results shown in Table 7-8 with the results in Table **7-5**, the increase of R^2 is limited when MPD and maximum absorption coefficient are added. This is because the effects of MPD and maximum absorption coefficient are already expressed by the material properties to a great extent as shown in Table 7-6.

Table 7-8 Regression results for Model 9

	$L_{A,eq}$	L_{315}	L_{400}	L_{500}	L_{630}	L_{800}	L_{1000}	L_{1250}	L_{1600}	L_{2000}	L_{2500}	L_{3150}
Constant	59.96	47.38	46.91	59.13	84.55	68.70	35.13	7.64	-11.99	14.72	90.63	100.99
Max Aggregate size	0.40	0.87	0.81	0.50	-0.10	0.13	0.93	1.47	1.92	1.65	-0.31	-0.74
Coarse aggregate content	0.52	0.02	0.11	0.02	-0.14	0.29	0.61	0.96	1.29	0.96	0.15	0.05
Fine aggregate content	0.34	0.08	0.14	0.08	-0.07	0.18	0.40	0.66	0.91	0.69	0.06	-0.02
Binder content	-0.36	1.67	1.19	0.83	0.27	-0.26	0.25	0.63	0.86	0.29	-2.36	-2.77
Air voids content	-0.12	0.06	0.04	0.02	0.02	-0.03	-0.07	-0.12	-0.16	-0.14	-0.39	-0.48
Thickness	-0.35	0.04	-0.02	0.08	0.15	-0.21	-0.33	-0.69	-1.12	-0.88	0.11	0.19
MPD	0.46	2.56	3.59	6.13	6.30	1.96	1.46	-0.54	-4.20	-5.52	-2.33	-1.64
Max. Absorption	-1.77	2.12	0.20	0.24	1.17	-1.35	-2.12	-2.53	-6.16	-10.34	-6.84	-2.19
R^2	0.94	0.88	0.97	0.98	0.98	0.96	0.95	0.91	0.88	0.94	0.96	0.97
Adjusted R^2	0.88	0.77	0.95	0.97	0.97	0.93	0.90	0.83	0.77	0.89	0.93	0.93

7.3.2 Modeling with variable selection

In this sub-section, an example of the regression analysis by means of variable selection is given. It aims to set up Model 2 shown in Figure 7-6. The model relates the noise levels directly to the selected material properties. The selections are performed by using backward elimination and stepwise selection respectively. For certain noise levels, the regression equation with the better fit based on the two methods is held for further consideration.

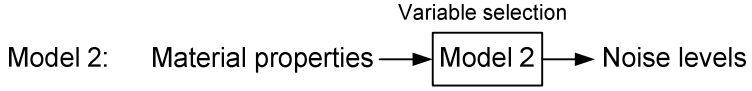

Figure 7-6 Example for modeling with variable selection method

The regression results by the backward and stepwise selection are given in Table 7-9 and Table 7-10 respectively. It can be seen that the two selection

procedures lead to different models except in the cases for L_{2500} and L_{3150}, in which identical variables are selected. In Table 7-9, the maximum aggregate size, the content of coarse and fine aggregate are selected in the models for overall noise level and noise below 2000 Hz. The binder content is not included in any model from the backward elimination. The air voids content is kept for predicting the overall noise level and noise at frequencies ≥ 2000 Hz. According to Table 7-10, a smaller number of variables are retained by the stepwise selection for most of the models compared to backward elimination. In comparison with the models from backward elimination, the binder is selected as a predictor for most of the models, but the coarse and fine aggregate content are excluded in all cases.

From the regression results with the two variable selection methods, it is learned that the noise levels can be evaluated by combinations of different selected material properties. However, when considering the fit of the models, the models from the backward elimination are appreciated, as the R^2 of the models are generally higher than or equal to those from the stepwise selection. This can be seen by comparing Table 7-9 and Table 7-10. In this case, the models shown in Table 7-9 are considered as the final selection of Model 2.

Table 7-9 Regression results for Model 2 with backward elimination

	$L_{A,eq}$	L_{315}	L_{400}	L_{500}	L_{630}	L_{800}	L_{1000}	L_{1250}	L_{1600}	L_{2000}	L_{2500}	L_{3150}
Constant	55.43	56.07	47.54	43.37	61.44	60.86	36.25	23.78	29.17	79.91	76.35	73.14
Max. Aggregate size	0.64	0.44	0.80	0.88	0.60	0.58	1.10	1.24	1.22	0.63	-	-
Coarse aggregate content	0.52	0.14	0.28	0.33	0.20	0.35	0.62	0.82	0.83	-	-	-
Fine aggregate content	0.35	0.12	0.24	0.27	0.15	0.23	0.42	0.57	0.61	-	-	-
Binder content	-	-	-	-	-	-	-	-	-	-	-	-
Air voids content	-0.12	-	-	-	0.08	-	-0.10	-0.19	-0.34	-0.37	-0.43	-0.38
Thickness	-0.34	-	-0.15	-	-	-0.26	-0.36	-0.64	-0.91	-	0.30	0.35
R^2	0.93	0.76	0.93	0.93	0.94	0.95	0.94	0.90	0.85	0.80	0.93	0.94
Adjusted R^2	0.90	0.71	0.91	0.91	0.92	0.94	0.92	0.86	0.78	0.77	0.92	0.94

Table 7-10 Regression results for Model 2 with stepwise selection

	$L_{A,eq}$	L_{315}	L_{400}	L_{500}	L_{630}	L_{800}	L_{1000}	L_{1250}	L_{1600}	L_{2000}	L_{2500}	L_{3150}
Constant	87.05	78.53	77.98	87.92	98.99	92.56	85.63	72.68	75.96	97.75	76.35	73.14
Max. Aggregate size	1.02	-	0.39	0.38	-	0.48	1.24	1.74	1.37	-	-	-
Coarse aggregate content	-	-	-	-	-	-	-	-	-	-	-	-
Fine aggregate content	-	-	-	-	-	-	-	-	-	-	-	-
Binder content	-	-0.98	-0.99	-1.76	-2.22	-1.17	-1.14	-	-	-1.80	-	-
Air voids content	-	-	-	-	-	-	-	-	-0.22	-0.48	-0.43	-0.38
Thickness	-	-	-	-	-	-	-	-	-	-	0.30	0.35
R^2	0.69	0.65	0.80	0.87	0.90	0.83	0.82	0.69	0.60	0.80	0.93	0.94
Adjusted R^2	0.67	0.63	0.78	0.85	0.89	0.81	0.80	0.67	0.55	0.78	0.92	0.94

7.3.3 Modeling with surface characteristic combination 2 and 3

In addition to MPD and the maximum absorption coefficient, there are two surface characteristic combinations containing texture level on the spectrum

band of wavelength and the absorption coefficient on the frequency band. In Table 7-3 they are respectively named combination 2 and combination 3. The texture levels are included in both the combinations. In terms of sound absorption, a selected absorption coefficient on a certain frequency is taken into account in combination 2, while the maximum absorption coefficient is used in combination 3. In Chapter 6, it was shown that the generation of tyre - road noise levels is attributed to surface characteristics in three groups:
1) texture level at long wavelengths (≥8 mm);
2) texture level at short wavelength (≤4 mm);
3) sound absorption coefficients.

According to the results of the principal component regression analysis given in Table 6-13, the noise levels can be expressed by a linear combination of energetic averaged texture levels with a wavelength from 1 mm to 250 mm and sound absorption coefficients from 1000 Hz to 3150 Hz. It is possible to use the PCA regression equation for predicting noise levels, but it contains 15 explanatory variables, which makes the model redundant for engineering applications. According to Chapter 6 (as shown in Table 6-8), there are high inter-correlations between each texture level, and the sound absorption at neighbouring frequencies are also significantly correlated. Therefore, it is reasonable to choose one representative parameter from each group to denote the long wavelength texture level, short wavelength texture level and sound absorption respectively. This can be considered as a pre-selection of variables.

The selection of the surface characteristic parameter is based on Table 6-13. In each of the three surface characteristic groups, the parameter which has the largest standardized regression coefficient from those shown to have an important influence on the noise level (with standardized coefficients higher than 0.1) is chosen. The following representative parameters are selected:

1) Texture level at long wavelength (≥8 mm): for the overall noise level and noise at frequencies ≤ 2000 Hz, the regression coefficients of texture level from 16 mm to 250 mm are quite similar. According to the previous study [16], the texture level at 63 mm is generally used as predictor of noise at low frequencies (below 1000 Hz). Therefore the averaged texture level at 63 mm is also selected to present the texture level at long wavelength in this study.
2) Texture level at short wavelength (≤4 mm): the short wavelength texture level mainly influences the noise at high frequencies (≥ 1600 Hz). So the parameter is only selected for modeling the noise level at frequencies ≥ 1600 Hz. The texture level at 1 mm has the highest regression coefficient for noise level between 1600 Hz and 3150 Hz, and is therefore selected in the modeling.
3) Sound absorption coefficients: for thin layer surfacings, the sound absorption reduces the noise level above 800 Hz. Absorption coefficients at different frequencies are included in the modeling

corresponding to various noise levels. For the overall noise level, the sound absorption at 1000 Hz is taken as predictor. An overview of the input variable selection for combination 2 is shown in Table 7-11.

Table 7-11 Selected variables for surface characteristic combination 2

	$L_{A,eq}$	L_{315}	L_{400}	L_{500}	L_{630}	L_{800}	L_{1000}	L_{1250}	L_{1600}	L_{2000}	L_{2500}	L_{3150}
Long wavelength texture level	TL_{63}	TL_{63}	TL_{63}	TL_{63}	TL_{63}	TL_{63}	TL_{63}	TL_{63}	TL_{63}	TL_{63}	-	-
Short wavelength texture level	-	-	-	-	-	-	-	-	TL_1	TL_1	TL_1	TL_1
Sound absorption coefficient	AL_{1000}	-	-	-	-	AL_{1000}	AL_{1000}	AL_{1000}	AL_{1250}	AL_{1600}	AL_{2500}	AL_{2500}

As to the surface characteristic combination 3, the maximum absorption coefficient is used instead of all the sound absorption coefficients shown in Table 7-11. The selected variables for combination 3 are shown in Table 7-12. The selected variables for surface characteristic combination 2 and 3 will also be used in the modeling with all types of surfaces as described in Section 7.3.4. All the selections were made based on the thin layer surfacings. The choices could be different when other types of surfaces are included. The influence on other types of surfaces needs to be determined in future work.

Table 7-12 Selected variables for surface characteristic combination 3

	$L_{A,eq}$	L_{315}	L_{400}	L_{500}	L_{630}	L_{800}	L_{1000}	L_{1250}	L_{1600}	L_{2000}	L_{2500}	L_{3150}
Long wavelength texture level	TL_{63}	TL_{63}	TL_{63}	TL_{63}	TL_{63}	TL_{63}	TL_{63}	TL_{63}	TL_{63}	TL_{63}	-	-
Short wavelength texture level	-	-	-	-	-	-	-	-	TL_1	TL_1	TL_1	TL_1
Sound absorption coefficient	AL_{max}	-	-	-	-	AL_{max}	AL_{max}	AL_{max}	AL_{max}	AL_{max}	AL_{max}	AL_{max}

In this sub-section, the models are developed by using the representative variables of texture level and absorption coefficients which are given in Table 7-11 and Table 7-12. The regression results of Model 6 and Model 8 are shown as examples of modeling by using surface characteristic combination 2 and 3 respectively as input. The models are illustrated in Figure 7-7.

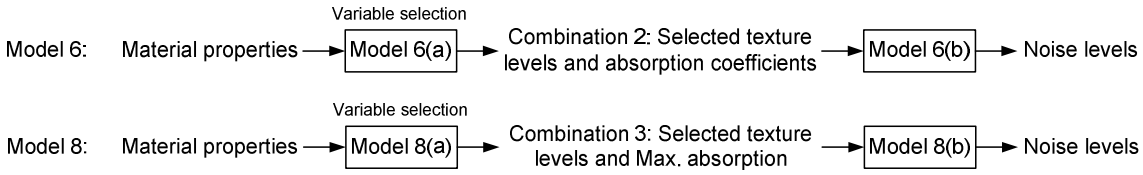

Figure 7-7 Modeling with surface characteristic combination 2 and 3

Table 7-13 gives the regression coefficients for Model 6(a) which relates the representative surface characteristics of combination 2 with the basic material properties. The results are from the variable selection methods. In the last row, the variable selection methods from which the regression coefficients are achieved are shown. According to the results shown in the table, the texture level TL_{63} and TL_1 can be estimated from the maximum aggregate size and the air voids content with a high R^2 value. However, in terms of sound absorption coefficients, good regression results are not found for all the cases. R^2 for the equations of AL_{1000} and AL_{1250} are very low, which means poor linear

relationships. It also indicates that the absorption coefficients at 1000 Hz and 1250 Hz cannot be well evaluated by the linear combination of the five material properties. As a result, Model 6(a) is rejected because of the low fit.

Table 7-13 Regression results for Model 6(a)

	TL_{63}	TL_1	AL_{1000}	AL_{1250}	AL_{1600}	AL_{2500}
Constant	19.39	33.14	0.05	0.02	-0.31	1.28
Max. Aggregate size	2.85	0.29	-	-	-	-0.02
Coarse aggregate content	-	-	-	-	-	-
Fine aggregate content	-	-	-	-	-	-
Binder content	-	-	-	-	-	-0.13
Air voids content	0.19	0.18	0.01	0.01	0.01	-
R^2	0.95	0.88	0.26	0.41	0.51	0.52
Adjusted R^2	0.94	0.86	0.25	0.40	0.49	0.50
Selection method	S*	B**&S	B&S	B&S	B	B

*Stepwise selection;
**Backward elimination.

Regression results of Model 6(b) are summarized in Table 7-14. Good linear regression equations are found for nearly all the noise levels. For the overall level and noise at frequencies above 500 Hz, the R^2 values are higher than 0.9. This means the noise levels can be well described by the selected surface characteristic parameters. Furthermore, the number of input variables in each sub-model is not more than 3. According to Table 7-13, the sound absorption coefficients AL_{1000} and AL_{1250} cannot be evaluated from the material properties; Model 6 is not able to make predictions based on material properties. However sub-model Model 6(b) is suggested to be used independently to deduce the noise levels in cases when surface characteristics are measured from the existing road surface or the sound absorption coefficients are predicted by other methods, such as the physical model built in Section 5.4.3.

Table 7-14 Regression results for Model 6(b)

	$L_{A,eq}$	L_{315}	L_{400}	L_{500}	L_{630}	L_{800}	L_{1000}	L_{1250}	L_{1600}	L_{2000}	L_{2500}	L_{3150}
Constant	85.89	65.10	63.65	63.78	70.38	77.71	69.99	71.57	111.74	121.97	133.86	117.73
TL_{63}	0.23	0.17	0.25	0.36	0.33	0.27	0.44	0.38	0.58	0.40	-	-
TL_1	-	-	-	-	-	-	-	-	-1.37	-1.55	-1.47	-1.05
AL_{1000}	-12.45	-	-	-	-	-7.51	-14.60	-22.39	-	-	-	-
AL_{1250}	-	-	-	-	-	-	-	-	-10.66	-	-	-
AL_{1600}	-	-	-	-	-	-	-	-	-	-7.67	-	-
AL_{2500}	-	-	-	-	-	-	-	-	-	-	-4.74	-7.83
R^2	0.92	0.71	0.80	0.84	0.91	0.94	0.96	0.93	0.90	0.96	0.93	0.95
Adjusted R^2	0.88	0.65	0.76	0.81	0.89	0.90	0.94	0.89	0.84	0.93	0.90	0.92

Table 7-15 and Table 7-16 show the modeling results when the surface characteristic combination 3 is considered. The regression equations for TL_{63} and TL_1 are the same as those with combination 2 in Table 7-13. As shown in Table 7-15, the maximum absorption is linearly related with the coarse aggregate content and the air voids content; a high R^2 of 0.86 is obtained. In

Table 7-16, model 8(b) provides a good prediction of the noise levels with the three surface parameters in combination 3. Comparing Table 7-16 with Table 7-14 shows that only for the noise level at 1600 Hz, a lower R^2 is obtained by using the maximum absorption coefficient instead of AL_{1250}.

Table 7-15 Regression results for Model 8(a)

	TL_{63}	TL_1	Max. Absorption
Constant	19.39	33.14	-0.42
Max. Aggregate size	2.85	0.29	-
Coarse aggregate content	-	-	0.01
Fine aggregate content	-	-	-
Binder content	-	-	-
Air voids content	0.19	0.18	0.02
R^2	0.95	0.88	0.86
Adjusted R^2	0.94	0.86	0.85
Selection method	S	B&S	B&S

Table 7-16 Regression results for Model 8(b)

	$L_{A,eq}$	L_{315}	L_{400}	L_{500}	L_{630}	L_{800}	L_{1000}	L_{1250}	L_{1600}	L_{2000}	L_{2500}	L_{3150}
Constant	79.90	65.10	63.65	63.78	70.38	76.14	64.06	60.22	127.69	114.80	115.15	122.46
TL_{63}	0.35	0.17	0.25	0.36	0.33	0.28	0.55	0.62	0.67	0.45	-	-
TL_1	-	-	-	-	-	-	-	-	-1.95	-1.37	-0.94	-1.21
Max. absorption	-1.79	-	-	-	-	1.00	-1.00	-3.82	0.05	-8.09	-5.94	-1.82
R^2	0.90	0.71	0.80	0.84	0.91	0.92	0.93	0.87	0.76	0.88	0.93	0.90
Adjusted R^2	0.87	0.65	0.76	0.81	0.89	0.90	0.92	0.84	0.71	0.85	0.92	0.88

7.3.4 Modeling with data from all surfaces

As mentioned before, data from other road surfaces were also available and therefore an attempt was made to develop a model for tyre - road noise predictions using the data sets from all types of road surface. The development of Model 24 is taken as an example. The framework of the model is shown in Figure 7-8. The model generates noise levels from a combination of material properties, MPD and maximum absorption coefficient; the variable selection regression method was used. For two-layer porous asphalt, the material properties used for regression are from the top layer. The thickness taken into account is also that of the top layer. Mixture compositions and the thickness of the bottom layer of two-layer porous asphalt concrete are not considered in the regression analysis.

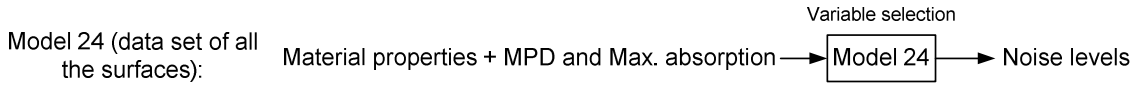

Figure 7-8 Example for modeling with data sets of all the surfaces

Models obtained from regression analyses with data of all the road surfaces are shown in Table 7-17. From the results shown in Table 7-17, it can be seen that the R^2 (or adjusted R^2) values are generally lower in comparison with those

from the models based on thin layer surfacings. However, the predictions are still good for the overall noise level and noise level at most of the frequencies. Only at frequencies between 1000 Hz and 1600 Hz, the R^2 is lower than 0.7.

Table 7-17 Regression results for Model 24 (with data set of all the surfaces)

	$L_{A,eq}$	L_{315}	L_{400}	L_{500}	L_{630}	L_{800}	L_{1000}	L_{1250}	L_{1600}	L_{2000}	L_{2500}	L_{3150}
Constant	92.25	64.17	68.79	72.15	81.47	82.43	82.70	74.93	79.83	83.14	82.18	80.05
Max Aggregate size	0.33	0.20	0.18	0.29	0.32	0.48	0.48	0.54	0.27	-	-	0.16
Coarse aggregate content	-	-	-	-	-	0.06	-	0.11	0.06	-	-	-
Fine aggregate content	-	0.04	0.05	0.06	-	-	-	-	-	-	-	-
Binder content	-	0.42	-	-	-	-	-	-	-	-	-	-
Air voids content	-0.06	-	-0.07	-	0.11	0.14	-	-0.14	-0.30	-0.34	-0.30	-0.29
Thickness	-0.07	-	-0.02	-0.07	-0.13	-0.11	-0.07	-0.03	-	0.02	-	-0.02
MPD	2.27	3.38	4.61	5.63	3.30	-	3.01	-	-	1.51	1.53	-
Max. Absorption	-	-	1.76	2.32	-	-4.22	-3.25	-	-	-2.49	-3.48	-
R^2	0.84	0.93	0.94	0.87	0.85	0.72	0.63	0.60	0.69	0.84	0.86	0.89
Adjusted R^2	0.83	0.92	0.93	0.86	0.83	0.69	0.60	0.57	0.67	0.83	0.85	0.88
Selection method	B&S	B	B	B	B	B	B	B	B	B	B	B&S

7.3.5 Model selection

In total 28 models have been developed and the question now is which of these models are to be preferred. It has been mentioned that the adjusted R^2 helps to check the goodness of fit of the multiple regression models without being influenced by the number of input variables. So an initial selection of the models was performed by investigating the adjusted R^2.

Models of Type 2 consist of two parts. Type 2(a) relates the surface characteristics to the material properties, and Type 2(b) generates the tyre - road noise from the surface characteristics. The models of Type 2(a) are firstly discussed. The adjusted R^2 values for various models are shown in Table 7-18. The surface group, meaning only thin layer or all surfaces, regression method and surface characteristic combination for each model are also listed. From the table, it can be seen that most of the regression models show a good fit except for those used for evaluating the sound absorption from 1000 to 2500 Hz. This reveals that the sound absorption on 1/3 octave band cannot be explained well by a linear combination of material properties. Therefore models 5(a), 6(a), 19(a) and 20(a) are excluded from the selection.

As to modeling with different regression methods, the adjusted R^2 from the least square regressions and the variable selection methods are similar. In some cases, the adjusted R^2 from variable selection regressions are even higher. It reveals that variables with less effect on the regression fit are eliminated from the model. After the selection, there are generally less input variables in an equation, and such an equation is more appropriate for being used in practice. Therefore only these models are considered for further testing in a next step. When considering the surface groups, models developed by using all types of

surfaces show a lower adjusted R^2. However, those adjusted R^2 values are still quite high in general (≥ 0.76). In this case, models for both surface groups are taken into account.

In summary, four sub-models are selected based on investigating the adjusted R^2 and considering the number of the input variables. In Table 7-18 they are Model 4(a), 8(a), 18(a) and 22(a). Because those models do not predict directly the noise levels, the final selection was made after models of Type (b) were evaluated.

Table 7-18 Adjusted R^2 for sub-models relating material properties to surface characteristics

Surface group	Model number	Regression method	Surface characteristic combination	MPD	TL_{63}	TL_1	Max. absorption	AL_{1000}	AL_{1250}	AL_{1600}	AL_{2500}
Thin layer surfacing	3(a)	Least square	1	0.93			0.83				
	4(a)	Variable selection	1	0.92			0.85				
	5(a)	Least square	2		0.95	0.85		0.24	0.04	0.64	0.61
	6(a)	Variable selection	2		0.94	0.86		0.00	0.24	0.68	0.62
	7(a)	Least square	3		0.95	0.85	0.83				
	8(a)	Variable selection	3		0.94	0.86	0.86				
All the surfaces	17(a)	Least square	1	0.85			0.84				
	18(a)	Variable selection	1	0.85			0.84				
	19(a)	Least square	2		0.86	0.77		0.29	0.47	0.51	0.55
	20(a)	Variable selection	2		0.86	0.75		0.25	0.43	0.49	0.50
	21(a)	Least square	3		0.86	0.77	0.84				
	22(a)	Variable selection	3		0.86	0.76	0.84				

The second round of model selection is accomplished by investigating the adjusted R^2 of the regression models which work for evaluating noise levels. The adjusted R^2 for all the models are shown in Table 7-19. The following comments are made:

For models developed by using data purely from thin layer surfacings, most equations have a high adjusted R^2 (higher than 0.7). This implies that nearly all the models are able to predict the noise levels by using different input variables. Considering the first round of model selection, both the (a) and (b) parts for model 4 and 8 show good regression results. Therefore, model 4 and 8 are selected for further testing. Models numbered 3, 5, 6 and 7 are left out. However, model 6(b) has a good fit with the data, and can be used independently to calculate the noise levels from known surface characteristic parameters. Moreover, models from the variable selection method generally possess similar adjusted R^2 as those from the least square regressions but with less input variables. Herein, models with selected variables are retained. In summary, the models selected for the thin surface group are model 2, 4, 6(b), 8, 10, 12 and 14.

When all types of surfaces are considered, high adjusted R^2 values are mainly found at frequencies below 630 Hz or above 1250 Hz for most of the models. For the overall noise level and noise levels between 630 Hz and 1250 Hz, the fit is generally poor. In comparison with models for the thin layer surfacing group, the adjusted R^2 for models for all surfaces generally smaller, except for predicting noise at 315 Hz and 400 Hz. From these observations, it is concluded that the noise levels are not well linearly related with the material properties or the selected indicators for surface characteristics at all the frequencies. This indicates that it is necessary to focus on a certain type of road surface when developing linear regression models. In this study, only two models with a relatively good R^2 for all frequencies are selected for validation; they are Model 16 and Model 24 (see Table 7-19). Others are not studied any more.

According to the model selection process in this section, nine models are chosen as candidates for application. They are to be validated by comparing predicted values with the measurement data from practical road surfaces. The selected models are numbered as 2, 4, 6(b), 8, 10, 12, 14, 16 and 24. The specific regression coefficients of the models can be found in Appendix C.

Table 7-19 Adjusted R^2 of models for calculating noise levels

Surface group	Model number	Regression method	Model Type	Surface characteristic combination	$L_{A,eq}$	L_{315}	L_{400}	L_{500}	L_{630}	L_{800}	L_{1000}	L_{1250}	L_{1600}	L_{2000}	L_{2500}	L_{3150}
Thin layer surfacing	1	Least square	1	-	0.89	0.74	0.92	0.92	0.91	0.93	0.92	0.85	0.78	0.84	0.91	0.94
	2	Variable selection		-	0.90	0.71	0.91	0.91	0.92	0.94	0.92	0.86	0.78	0.77	0.92	0.94
	3(b)	Least square	2	1	0.75	0.72	0.89	0.93	0.96	0.91	0.86	0.72	0.53	0.77	0.80	0.67
	4(b)	Variable selection		1	0.75	0.73	0.89	0.93	0.96	0.90	0.86	0.72	0.53	0.77	0.80	0.65
	5(b)	Least square		2	0.88	0.57	0.69	0.77	0.86	0.90	0.94	0.89	0.84	0.93	0.90	0.92
	6(b)	Least square		2	0.88	0.57	0.69	0.77	0.86	0.90	0.94	0.89	0.84	0.93	0.90	0.92
	7(b)	Least square		3	0.87	0.65	0.76	0.81	0.89	0.90	0.92	0.84	0.71	0.85	0.92	0.88
	8(b)	Least square		3	0.87	0.65	0.76	0.81	0.89	0.90	0.92	0.84	0.71	0.85	0.92	0.88
	9	Least square	3	1	0.88	0.77	0.95	0.97	0.97	0.93	0.90	0.83	0.77	0.89	0.93	0.93
	10	Variable selection		1	0.90	0.73	0.95	0.97	0.97	0.94	0.92	0.86	0.78	0.90	0.94	0.94
	11	Least square		2	0.97	0.59	0.90	0.93	0.93	0.96	0.97	0.96	0.91	0.93	0.97	0.98
	12	Variable selection		2	0.92	0.75	0.91	0.93	0.93	0.95	0.94	0.91	0.94	0.94	0.93	0.97
	13	Least square		3	0.95	0.72	0.92	0.91	0.90	0.96	0.95	0.90	0.83	0.89	0.94	0.96
	14	Variable selection		3	0.90	0.75	0.91	0.93	0.93	0.94	0.92	0.86	0.86	0.89	0.95	0.97
All the surfaces	15	Least square	1	-	0.45	0.74	0.73	0.55	0.06	0.15	0.39	0.54	0.70	0.82	0.83	0.87
	16	Variable selection		-	0.78	0.75	0.76	0.75	0.79	0.67	0.58	0.57	0.67	0.82	0.84	0.88
	17(b)	Least square	2	1	0.42	0.84	0.84	0.68	0.24	0.26	0.41	0.34	0.29	0.56	0.64	0.63
	18(b)	Least square		1	0.42	0.84	0.84	0.68	0.24	0.26	0.41	0.34	0.29	0.56	0.64	0.63
	19(b)	Least square		2	0.66	0.81	0.84	0.76	0.40	0.36	0.68	0.87	0.92	0.94	0.90	0.92
	20(b)	Least square		2	0.66	0.81	0.84	0.76	0.40	0.36	0.68	0.87	0.92	0.94	0.90	0.92
	21(b)	Least square		3	0.60	0.81	0.83	0.65	0.17	0.26	0.53	0.65	0.70	0.85	0.87	0.88
	22(b)	Least square		3	0.60	0.81	0.83	0.65	0.17	0.26	0.53	0.65	0.70	0.85	0.87	0.88
	23	Least square	3	1	0.58	0.93	0.93	0.72	0.20	0.25	0.50	0.58	0.70	0.86	0.87	0.89
	24	Variable selection		1	0.83	0.92	0.93	0.85	0.83	0.67	0.59	0.50	0.66	0.82	0.85	0.88
	25	Least square		2	0.66	0.91	0.92	0.84	0.45	0.33	0.69	0.87	0.91	0.95	0.91	0.94
	26	Variable selection		2	0.52	0.89	0.89	0.71	0.22	0.21	0.55	0.85	0.90	0.95	0.85	0.92
	27	Least square		3	0.60	0.93	0.93	0.71	0.13	0.23	0.53	0.65	0.74	0.88	0.90	0.92
	28	Variable selection		3	0.53	0.89	0.89	0.71	0.22	0.24	0.51	0.58	0.75	0.88	0.88	0.90

7.4 Validation of the Models

Validation of the model is performed by comparing the predicted noise levels with those measured on practical road sections. Table 7-20 summarizes all the candidate models which are to be validated together with the input variables.

Table 7-20 Input variable combinations and the corresponding models

Input variables	Models to be validated
Material properties	Model 2, Model 4, Model 8, Model 16
MPD, Max. absorption	Model 4(b)
TL_{63}, TL_1, AL_{1000}, AL_{1250}, AL_{1600}, AL_{2500}	Model 6(b)
TL_{63}, TL_1, Max. absorption	Model 8(b)
Material properties, MPD, Max. absorption	Model 10, Model 24
Material properties, TL_{63}, TL_1, AL_{1000}, AL_{1250}, AL_{1600}, AL_{2500}	Model 12
Material properties, TL_{63}, TL_1, Max. absorption	Model 14

7.4.1 Road surfaces for validation

As introduced in Section 7.2.2, the data used for validation are from four thin layer surfacing sections on highway A6. The sections were built in 2006 by different contractors. The basic material properties of the four surfaces are given in Table 7-21. These material properties are from the quality control reports made during production. In the validation, the thickness of all the surfaces is considered to be 30 mm.

Table 7-21 Material properties of road surfaces for validation

Section number	Aggregate type	Max. Aggregate size	Coarse aggregate (>2mm) content, % by mass	Fine aggregate (0.063mm-2mm) content,% by mass	Binder type	Binder content, % by mass ratio with mineral aggregate	Air voids content, % by volume
1	Bestone	6	81	11	SH periphalt 45A spec	6.5	17.9
2	Augit Rheolit	6	74	18	Cariphalte ZSA SD	7	11.5
3	Gres D'Ardennes	6	76.9	14.8	Cariphalte XS	6.5	10.7
4	Bestone	6	72.4	22.4	Cariphalte DA	6.3	12.3

Four 1 km long sections were constructed with the mixtures shown in Table 7-21. Tyre - road noise levels, surface texture and sound absorption coefficients were measured on the newly built sections in 2006 as well as after half a year service of the road in 2007. In this study, as the material properties are given for the newly produced mixtures, only the measurement data in 2006 are used. The measurement positions on each lane of the road and the available data obtained from the different tests are listed in Table 7-22. According to the table, sound absorption coefficients were only determined at 6 positions on each lane. So the surface texture and CPX noise levels recorded at the same positions as well as the sound absorption measurements are used in the validation. This ensures that the results of different measurements are all from the same

positions. In total six sets of measurement data of surface characteristics and noise levels for each section are available, which brings the total number of data sets available for the validation at 6 × 4=24.

From Table 7-22, it is also known that just the MPD was recorded for denoting the surface texture, and no texture level on the octave band of wavelength was provided. However, for certain models, texture levels TL_{63} and TL_1 are required for performing the evaluation. In this study, the TL_{63} and TL_1 are determined by using the Model 8(a), see Table 7-15. It should be noted that measured data are always to be preferred for model validation. The author strongly recommends that the models with TL_{63} and TL_1 are validated with measured data in the future. In terms of the CPX measurements, different types of tyres were involved. As the present model is developed purely with a passenger car tyre moving at 80 km/h, only the CPX noise levels measured by using the standard passenger car tyre, namely type A in ISO/CD 11819-2 [15], are used in the validation. The driving speed was 80 km/m.

Table 7-22 Measurement positions and the recording form of the test results

Item	Test positions on one lane	Total test number recorded on one lane	Recorded data
Surface texture	every 10 meters on the whole lane	100	MPD
Absorption coefficient	every 100 meters on the central part of the lane	6	Absorption coefficients on 1/3 octave band
Near field noise measured by CPX	on the whole lane	50 for each test	Overall noise level and noise level on 1/3 octave band

7.4.2 Final model selection

Noise levels are calculated by using the models listed in Table 7-20. The root mean square error (RMSE) is calculated to assess the predictive power of the model. RMSE is a measure for the difference between predicted value from a model and the value actually observed. A smaller RMSE implies higher accuracy of the prediction. Calculation of RMSE is based on the following equation:

$$\mathrm{RMSE} = \sqrt{\frac{\sum_{i=1}^{n} (Y_{obs,i} - Y_{model,i})^2}{n}} \tag{7-5}$$

Where $Y_{obs,i}$ is the observed values and $Y_{model,i}$ is the predicted value from the model. n is the number of observations. In this study, n=24. RMSE has the same units as the quantity being estimated.

The calculated RMSE values are given in Table 7-23. The models are listed in decreasing sequence of RMSE for the overall noise level $L_{A,eq}$. In addition, the maximum number of input parameters required by each model and the input parameter type are also shown. A final selection of the model was made by investigating the validation results.

The ideal model is considered to have the following characteristics:
1) A high adjusted R^2 of the regression equation. This has been examined in Section 7.3.6, and all the candidate models included in the validation process have a high adjusted $R^{2.}$
2) A low RMSE value when comparing the predicted with the measured data.
3) A low number of input variables.
4) The input variables are material properties.
5) The regression relationship is physically correct.

Based on these considerations, the following models were finally selected.

1) Modeling tyre - road noise from surface characteristics

Model 4(b) and Model 8(b) calculate the noise levels from the surface characteristics, and have a better prediction power in comparison with other models on most of the noise levels. Model (4) provides the best prediction of the overall noise level and shows a good fit with the measured data at frequencies below 2000 Hz. This reveals that these noise levels can be well predicted from the linear combination of MPD and the maximum absorption coefficient. In previous studies, the MPD is not always considered as a good predictor for tyre - road noise. However, from this research, it is found that when concentrating on a certain type of surface, the thin layer surfacing in this study, the MPD can be used very well to predict the tyre - road noise levels.

In the 2000 Hz and 2500 HZ frequency band, the RMSEs for Model 8(b) are lower which denotes a better prediction power. This is because the noise level at a high frequency is greatly influenced by the short wavelength texture level (see Chapter 6), and using TL_1 as an input variable is thought to improve the prediction capability of Model 8(b). Towards a better prediction, a new model is set up by combining certain equations selected from Model 4(b) and Model 8(b). In the new model, equations for overall noise level and noise levels from 315 Hz to 1600 Hz are from Model 4(b), and equations for noise levels above 2000 Hz are from Model 8(b). The selection is marked by the blue color in Table 7-23. The new model is called Model I, and can be used to predict the noise levels on thin layer surfacings with MPD, maximum absorption coefficient, TL_{63} and TL_1 as input parameters. A summary of the regression coefficient of Model I is given in Table 7-24.

2) Modeling tyre - road noise from material properties

As shown in Table 7-23, Model 8 performs the best among the models for predicting noise level from material properties. The model calculates the noise level from the evaluated TL_{63} and TL_1 and maximum absorption coefficient based on the material properties. Only three material properties, namely maximum aggregate size, coarse aggregate content and air voids content are required as input variables. This means that the tyre - road noise can be evaluated from the three material properties. According to Table 7-15, the sign of the regression coefficients for the three material parameters are also in

accordance with the analysis of the laboratory measurement results described in Chapter 5. All the findings reflect that Model 8 satisfies the requirements of being an ideal model. The model is suggested to be used for predicting noise levels from material properties (green colour in Table 7-23), and it is renamed as Model II. For the regression coefficients of Model II, the reader is referred to Table 7-15 and Table 7-16.

Model 24 also has a low RMSE for most of the predicted noise levels. The number of input variables is considered to be too high in comparison with Model I and Model II as eight input variables including both material properties and surface characteristics are required. This model is for that reason not recommended in this study. However, the model is developed by using data from all types of road surfaces. This shows that the model has the potential to predict tyre - road noise for all types of pavements in addition to thin layer surfacings. The author suggests that the model should be validated for other types of surfaces as well. If good predictions are made on other surfaces too, the model can be rated as a general model which is applicable for all types of surfaces.

Table 7-23 RMSE between the observed and predicted noise levels

	$L_{A,\,eq}$	L_{315}	L_{400}	L_{500}	L_{630}	L_{800}	L_{1000}	L_{1250}	L_{1600}	L_{2000}	L_{2500}	L_{3150}	Maximum number of input parameter	Input variable type
Model 4(b)	1.84	0.97	1.89	2.48	3.13	3.49	3.11	2.51	3.25	5.89	4.87	1.35	2	Surface
Model 8(b)	2.23	0.89	1.76	2.43	2.72	3.44	3.43	3.33	4.37	3.85	2.72	1.53	3	Surface
Model 24	2.35	0.87	2.11	2.75	2.57	3.00	3.25	3.77	4.36	3.20	2.84	1.73	8	Material and surface
Model 8	2.45	0.91	1.78	2.47	2.76	3.42	3.52	3.63	4.44	4.02	2.95	1.80	3	Material
Model 12	2.50	0.81	2.17	2.48	3.08	2.41	4.17	6.01	5.18	3.20	3.01	3.28	12	Material and surface
Model 16	2.51	1.21	1.80	2.85	3.03	3.06	3.60	3.77	4.36	3.22	2.86	1.73	6	Material
Model 2	2.53	1.07	2.17	2.57	2.98	3.03	3.70	4.11	6.40	3.74	2.37	3.23	6	Material
Model 14	2.53	0.81	2.17	2.48	3.08	3.02	3.70	4.11	6.52	6.38	2.27	3.28	9	Material and surface
Model 10	2.53	0.97	2.01	2.66	3.38	3.33	3.70	4.11	6.40	7.10	2.30	3.23	8	Material and surface
Model 4	2.68	1.01	1.77	2.47	2.91	3.67	3.71	3.89	4.68	4.07	3.38	1.68	4	Material
Model 6(b)	3.05	0.89	1.76	2.43	2.72	2.52	4.95	6.03	3.27	3.20	2.96	1.83	6	Surface

For other models, the amount of input variables is generally large, and the RMSE values are higher than those of Model I and Model II. These models are excluded from the investigation.

Table 7-24 Regression coefficients for Model I

	$L_{A,eq}$	L_{315}	L_{400}	L_{500}	L_{630}	L_{800}	L_{1000}	L_{1250}	L_{1600}	L_{2000}	L_{2500}	L_{3150}
Constant	90.08	69.95	70.77	74.07	80.01	84.21	79.96	78.08	78.88	114.80	115.15	122.46
MPD	6.32	2.33	4.70	6.06	4.22	4.33	9.47	10.85	9.92	-	-	-
TL_{63}	-	-	-	-	-	-	-	-	-	0.45	-	-
TL_1	-	-	-	-	-	-	-	-	-	-1.37	-0.94	-1.21
Max. absorption	-4.56	0.00	-2.18	-1.59	1.46	0.00	-4.93	-8.44	-14.97	-8.09	-5.94	-1.82
R^2	0.78	0.75	0.90	0.94	0.96	0.91	0.87	0.75	0.59	0.88	0.93	0.90
Adjusted R^2	0.75	0.73	0.89	0.93	0.96	0.90	0.86	0.72	0.53	0.85	0.92	0.88

7.4.3 Validation of the final models

Model I and Model II are finally selected. The noise levels predicted with these two models are compared to the noise levels measured on the four sections. The results are shown in Figure 7-9 and Figure 7-10 respectively. The error bars in the figures denote the standard deviation of the measured or predicted values on a certain road surface.

From Figure 7-9 (a), it can be seen that Model I makes very good predictions of the overall tyre - road noise levels on sections 1, 2 and 4. On section 3, the model underestimates the noise level with around 3 dB (A). In Figure 7-10 (a), the overall noise level is perfectly predicted by Modell II on surface 1. On other sections, the difference between the prediction and the measurement is between 2.5 dB (A) to 3 dB (A).

For noise levels on 1/3 octave band, as shown in Figure 7-9 (b) to (e) and Figure 7-10 (b) to (e), the modeled curves generally have similar shapes as those from the measurements. At most of the frequencies, especially frequencies below 800 Hz, the predicted noise levels are in agreement with the measured ones, with a difference not larger than 2 dB (A). The noise levels are underestimated between 1600 Hz and 2500 HZ on surface 1, and between 1000 Hz and 2500 Hz for surface 2. There are overestimations of noise levels between 630 Hz and 1250 Hz on surface 3. The best predictions are obtained for surface 4 by means of Model I and Model II.

It should be noticed that the models are developed based on the averaged CPX levels from 10 different passenger car tyres. In the validation, the measurement data are just from one type of tyre. Considering the variations of noise among the tyres, the prediction results are rather good, as the predicted noise levels are generally close to the measured data, and the distribution of the noise levels over the frequencies is also fairly well predicted by the models.

The fact that both models only need a small amount of input variables is considered to be an advantage. The change of noise level with changing basic

material properties can also be determined with Model II. This is an improvement in comparison with existing models like AOT. Therefore, the models are recommended to be used for the following applications:

1) prediction of the tyre - road noise level when designing thin layer surfacings (Model II);

2) evaluation of the tyre - road noise level based on collected surface characteristic data (Model I).

It is suggested that the proposed models are examined and improved in the future by using more measurement data. The models can be seen as a basic module and need to be extended for wider usage. As the current model only predicts the CPX noise level from passenger car tyres, future work should take into account the influence of truck tyres and the far field receiver positions, such as SPB test positions [17, 18]. The same method is also suitable to develop models for other types of road surfaces. It is recommended that similar models are to be developed for different types of road surfaces, such as dense surfaces, porous asphalt and two-layer asphalt.

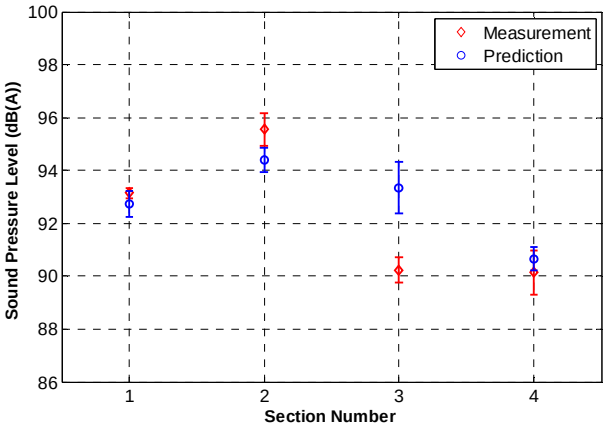

(a) Overall noise level

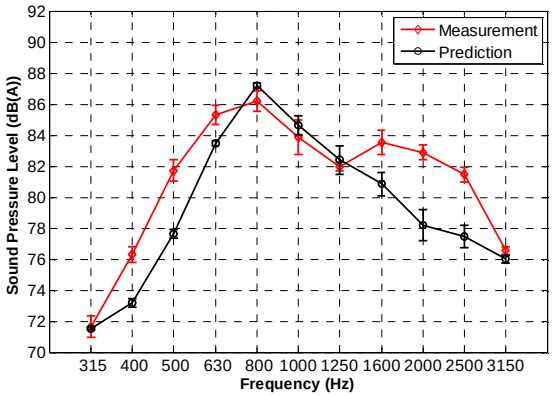

(b) Validation surface 1

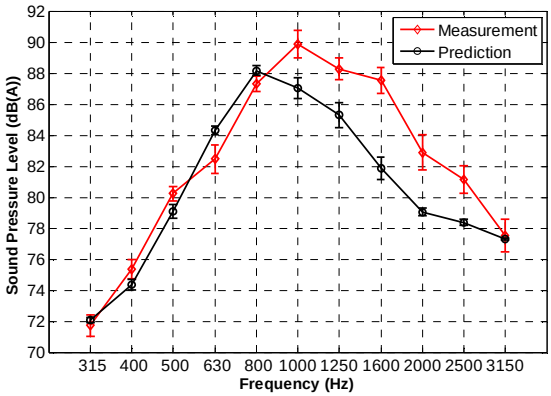

(c) Validation surface 2

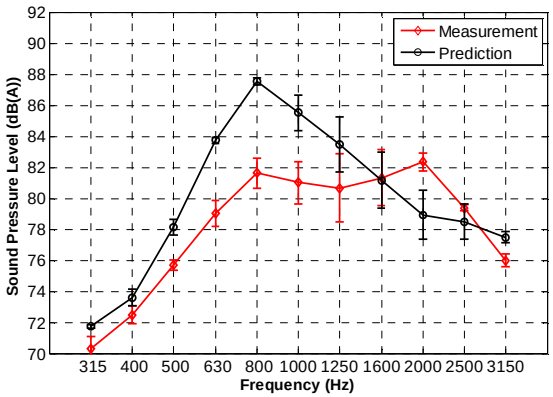

(d) Validation surface 3

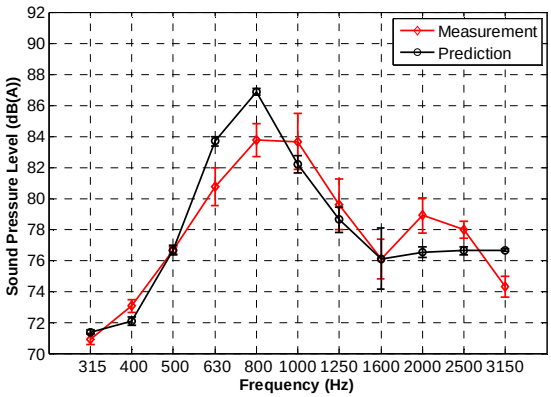

(e) Validation surface 4

Figure 7-9 Noise levels from measurements and predictions with Model I

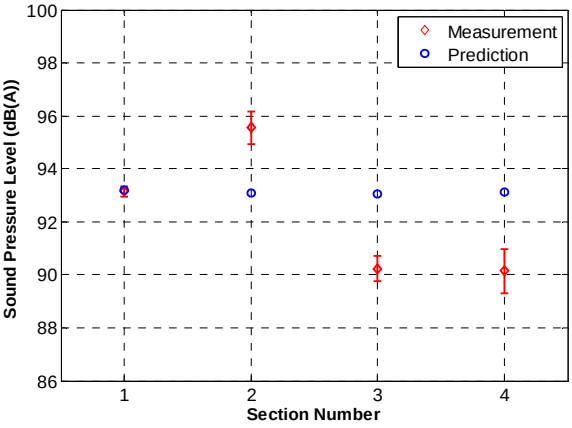

(a) Overall noise level

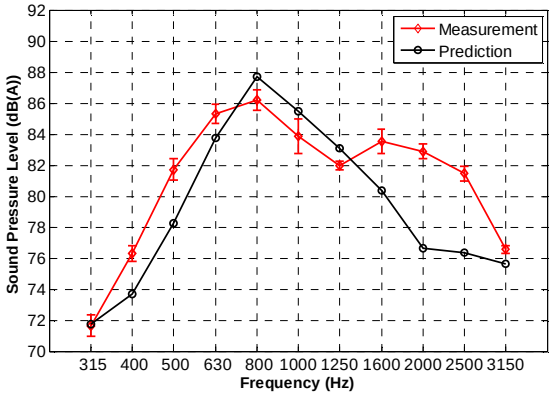

(b) Validation surface 1

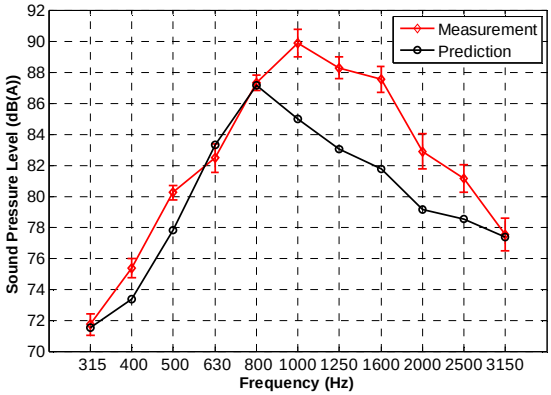

(c) Validation surface 2

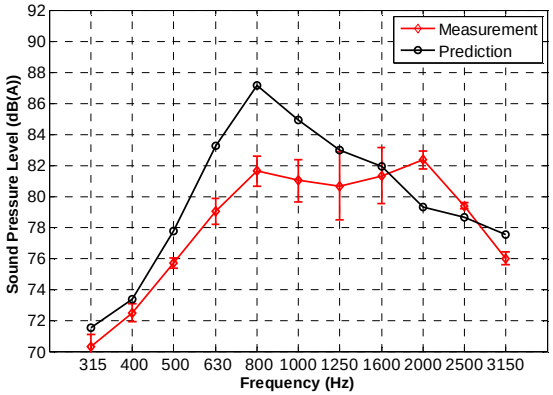

(d) Validation surface 3

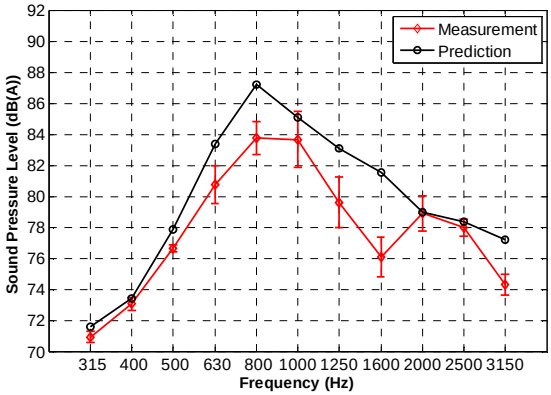

(e) Validation surface 4

Figure 7-10 Noise levels from measurements and predictions with Model II

7.5 Summary

The goal of this chapter was to develop models for predicting tyre - road noise levels from material properties and surface characteristics of thin layer surfacings. The modeling was accomplished by linear regression with data from laboratory and field measurements. 28 models were initially constructed using different input variable combinations, regression methods and surface types. An initial selection of appropriate models was performed by investigating the adjusted R^2. It was found that the models developed by the variable selection methods generally have a similar prediction power as those set up by least square regressions, but with less input variables. Nine candidate models were collected from the initial model selection. The models are validated with measurement data from thin layer surfacings on highway A6 in the Netherlands. By comparing the prediction results obtained with the candidate models from the measured values and considering the number and type of the input variables, two models were finally proposed as outcome of the study.

The near field noise at the CPX positions can be evaluated with the models. Model I generates the noise level from the given surface characteristics. The MPD and maximum absorption are used to predict the overall noise level and noise level at frequencies below 2000 Hz. Above 2000 Hz, the energetic averaged texture levels are used as predictors together with the maximum absorption. The input variables for Model II are three basic material properties, namely maximum aggregate size, coarse aggregate content and air voids content. The tyre - road noise levels are calculated from the surface characteristics simulated by these three material properties. The change of the noise levels caused by the variations of material properties can also be investigated by using Model II.

By comparing the prediction results of the two models with field data, it is shown that the predictions are reliable. The models are of importance for road engineers. Model I can be used to determine the tyre - road noise levels from existing thin layer surfacings of which the surface characteristics are measured. Model II is applicable for making predictions of tyre - road noise during the design process, before the pavements are constructed. It would help the road engineers to compare the noise levels from surfaces with different material properties and in turn to optimize the designs. However, it is suggested to further validate the models with extra data from practical road surfaces. Improvements could be made towards a higher prediction accuracy. Moreover, the present models need to be extended by considering different types of road surfaces and truck tyres.

References

1. Bekke, D.A., Wijnant, Y.H., and Boer de, A., *Experimental review on interior tire-road noise models*, in *International Conference on Noise and Vibration Engineering, ISMA 2010*. 2010, Katholieke Universiteit Leuven: Leuven, Belgium.
2. Kuijpers, A.H.W.M.. and van Blokland, G.J., *Tyre/road noise models in the last two decades: a critical evaluation*. in *Proceedings of The 2001 International Congress and Exhibition on Noise Control Engineering*. 2001. the Hague, The Netherlands.
3. Klein, P. and Hamet, J.F., *END_T, Expected pass-by noise level difference from texture level variation of the road surface*, in *SILVIA Report SILVIA-INRETS-021-01-WP2-070705*. 2005.
4. Hamet, J.F. and Klein, P., *ENRa, Expected pass-by noise level reduction from acoustic absorption of the road surface*, in *SILVIA Project Report SILVIA-INRETS-018-02-WP2-040505*. 2005.
5. Losa, M., Leandri, P., and Rand Bacci, R., *Empirical Rolling Noise Prediction Models Based on Pavement Surface Characteristics* International Journal of Road Materials and Pavement Design - EATA10, 2010. **11**(special issue): p. 487-506.
6. Schutte, A., *Numerical Simulation of Tyre/Road Noise*. 2011, University of Twente: Enschede, The Netherlands.
7. Larsson, K., Barrelet, S., and Kropp, W., *The modelling of the dynamic behaviour of tyre tread blocks.* Applied Acoustics, 2002. **63**(6): p. 659-677.
8. O'Boy, D.J. and Dowling, A.P., *Tyre/road interaction noise—Numerical noise prediction of a patterned tyre on a rough road surface.* Journal of Sound and Vibration, 2009. **323**(1–2): p. 270-291.
9. Li, M., van Keulen, W., van de Ven, M. and Molenaar, A.A.A., *Development of a New Type of Prediction Model for Predicting Tyre/Road Noise*, in *Sustainable Construction Materials 2012*. p. 408-420.
10. Kuijpers, A.H.W.M., Peeters, H.M., Kropp, W., and Beckenbauer, T., *Acoustic optimization tool, RE4 - Modelling refinements in the SPERoN framework*, in *M+P Report DWW.06.04.7*. 2007: Vught, the Netherlands.
11. Morgan, P.A., *IPG Research Report - Innovative mitigation measures for road traffic noise*, in *Report DVS-2008-018*. 2008, Road and Hydraulic Engineering Division of Rijkswaterstaat: Delft, the Netherlands.
12. Hocking, R.R., *The Analysis and Selection of Variables in Linear Regression.* Biometrics, 1976. **32**: p. 1-49.
13. Draper, N.R. and Smith, H., *Applied Regresion Analisis*. 1981, New York: John Wiley & Sons, Inc
14. Hamilton, L.C., *Regression with graphics : a second course in applied statistics*. 1992, Belmont, Calif.: Duxbury Press.

15. ISO11819-2, *Acoustics - Method for measuring the influence of road surfaces on traffic noise -- Part 2: Close-proximity method*. 2000, International Organisation for Standardization (ISO): Geneva, Switzerland.
16. Sandberg, U. and Ejsmont, J., *Tyre/Road Noise Reference Book*. 2002, Kisa, Sweden: Informex.
17. ISO11819-1, *Acoustics - Measurement of the influence of road surfaces on traffic noise -- Part 1: Statistical Pass-By method*. 1997, International Organisation for Standardization (ISO): Geneva, Switzerland.
18. Schwanen, W., van Blokland, G.J., and van Leeuwen, H.M., *IPG 1.4 Robust CPX - Comparison of potential CPX tyres -Comparison of CPX- and SPB-measurements (M+P.DWW.07.04.1, Revision 3)*, in *M+P Report*. 2008, M+P Raadgevende Ingenieurs bv: Vught, the Netherlands.

CHAPTER 8

CONCLUSIONS AND RECOMMENDATIONS

8.1 Highlights of the Thesis

The thesis focuses on tyre - road noise from thin layer surfacings. Measurements, including laboratory and field measurements, were carried out for studying the influence of road material properties on the surface characteristics. Next, statistical analyses were performed to investigate the influence of road surface characteristics on the tyre - road noise levels. In the end, statistical models were developed for evaluating the tyre - road noise from thin layer surfacings in practical circumstances. In this thesis, the following contributions have been made to the existing research work of tyre - road noise:

- The connected air voids content and degree of connectivity were calculated by means of a cluster-labeling algorithm applied on CT scanning results of the test samples. The degree of connectivity was related to the overall air voids content and the sound absorption coefficients.
- P-U technology was used to measure sound absorption. Continuous curves of the absorption coefficient in the frequency domain could be achieved by this method. Procedures were developed for performing this test on slab and core samples in the laboratory.
- A relationship between the mechanical impedance and mixture stiffness was developed. From the relation, the mechanical impedance can be deduced from stiffness measurement.
- PCR and PLS methods were employed to investigate the influence of surface texture and sound absorption on noise levels. The mullticollinearity of the explanatory variables was reduced by using these methods. The influence of each road surface parameters on noise levels can be determined from the developed linear regression equations.
- Statistical models which predict tyre - road noise on thin layer surfacings were developed. The models are proposed to be used in the design of noise reducing road surfaces. The advantages of the models are: they use material properties as input; they have simple structure and are convenient for extension; a small number of inputs are required; and they give reliable predictions.

8.2 Conclusions

As presented in Chapter 1, the main objectives of this PhD thesis are:

- Develop and improve laboratory measurement methods of surface characteristics which are related to tyre - road noise.
- Investigate the influence of material properties on the surface characteristics which are related to tyre - road noise of thin layer surfacings.
- Investigate the influence of surface characteristics on tyre - road noise for thin layer surfacings.
- Develop a practical model which is suitable for predicting the tyre - road noise of thin layer surfacings and which can be applied for road engineers.

With respect to the objectives of the research, the following conclusions can be drawn from this PhD research:

8.2.1 Measurement methods (Chapter 4)

The surface impedance setup based on P-U technology was applied in the sound absorption measurements. The test provides sound absorption coefficients on a much larger frequency range compared with the impedance tube method. P-U technology is suggested to be used for measuring sound absorption of the road surface in both laboratory and in-situ conditions.

Requirements for using this method in laboratory tests were proposed. It requires that the test surface should be large enough, with the dimension of a sample not smaller than 400 mm × 400 mm. Core samples are not suggested to be used for evaluating the sound absorption of a road surface. In case a core sample has to be tested, the assisting platform should be used. The influence of the height of the core can be eliminated in the test with the platform.

8.2.2 Conclusions from the measurements (Chapter 5)

Mixture compositions:

The mixture compositions of the samples were obtained by means of CT scanning. It was shown that the division in stone fraction, mortar and voids content worked well for the purpose of contribution to noise. The degree of connectivity of the road surface was obtained by means of a cluster-labeling algorithm. It was found that the connectivity highly depends on the air voids content. For a mixture with an air voids content less than 12%, the degree of connectivity is generally below 0.1 and close to 0. For mixtures with an air voids content higher than 19%, a large amount of connected air voids were observed, with the degree of connectivity degree close to or exceeding 0.9. A relation between the degree of connectivity and air voids content was developed in this

study and can be used for estimating the degree of connectivity from the air voids content in future studies.

Surface texture:
Surface profile data were collected by means of a laser profilometer. The measurement results show that the maximum aggregate size is the most important factor influencing the surface texture. A material with a larger stone size shows a higher peak value of the texture level and MPD. The peak texture level generally occurs at a wavelength which is equal or close to the maximum aggregate size. A linear relationship was developed between the maximum aggregate size and the MPD. The test results also showed that the surface texture increases with increasing air voids content and increasing coarse aggregate content.

Sound absorption:
Sound absorption was measured with the P-U surface impedance setup. High absorption coefficient peaks, equal to or higher than 0.7, were generally observed for surfaces with an air voids content higher than 17% and with exposed pores at the surface. For a surface layer with a designed air voids content below 12%, or with a clogged surface, a first peak of the absorption coefficient is generally observed between 800 Hz and 1250 Hz; the absorption coefficient is then smaller than 0.35. Regression analysis showed that the first absorption coefficient peak increases linearly with the connected air voids content and the overall air voids content. The connected air voids content is considered to be an essential parameter determining the maximum absorption. The coarse aggregate content and mortar content are together contributing to the connected air voids content in the surface layer after compaction.

Acoustical models were developed for simulating the sound absorption curves of thin layer surfacing slabs. From the models, it can be seen that the overall air voids content can be used directly to simulate the sound absorption of a semi-open surfaces. For a semi-dense type of thin layer surfacing, a better fit is achieved when connected the air voids content is used.

Mechanical impedance:
The mechanical impedance tests showed that the cores from the road sections have comparable mechanical impedance independent on the type of asphalt mixtures. Also slab samples made in the lab have a similar mechanical impedance. When comparing two materials, the difference in mechanical impedance of materials is only significant when they have a great difference in stiffness.

A relationship between the mechanical impedance and stiffness was developed. It was shown that the mechanical impedance is linearly related to the logarithm of the resilient modulus. From the relationship, it is learned that an effective way to reduce the mechanical impedance is by using low stiffness materials, such as

poro-elastic materials. It will not be possible to produce low mechanical impedance layers using standard asphalt concrete mixtures.

8.2.3 Influence of surface characteristics on tyre - road noise (Chapter 6)

Surface characteristics:

Texture levels and sound absorption coefficients can be categorized in three groups being: the long wavelength (≥8 mm) texture level, the short wavelength (≤4 mm) texture level and the sound absorption. In general, the long wavelength texture level increases the noise level below 2000 Hz, and texture with short wavelengths reduces the noise level at frequencies higher than 1600 Hz. Increasing sound absorption results in a noise reduction above 800 Hz. Similar results can also be found when using MPD to present surface texture or the maximum absorption coefficient to denote the sound absorption of the road surface.

Noise levels:

The overall noise level mainly increases with larger texture levels at long wavelength (≥8 mm) and is effectively reduced by the sound absorption at 1000 Hz and 1250 Hz. Therefore, decreasing the long wavelength texture level and increasing the sound absorption at 1000 Hz and 1250 Hz are considered as two important ways to eliminate the tyre - road noise production on thin layer surfacings.

The noise level at low frequencies (below 800 Hz) is highly related with the long wavelength surface texture level, and the noise is considered to be caused by impact mechanisms between tyre and road surface. Generation of noise in the medium frequency range (from 1000 Hz to 2000 Hz) is considered as a combined consequence of the impact and air pumping mechanisms, because all the surface parameters show to have a great influence on the noise levels. At high frequencies, tyre - road noise is mainly caused by the air pumping mechanism. An increase of the short wavelength (≤4 mm) texture level and increasing the sound absorption leads to a reduction of noise levels at high frequencies.

A new type of modeling was developed which relates the change of noise level to the changes in surface characteristics. The method provides a direct description of the noise reduction or increase on thin layer surfacing, and it can help to correct existing models by taking into account the change of the noise level due to the small changes of road surface characteristics.

Vehicle speed:

Speed has a strong influence on noise. Speed is completely independent from the road surface characteristics in the regression analysis. The noise levels are increasing linearly with the increasing speed for any combination of surface characteristics.

Truck tyre:
On thin layer surfacings, the surface texture is relatively small compared with other types of surface layers. The influence of texture is not that significant between different surfaces when truck tyres are considered. In the low frequency band, only noise at 500 Hz and 630 Hz is strongly affected by the texture level. The short wavelength texture level and sound absorption effectively decrease the noise level at frequencies above 1000 Hz. Thus increasing the texture level at short wavelengths and sound absorption coefficients are considered as essential factors for reducing the noise from the truck tyre rolling on thin layer surfacing.

8.2.4 Tyre - road noise modelling (Chapter 7)

Models for predicting tyre - road noise levels from the material properties and surface characteristics of thin layer surfacings were developed. Two models were finally selected as outcome of the study.

The models are used for predicting the near field noise at the CPX positions. Model I generates the noise level from the given surface characteristics. The MPD and maximum absorption are used to predict the overall noise level and noise levels at frequencies below 2000 Hz. Above 2000 Hz, selected texture levels are used as predictors together with the maximum absorption. The input variables for Model II are three basic material properties, namely maximum aggregate size, coarse aggregate content and air voids content. In Model II, the tyre - road noise levels are calculated from the surface characteristics which are simulated by these three material properties. The change of the noise levels caused by the variations of material properties can also be investigated by using Model II.

By comparing the prediction results of the two models with the measurement data obtained on thin surface layers, it was concluded that the models give rather accurate predictions. The models are proposed to be applied by road engineers. Model I can be used in the cases where surface characteristics are measured. The tyre - road noise levels are to be deduced from those measured surface characteristics. Model II is applicable for making predictions of tyre - road noise in the mixture design process, before the pavement is constructed. It will help road engineers to compare the noise levels from surfaces with different material properties and to optimize the designs.

8.3 Recommendations

Although some promising results have been obtained from the research in this thesis, much work still needs to be carried out. The recommendations for future research are as follows:

- The study has focused on a certain type of road surface, namely the thin layer surfacing. Similar analyses as used in this thesis, including laboratory measurements, statistical analyses and modeling can also be adopted for other surface types, such as a dense asphalt surfaces, porous asphalt and two-layer

porous asphalts. It should be noted that the surface characteristics or material properties to be taken into account can change depending on the type of surface for which the model is developed. For example, there is nearly no sound absorption ability in case of dense surfaces. For porous asphalt, the depth of an exposed pore in the surface does not work for noise generation from tyre vibration when it is beyond a certain critical value. Then the enveloped surface texture could be used for denoting the road surface profile instead of the raw texture.

- The measurements in this thesis are mainly performed on test samples in the laboratory. It is essential to measure the tyre - road noise on the field road surfaces with the same material properties as in the lab. With in-situ tests, researchers can compare the surface characteristics of laboratory made samples with those of real road surfaces. This helps to calibrate and improve the present laboratory tests for a better simulation of practice. Relationships can be built between the surface characteristics measured in the lab and the noise levels from the road surface. These relationships are important for evaluating the tyre - road noise based on the laboratory tests on surface characteristics.

- The models developed in this thesis need to be examined and improved in the future by using more measurement data. The models can be seen as a basic module and need to be extended for wider usage. In future work, the influence of truck tyres and the far field receiver positions, such as SPB test positions, should be taken into account for improving the models. Similar models are also recommended to be developed for different types of road surfaces, such as dense asphalt surfaces, porous asphalt and two-layer asphalt.

Appendix A

Noise level from passenger car tyres on thin layer surfacings

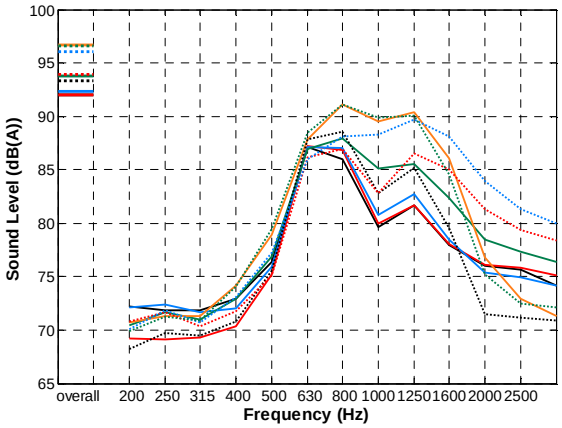

Tyre 01: Michelin Energy 175/65R14

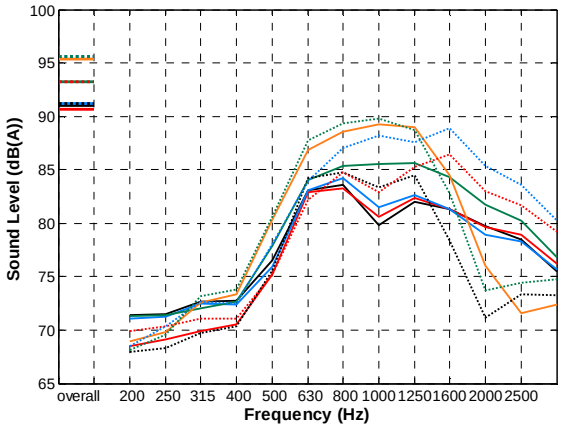

Tyre 02: Goodyear GT3

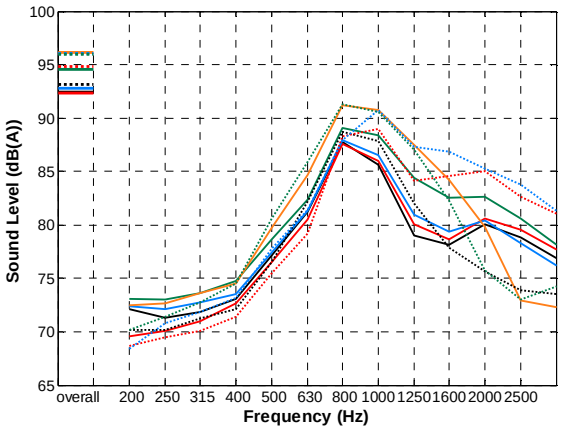

Tyre 03: Pirelli P3000 Energy

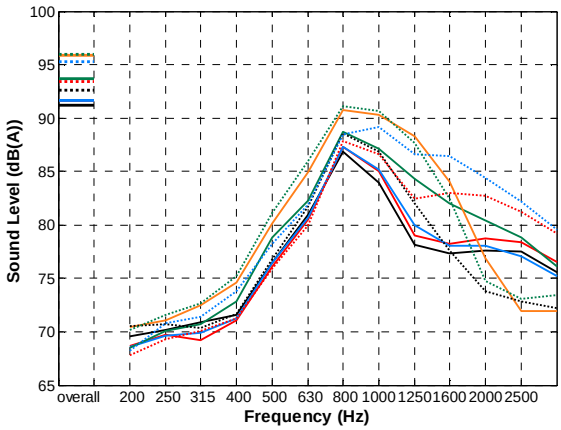

Tyre 04: Continental ContiEcoContact EP

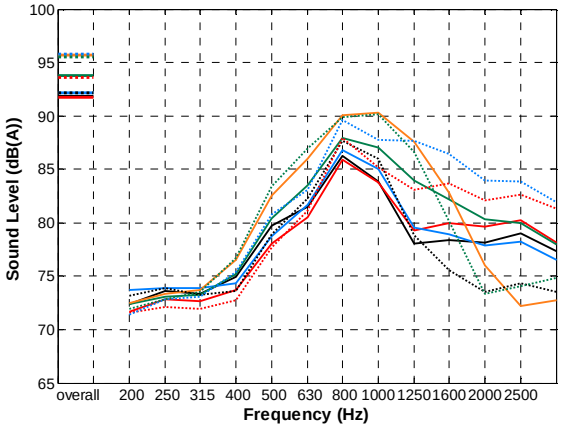

Tyre 05: Michelin Energy 195/65R15

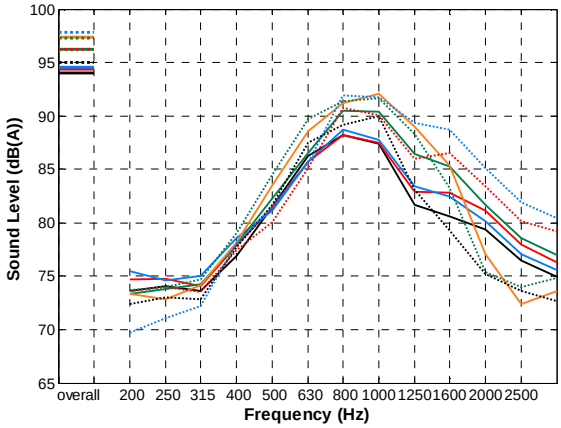

Tyre 06: Vredestein Hi-Trac

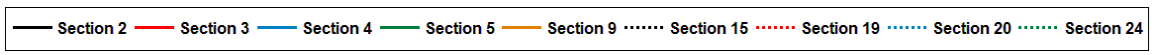

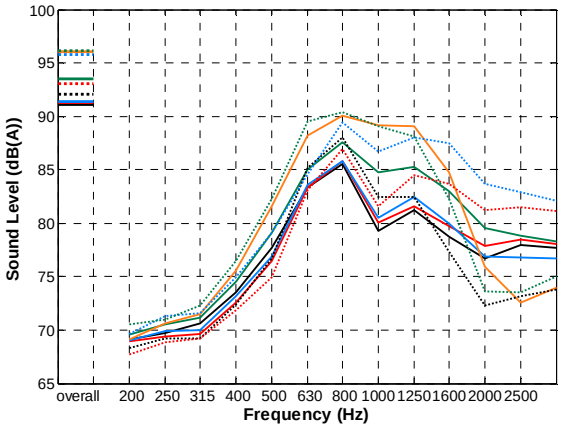

Tyre 07: Continental ContiPremiContact

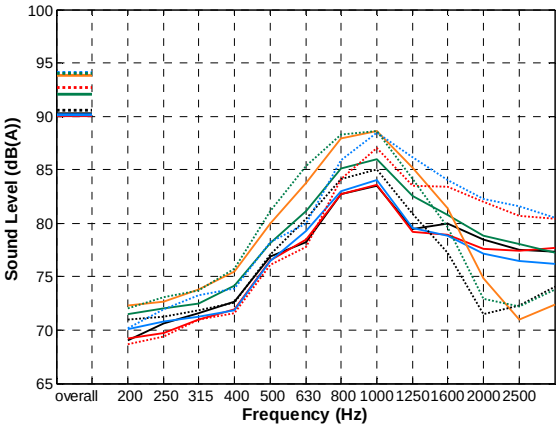

Tyre 09: Goodyear Ultragrip 7

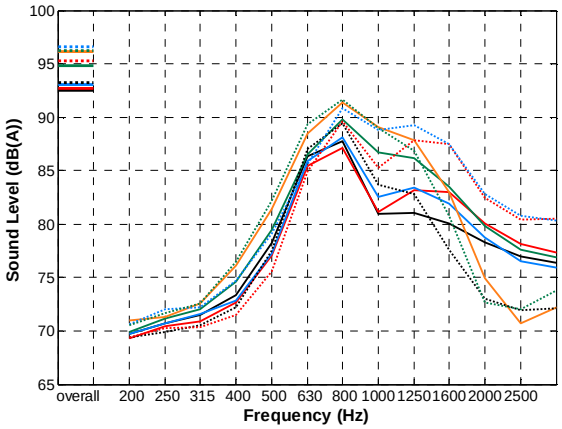

Tyre 10: Vredestein Snowtrac2

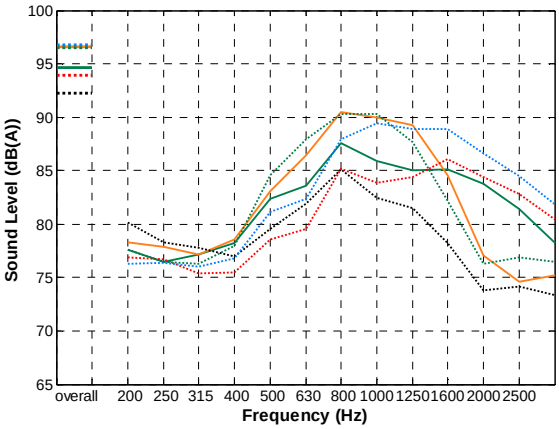

Tyre 11: Avon ZV1

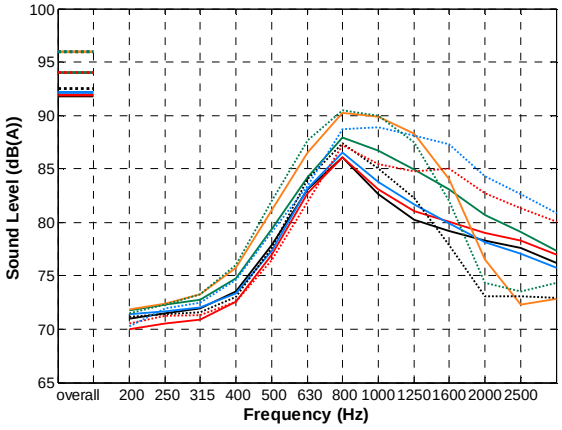

Average of the ten tyres

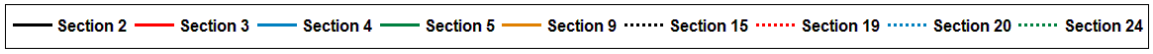

Appendix B

Standardized coefficients from PLS with variable combination 1

	$L_{A,\,eq}$	L_{315}	L_{400}	L_{500}	L_{630}	L_{800}	L_{1000}	L_{1250}	L_{1600}	L_{2000}	L_{2500}	L_{3150}
TL_{250}	0.17	0.15	0.15	0.14	0.09	0.14	0.16	0.17	0.15	0.10	0.08	0.08
TL_{125}	0.17	0.13	0.15	0.14	0.10	0.13	0.16	0.17	0.14	0.09	0.07	0.07
TL_{63}	0.16	0.14	0.15	0.14	0.10	0.14	0.16	0.16	0.14	0.09	0.07	0.07
TL_{32}	0.16	0.14	0.15	0.14	0.10	0.13	0.16	0.16	0.14	0.08	0.06	0.07
TL_{16}	0.15	0.12	0.14	0.13	0.10	0.13	0.15	0.15	0.12	0.07	0.05	0.06
TL_{8}	0.11	0.09	0.10	0.10	0.09	0.11	0.12	0.11	0.06	0.01	0.00	0.01
TL_{4}	0.02	0.04	0.05	0.06	0.09	0.06	0.05	0.02	-0.06	-0.09	-0.09	-0.09
TL_{2}	-0.06	0.02	0.01	0.04	0.08	0.01	-0.02	-0.06	-0.15	-0.17	-0.16	-0.16
TL_{1}	-0.09	0.02	0.00	0.04	0.09	-0.01	-0.05	-0.10	-0.19	-0.21	-0.20	-0.21
AL_{1000}	-0.24	0.01	-0.07	-0.07	-0.06	-0.18	-0.20	-0.24	-0.23	-0.10	-0.04	-0.08
AL_{1250}	-0.17	0.00	-0.04	0.01	0.09	-0.08	-0.12	-0.20	-0.30	-0.25	-0.13	-0.12
AL_{1600}	-0.07	-0.01	-0.02	0.04	0.14	0.01	-0.03	-0.11	-0.25	-0.29	-0.18	-0.12
AL_{2000}	-0.03	0.00	-0.02	-0.01	0.03	0.03	-0.01	-0.02	-0.10	-0.17	-0.22	-0.22
AL_{2500}	-0.04	0.01	-0.02	-0.04	-0.02	0.01	-0.02	-0.03	-0.05	-0.08	-0.17	-0.21
AL_{3150}	-0.05	0.01	-0.02	-0.02	-0.01	0.01	-0.03	-0.04	-0.07	-0.09	-0.17	-0.21
R^2	0.88	0.70	0.77	0.82	0.89	0.91	0.93	0.90	0.86	0.88	0.88	0.90
Number of components selected	2	2	2	2	2	2	2	2	2	2	2	2

Standardized coefficients from PLS with variable combination 3

	$L_{A,\,eq}$	L_{315}	L_{400}	L_{500}	L_{630}	L_{800}	L_{1000}	L_{1250}	L_{1600}	L_{2000}	L_{2500}	L_{3150}
TL_{250}	0.24	0.16	0.18	0.15	0.07	0.17	0.21	0.25	0.25	0.18	0.14	0.15
TL_{125}	0.23	0.14	0.18	0.15	0.07	0.17	0.21	0.24	0.23	0.16	0.12	0.13
TL_{63}	0.23	0.14	0.18	0.16	0.08	0.17	0.21	0.23	0.22	0.16	0.12	0.13
TL_{32}	0.23	0.15	0.18	0.16	0.09	0.17	0.21	0.23	0.22	0.15	0.11	0.12
TL_{16}	0.20	0.12	0.15	0.13	0.08	0.16	0.19	0.20	0.19	0.12	0.09	0.09
TL_{8}	0.12	0.08	0.09	0.09	0.08	0.12	0.13	0.12	0.07	0.01	-0.01	0.00
TL_{4}	-0.04	0.02	0.01	0.03	0.10	0.04	0.00	-0.05	-0.15	-0.19	-0.19	-0.19
TL_{2}	-0.19	0.00	-0.05	0.00	0.11	-0.05	-0.12	-0.20	-0.34	-0.34	-0.33	-0.34
TL_{1}	-0.25	0.02	-0.05	0.01	0.14	-0.08	-0.16	-0.26	-0.41	-0.41	-0.40	-0.42
Max.absorption	-0.10	0.04	-0.02	0.05	0.21	0.05	-0.05	-0.13	-0.33	-0.44	-0.42	-0.38
R^2	0.83	0.70	0.78	0.82	0.88	0.87	0.89	0.82	0.75	0.89	0.93	0.89
Number of components selected	2	2	2	2	2	2	2	2	2	2	2	2

Appendix C

Regression results for Model 2

	$L_{A,eq}$	L_{315}	L_{400}	L_{500}	L_{630}	L_{800}	L_{1000}	L_{1250}	L_{1600}	L_{2000}	L_{2500}	L_{3150}
Constant	55.43	56.07	47.54	43.37	61.44	60.86	36.25	23.78	29.17	79.91	76.35	73.14
Max. Aggregate size	0.64	0.44	0.80	0.88	0.60	0.58	1.10	1.24	1.22	0.63	-	-
Coarse aggregate content	0.52	0.14	0.28	0.33	0.20	0.35	0.62	0.82	0.83	-	-	-
Fine aggregate content	0.35	0.12	0.24	0.27	0.15	0.23	0.42	0.57	0.61	-	-	-
Binder content	-	-	-	-	-	-	-	-	-	-	-	-
Air voids content	-0.12	-	-	-	0.08	-	-0.10	-0.19	-0.34	-0.37	-0.43	-0.38
Thickness	-0.34	-	-0.15	-	-	-0.26	-0.36	-0.64	-0.91	-	0.30	0.35
R^2	0.93	0.76	0.93	0.93	0.94	0.95	0.94	0.90	0.85	0.80	0.93	0.94
Adjusted R^2	0.90	0.71	0.91	0.91	0.92	0.94	0.92	0.86	0.78	0.77	0.92	0.94
Selection method	B	B	B	B	B	B	B	B	B	B	B&S	B&S

Regression results for Model 4(a)

	MPD	Max. Absorption
Constant	-3.29	-0.42
Max. Aggregate size	0.15	-
Coarse aggregate content	0.03	0.01
Fine aggregate content	0.03	-
Binder content	-	-
Air voids content	0.01	0.02
R^2	0.94	0.86
Adjusted R^2	0.92	0.85
Selection method	B&S	B&S

Regression results for Model 4(b)

	$L_{A,eq}$	L_{315}	L_{400}	L_{500}	L_{630}	L_{800}	L_{1000}	L_{1250}	L_{1600}	L_{2000}	L_{2500}	L_{3150}
Constant	90.08	69.95	70.77	74.07	80.01	84.21	79.96	78.08	78.88	79.86	80.29	79.72
MPD	6.32	2.33	4.70	6.06	4.22	4.33	9.47	10.85	9.92	6.36	3.11	-
Max. Absorption	-4.56	-	-2.18	-1.59	1.46	0.00	-4.93	-8.44	-14.97	-18.26	-15.26	-9.29
R^2	0.78	0.75	0.90	0.94	0.96	0.91	0.87	0.75	0.59	0.80	0.82	0.67
Adjusted R^2	0.75	0.73	0.89	0.93	0.96	0.90	0.86	0.72	0.53	0.77	0.80	0.65
Selection method	B&S	B&S	B&S	B	B&S	B&S	B&S	B&S	B	B&S	B	B&S

Regression results for Model 6(b)

	$L_{A,eq}$	L_{315}	L_{400}	L_{500}	L_{630}	L_{800}	L_{1000}	L_{1250}	L_{1600}	L_{2000}	L_{2500}	L_{3150}
Constant	85.89	65.10	63.65	63.78	70.38	77.71	69.99	71.57	111.74	121.97	133.86	117.73
TL_{63}	0.23	0.17	0.25	0.36	0.33	0.27	0.44	0.38	0.58	0.40	-	-
TL_1	-	-	-	-	-	-	-	-	-1.37	-1.55	-1.47	-1.05
AL_{1000}	-12.45	-	-	-	-	-7.51	-14.60	-22.39	-	-	-	-
AL_{1250}	-	-	-	-	-	-	-	-	-10.66	-	-	-
AL_{1600}	-	-	-	-	-	-	-	-	-	-7.67	-	-
AL_{2500}	-	-	-	-	-	-	-	-	-	-	-4.74	-7.83
R^2	0.92	0.71	0.80	0.84	0.91	0.94	0.96	0.93	0.90	0.96	0.93	0.95
Adjusted R^2	0.88	0.65	0.76	0.81	0.89	0.90	0.94	0.89	0.84	0.93	0.90	0.92

Regression results for Model 8(a)

	TL_{63}	TL_1	Max. Absorption
Constant	19.39	33.14	-0.42
Max. Aggregate size	2.85	0.29	-
Coarse aggregate content	-	-	0.01
Fine aggregate content	-	-	-
Binder content	-	-	-
Air voids content	0.19	0.18	0.02
R^2	0.95	0.88	0.86
Adjusted R^2	0.94	0.86	0.85
Selection method	S	B&S	B&S

Regression results for Model 8(b)

	$L_{A,eq}$	L_{315}	L_{400}	L_{500}	L_{630}	L_{800}	L_{1000}	L_{1250}	L_{1600}	L_{2000}	L_{2500}	L_{3150}
Constant	79.90	65.10	63.65	63.78	70.38	76.14	64.06	60.22	127.69	114.80	115.15	122.46
TL_{63}	0.35	0.17	0.25	0.36	0.33	0.28	0.55	0.62	0.67	0.45	-	-
TL_1	-	-	-	-	-	-	-	-	-1.95	-1.37	-0.94	-1.21
Max. Absorption	-1.79	-	-	-	-	1.00	-1.00	-3.82	0.05	-8.09	-5.94	-1.82
R^2	0.90	0.71	0.80	0.84	0.91	0.92	0.93	0.87	0.76	0.88	0.93	0.90
Adjusted R^2	0.87	0.65	0.76	0.81	0.89	0.90	0.92	0.84	0.71	0.85	0.92	0.88

Regression results for Model 10

	$L_{A,eq}$	L_{315}	L_{400}	L_{500}	L_{630}	L_{800}	L_{1000}	L_{1250}	L_{1600}	L_{2000}	L_{2500}	L_{3150}
Constant	55.43	69.95	67.20	70.88	79.94	72.57	36.25	23.78	29.17	41.99	86.47	73.14
Max Aggregate size	0.64	-	0.41	0.29	-	-	1.10	1.24	1.22	0.81	-	-
Coarse aggregate content	0.52	-	-	-	-0.03	0.20	0.62	0.82	0.83	0.64	-	-
Fine aggregate content	0.35	-	0.05	0.05	-	0.12	0.42	0.57	0.61	0.45	-	-
Binder content	-	-	-	-	-	-	-	-	-	-	-1.12	-
Air voids content	-0.12	-	-	-	-	-0.06	-0.10	-0.19	-0.34	-0.19	-0.36	-0.38
Thickness	-0.34	-	-	-	0.08	-0.14	-0.36	-0.64	-0.91	-0.69	0.22	0.35
MPD	-	2.33	3.63	5.73	4.78	3.43	-	-	-	-	-	-
Max. Absorption	-	-	-	-	1.56	-	-	-	-	-10.76	-5.10	-
R^2	0.93	0.75	0.96	0.98	0.98	0.96	0.94	0.90	0.85	0.93	0.96	0.94
Adjusted R^2	0.90	0.73	0.95	0.97	0.97	0.94	0.92	0.86	0.78	0.90	0.94	0.94
Selection method	B	B&S	B	B	B	B	B	B	B	B	B	B&S

Regression results for Model 12

	$L_{A,eq}$	L_{315}	L_{400}	L_{500}	L_{630}	L_{800}	L_{1000}	L_{1250}	L_{1600}	L_{2000}	L_{2500}	L_{3150}
Constant	64.32	61.37	47.54	47.73	80.53	67.40	26.99	2.18	125.23	121.97	114.73	103.96
Max Aggregate size	-	-	0.80	-	-0.79	-	1.54	2.17	-2.70	-	-	-
Coarse aggregate content	0.33	-	0.28	0.17	-	0.20	0.55	0.73	-	-	-	-
Fine aggregate content	0.23	0.03	0.24	0.17	-	0.14	0.40	0.56	-	-	-	-
Binder content	-	-	-	-	-1.10	-	1.26	2.58	-	-	-1.38	-0.95
Air voids content	-0.11	-	-	-	-	-	-	-	-	-	-0.36	-0.32
Thickness	-0.26	-	-0.15	-	-	-0.19	-0.26	-0.47	-0.46	-	-	0.28
TL_{63}	0.25	0.24	-	0.38	0.40	0.22	-	-	1.63	0.40	-	-
TL_{1}	-	-	-	-	-	-	-	-	-2.10	-1.55	-0.61	-0.62
AL_{1000}	-6.21	-	-	-	-	-5.09	-8.16	-14.07	-	-	-	-
AL_{1250}	-	-	-	-	-	-	-	-	-8.57	-	-	-
AL_{1600}	-	-	-	-	-	-	-	-	-	-7.67	-	-
AL_{2500}	-	-	-	-	-	-	-	-	-	-	-	-
R^2	0.95	0.78	0.93	0.95	0.95	0.97	0.96	0.94	0.96	0.95	0.94	0.97
Adjusted R^2	0.92	0.75	0.91	0.93	0.93	0.95	0.94	0.91	0.94	0.94	0.93	0.97
Selection method	B	B&S	B	B	B	B	B	B	B&S	B	B	B

Regression results for Model 14

	$L_{A,eq}$	L_{315}	L_{400}	L_{500}	L_{630}	L_{800}	L_{1000}	L_{1250}	L_{1600}	L_{2000}	L_{2500}	L_{3150}
Constant	55.43	61.37	47.54	47.73	80.53	58.95	36.25	23.78	107.41	119.55	104.86	103.96
Max Aggregate size	0.64	-	0.80	-	-0.79	-	1.10	1.24	-	-	-	-
Coarse aggregate content	0.52	-	0.28	0.17	-	0.33	0.62	0.82	0.39	-	-	-
Fine aggregate content	0.35	0.03	0.24	0.17	-	0.22	0.42	0.57	0.31	-	-	-
Binder content	-	-	-	-	-1.10	-	-	-	-	-	-1.28	-0.95
Air voids content	-0.12	-	-	-	-	-0.04	-0.10	-0.19	-	-	-0.30	-0.32
Thickness	-0.34	-	-0.15	-	-	-0.25	-0.36	-0.64	-0.80	-0.40	0.23	0.28
TL_{63}	-	0.24	-	0.38	0.40	0.19	-	-	0.75	0.52	-	-
TL_{1}	-	-	-	-	-	-	-	-	-1.89	-1.32	-0.49	-0.62
Max. Absorption	-	-	-	-	-	-	-	-	-	-6.55	-4.24	-
R^2	0.93	0.78	0.93	0.95	0.95	0.96	0.94	0.90	0.90	0.92	0.97	0.97
Adjusted R^2	0.90	0.75	0.91	0.93	0.93	0.94	0.92	0.86	0.86	0.89	0.95	0.97
Selection method	B	B&S	B	B	B	B	B	B	B	B	B	B

Regression results for Model 16

	$L_{A,eq}$	L_{315}	L_{400}	L_{500}	L_{630}	L_{800}	L_{1000}	L_{1250}	L_{1600}	L_{2000}	L_{2500}	L_{3150}
Constant	88.05	74.74	57.40	60.58	92.88	85.62	76.86	74.93	79.83	81.90	80.94	80.05
Max Aggregate size	0.52	0.22	0.32	0.30	0.30	0.55	0.71	0.54	0.27	0.24	0.19	0.16
Coarse aggregate content	0.06	0.04	0.26	0.37	0.05	0.00	0.08	0.11	0.06	0.00	0.00	0.00
Fine aggregate content	0.00	0.00	0.18	0.26	0.00	0.00	0.00	0.00	0.00	0.00	0.00	0.00
Binder content	0.00	-0.99	-1.04	-1.97	-1.74	0.00	0.00	0.00	0.00	0.00	0.00	0.00
Air voids content	0.00	0.00	0.00	0.00	0.11	0.10	0.00	-0.14	-0.30	-0.30	-0.31	-0.29
Thickness	-0.07	-0.01	-0.03	-0.08	-0.14	-0.11	-0.08	-0.03	0.00	0.00	0.00	-0.02
R^2	0.79	0.77	0.78	0.77	0.81	0.68	0.61	0.60	0.69	0.83	0.84	0.89
Adjusted R^2	0.78	0.75	0.76	0.75	0.79	0.67	0.58	0.57	0.67	0.82	0.84	0.88
Selection method	B&S	B	B	B&S	B	B&S	B&S	B	B	B&S	B&S	B&S

Regression results for Model 24

	$L_{A,eq}$	L_{315}	L_{400}	L_{500}	L_{630}	L_{800}	L_{1000}	L_{1250}	L_{1600}	L_{2000}	L_{2500}	L_{3150}
Constant	92.25	64.17	68.79	72.15	81.47	82.43	82.70	74.93	79.83	83.14	82.18	80.05
Max Aggregate size	0.33	0.20	0.18	0.29	0.32	0.48	0.48	0.54	0.27	-	-	0.16
Coarse aggregate content	-	-	-	-	-	0.06	-	0.11	0.06	-	-	-
Fine aggregate content	-	0.04	0.05	0.06	-	-	-	-	-	-	-	-
Binder content	-	0.42	-	-	-	-	-	-	-	-	-	-
Air voids content	-0.06	-	-0.07	-	0.11	0.14	-	-0.14	-0.30	-0.34	-0.30	-0.29
Thickness	-0.07	-	-0.02	-0.07	-0.13	-0.11	-0.07	-0.03	-	0.02	-	-0.02
MPD	2.27	3.38	4.61	5.63	3.30	-	3.01	-	-	1.51	1.53	-
Max. Absorption	-	-	1.76	2.32	-	-4.22	-3.25	-	-	-2.49	-3.48	-
R^2	0.84	0.93	0.94	0.87	0.85	0.72	0.63	0.60	0.69	0.84	0.86	0.89
Adjusted R^2	0.83	0.92	0.93	0.86	0.83	0.69	0.60	0.57	0.67	0.83	0.85	0.88
Selection method	B&S	B	B	B	B	B	B	B	B	B	B	B&S

Curriculum Vitae
M. Li

Personal Information

Name: Mingliang Li

Gender: Male

Date of birth: February 17, 1982

Place of birth: Fuxin, Liaoning Province, China

E-mail: isl0330y@gmail.com; lis.1221@163.com

Education

Oct. 2008- present

PhD candidate in Section of Road and Railway Engineering, Faculty of Civil Engineering and Geosciences, Delft University of Technology, the Netherlands.

Sep. 2005- Jan. 2008

Master of Science, majored in Municipal Engineering, School of Civil and Hydraulic Engineering, Dalian University of Technology, China.

Sep. 2001-July 2005

Bachelor of Engineering, majored in Civil Engineering, School of Civil and Hydraulic Engineering, Dalian University of Technology, China.

Previous Employment

Apr.- Oct. 2007

Research Assistant in the Hong Kong Road Research Laboratory of the Hong Kong Polytechnic University, Hong Kong.